

Final

Setup, Calibration, and Validation for Illinois River Watershed Nutrient Model and Tenkiller Ferry Lake EFDC Water Quality Model

Prepared by

Michael Baker Jr., Inc.

3601 Eisenhower Avenue, Alexandria, VA 22304

Aqua Terra, Consultants

2685 Marine Way, Suite 1314
Mountain View, CA 94043-1115

Dynamic Solutions, LLC

6421 Deane Hill Dr. Suite 1
Knoxville, TN 37919

Submitted to

US EPA Region 6

Dallas, TX 75202

Under

EPA Contract EP-C-12-052 Order No. 0002

Dated 15 September 2013

August 7, 2015



Table of Contents

Section 1 Introduction	1
Section 2 Illinois River Watershed Nutrient Modeling: Model Calibration and Validation	4
2.1 Background and Study Objectives	4
2.2 Prior Modeling Studies and Management Plans	7
2.3 Modeling Approach.....	9
2.3.1 Model Application	9
2.4 Time Series Data Availability for the IRW Model.....	12
2.4.1 Precipitation.....	13
2.4.2 Evapotranspiration and Other Meteorological Data	18
2.4.3 Streamflow	19
2.4.4 Water Quality Data	21
2.4.5 Point Sources	22
2.4.6 Atmospheric Deposition	26
2.5 Segmentation and Characterization of the IRW	27
2.5.1 Topography and Elevation	28
2.5.2 Hydrography/Drainage Patterns.....	29
2.5.3 Land Use	32
2.5.4 Soils Data	37
2.5.5 Final Segmentation	43
2.6 Calibration and Validation of the IRW Model.....	47
2.6.1 Calibration and Validation Time Periods	47
2.6.2 Hydrology Calibration/Validation Procedures and Results.....	52
2.6.3 Water Quality and Sediment Calibration Procedures and Comparisons.....	64
2.6.4 Nonpoint Loading Calibration and Results	79
2.6.5 Instream Water Quality Calibration Results.....	90
2.7 TP and TN Loading and Load Allocation Analyses	97
2.7.1 Loading Analyses at AR/OK Stateline and Tahlequah.....	97
2.7.2 Load Allocation at AR/OK Stateline and Tahlequah.....	105
Section 3 Tenkiller Ferry Lake EFDC Water Quality Model Analysis	109
3.1 Overview of the EFDC Model	109
3.2 Model Simulation Period.....	109
3.3 Grid Development.....	110
3.4 Shoreline and Bathymetry	110

3.5	Meteorological Data.....	112
3.6	Boundary Conditions	114
3.7	HSPF-EFDC Linkage	117
Section 4	Water Quality and Sediment Flux Model	120
4.1	Water Quality Model	120
4.2	Sediment Flux Model.....	130
Section 5	Calibration and Validation Stations	138
5.1	Stage Calibration and Validation Stations	138
5.2	Water Quality Calibration Stations.....	139
Section 6	Model Performance Statistics	142
6.1	Model Performance Statistics.....	142
Section 7	Hydrodynamic Model Calibration and Validation	144
7.1	Lake Stage Calibration	144
7.2	Lake Stage Validation.....	145
7.3	Lake Hydraulic Residence Time Calibration and Validation	145
Section 8	Water Quality Model Calibration and Validation	149
8.1	Introduction.....	149
8.2	Water Temperature Calibration and Validation	149
8.3	Total Suspended Solids Calibration and Validation.....	159
8.4	Dissolved Oxygen Calibration and Validation.....	165
8.5	Algae and Tropic State Index Calibration and Validation	174
8.6	Organic Carbon Calibration and Validation	180
8.7	Nitrogen Calibration and Validation	185
8.8	Phosphorus Calibration and Validation	196
Section 9	Summary and Conclusions	209
9.1	Summary	209
9.2	Conclusions	210
Section 10	References.....	212

List of Figures

Figure 1-1. Location of Tenkiller Ferry Lake	3
Figure 2-1. Illinois River Watershed Location map	5
Figure 2-2. Section 303(d) 2008 Listed Impaired Segments within the Illinois River Watershed.	6
Figure 2-3 Pervious Land Simulation (PERLND) Module in HSPF	10
Figure 2-4 Soil Phosphorus Cycle in HSPF AGCHEM	11
Figure 2-5 Instream Phosphorus Processes in HSPF RCHRES	12
Figure 2-6 Precipitation Stations Selected for Use in the IRW Model.....	15
Figure 2-7 Annual Isohyetal Map of the IRW	17
Figure 2-8 USGS Stream Gage Locations in the IRW	20
Figure 2-9 Derived from a 10-Meter DEM from the USGS Seamless Server	30
Figure 2-10 Stream Hydrography Coverage for the IRW from NHDPlus.....	31
Figure 2-11 National Land Cover Data (NLCD) for 2001 and 2006	35
Figure 2-12 Distribution of NRCS Hydrologic Soil Groups for the IRW.....	38
Figure 2-13 The cross-section of a riffle at site OSG1	41
Figure 2-14 Final Segmentation of the IRW.....	43
Figure 2-15 Annual Rainfall Data for Fayetteville, Kansas, and Odell for 1980-2009.....	49
Figure 2-16 R and R ² Value Ranges for Model Performance	54
Figure 2-17 Daily Flow Duration Comparisons for the State Line (Reach 630) and Tahlequah (Reach 870) for the Calibration Period	60
Figure 2-18 Daily Flow Duration Comparisons for the State Line (Reach 630) and Tahlequah (Reach 870) for the Validation Period.....	61
Figure 2-19 Daily Flow Time Series Comparisons for the State Line (Reach 630) and Tahlequah (Reach 870) for the Calibration Period	62
Figure 2-20 Daily Flow Time Series Comparisons for the State Line (Reach 630) and Tahlequah (Reach 870) for the Validation Period.....	63
Figure 2-21 Sediment Calibration Plots for Osage Creek (Reach 316).....	69
Figure 2-22 Sediment Calibration Plots for Ballard Creek (Reach 609).....	70

Figure 2-23 Sediment Calibration Plots for Illinois River south of Siloam Springs (Reach 630) 71

Figure 2-24 Sediment Calibration Plots for Illinois River near Tahlequah (Reach 870)..... 72

Figure 2-25 Water Temperatures Graphs for Illinois River at Savoy (Reach 150) for Calibration (top) and Validation (bottom) periods 76

Figure 2-26 Water Temperatures Graphs for Illinois River South of Siloam Springs (Reach 630) for Calibration (top) and Validation (bottom) periods 77

Figure 2-27 Water Temperatures Graphs for Illinois River near Tahlequah (Reach 870) for Calibration (top) and Validation (bottom) periods 78

Figure 2-28 Meteorologic Segments for the IRW..... 80

Figure 2-29 Simulated and Observed DO (top) and TN (bottom) at Illinois River below Siloam Springs, AR (Reach 630, USGS 07195430)..... 93

Figure 2-30 Simulated and Observed PO4-P (top) and TP (bottom) at Illinois River below Siloam Springs, AR (Reach 630, USGS 07195430)..... 94

Figure 2-31 Simulated and Observed DO (top) and TN (bottom) at Illinois River near Tahlequah, OK (Reach 630, USGS 07196500)..... 95

Figure 2-32 Simulated and Observed PO4-P (top) and TP (bottom) at Illinois River near Tahlequah, OK (Reach 870, USGS 07196500)..... 96

Figure 2-33 Scatterplots of TP (top) and TN (bottom) Monthly Loads at the IR South of Siloam Springs, AR (RCH630) 99

Figure 2-34 Flow and load rating curves of TP (top) and TN (bottom) at the IR South of Siloam Springs, AR (RCH630) 100

Figure 2-35 Comparison of Monthly Loading (lbs/mo) of TP (top) and TN (bottom) estimated with LOADEST and the HSPF IRW model at the Illinois River near Tahlequah (RCH870) 103

Figure 2-36 Flow and load rating curves of TP (top) and TN (bottom) at the Illinois River near Tahlequah (RCH870)..... 104

Figure 3-1. Modeling Domain of the Tenkiller Ferry Lake EFDC 111

Figure 3-2. Tenkiller Ferry Lake Stage and Storage Volume. Comparison of Observed Data and EFDC Model 112

Figure 3-3. Location of the MESONET station COOK 113

Figure 3-4. HSPF tributary and catchment locations 116

Figure 4-1. Spatial water quality kinetic zones defined for Tenkiller Ferry Lake 125

Figure 4-2. Location of the Atmospheric Deposition Monitoring Stations 129

Figure 4-3. Location of the CDM Sediment Core and Shallow Benthic Stations	135
Figure 5-1. Location of the USACE Stage Monitoring Station TENO2	138
Figure 5-2. Location of the OWRB Monitoring Stations	140
Figure 5-3. Location of the CDM/USGS Monitoring Stations	141
Figure 7-1. Comparison of Simulated and Observed Water Level during January 2006 to December 2006	144
Figure 7-2. Comparison of Simulated and Observed Water Level during January 2005 to December 2005	145
Figure 8-1. Surface Layer Water Temperature Calibration Plot at Station LK-01	151
Figure 8-2. Bottom Layer Water Temperature Calibration Plot at Station LK-01	151
Figure 8-3. Surface Layer Water Temperature Calibration Plot at Station LK-03	152
Figure 8-4. Bottom Layer Water Temperature Calibration Plot at Station LK-03	152
Figure 8-5. Surface Layer Water Temperature Validation Plot at Station LK-01	153
Figure 8-6. Bottom Layer Water Temperature Validation Plot at Station LK-01	153
Figure 8-7. Surface Layer Water Temperature Validation Plot at Station LK-03	154
Figure 8-8. Bottom Layer Water Temperature Validation Plot at Station LK-03	154
Figure 8-9. Water Temperature Vertical Profile Comparison Plot at Station LK-01 (5 May 2005 – 28 March 2006) (page 2-1)	155
Figure 8-10. Water Temperature Vertical Profile Comparison Plot at Station LK-01 (6 April 2005 – 14 September 2006) (page 2-2)	156
Figure 8-11. Water Temperature Vertical Profile Comparison Plot at Station LK-03 (18 May 2005 – 16 November 2005) (page 2-1)	157
Figure 8-12. Water Temperature Vertical Profile Comparison Plot at Station LK-03 (28 March 2006 – 14 September 2006) (page 2-2)	158
Figure 8-13. Surface Layer TSS Calibration Plot at Station LK-01	161
Figure 8-14. Bottom Layer TSS Calibration Plot at Station LK-01	161
Figure 8-15. Surface Layer TSS Calibration Plot at Station LK-03	162
Figure 8-16. Bottom Layer TSS Calibration Plot at Station LK-03	162
Figure 8-17. Surface Layer TSS Validation Plot at Station LK-01	163

Figure 8-18. Bottom Layer TSS Validation Plot at Station LK-01	163
Figure 8-19. Surface Layer TSS Validation Plot at Station LK-03	164
Figure 8-20. Bottom Layer TSS Validation Plot at Station LK-03	164
Figure 8-21. Surface Layer DO Calibration Plot at Station LK-01.....	167
Figure 8-22. Bottom Layer DO Calibration Plot at Station LK-01.....	167
Figure 8-23. Surface Layer DO Calibration Plot at Station LK-03.....	168
Figure 8-24. Bottom Layer DO Calibration Plot at Station LK-03.....	168
Figure 8-25. Surface Layer DO Validation Plot at Station LK-01	169
Figure 8-26. Bottom Layer DO Validation Plot at Station LK-01	169
Figure 8-27. Surface Layer DO Validation Plot at Station LK-03	170
Figure 8-28. Bottom Layer DO Validation Plot at Station LK-03	170
Figure 8-29. Dissolved Oxygen Vertical Profile Comparison Plot at Station LK-01 (18 May 2005 – 28 March 2006) (page 2-1).....	171
Figure 8-30. Dissolved Oxygen Vertical Profile Comparison Plot at Station LK-01 (6 April 2005 – 14 September 2006) (page 2-2)	172
Figure 8-31. Dissolved Oxygen Vertical Profile Comparison Plot at Station LK-03 (18 May 2005 – 16 November 2005) (page 2-1)	173
Figure 8-32. Surface Layer Chlorophyll a Calibration Plot at Station LK-01	176
Figure 8-33. Surface Layer Chlorophyll a Calibration Plot at Station LK-03	176
Figure 8-34. Bottom Layer Chlorophyll a Calibration Plot at Station LK-03	177
Figure 8-35. Surface Layer Chlorophyll a Validation Plot at Station LK-01	177
Figure 8-36. Bottom Layer Chlorophyll a Validation Plot at Station LK-01	178
Figure 8-37. Surface Layer Chlorophyll a Validation Plot at Station LK-03	178
Figure 8-38. Bottom Layer Chlorophyll a Validation Plot at Station LK-03	179
Figure 8-39. Comparison of Carlson’s TSI for Chlorophyll-a and Oklahoma Water Quality Criteria at LK-03 for a Nutrient Limited Watershed.....	179
Figure 8-40. Surface Layer TOC Calibration Plots at Station LK-01.....	181
Figure 8-41. Bottom Layer TOC Calibration Plots at Station LK-01.....	182

Figure 8-42. Surface Layer TOC Calibration Plots at Station LK-03.....	182
Figure 8-43. Bottom Layer TOC Calibration Plots at Station LK-03.....	183
Figure 8-44. Surface Layer TOC Validation Plots at Station LK-01	183
Figure 8-45. Bottom Layer TOC Validation Plots at Station LK-01	184
Figure 8-46. Surface Layer TOC Validation Plots at Station LK-03	184
Figure 8-47. Bottom Layer TOC Validation Plots at Station LK-03	185
Figure 8-48. Surface Layer NH4 Calibration Plots at Station LK-01	187
Figure 8-49. Bottom Layer NH4 Calibration Plots at Station LK-01	188
Figure 8-50. Surface Layer NH4 Calibration Plots at Station LK-03	188
Figure 8-51. Bottom Layer NH4 Calibration Plots at Station LK-03	189
Figure 8-52. Surface Layer TKN Calibration Plots at Station Site1	189
Figure 8-53. Surface Layer TKN Calibration Plots at Station Site3	190
Figure 8-54. Surface Layer TKN Validation Plots at Station Site1.....	190
Figure 8-55. Surface Layer TKN Validation Plots at Station Site3.....	191
Figure 8-56. Surface Layer NO3 Calibration Plots at Station LK-01	191
Figure 8-57. Bottom Layer NO3 Calibration Plots at Station LK-01	192
Figure 8-58. Surface Layer NO3 Calibration Plots at Station LK-03.....	192
Figure 8-59. Bottom Layer NO3 Calibration Plots at Station LK-03.....	193
Figure 8-60. Surface Layer NO3 Validation Plots at Station LK-01	193
Figure 8-61. Bottom Layer NO3 Validation Plots at Station LK-01	194
Figure 8-62. Surface Layer NO3 Validation Plots at Station LK-03	194
Figure 8-63. Bottom Layer NO3 Validation Plots at Station LK-03	195
Figure 8-64. HSPF NO3 Boundary at Illinois River in 2005. USGS Tahlequah station is approximately 9 miles upstream of the EFDC upstream boundary at Illinois River.	195
Figure 8-65. HSPF NO3 Boundary at Illinois River in 2006. USGS Tahlequah station is approximately 9 miles upstream of the EFDC upstream boundary at Illinois River.	196
Figure 8-66. Surface Layer TPO4 Calibration Plots at Station LK-01	199

Figure 8-67. Bottom Layer TPO4 Calibration Plots at Station LK-01	200
Figure 8-68. Surface Layer TPO4 Calibration Plots at Station LK-03	200
Figure 8-69. Bottom Layer TPO4 Calibration Plots at Station LK-03	201
Figure 8-70. HSPF TPO4 Boundary in the Illinois River in 2006. USGS Tahlequah station is approximately 9 miles upstream of the EFDC upstream boundary at Illinois River.	201
Figure 8-71. HSPF Flow Boundary in the Illinois River in 2006	202
Figure 8-72. Surface Layer TPO4 Validation Plots at Station LK-01	202
Figure 8-73. Bottom Layer TPO4 Validation Plots at Station LK-01	203
Figure 8-74. Surface Layer TPO4 Validation Plots at Station LK-03	203
Figure 8-75. Bottom Layer TPO4 Validation Plots at Station LK-03	204
Figure 8-76. Surface Layer TP Calibration Plots at Station LK-01	204
Figure 8-77. Bottom Layer TP Calibration Plots at Station LK-01	205
Figure 8-78. Surface Layer TP Calibration Plots at Station LK-03	205
Figure 8-79. Bottom Layer TP Calibration Plots at Station LK-03	206
Figure 8-80. Surface Layer TP Validation Plots at Station LK-01	206
Figure 8-81. Bottom Layer TP Validation Plots at Station LK-01	207
Figure 8-82. Surface Layer TP Validation Plots at Station LK-03	207
Figure 8-83. Bottom Layer TP Validation Plots at Station LK-03	208

List of Tables

Table 2-1	Precipitation Stations in/near the Illinois River Watershed	16
Table 2-2	Meteorological Stations in/near the Illinois River Watershed.....	19
Table 2-3	USGS Stream Gages Containing Flow Data	21
Table 2-4	USGS Stream Gages with Water Quality Data in the IRW	22
Table 2-5	Point Sources in Illinois River Watershed.....	23
Table 2-6	Data Availability and Measurement Frequency of Point Sources.....	25
Table 2-7	Average Daily Point Source Loads for 1990-2009.....	25
Table 2-8	Annual Loads (lbs/year) of TP, TN, and CBOD _u for 2009.....	26
Table 2-9	Distribution of NLCD Land Use for 1992, 2001, and 2006	34
Table 2-10	Aggregation of NLCD Land Use to Model Categories	34
Table 2-11	Total Impervious Areas (TIA) and Percent Imperviousness of Each Urban Land Use for NLCD 2001 v2, and NLCD 2006, and Calculation of EIA.....	36
Table 2-12	Effective Impervious Area Percentage in Developed Land Use Classes in the IRW	37
Table 2-13	Example FTABLEs for Reaches 302 and 312	42
Table 2-14	IRW Stream Reach Characteristics	44
Table 2-15	IRW Gage Stations for Watershed Model Calibration and Validation.....	51
Table 2-16	General Calibration/Validation Targets or Tolerances for HSPF Applications (Donigian, 2000)	54
Table 2-17	Calibration (top) and Validation (bottom) Summary Statistics	57
Table 2-18	Annual Flow Volumes in Inches for the Illinois River South of Siloam Springs (Reach 630) for the Calibration (top) and Validation (bottom) Periods.....	58
Table 2-19	Annual Flow Volumes in Inches for the Illinois River near Tahlequah (Reach 870) for the Calibration (top) and Validation (bottom) Periods.....	59
Table 2-20	Annual Sediment Loading Rates (tons/acre/year) for the IRW	67
Table 2-21	Instream Reach Sediment Balance for IRW	73
Table 2-22	Modeled Nonpoint Source Loading Rates (lb/ac/yr) for the IRW	81
Table 2-23	“Target” Nonpoint Source Loadings Rates (lb/ac/yr) for the IRW	82

Table 2-24 Comparison of Factors Converting Generic Organic Matter (BOD/Organics) from the Land to Organic Species in Streams	83
Table 2-25 Final Litter Application Rates (tons/acre/year) Used in the IRW HSPF Model	88
Table 2-26 Sample AGCHEM Phosphorus Balance for Pasture-Litter for Met Segment 140 ...	89
Table 2-27 LOADEST Summary Statistics for TP and TN loads at the Illinois River near Tahlequah (RCH870).....	101
Table 2-28 Annual Loadings of TN and TP (tons/year) by LOADEST and the HSPF IRW model at the Illinois River near Tahlequah (RCH870).....	102
Table 2-29 Load Allocation for TP for Selected Reaches within the IRW	106
Table 2-30 Load Allocation for TN for Selected Reaches within the IRW.....	107
Table 3-1. Tenkiller Ferry Lake EFDC Model Flow Boundaries and Data Source.....	115
Table 3-2. HSPF State Variables and Units for the Tenkiller Ferry Lake Watershed Model.....	117
Table 3-3. HSPF-EFDC Linkage.....	118
Table 3-4. Refractory, Labile and Dissolved Splits for Organic Matter	119
Table 4-1. EFDC State Variables.....	120
Table 4-2. EFDC Model Parameter Values for Cohesive Solids	123
Table 4-3. Dry and Wet Atmospheric Deposition for Nutrients	128
Table 4-4. EFDC Sediment Diagenesis Model State Variables.....	131
Table 4-5. Sediment Phosphorus Data.....	136
Table 4-6. Sediment Bed Data used for Water Quality Zones.....	137
Table 5-1. Calibration and Validation Stations for the Tenkiller Ferry Lake EFDC Model	139
Table 7-1. Summary Model Performance Statistics for Hydrodynamic Model of Tenkiller Ferry Lake Calibration and Validation Periods.....	144
Table 7-2. Comparison of Observed and Simulated Whole Lake Hydraulic Residence Time: January-December	147
Table 7-3. Comparison of Observed and Simulated Whole Lake Hydraulic Residence Time: April-September.....	147
Table 8-1. Summary Statistics of Water Temperature (°C)	150
Table 8-2. Summary Statistics of TSS (mg/l).....	160

Table 8-3. Summary Statistics of DO (mg/l)	166
Table 8-4. Summary Statistics of Chlorophyll a (µg/l).....	175
Table 8-5. Summary Statistics of TOC (mg/l)	181
Table 8-6. Summary Statistics of NO3 (mg/l)	186
Table 8-7. Summary Statistics of TPO4 (mg/l)	198
Table 8-8. Summary Statistics of TP (mg/l)	198

List of Acronyms and Abbreviations

Chl-a	Chlorophyll-a
COD	Chemical Oxygen Demand
COE	United States Army Corps of Engineers
ODEQ	Oklahoma Department of Environmental Quality
DO	Dissolved Oxygen
DOC	Dissolved Organic Carbon
DOM	Dissolved Organic Matter
DON	Dissolved Organic Nitrogen
DOP	Dissolved Organic Phosphorus
DSLLC	Dynamic Solutions, LLC
EFDC	Environmental Fluid Dynamics Code
EPA	Environmental Protection Agency
HSPF	Hydrologic Simulation Program - Fortran
HUC	Hydrologic Unit Code
LPOC	Labile particulate organic carbon
LPON	Labile particulate organic nitrogen
LPOP	Labile particulate organic phosphorus
NLW	Nutrient Limited Waterbody
NPS	Nonpoint Source
OCC	Oklahoma Conservation Commission
OWRB	Oklahoma Water Resources Board
POM	Particulate Organic Matter
PON	Particulate Organic Nitrogen
POP	Particulate Organic Phosphorus
RMS	Root Mean Square
RMSE	Root Mean Square Error
RPOC	Refractory particulate organic carbon
RPON	Refractory particulate organic nitrogen
RPOP	Refractory particulate organic phosphorus
SOD	Sediment Oxygen Demand
TKN	Total Kjeldhal Nitrogen (Total Organic Nitrogen + Ammonia-N)
TMDL	Total Maximum Daily Load
TN	Total Nitrogen
TOC	Total Organic Carbon
TON	Total Organic Nitrogen
TOP	Total Organic Phosphorus
TP	Total Phosphorus
TPO4	Total Phosphate
TSI	Trophic State Index
TSS	Total Suspended Solids
USGS	United States Geological Survey

Section 1 Introduction

Tenkiller Ferry Lake is located in the Illinois River watershed (Hydrologic Unit Code 11110103), which crosses the Oklahoma-Arkansas boundary and covers 1,053,032 acres. The Illinois River flows west-southwest from Arkansas and into Oklahoma, where it drains into Tenkiller Ferry Lake before flowing into the Arkansas River. Tenkiller Ferry Lake is located in the southwestern portion of the basin with an area of 12,900 acres (OWRB, 2013). The main tributaries to the lake include the Illinois River, Baron Fork, Tahlequah Creek, Flint Creek, and Caney Creek. Figure 1-1 shows the location of the Illinois River watershed, the Tenkiller Ferry Lake drainage basin, Tenkiller Ferry Lake, and its main tributaries.

Tenkiller Ferry Lake is identified on Oklahoma's 2010 303(d) list as impaired because of elevated nutrients, and it is a high-priority target for TMDL development (ODEQ, 2010). Tenkiller Ferry Lake is also listed as a Nutrient Limited Waters (NLW) indicating that the aesthetics beneficial use is considered threatened by nutrients (OWRB, 2013). Water quality impairments in the lake are for dissolved oxygen (DO), chlorophyll a, and trophic state index (TSI). Analysis of the water quality data collected by OWRB indicates that eutrophication of the lake occurs during summer periods, which is primarily attributed to excess phosphorus inputs from both point and nonpoint sources, especially from the untreated poultry litter on watershed pasture (Cooke et al., 2011).

In order to address the water quality issues in Tenkiller Ferry Lake, DSLLC developed a 3-dimensional water quality model using the Environmental Fluid Dynamic Code (EFDC) in 2006 (DSLLC, 2006). The developed EFDC water quality model was calibrated and validated to the observed data from the Clean Lakes Program (OWRB et al., 1996). Several data issues have limited the performance of the EFDC water quality model. These issues are listed below:

- There was no detailed lake bathymetry data available: bathymetry data were based on historical USGS quadrangle maps that represented the topography of the area before construction of the dam in the early 1950s (DSLLC, 2006);
- Sediment bed chemistry data were not available to support the setup of a full diagenesis model of EFDC.

In 2005, detailed contemporary bathymetry data were collected to support the collection of sediment cores (Fisher, 2008; Fisher et al., 2009) and the development of a laterally-averaged hydrodynamic and water quality model of Tenkiller Ferry Lake using CE-QUAL-W2 (Wells et al., 2008). During 2005 to 2007, CDM/USGS collected water quality data in both the water column and sediment bed (Olsen, 2008). Inclusion of these most current data into the lake EFDC water quality model will greatly enhance the model reliability of the EFDC model as management tools to address the water quality issues and assistance in the development of the TMDLs.

The setup, calibration, and validation of Lake Tenkiller EFDC water quality model using the most current data are summarized in this report. The scope of the project included the following elements:

- Refine the EFDC model grid from earlier DSLLC study (DSLLC, 2006);
- Setup and develop data linkages between AQUA TERRA developed HSPF watershed runoff model and the EFDC lake model of hydrodynamics and water quality. The HSPF model results are used to provide streamflow, water temperature, suspended solids

(TSS), organic carbon, nutrients (N,P), algae biomass, and dissolved oxygen as input data for the EFDC lake model;

- Update the bottom elevation data for the refined model grid with detailed contemporary bathymetric data available from a 2005 survey that was conducted to support the collection of sediment cores (Fisher, 2008; Fisher et al., 2009) and the development of a laterally-averaged hydrodynamic and water quality model of Lake Tenkiller (Wells et al., 2008);
- Analyze, process and format lake surface elevation, storage volume and release flow measured at the dam at Station TENO2 by the US Army Corps of Engineers Tulsa District;
- Analyze, process and format wind and meteorological input data from Oklahoma MesoNet at Station COOK;
- Analyze, process, and format available station data to describe time series and vertical profiles of water temperature and dissolved oxygen from CDM/USGS and OWRB;
- Analyze, process, and format available station data to describe time series of nutrients, chlorophyll a and TSS from CDM/USGS and OWRB;
- Analyze, process, and format available station data to describe sediment bed distributions of solids, nitrogen and phosphorus from CDM/USGS;
- Process all data in formats required for input to the EFDC model for setup of the hydrodynamic, sediment transport, water quality and sediment diagenesis model;
- Calibrate the hydrodynamic and water quality model for the 365 day period from 1 January 2006 through 31 December 2006 to records for water level elevation, water temperature, suspended solids, dissolved oxygen, organic carbon, nutrients (N,P) and algae biomass as chlorophyll-a at four (4) station locations in Tenkiller Ferry Lake;
- Validate the hydrodynamic and water quality model for the 365 day period from 1 January 2005 through 31 December 2005 to records for water level elevation, water temperature, suspended solids, dissolved oxygen, organic carbon, nutrients (N,P) and algae biomass as chlorophyll-a at four (4) station locations in Tenkiller Ferry Lake;
- Prepare and submit draft and final technical reports documenting the development, calibration and validation of the Tenkiller Ferry Lake EFDC hydrodynamic and water quality model.
- Conduct the sensitivity analyses with a total of four (4) model input parameters and eight (8) EFDC runs;
- Conduct the uncertainty analysis by evaluating the combined set of four (4) model input parameters (watershed TP load + 3 other model input parameters) using results of the calibration run; and
- Using the calibrated HSPF watershed and EFDC lake models simulate the in-lake response to load allocation scenarios.

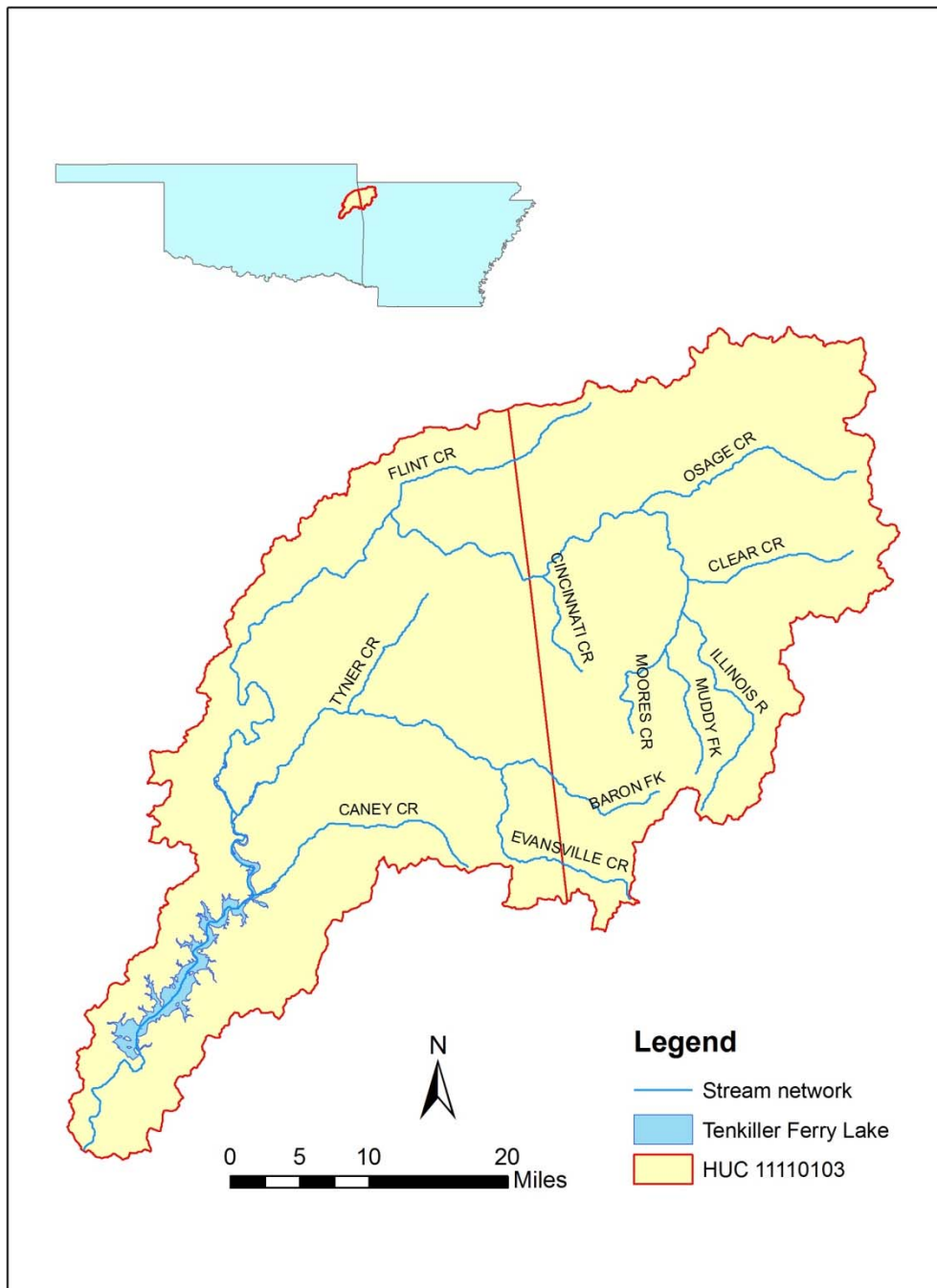


Figure 1-1. Location of Tenkiller Ferry Lake

Section 2 Illinois River Watershed Nutrient Modeling: Model Calibration and Validation

2.1 Background and Study Objectives

The Illinois River is a multi-jurisdictional tributary of the Arkansas River, approximately 160 miles long, in the states of Arkansas and Oklahoma. The objective of this study is to develop a scientifically robust and defensible watershed model to determine reductions in phosphorus loads needed to meet water quality standards in both states, Arkansas and Oklahoma. This watershed model serves as a tool for sound technical decisions on appropriate point and nonpoint source controls to meet those standards. Ultimately, the intent is development of a tool that can lead to scientifically sound TMDLs and a basin-wide water quality restoration plan.

The U.S. Environmental Protection Agency's (EPA's) Region 6 is funding this project through EPA Purchase Order #EP-11-000023, and Work Assignments #3-36, #4-36, and 5-36 -- Water Quality Modeling and TMDL Development for the Illinois River Watershed -- under EPA's BASINS contract (# EP-C-06-029) with AQUA TERRA Consultants, Mountain View, California. In addition, under EPA PO EP-G126-00097, AQUA TERRA performed application of detailed nutrient modeling (i.e., use of AGCHEM module within the HSPF watershed model), along with sensitivity and uncertainty analyses of the model results. AQUA TERRA conducted work for this project in conformance with the procedures detailed in the Quality Assurance Project Plan (QAPP) developed for this effort (AQUA TERRA Consultants, 2010a; M. Baker, Jr., 2013).

The Illinois River begins in the Ozark Mountains in the northwest corner of Arkansas, and flows for 50 miles west into northeastern Oklahoma (See Figure 2-1). The Arkansas portion of the Illinois River Watershed is characterized by rapidly developing urban areas and intensive agricultural animal production. It includes Benton, Washington and Crawford Counties and according to the US Census Bureau, the population of Benton and Washington Counties increased by 45% between 1990 and 2000. This growth rate continued through 2010 with Benton County growing at 44% and Washington County at 29%. Arkansas ranked second in the nation in broiler production in 1998. Benton and Washington Counties ranked first and second respectively in the state. Other livestock production such as turkey, cattle and hogs are also all significant in this area. Upon entering Oklahoma, the river flows southwest and then south through the mountains of eastern Oklahoma for 65 miles, until it enters the Tenkiller Ferry Lake reservoir, also known as Lake Tenkiller. The upper section of the Illinois River in Oklahoma is a designated scenic river and home to many native species of bass with spring runs of white bass. The lower section, below Tenkiller dam flows for 10 miles to the Arkansas River, and is a designated year-round trout stream, stocked with rainbow and brown trout.

Several segments of the Illinois River have been and currently are on the State of Oklahoma's 303(d) list for Total Phosphorus (TP), while the mainstem Illinois River in Arkansas is not listed for TP. However, several tributaries to the Illinois River in Arkansas (e.g. Osage Creek, Muddy Fork, and Spring Creek) are designated as Phosphorus-impaired and included in the State's Clean Water Act 303(d) list. (See Figure 2-2). On 19 January 2010 a Call for Data was published in the Federal Register (FR) requesting that data relevant to this project be submitted before 3 March 2010. On 4 February 2010, EPA organized meetings in Fort Smith AR with the core state and federal agencies participating in the study, and with local stakeholder groups. These meetings provided an overview of the project and its objectives, and further elaborated on the data needs included in the FR Call for Data. Following the Fort Smith meeting and the FR Notice, a wide range of groups and agencies at all levels – federal, state, local, university –

have been supportive of the effort by providing reports, documents, references, and data for use in the study.

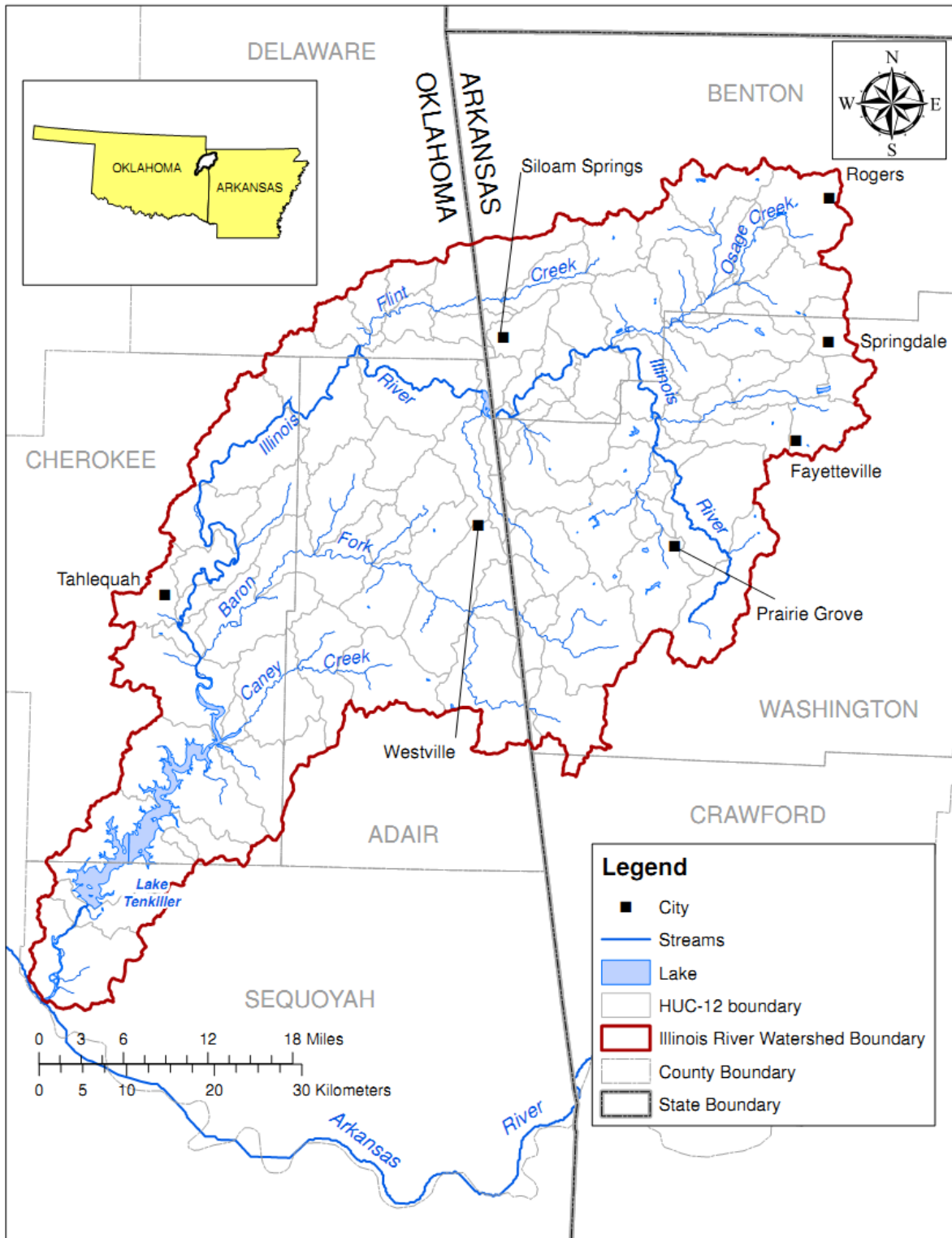


Figure 2-1. Illinois River Watershed Location map

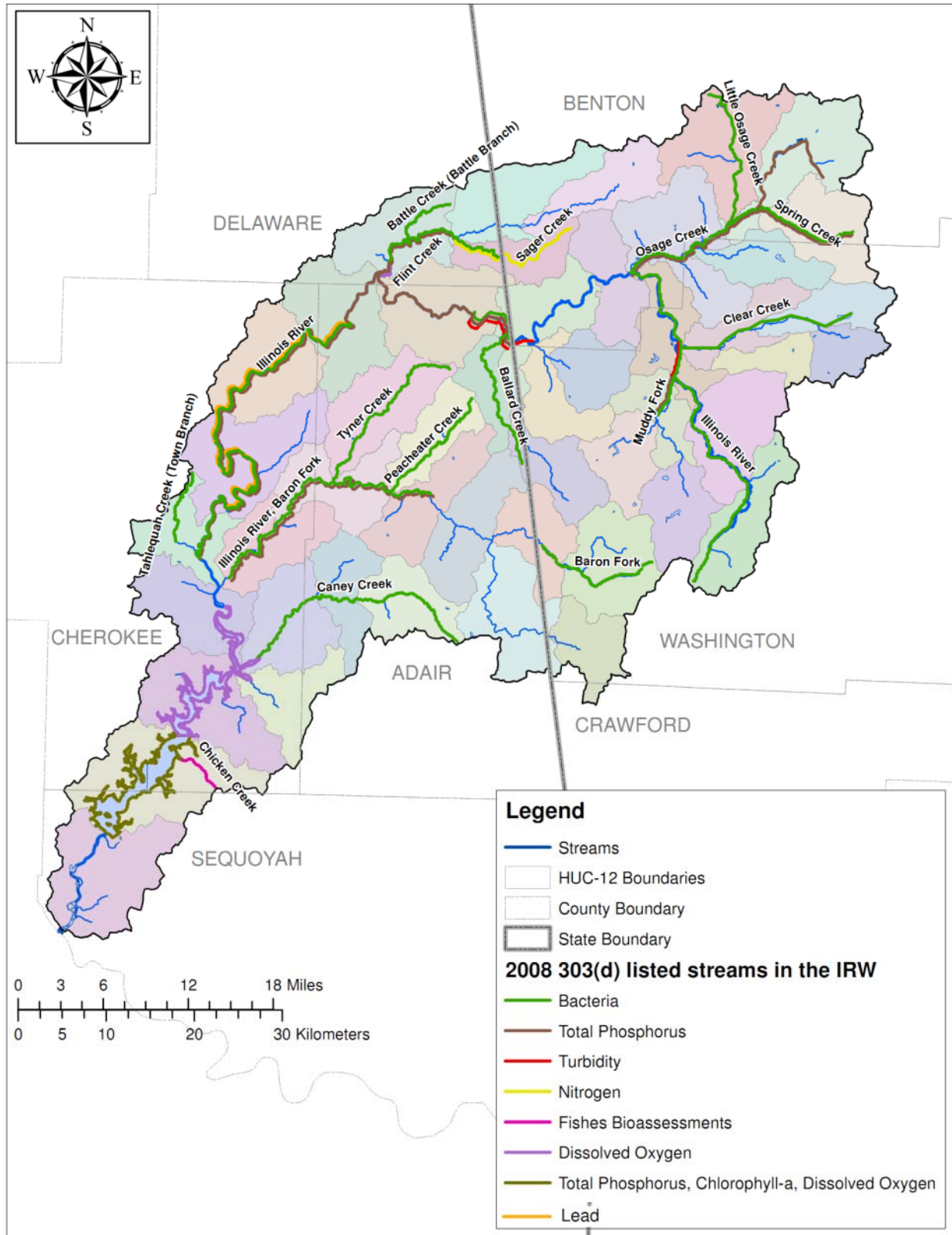


Figure 2-2. Section 303(d) 2008 Listed Impaired Segments within the Illinois River Watershed

In addition, individuals in each lead State agency – OK Department of Environmental Quality and AR Department of Environmental Quality – were identified and designated as the primary Points of Contact (POC) within each State.

The data gathering and accumulation efforts continued throughout 2010 and into 2011 and 2012, with a significant increase in the volume of data and reports arriving after each of numerous project coordination and stakeholder meetings. In addition, review comments on the Data Report were received from a number of stakeholders, providing additional contacts and direction for data gaps identified in the report. The Final Data Report was provided in September 2011 (AQUA TERRA Consultants, 2011).

As part of the study effort, a model selection task was performed and produced a Draft Model Selection Technical Memorandum dated November 22, 2010 (Donigian and Imhoff, 2010). This model comparison and selection process resulted in the recommendation that the US EPA HSPF (Hydrological Simulation Program – FORTRAN (Bicknell et al., 2005)) watershed model and the US EPA EFDC (Environmental Fluid Dynamics Code (Hamrick 1992, Tetra Tech 2007)) lake model be used in a linked application to provide the necessary modeling framework for performing this study. Following receipt of review comments, the Final Memo was submitted in September 2011 (Donigian and Imhoff, 2011).

This Final Report repeats some of the information from the Simulation Plan, by describing details of the model application, including model setup procedures and assumptions, calibration and validation time periods, constituents to be simulated, model scales and resolution, and model performance targets, so that readers have the background needed to understand and interpret the model results presented. Thus, the previous documents are viewed as companion and supporting information to this Final Report (Draft), and numerous references are made to information in those documents to avoid further duplication herein.

This Final Report presents model calibration and validation results for hydrology (flow), water temperature, sediment (TSS), and water quality. Water quality results were finalized as part of the AGCHEM model application funded under EPA PO G126-00097. Since the AGCHEM application to the pasture areas covers essentially all subbasins within the IRW, the water quality calibration could not be finalized until those loadings were completed and subsequent instream water quality calibration could be performed. Consequently, this report is a revision of an earlier Draft Final Report (January 2014) to include final water quality results.

2.2 Prior Modeling Studies and Management Plans

The initial step in any modeling and/or data assessment effort is to review prior modeling studies that may identify and compile relevant data on the IRW, since all modeling efforts essentially use the same general types and categories of watershed data. This section summarizes the major prior modeling efforts on the IRW and Lake Tenkiller, along with recent watershed management plans published for both sides of the state line.

Over the recent past, the IRW has been the focus of at least two previous modeling efforts by Donigian et al., (2009) and Storm et al., (2006 and 2009) which focused on the entire IRW. Under WA 2-11 of EPA Contract EP-C-06-029, AQUA TERRA and Eco Modeling completed an integrated-linked watershed and ecosystem modeling effort of the Illinois River and Tenkiller Reservoir, using the US EPA HSPF watershed model and AQUATOX ecosystem model (Donigian et al., 2009). This effort was directed to nutrient criteria development and was based on a relatively limited period of available data. The watershed simulation covered a 20-year

period from 1984 through 2003, but available water quality data (at that time) limited the TN calibration to the period 1990-1996 and the TP calibration from 1999-2003, with downstream stations primarily in OK. In this HSPF/AQUATOX effort, the AQUATOX calibrations were limited to 1992-1993 using Clean Lakes Program data from Oklahoma State University (1996).

The watershed modeling effort by Storm et al. (2006) used the USDA SWAT model to represent the IRW, including specific consideration of the poultry litter applied to pasture areas, and subsequent runoff to the river system. That effort used relatively simple instream algorithms to approximate the complex instream fate and transport interactions of dissolved and particulate phosphorus. SWAT model runs were performed for the period of 1980 through 2006, including both calibration and validation; water quality calibration for TP (and dissolved P) was performed for 1990 through 2006. The OK DEQ provided to EPA and AQUA TERRA the most recent modeling report submitted by Dr. Storm (Storm et al., 2009), along with the model input and data files, including GIS files used in this SWAT model setup, for possible use in this effort.

There have been at least two studies of Lake Tenkiller using the US EPA HSPF watershed model for loadings and the US EPA EFDC model for hydrodynamics and water quality simulation of the lake. These include an initial study performed in support of TMDL development by EPA Region 6 and OK DEQ (US EPA and OK DEQ, 2001), with Tetra Tech contracted to perform the modeling, and a subsequent revision and refinement of that effort performed by Dynamic Solutions LLC (2006) with AQUA TERRA Consultants (2005) subcontracted to upgrade the HSPF model of the IRW. Water quality calibrations were performed with available Clean Lakes Program data for 1992 and 1993, the same period as the subsequent AQUATOX application noted above.

Saraswat et al., (2010) and White (2009) have published modeling efforts using the SWAT model applied to the AR portion of the IRW. The Saraswat effort focused on the 12-Digit HUC (Hydrologic Unit Code) spatial level within the IRW, and addressed issues of impaired water quality for the Illinois River and selected tributaries within AR. White's study appears to be a refinement of the previous study by Storm et al (2009), with greater detail on the AR side. Both efforts were primarily directed to monthly comparisons of observed and simulated loads and concentrations, but include a comprehensive assessment of phosphorus sources and potential impacts of conservation efforts and management practices. More recently, Storm and Mittelstet (2014) applied the SWAT model to the entire IRW, including both the AR and OK portions as a current (and possibly ongoing) assessment of phosphorus sources and impacts of management practices.

All of these modeling studies were part of development efforts for watershed management planning for the IRW on both sides of the state line. Near the end of 2010, a draft watershed management plan (WMP) was published by the Illinois River Watershed Partnership (IRWP) Watershed Management Plan (IRWP, 2010), and subsequently finalized (FTN Assoc., 2012). This WMP presents a watershed management strategy with the goal to "improve water quality in the Illinois River and its tributaries so that all waters meet their designated uses both now and in the future." Although this document focuses on the AR portion of the IRW, a comparable effort was ongoing for the OK portion by the Oklahoma Conservation Commission (OCC), who recently finalized their draft plan (OCC, 2010). Both of these plans have been very helpful in our efforts to identify previous studies, available data, water quality issues of concern, and potential remediation and restoration alternatives within their respective portions of the IRW. For example, the watershed plans identified stream bank erosion as a source for both sediment and phosphorus, along with areas within the watershed where this is a concern and studies with relevant data.

2.3 Modeling Approach

In order to develop a scientifically sound modeling system to represent the entire IRW, including the land areas, the stream channels and Lake Tenkiller, models must be selected to represent each of these components. If the selected models are not already integrated within a single modeling system, the models must be linked to provide a comprehensive tool that addresses the watershed hydrology, generation of pollutants, fate/transport within the stream system, and ultimately dynamics and impacts on Lake Tenkiller.

As part of the study effort, a model selection task was performed and produced a Draft Model Selection Technical Memorandum dated November 22, 2010 (Donigian and Imhoff, 2010). This model comparison and selection process resulted in the recommendation that the US EPA HSPF (Hydrological Simulation Program – FORTRAN (Bicknell et al., 2005)) watershed model and the US EPA EFDC (Environmental Fluid Dynamics Code (Hamrick 1992, Tetra Tech 2007)) lake model be used in a linked application to provide the necessary modeling framework for performing this study. Following review and comments from project stakeholders, EPA subsequently agreed to the model recommendations and selected the HSPF watershed model and the EFDC lake model for this TMDL effort (M. Flores, personal communication, email to Project Stakeholders dated January 13, 2011). The Model Selection Memoranda was subsequently finalized in September 2011, following responses to review comments (Donigian and Imhoff, 2011).

HSPF was selected for the watershed because it provides a strong dynamic (i.e. short time step, hourly) hydrologic and hydraulic model simulation capability, and a moderately complex instream fate/transport simulation of sediment and phosphorus, both of which are linked to soil nutrient and runoff models; this combination provides a strong and established capability to relate upstream watershed point and nonpoint source contributions to downstream conditions and impacts at both the AR/OK state line and to Lake Tenkiller.

EFDC was selected because it allows a more mechanistic modeling of thermal stratification and is capable of a high level of spatial resolution in Lake Tenkiller, both of which are essential to support water quality compliance issues in OK, particularly time- and space-varying anoxic conditions. EFDC also provides moderately complex *biochemical* process representation that enables modeling and evaluation of chlorophyll *a* concentrations expressed as Carlson's Trophic State Index (TSI). Oklahoma statutes use TSI values to determine whether or not water bodies are threatened by nutrients.

For those readers not familiar with the HSPF and EFDC models, brief summaries are provided in both the Simulation Plan and the Model Selection Memo.

2.3.1 Model Application

HSPF represents a watershed as comprised of two primary components: land areas and stream channels or lakes and reservoirs. Each is represented by a different module(s) within HSPF: the land areas are represented with the PERLND and IMPLND modules for pervious and impervious areas, respectively, while the waterbodies, whether a free-flowing stream or a lake/reservoir, are represented with the RCHRES module.

Figure 2-3 shows the various components and capabilities of the PERLND module of HSPF. Each of the boxes in Figure 2-3 identifies a capability used by HSPF to model the corresponding process, or processes, that occur on each category of land; thus, the PWATER subroutine

models the water budget, SEDMNT models soil erosion and delivery to the stream, PSTEMP models soil temperatures, etc. For runoff loadings of water quality constituents, HSPF provides alternative methods, among which the user can select, to calculate loadings either with simple, empirical build-up and washoff algorithms used in the PQUAL subroutine, or the detailed mass balance formulations used within the group of subroutines within the dashed-line box marked as AGCHEM. The PQUAL (and IQUAL for impervious surfaces) are commonly used for urban land uses, as the buildup/washoff formulations have traditionally been applied for urban runoff quality models, and for applications that are primarily focused on impacts of urbanization and a general assessment of land use changes. For watersheds that are dominated by agriculture, and agricultural practices and impacts are key elements of the assessment, the AGCHEM module is often required as it allows a more process, and mass-balance based, evaluation of land management practices including nutrient application practices.

For the IRW application of HSPF, the AGCHEM subroutines are applied for the pasture lands that are the primary recipients of fertilizer, manure, and litter applications, and then the simpler PQUAL routines are applied for all other land uses. The data requirements and calibration effort associated with using the AGCHEM routines is much greater than for the PQUAL routine, but the end result is a capability to quantify the impacts of changes in nutrient application rates on the resulting runoff, and subsequently assess scenarios of alternative management practices and their impacts on water quality

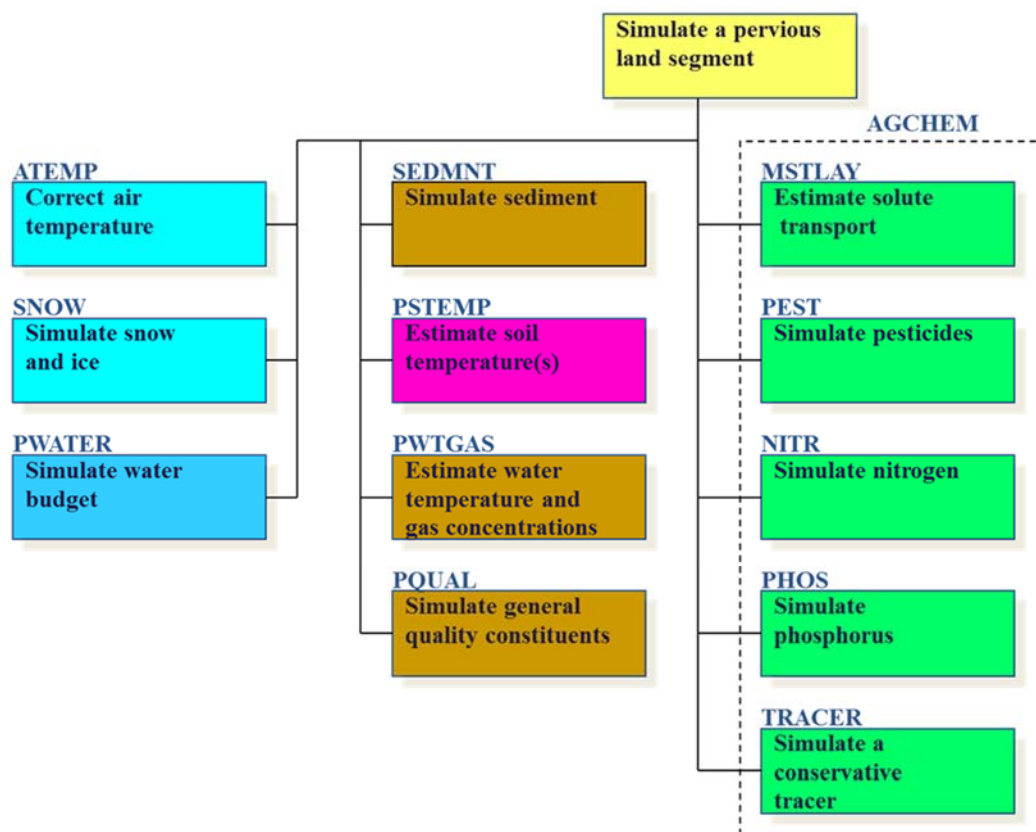


Figure 2-3 Pervious Land Simulation (PERLND) Module in HSPF

Figure 2-4 shows the phosphorus cycling capability and processes simulated with the AGCHEM routines; these process simulations are performed within each soil layer and then utilize the simulated flow and sediment fluxes to calculate the associated dissolved and sorbed

phosphorus contributions to the stream channel. For the channel system, Figure 2-5 shows phosphorus fate and transport processes that are modeled to calculate concentrations of the various forms of phosphorus and its subsequent downstream transport. Complete descriptions of the HSPF modules and algorithms are available in the HSPF User Manual (Bicknell et al., 2005) and the other references cited above.

The distinction between the HSPF simulation modules for the land area and channels within the IRW, noted above, is also important for the linkage interface between HSPF and EFDC. For Lake Tenkiller, the local drainage that enters the Lake directly without first entering a modeled stream channel will be provided by the PERLND and IMPLND modules for all relevant land use categories within the local area, whereas the HSPF RCHRES module will provide the loadings entering from all the major tributary streams including the Illinois River, downstream from its confluence with Baron Fork, and Caney Creek. In addition, a few other selected smaller tributaries are modeled with a channel reach either due to their size or due to being listed as impaired.

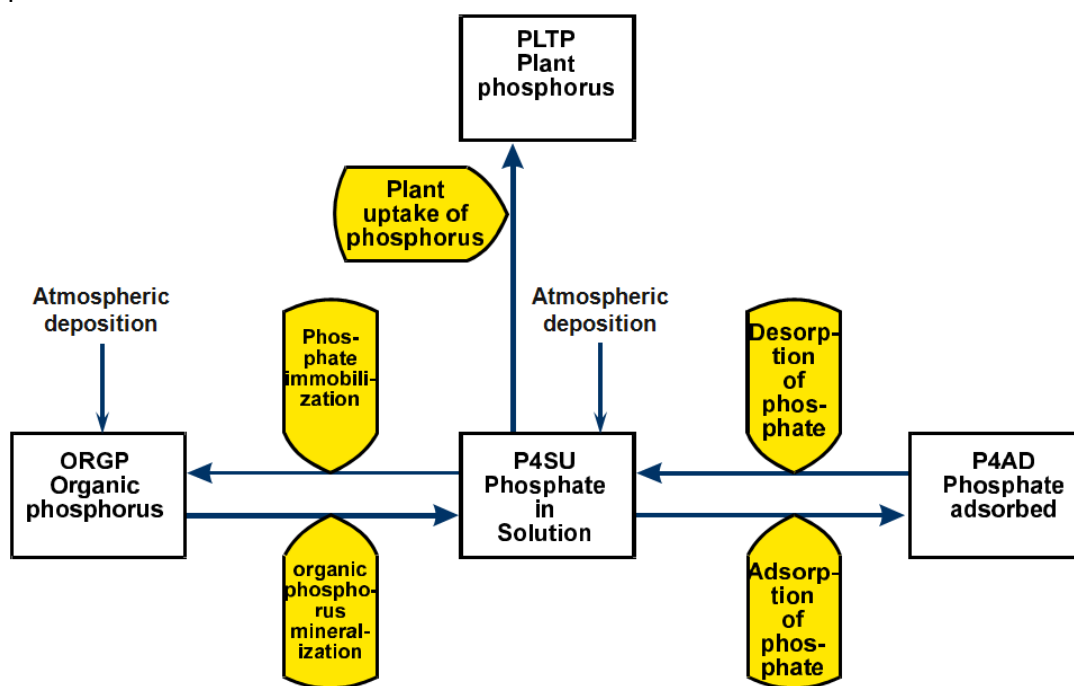


Figure 2-4 Soil Phosphorus Cycle in HSPF AGCHEM

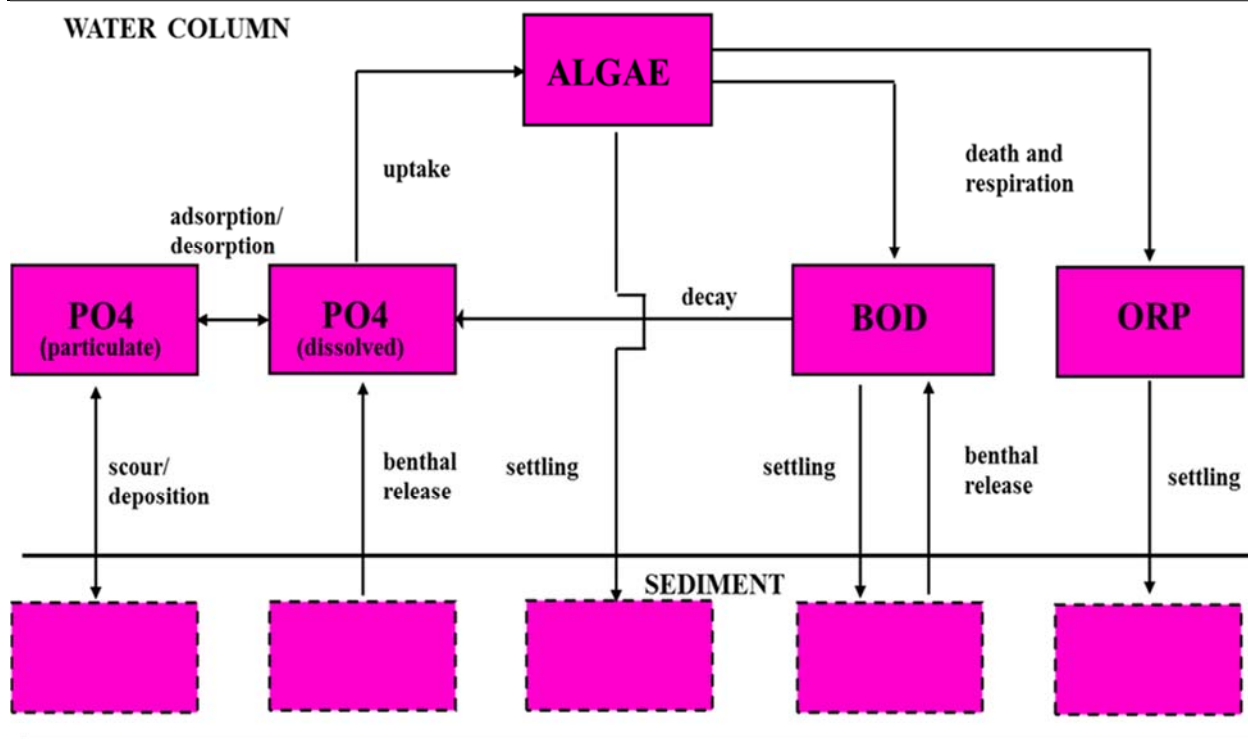


Figure 2-5 Instream Phosphorus Processes in HSPF RCHRES

As noted above, this report presents the Final Report for the IRW, including details of the model application effort for HSPF, model setup procedures and assumptions, calibration and validation time periods, constituents to be simulated, model scales and resolution, and model results for flow (hydrology) water temperature, sediment (TSS), and water quality. Following this introduction, Section 2 describes the time series data available to support watershed model setup and operation, and Section 3 describes the model segmentation characterization of the IRW. Section 4 follows with a description of the watershed model calibration and validation procedures, along with the model calibration and validation results for flow, water temperature, sediment, and water quality. Section 5 completes the report with a presentation of the TP and TN load analyses at the AR/OK Stateline and at Tahlequah, along with allocation of the loads at various points in the watershed to the sources of both TP and TN.

2.4 Time Series Data Availability for the IRW Model

Simulation of hydrology and water quality within the IRW requires the following types of time series data:

1. Precipitation
2. Potential evapotranspiration
3. Other meteorologic data (e.g. air temperature, wind, solar radiation, dewpoint, cloud cover)
4. Streamflow
5. Water quality observations
6. Other data (e.g. points sources, diversions, withdrawals, atmospheric deposition)

This section discusses the availability and selection of these time series data used in the watershed modeling. In addition, other data types, such as point sources, diversions, atmospheric deposition, etc. are also discussed as they help to define the inflow, outflow, and quality of water in the watershed, and their use in the modeling effort. Quality Assurance and Quality Control (QA/QC) procedures followed throughout the effort, in accordance with the Project QAPP, are discussed in Appendix F (separate document).

2.4.1 Precipitation

For hydrology calibration of the IRW, all watershed models require precipitation timeseries that are complete records (*i.e.*, no missing data) at a daily or shorter timestep, depending on the selected model, and with adequate spatial coverage and density across the model domain. Precipitation is the critical forcing function for all watershed models as it drives the hydrologic cycle and provides the foundation for transport mechanisms, both flow and sediment, that move pollutants from the land to the waterbody where their impacts are imposed.

For this study, long-term precipitation data have been obtained from the following primary sources:

- a. Prior modeling efforts with BASINS/HSPF and SWAT
- b. Online databases (e.g., NOAA, USGS) accessed through the BASINS download data capability
- c. OK Mesonet data network (provided by ODEQ)
- d. Daily NEXRAD data (provided for AR by Drs Matlock and Saraswat at the University of Arkansas (Personal communication, 1 January 2011))
- e. BASINS data extended through 12/31/09 (from an ongoing BASINS data project)

The last two precipitation data items (listed above) were obtained since the publication of the Draft Data Report in August 2010. Figure 2-6 shows the precipitation stations used in the IRW modeling effort. These stations are a subset of all the available stations, following a screening of the data to ensure recent and complete records from about 1980 through 2009. This time period provides a 30-year database to support longterm model runs for evaluation of watershed scenarios over a wide range of meteorologic conditions.

In addition to the actual precipitation gage stations, Figure 2-6 shows the 'pseudo' stations for the NEXRAD data (discussed below) for the AR portion of the watershed, and a Thiessen polygon analysis for the OK side of the watershed based on the locations of the NWS and OK Mesonet station locations. Thus a hybrid approach is used, *i.e.* Thiessen analysis of gage stations on the OK side, and NEXRAD data on the AR side, to make use of the best available precipitation data on both sides of the watershed. Both of these approaches are further discussed below.

The Data Report identified an area of relatively sparse coverage on the AR side of the watershed, about the center of the area where the Illinois River bends toward the west (see Figure 2-6). The study was fortunate to obtain daily precipitation data from Drs Matlock and Saraswat at the University of Arkansas for 28 'pseudo' gage sites (shown as the yellow circles in Figure 2-6), located at the approximate centroid of the HUC12 subwatersheds. This daily data set was developed as a combination of three NWS stations (Bentonville, Fayetteville, and

Gravette) for the period 1981-93, and NWS NEXRAD (Next Generation Weather Radar) data for the period 1994-2008.

The station data for the early period (1981-93) were adjusted to the subwatershed centroids using an inverse distance weighting method developed by Zhang and Srinivasan (2009). The extension of these data through 2008 was derived from the NEXRAD Stage III data for 82 4x4 km grid cells within the IRW. In the words of Dr. Saraswat ... "The data required several levels of post processing including unzipping, untarring, and transformation from the NEXRAD hydrological rainfall analysis project (HRAP) grid to a geographical coordinate system..... All NEXRAD grid points falling within a subwatershed were aggregated; an average value calculated; and assigned to pseudo weather stations at the centroid of the ... subwatersheds." (Saraswat, 2010, pg. 18). These data help to fill in the sparse coverage on the AR portion of the IRW; however, due to the manner in which NWS observed data was processed and then combined with NEXRAD data to cover the 1981-2008 period for the 'pseudo' stations, further analysis and evaluation of these data sets was needed as part of the model setup and calibration efforts.

It is critical that the precipitation data demonstrate consistency across the entire IRW in order to produce a scientifically sound hydrologic model. Initial calibration runs demonstrated selected storms with extreme precipitation and little or no response at downstream flow gages, mostly in the AR portion of the watershed which received NEXRAD rainfall data. We referred to these as 'phantom' events since there was no evidence that such extreme rainfall events even occurred. Further analysis identified 10-15 events with rainfall totals at some of the NEXRAD 'pseudo' stations with extreme daily amounts in the range of 10 to 22 inches in a single day. Analysis of the NWS and OK Mesonet stations showed no single day rainfall greater than 8 inches for the entire record from 1981 to 2009. Consequently, for these selected events we adjusted the rainfall for the outlier site based on rainfall amounts at neighboring sites. This does raise questions regarding the accuracy of the NEXRAD data for other non-extreme events.

On the OK side of the IRW, four Mesonet stations are combined with up to seven NWS stations, (denoted as BASINS in Figure 2-6, since they are available by download) to provide a reasonable coverage of the watershed within OK. An initial Thiessen analysis is shown in Figure 2-6 (green lines) for the OK side. A Thiessen analysis is a standard hydrologic technique to define the watershed area that will receive rainfall recorded at a specific gage; it involves constructing polygons around each gage using perpendicular bisecting lines drawn at the midpoint of connecting lines between each gage. In other words, the first step is to draw lines connecting the gages, then at the midpoint draw a perpendicular line, then erase the connecting lines; the result is a polygon around each gage. In Figure 2-6, there are nine gages for which the Thiessen analysis produced nine polygons; in the final model, this was reduced to seven polygons, as the Rose Tower gage was eliminated, and the Tahlequah and Webber Falls/Tenkiller polygons were combined into two polygons.

Table 2-1 tabulates all the available precipitation stations, and identifies the Mesonet sites and the specific stations used by Donigian et al (2009) in a prior HSPF/AQUATOX study. In addition to providing detailed 5-minute data, the Mesonet stations by their locations appear to fill in some areas with otherwise sparse gage coverage in the southern and western portions of the IRW. The Mesonet stations also provide extensive meteorologic data, discussed below.

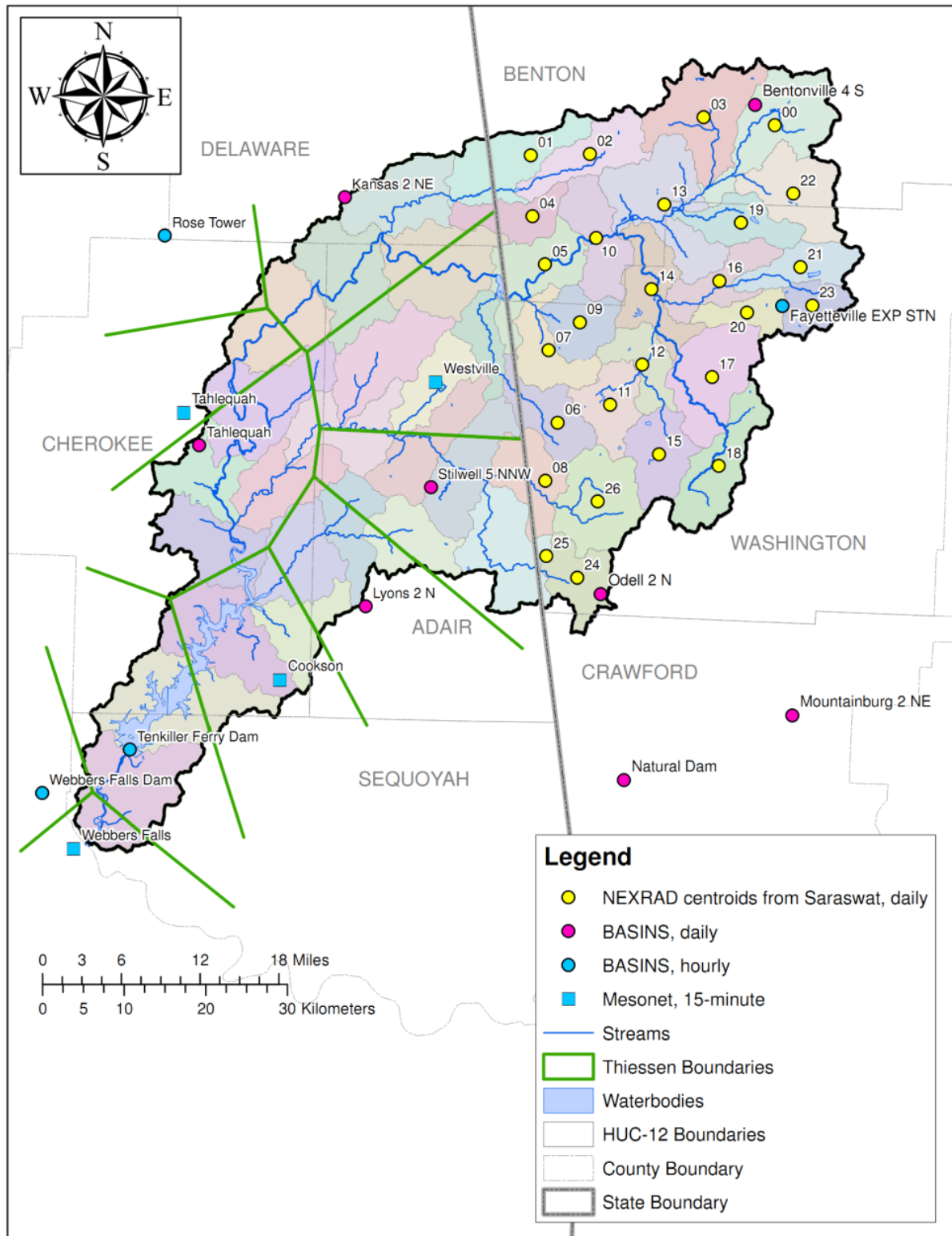


Figure 2-6 Precipitation Stations Selected for Use in the IRW Model

Table 2-1 Precipitation Stations in/near the Illinois River Watershed

Site Name	Site Number	Source	Start	End	Av Annual Precip (in)
Bentonville 4S	AR030586	BASINS daily	12/31/1947	2/28/2007	46.79
Cookson	31	Mesonet 5-min	1/1/1994	5/26/2010	50.50
Fayetteville Exp Sta*	AR032444	BASINS hourly	4/1/1966	3/31/2006	46.17
Fayetteville Exp Sta*	AR032444	BASINS daily	12/14/1926	8/31/2003	46.17
Mountainburg 2NE	AR035018	BASINS daily	8/31/1985	12/31/2009	50.61
Natural Dam	AR035160	BASINS daily	12/31/1962	12/31/2009	49.39
Odell 2 N*	AR035354	BASINS daily	12/31/1947	12/31/2009	51.56
Kansas 2 NE*	OK344672	BASINS daily	3/31/1959	12/31/2009	48.23
Lyons 2 N*	OK345437	BASINS daily	12/31/1947	9/30/2003	47.75
Rose Tower*	OK347739	BASINS hourly	1/1/1974	12/31/2003	46.79
Stilwell 5 NNW*	OK348506	BASINS daily	9/30/1948	4/30/2003	49.11
Tahlequah*	OK348677	BASINS daily	12/31/1947	12/31/2006	47.64
Tahlequah	92	Mesonet 5-min	1/1/1994	5/26/2010	47.50
Tenkiller Ferry Dam*	OK348769	BASINS hourly	4/1/1949	1/31/1999	46.33
Webbers Falls	103, 132	Mesonet 5-min	1/1/1994	5/26/2010	46.50
Westville	104	Mesonet 5-min	1/1/1994	5/26/2010	48.90

*This station was previously used in the HSPF/AQUATOX study by Donigian et al (2009).

Based on the previous HSPF and SWAT modeling efforts, and the precipitation stations identified in Table 2-1 and Figure 2-6, the coverage of daily stations appears sufficient for coverage of the IRW, especially with the addition of the Mesonet stations on the Oklahoma side and the NEXRAD data for the Arkansas side.

To simulate individual storm events, HSPF requires hourly data, and the conventional practice is to use nearby hourly stations to disaggregate daily precipitation values to hourly increments. The BASINS procedures for performing this disaggregation involve identifying up to 30 nearby stations, selecting the hourly station based on both geographic distance (proximity) and similarity of daily values, and then using the hourly distribution at that station to transform the daily station value into 24 hourly values. A tolerance threshold is used to only select stations whose daily total is within a certain percentage of the daily value for the station being disaggregated. Typical tolerance values are in the range of 30% to 90%, depending on the availability of nearby alternate gages.

For the IRW, there are seven hourly stations, which include four Mesonet and three BASINS stations derived from NWS data. The combined Mesonet and BASINS hourly sites provide a good distribution for the OK side of the watershed, whereas hourly distributions for the AR side were derived from the Fayetteville, AR and from the Westville Mesonet site in OK.

Another indicator of rainfall patterns on the watershed is an annual isohyetal map, as shown in Figure 2-7, which displays lines of equal annual rainfall (i.e., isohyets) across the watershed, based on the 1971-2000 period. The data for this map were obtained from the Oregon State University web site for their PRISM model (Parameter-elevation Regressions on Independent Slopes Model) (www.ocs.orst.edu/prism/). Gridded data, generated by this model based on point rainfall data, a DEM for topographic data, and other GIS data, was processed to produce the isohyets shown in the map. The information from Figure 2-7 can be helpful to assess the consistency of other rainfall estimates, and allow a determination of whether point rainfall data should be adjusted to better represent the area it is applied to. The pattern shows an overall

range of 47 to 52 inches per year, but the large majority of the watershed experiences an annual range of only 48 to 50 inches.

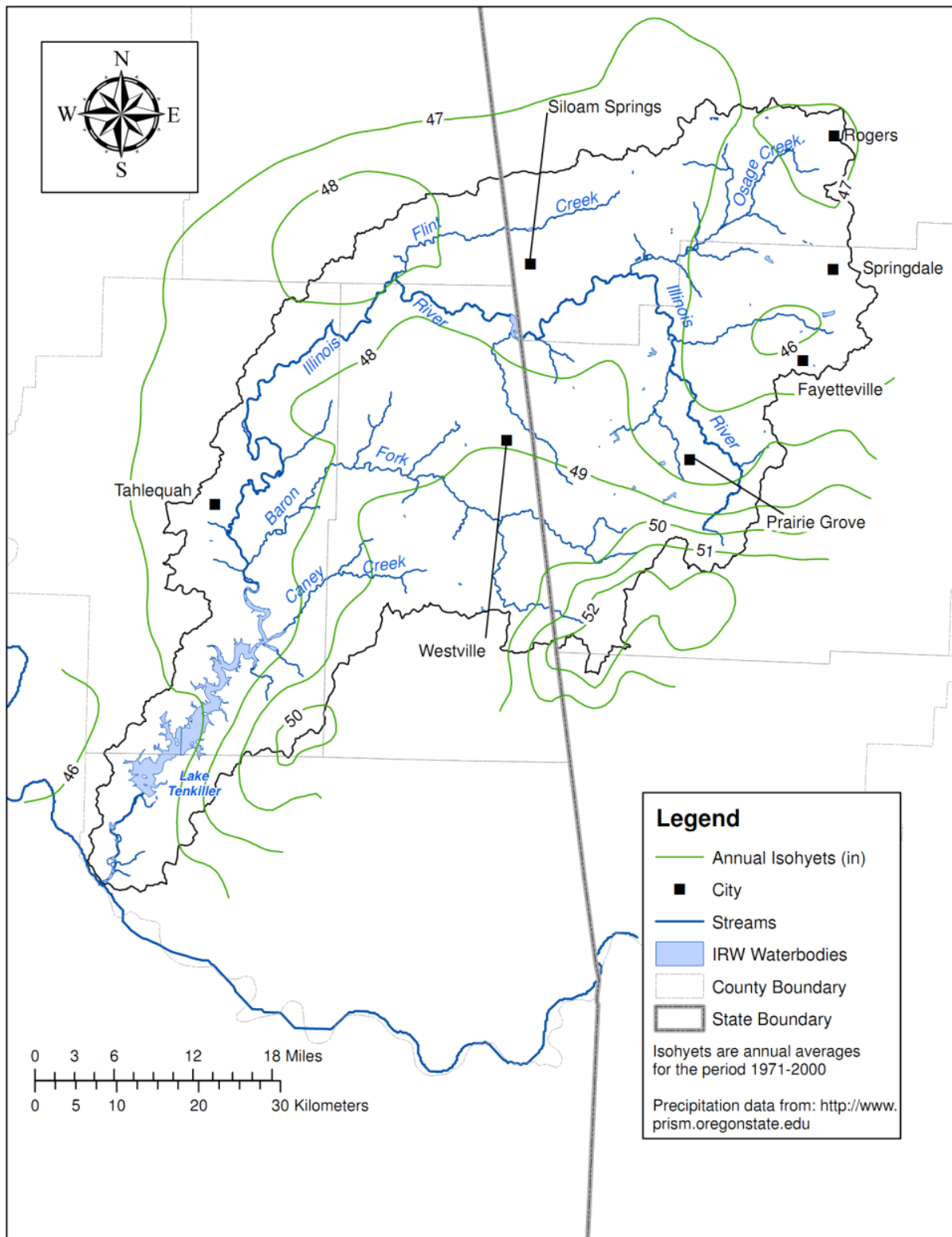


Figure 2-7 Annual Isohyetal Map of the IRW

2.4.2 Evapotranspiration and Other Meteorological Data

Watershed models require evaporation data as a companion to precipitation to drive the water balance calculations inherent in the hydrologic algorithms contained in these types of models. In addition, other meteorologic time series are also often required in temperate climates where snow accumulation and melt are a significant component of the hydrologic cycle and water balance. These same time series, such as air temperature, solar radiation, dewpoint temperature, wind, and cloud cover, are often required if soil and/or water temperatures are simulated. Water temperature is subsequently used to adjust rate coefficients in most water quality processes, and other time series are used in selected calculations, like solar radiation affecting algal growth.

Both HSPF and SWAT have similar weather data requirements (with some slight differences), so the availability of weather data is expected to be adequate for model application, considering both models have been previously applied to the IRW.

HSPF generally uses measured pan evaporation to derive an estimate of lake evaporation, which is considered equal to the potential evapotranspiration (PET) required by model algorithms, i.e., $PET = (\text{pan evap}) \times (\text{pan coefficient})$. The actual simulated evapotranspiration is computed by the program based on the model algorithms that calculate dynamic soil moisture conditions, ET parameters, and the input PET data. Where pan evaporation is not available, potential evapotranspiration (PET) can be computed from minimum and maximum daily air temperatures using the Hamon formula (Hamon, 1961). This method was used to compute the PET data included in the BASINS database of available meteorologic time series. The Hamon method generates daily potential evapotranspiration (inches) using air temperature (F or C), a monthly variable coefficient, the number of daylight hours (computed from latitude), and absolute humidity (computed from air temperature).

Recently, BASINS has been enhanced to also allow computation of PET according to the Penman-Monteith method, which involves a more detailed computation requiring air temperature, solar radiation, relative humidity, and wind speed, along with other coefficients. The method incorporated into BASINS was based on procedures included in the SWAT model. As part of the model setup effort, PET estimates from both the Hamon and Penman-Monteith methods were compared, along with available pan evaporation data, and the Hamon method was selected as most representative of IRW. Initial calibration runs confirmed that the Hamon values were more consistent with the expected PET for the IRW.

The primary source of evapotranspiration and the other meteorologic data was the BASINS database of thousands of stations across the US; the download capability within BASINS allows users to identify their selected watersheds and then access all the data available, including meteorologic data. Figure 2-6 shows the available meteorologic stations in and near the IRW available through BASINS; it also shows the nearest OK Mesonet stations. The OK Mesonet is an automated network of hundreds of remote meteorologic stations across OK instrumented to monitor and measure soil and meteorologic conditions. As shown in Figure 2-6, there are four Mesonet stations within or near the IRW.

Table 2-2 lists the meteorologic stations found through BASINS along with the Mesonet sites. The nearest pan evaporation station to the IRW is the Blue Mountain Dam NWS site approximately 30 miles southeast of the watershed. This site was used as the only evaporation data station for the HSPF/AQUATOX study; since PET generally demonstrates little spatial variability in this climate region, compared to rainfall variability, the distance was not considered excessive. Table 2-2 shows 14 sites with BASINS computed evapotranspiration data providing

sufficient coverage for the IRW. Also, the stations available for the remaining weather data, combined with the Mesonet sites, appear to provide a similar level of coverage. As noted above, the various estimates of PET – Blue Mountain Dam pan data, Hamon method, Penman-Monteith method – were compared and the Hamon method was determined the most representative method to use for this study. In addition, Thiessen analyses, analogous to what was discussed above for the precipitation stations, were performed to identify the watershed areas for which each meteorological time series were applied. Since PET and air temperature are the more critical of the meteorologic forcing data sets, and more data sites are available, we have a denser network for PET and air temperature than for wind, solar radiation, dewpoint temperature, or cloud cover. The periods of available historic data for these meteorologic data, starting mostly about 1995, is consistent with our expected calibration and validation periods (discussed in Section 4).

Table 2-2 Meteorological Stations in/near the Illinois River Watershed

Site Name	Site Number	Source	Data Type	Start	End
Bentonville (AWOS)	AR723444	BASINS	ATEM, PET, WIND, SOLR, DEWP, CLOUD	1/1/1995	12/31/2009
Bentonville 4S	AR030586	BASINS	ATEM, PET	1/1/1948	2/28/2007
Blue Mountain Dam*1		previous study	ATEM, PET	1/1/1984	9/30/2004
Cookson	31	Mesonet	ATEM, BP, SOLR, WIND	1/1/1994	present
Fayetteville Exp Sta	AR032444	BASINS	ATEM, PET	8/26/1921	8/31/2003
Fayetteville FAA Airport	AR032443	BASINS	WIND, SOLR, DEWP, CLOUD	12/31/1994	12/31/2009
Kansas 2 NE	OK344672	BASINS	ATEM, PET	4/1/1959	1/1/2010
Muskogee	OK346130	BASINS	ATEM, PET	1/1/1948	12/31/2009
Rogers	AR723449	BASINS	ATEM, PET, WIND, SOLR, DEWP, CLOUD	1/1/1995	12/31/2009
Siloam Springs (AWOS)	AR723443	BASINS	ATEM, PET, WIND, SOLR, DEWP, CLOUD	1/1/1995	12/31/2009
Stilwell 5 NNW	OK348506	BASINS	ATEM, PET	1/1/1960	4/30/2003
Tahlequah	OK348677	BASINS	ATEM, PET	1/1/1948	12/31/2006
Tahlequah	92	Mesonet	ATEM, BP, SOLR, WIND	1/1/1994	present
Webbers Falls	103, 132	Mesonet	ATEM, BP, SOLR, WIND	1/1/1994	present
Webbers Falls Dam	OK349450	BASINS	ATEM, PET, WIND, SOLR, DEWP, CLOUD	1/1/1970	12/31/2009

2.4.3 Streamflow

Flow data is needed for both calibration and validation of the watershed model to ensure it is reproducing the hydrologic behavior of the IRW, and providing proper boundary inflows into Lake Tenkiller, along with its transport of sediment and water quality constituents. The BASINS download capability provided the means to access all the USGS flow (and water quality) data

for sites in the watershed. Figure 2-8 shows the locations of the USGS gaging sites within the watershed, and Table 2-3 lists their names, USGS ID numbers, periods of record, tributary areas, and elevations for selected sites. In addition, the Arkansas Water Resources Center (B. Haggard, personal communication, 2011) provided supplemental data for Ballard Creek and Moore's Creek for model application.

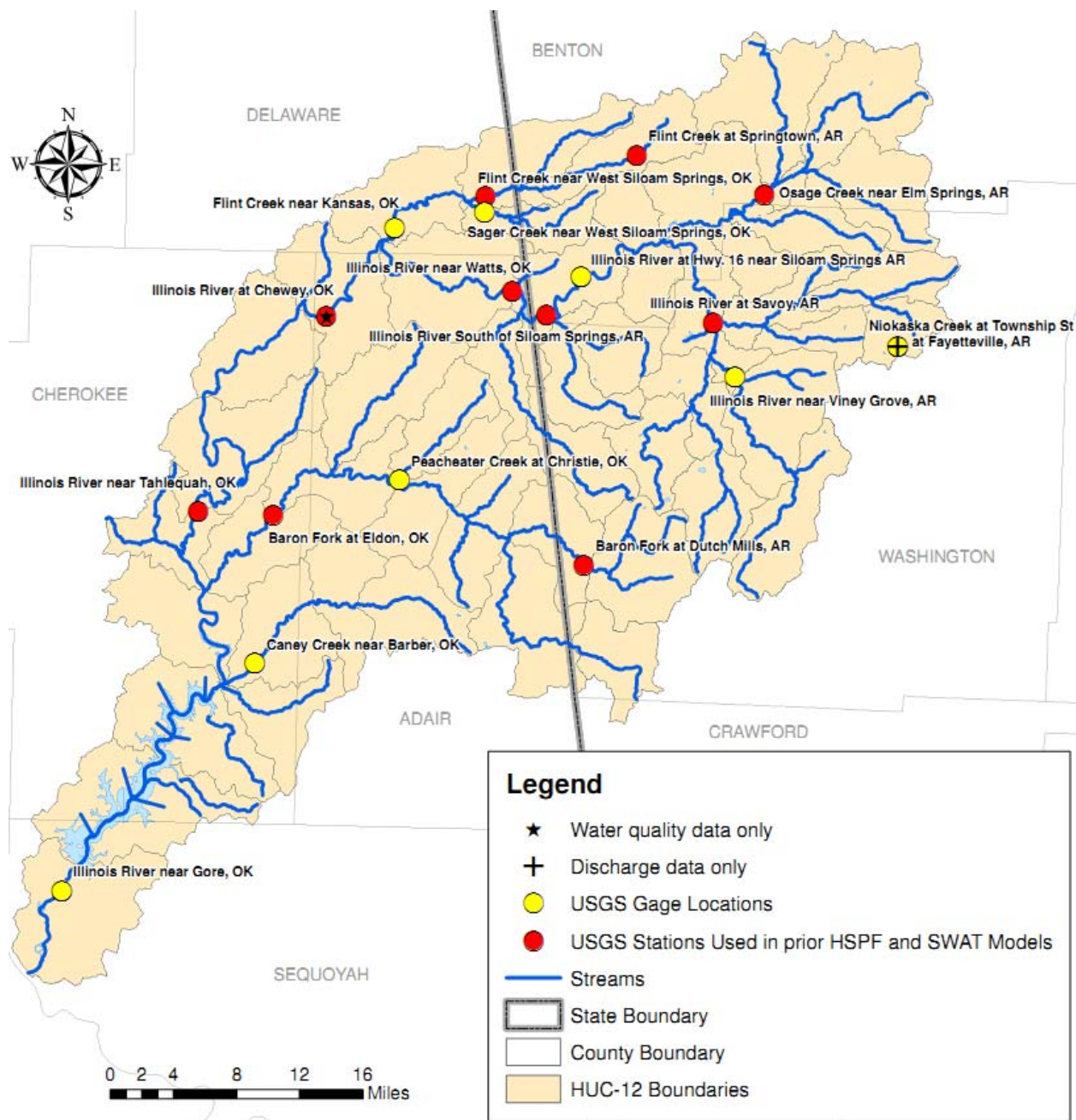


Figure 2-8 USGS Stream Gage Locations in the IRW

The USGS sites designated with red circles (●) are those used for model calibration and/or validation in the previous HSPF and SWAT model applications discussed above. However, no single model included ALL the gages shown in both states, until the current IRW modeling effort. Section 4 addresses the issue of selection of calibration/validation sites in both states,

and the corresponding time periods. There are adequate periods of record for three to five calibration sites within each state, as discussed in Section 4.

Table 2-3 USGS Stream Gages Containing Flow Data

Location	Gage Station	Period of Record		Tributary Area (mi ²)	Elevation (ft)
Illinois River near Tahlequah, OK	07196500	10/1/1935	present	959.0	664
Baron Fork at Eldon, OK	07197000	10/1/1948	present	307.0	701
Baron Fork at Dutch Mills, AR	07196900	4/1/1958	present	40.6	986
Illinois River near Watts, OK	07195500	10/1/1955	present	635.0	894
Illinois River near Viney Grove, AR	07194760	9/5/1985	10/16/1986	80.7	1051
Illinois River at Savoy, AR	07194800	6/21/1979	present	167.0	1019
Niokaska Creek at Township St at Fayetteville, AR	07194809	9/19/1996	present	1.2	1482
Osage Creek near Elm Springs, AR	07195000	10/1/1950	present	130.0	1052
Illinois River at Hwy. 16 near Siloam Springs AR	07195400	6/21/1979	2/7/2011	509.0	1170
Illinois River South of Siloam Springs, AR	07195430	7/14/1995	present	575.0	909
Flint Creek at Springtown, AR	07195800	7/1/1961	present	14.2	1173
Flint Creek near West Siloam Springs, OK	07195855	10/1/1979	present	59.8	954
Sager Creek near West Siloam Springs, OK	07195865	9/12/1996	present	18.9	960
Flint Creek near Kansas, OK	07196000	10/1/1955	present	110.0	855
Peacheater Creek at Christie, OK	07196973	9/1/1992	9/16/2004	25.0	802
Caney Creek near Barber, OK	07197360	10/1/1997	present	89.6	638
Illinois River near Gore, OK	07198000	3/25/1924	present	1626.0	468

2.4.4 Water Quality Data

Water quality data is used primarily for model calibration and validation, but also to help quantify source contributions and boundary conditions, such as for point sources, selected agricultural sources, and atmospheric deposition. A number of agencies contributed a wide variety water quality related data to be used in this effort. The Draft Data Report (AQUA TERRA Consultants, 2010b) listed the specific sites and constituents available, along with the period of record for each site and constituent, to support the model application.

The specific constituents modeled in this study include all constituents needed for modeling nutrients, with a specific focus on phosphorus species. The following list shows the conventional constituents that are modeled whenever nutrients are the purpose of a modeling effort:

1. Flow/discharge
2. TSS
3. water temperature
4. DO
5. BOD ultimate, or total BOD
6. NO₃/NO₂, combined
7. NH₃/NH₄
8. Total N
9. PO₄
10. Total P
11. Phytoplankton as Chl a
12. Benthic algae (as biomass)

These are the constituents that are modeled for the IRW; they include flow and TSS as the basic transport mechanisms for moving the nutrients, along with the environmental conditions (e.g. temperature) and other state variables (e.g. DO/BOD), that are involved in the aquatic fate, transport, and cycling of nutrients in aquatic systems.

For most modeling efforts of moderate to large watersheds, the USGS is the primary source of both flow and water quality data. In the IRW, the USGS works collaboratively with both the OK DEQ and AWRC for flow and water quality data collection efforts. Data was obtained from both the USGS NWIS system through direct downloading, along with files provided by the state agencies.

Table 2-4 lists the USGS flow gages that also include water quality data, along with their period of record. The Data Report provides a compilation of the number of data points and their period of record for each relevant water quality constituent, at each water quality observation gage.

As a supplement to the USGS water quality data, the AR Water Resources Center (AWRC) provided a series of annual reports, along with spreadsheets of loading calculations, for four sites within the AR portion of the IRW (B. Haggard, personal communication, 25 May 2010). Daily loads are available for the IR at Highway 59 (USGS gage #07195430), Ballard Creek, Moore's Creek, and Osage Creek, and for various time periods from 1999 to 2009 (see Nelson et al., 2006 as an example annual report).

Table 2-4 USGS Stream Gages with Water Quality Data in the IRW

Location	Gage Station #	Period of Record		Tributary Area (mi ²)	Elevation (ft)
Illinois River near Tahlequah, OK	07196500	8/23/1955	12/15/2009	959	664
Baron Fork at Eldon, OK	07197000	5/7/1958	12/14/2009	307	701
Baron Fork at Dutch Mills, AR	07196900	3/17/1959	8/25/2009	40.6	986
Illinois River near Watts, OK	07195500	9/12/1955	10/26/2009	635	893
Illinois River near Viney Grove, AR	07194760	9/6/1978	7/19/2007	80.7	1051
Illinois River at Savoy, AR	07194800	9/11/1968	8/25/2009	167	1019
Osage Creek near Elm Springs, AR	07195000	9/10/1951	8/25/2009	130	1052
Illinois River at Hwy. 16 near Siloam Springs AR	07195400	9/8/1978	9/20/1994	509	1170
Illinois River South of Siloam Springs, AR	07195430	10/3/1972	8/25/2009	575	909
Flint Creek at Springtown, AR	07195800	10/15/1975	7/1/1996	14.2	1173
Flint Creek near West Siloam Springs, OK	07195855	7/11/1979	8/28/1996	59.8	954
Sager Creek near West Siloam Springs, OK	07195865	5/24/1991	10/21/2009	18.9	960
Flint Creek near Kansas, OK	07196000	9/7/1955	10/26/2009	110	855
Peacheater Creek at Christie, OK	07196973	8/6/1991	5/16/1995	25.0	802
Caney Creek near Barber, OK	07197360	8/25/1997	10/27/2009	89.6	638
Illinois River at Chewey, OK	07196090	7/16/1996	10/27/2009	825	801
Illinois River near Gore, OK	07198000	4/12/1940	8/16/1995	1626	468

2.4.5 Point Sources

Data on point sources discharges have been compiled from a number of different sources of information, including data provided by EPA, State representatives, and the dischargers. Prior modeling efforts focused on the major dischargers, and ignored the contributions from the

numerous minor and smaller ones. A similar approach is followed in this effort as the detailed time series data needed is not available for the minor dischargers.

Point source loads have been developed for 13 primary facilities (Table 2-5) that discharge to the Illinois River and its tributaries. The primary basis for developing the point source loads were (1) internal monitoring data provided by individual facilities (Springdale, Fayetteville, Lincoln, Rogers, Siloam Springs, Tahlequah, Stilwell) and (2) Discharge Monitoring Report (DMR) data provided by Oklahoma DEQ (Andrew Fang) and Arkansas DEQ. Bicknell and Donigian (2012) document the data, procedures, and assumptions that were used to develop the loads.

Table 2-5 Point Sources in Illinois River Watershed

NPDES #	Facility	Discharge Location (Tributary)	Typical Flow (MGD)
AR0022098	Prairie Grove, City of	Muddy Fork	0.3
AR0020010	Fayetteville - Paul Noland WWTP	Mud Ck	4.5
AR0050288	Fayetteville - Westside WWTP	Goose Ck	5.8
AR0033910	USDA FS - Lake Wedington Rec. Area	Tributary to Illinois R	0.0013
AR0035246	Lincoln, City of	Bush Ck/Baron Fork	0.45
AR0022063	Springdale WWTP, City of	Spring Ck/Osage Ck	12
AR0043397	Rogers, City of	Osage Ck	6.5
AR0020184	Gentry, City of	SWEPCO Res/L Flint Ck	0.45
AR0020273	Siloam Springs, City of	Sager Ck/Flint Ck	3
AR0037842	SWEPCO Flint Ck Power Plant	SWEPCO Res/Flint Ck	5/400 *
OK0026964	Tahlequah Public Works Authority	Tahlequah Ck	2.7
OK0028126	Westville Utility Authority	Shell Branch/Baron Fork	0.2
OK0030341	Stilwell Area Development Authority	Caney Ck	0.85

* - Once-through cooling water outflow (400 MGD) and wastewater outflow (5 MGD)

The quantities that were generated are listed below. They include flow, heat, and the water quality-related constituents that are being modeled by HSPF.

<u>Quantity</u>	<u>Units</u>
Flow	MG (input as ac-ft)
Heat	BTU
TSS	lbs (input as tons)
DO	lbs O
NO3/NO2	lbs N
NH3/NH4	lbs N
Organic N	lbs N
PO4	lbs P
Organic P	lbs P
CBOD _u	lbs O
Organic C	lbs C

The data availability and frequency are summarized in Table 2-6, and the average daily values (in units of lbs/day) of all quantities for the full 1990-2009 period are shown in Table 2-7; spreadsheets of the daily and monthly values were provided to EPA and stakeholders November 2012. Total TN, TP, and CBOD_u loads for 2009 are shown in Table 2-8. Although these tables show summaries of average daily and annual loads, the model actually receives the daily loads as a timeseries for the entire period of 1990-2009; these values are included with the daily load spreadsheet provided to EPA and stakeholders.

Table 2-6 Data Availability and Measurement Frequency of Point Sources

NPDES #	Facility	Monthly DMR Data	Weekly/Daily Data
AR0022098	Prairie Grove, City of	1990/1 - 2009/12	n/a
AR0020010	Fayetteville - Paul Noland WWTP	1990/1 - 2008/6	1990/1 - 2008/6
AR0050288	Fayetteville - Westside WWTP	n/a	2008/6 - 2009/12
AR0033910	USDA FS - Lake Wedington Rec. Area	1990/1 - 2009/12	n/a
AR0035246	Lincoln, City of	1990/1 - 2009/12	2001/1 - 2009/12
AR0022063	Springdale WWTP, City of	1990/1 - 2009/12	1991/10 - 2009/12
AR0043397	Rogers, City of	1990/1 - 2009/12	1990/1 - 2009/12
AR0020184	Gentry, City of	1990/1 - 2009/12	n/a
AR0020273	Siloam Springs, City of	1990/1 - 2009/12	2002 - 2009/12
AR0037842	SWEPCO Flint Ck Power Plant	1990/1 - 2009/12	n/a
OK0026964	Tahlequah Public Works Authority	1990/1 - 2009/12	2001/1 - 2009/12
OK0028126	Westville Utility Authority	1990/1 - 2009/12	n/a
OK0030341	Stilwell Area Development Authority	1990/1 - 2009/12	2006/1 - 2009/12

Table 2-7 Average Daily Point Source Loads for 1990-2009

Facility	Flow mgd	Heat btu/day	DO lb/day	TSS lb/day	CBOD ₅ lb/day	CBOD _U lb/day	Ref Org C lb/day	TP lb/day	PO4 lb/day	Org P lb/day	TN lb/day	NH3 lb/day	NO3 lb/day	OrgN lb/day
Prairie Grove	0.27	7.5E+7	19	19	9.0	25.5	2.4	10	7.7	2.6	17.4	1.9	11	4.4
Fayetteville Noland (1990-2008/6)	3.9	1.1E+9	311	82	65	184	17	14	10	3.5	242	12	164	65
Fayetteville Westside (2008/6-2009)	5.8	1.7E+9	441	43	93	265	71	21	16	5.3	349	7.6	244	98
USDA-Lake Wedington	.0013	3.7E+5	0.095	0.063	0.050	0.14	0.014	.0046	.0035	.0012	.0864	0.011	0.054	0.022
Lincoln	0.46	1.1E+8	34	15	24	68	6.4	6.0	4.5	1.5	24.3	3.2	13	7.7
Springdale	11	3.2E+9	872	352	199	566	53	304	270	54	558	41	369	149
Rogers	5.5	1.5E+9	450	218	123	348	33	67	17	50	262	10	202	54
Gentry	0.47	1.3E+8	35	44	41	118	11	15	11	3.7	32	4	20	7.9
Siloam Springs	2.7	8.1E+8	187	203	73	207	19	76	57	19	290	13	231	46
SWEPCO	359	5.7E+11	2.7E+4	575	33*	94*	8.8*	15*	11*	3.7*	32*	4*	20*	7.9*
Tahlequah	2.7	7.7E+8	176	53	85	241	23	21	16	5.3	176	20	111	45
Westville	0.18	4.9E+7	13	38	18	50	4.7	3.1	2.3	0.8	13.2	2.8	7.5	3.0
Stilwell	0.71	2.0E+8	44	50	58	164	15	6.0	4.5	1.5	52.5	11.3	29	12

* SWEPCO nutrient loads based on Gentry data

Table 2-8 Annual Loads (lbs/year) of TP, TN, and CBOD_u for 2009

NPDES #	Facility	TP	TN	CBOD _u
AR0022098	Prairie Grove	3,400	7,100	5,310
AR0020010	Fayetteville - Noland (2007)	3,980	125,000	126,000
AR0050288	Fayetteville - Westside	7,910	139,000	106,000
AR0033910	USDA FS - Lake Wedington	4.54	92.5	192
AR0035246	Lincoln	1,540	11,500	6,020
AR0022063	Springdale	16,900	248,000	169,000
AR0043397	Rogers	5,380	192,000	75,400
AR0020184	Gentry	4,920	13,600	19,000
AR0020273	Siloam Springs	12,600	63,000	42,000
AR0037842	SWEPCO	*4,920	*13,600	*19,000
OK0026964	Tahlequah	3,910	75,000	55,400
OK0028126	Westville	489	6,910	7,910
OK0030341	Stilwell	1,920	26,100	57,500

* SWEPCO loads based on Gentry data

The primary data available for many of the facilities was derived from DMR sources, and consists of monthly averages of flow and the following constituents: CBOD₅, TSS, DO, NH₃, and TP. Eight of the facilities provided daily/weekly data for selected time periods, and those data were used when available. While it is likely that most flow rates are based on frequent (daily) measurements, the other constituent monthly averages were apparently obtained from one to two measurements per month. For five of the facilities, this type of monthly data are the only data available (facilities with "n/a" in Table 2-6); four of the facilities (Fayetteville-Noland, Fayetteville-Westside, Rogers, and Springdale) have essentially a complete period (1990/1/1 - 2009/12/31) of daily/weekly data; and the remaining four facilities (Lincoln, Siloam Springs, Tahlequah, and Stilwell) utilize monthly data for the earlier years, and are supplemented by more frequent measurements (typically weekly) for the later years. In general, where monthly and weekly (or daily) data overlapped in time, the more frequent measurements were used to develop the final loads.

Missing Data

The general methodology for filling missing values was interpolation or averaging. Very little of the monthly data were missing. However, the daily/weekly data were filled in to generate daily time series by interpolation and averaging. Also, at the facilities where the monthly data did not extend over the entire period of point source data development (1990/1/1 - 2009/12/31), the existing data were extended back in time using selected averages of the existing data for that facility. For example, at the Lincoln facility, many of the constituents were not available prior to 2001, and were therefore estimated from the available data from 2001 through 2009. The procedures applied for filling in missing data at each facility are documented in Bicknell and Donigian (2012).

2.4.6 Atmospheric Deposition

Atmospheric deposition of nutrients is commonly included in watershed modeling efforts that focus on nutrient issues, like the current study. Atmospheric deposition data were obtained

online through the National Atmospheric Deposition Program (NADP) (<http://nadp.sws.uiuc.edu/>) and the Clean Air Status and Trends Network (CASTNet) (<http://java.epa.gov/castnet/>). Sites in the NADP precipitation chemistry network began operations in 1978 with the goal of providing data on the amounts, trends, and geographic distributions of acids, nutrients, and base cations in precipitation. The network grew rapidly in the early 1980s funded by the National Acid Precipitation Assessment Program (NAPAP), established in 1981 to improve understanding of the causes and effects of acidic precipitation. Reflecting the federal NAPAP role in the NADP, the network name was changed to NADP National Trends Network (NTN). The NTN network currently has 250 sites.

CASTNet began collecting measurements in 1991 with the incorporation of 50 sites from the National Dry Deposition Network, which had been in operation since 1987. CASTNET provides long-term monitoring of air quality in rural areas to determine trends in regional atmospheric nitrogen, sulfur, and ozone concentrations and deposition fluxes of sulfur and nitrogen pollutants in order to evaluate the effectiveness of national and regional air pollution control programs. CASTNET operates more than 80 regional sites throughout the contiguous United States, Alaska, and Canada. Sites are located in areas where urban influences are minimal. The primary sponsors of CASTNET are the Environmental Protection Agency and the National Park Service.

The data available from NADP/NTN are wet deposition of NH_4 and NO_3 in the form of precipitation-weighted concentrations (mg-N/L) on a monthly basis from 1980-2009. There are two active stations near the watershed: one is in Fayetteville, AR, and the other is in McClain County, OK. Two inactive stations in Oklahoma at Lake Eucha and Stilwell have data only for a limited period (2000-2003). There are no phosphorus data available.

The CASTNet data available for the watershed are weekly, quarterly, seasonal, and annual dry deposition fluxes of NH_4 , HNO_3 , and NO_3^- for 10/88-12/09. The stations near the watershed are Cherokee Nation in Adair County, OK and Caddo Valley in Clark County, AR. The Caddo Valley station is near an NADP station, but not the Fayetteville station.

There are very little data available to estimate phosphorus deposition. Most of the literature concludes that atmospheric deposition is a small contributor to the total P budget. Based on the available data and literature, we assume that atmospheric deposition of phosphorus is negligible compared to other sources.

2.5 Segmentation and Characterization of the IRW

Whenever any watershed model is set up and applied to a watershed, the entire study area must undergo a process sometimes referred to as 'segmentation'. The purpose of watershed segmentation is to divide the study area into individual land and channel segments, or pieces, that are assumed to demonstrate relatively homogenous hydrologic/hydraulic and water quality behavior. This segmentation provides the basis for assigning similar or identical input and/or parameter values or functions to where they can be applied logically to all portions of a land area or channel length contained within a model segment. Since most watershed models differentiate between land and channel portions of a watershed, and each is modeled separately, each undergoes a segmentation process to produce separate land and channel segments that are linked together to represent the entire watershed area.

Watershed segmentation is based on individual spatial characteristics of the watershed, including topography, drainage patterns, land uses and distribution, meteorologic variability, and

soils conditions. The process is essentially an iterative procedure of overlaying these data layers and identifying portions of the watershed with similar groupings of these characteristics. The results of the land segmentation process are a series of model segments, sometimes call hydrologic response units (HRUs) that demonstrate similar hydrologic and water quality behavior. Over the past few decades, geographic information systems (GIS), and associated software tools, have become critical tools for watershed segmentation. Combined with advances in computing power, they have allowed the development of automated capabilities to efficiently perform the data-overlay process.

GIS data, or coverages, are used to spatially quantify the characteristics of the watershed landscape to develop the model input that informs the model as to how the watershed characteristics change across the study area. GIS data used in the segmentation process that affect the hydrologic and water quality response of a watershed are: topography and elevation, hydrography/drainage patterns, land use and land cover, soils information, and other various types of spatial data.

The primary sources for GIS data obtained for the IRW were those accessed through the use of the BASINS data download capability, from the SWAT 2009 modeling files provided by OK DEQ, and additional coverages provided by stakeholders in response to the Federal Register data request. Through the BASINS interface a wide range of GIS data layers were downloaded and displayed. BASINS accesses GIS data from a variety of sources such as The National Land Cover Data (NLCD), National Hydrography Dataset (NHD), and the USGS seamless data server (<http://seamless.usgs.gov/>). Other sources include the earlier HSPF modeling efforts, Geospatial One-Stop (<http://gos2.geodata.gov/wps/portal/gos>), and contacts with the OK DEQ and AR DEQ. Geospatial One-Stop is an e-government initiative sponsored by the Federal Office of Management and Budget (OMB) to make it easier, faster, and less expensive for all levels of government and the public to access geospatial information

The Data Report provided a catalog of the various GIS data coverages that were downloaded and are currently available for this study of the IRW. Below we discuss the major categories of GIS data used in model segmentation, display and discuss the major categories, and describe the model segmentation of the IRW.

2.5.1 Topography and Elevation

GIS layers of topography are important in setting up HSPF because they provide elevation and slope values for the project area, and are needed for characterizing the landscape and the land areas of the watershed. These elevation values are used to delineate subbasins, determine average elevations for each model subbasin, and/or to compute average slopes for model subbasins and land uses within a subbasin. A very detailed topographic layer (e.g. LIDAR data) can also be useful for determining stream cross-sections used to define the hydraulic characteristics of the streams.

The National Elevation Dataset (NED) available through BASINS 4.0 is a 30-meter Digital Elevation Model (DEM) grid, with vertical units in centimeters. A 10-meter resolution DEM was also available and was obtained from the USGS seamless site; this layer has been converted to feet and is shown in Figure 2-9. It was used in the lower slope areas for better spatial resolution, as needed.

2.5.2 Hydrography/Drainage Patterns

Hydrography includes GIS layers of stream segments, at various levels of detail, as well as subbasins or drainage boundaries, and waterbodies. Several layers of hydrographic data are available for use in the Illinois River Watershed modeling effort. A set of coverages that is commonly used in watershed modeling is the NHDPlus dataset. NHDPlus is an integrated suite of geospatial data sets that incorporates many of the best features of the National Hydrography Dataset (NHD), the National Elevation Dataset (NED), the National Land Cover Dataset (NLCD), and the Watershed Boundary Dataset (WBD).

The NHDPlus dataset includes elevation, flow accumulation, and flow direction grids. These grids can be used to automate the subbasin delineation process for reaches with high topographic variation, e.g., mountainous regions of the watershed. The grids have undergone significant processing to ensure that drainage patterns are consistent with the 1:100,000 scale NHD and WBD using the “New England Method” (Dewald, 2006). These grids are the most hydrologically accurate 30 meter DEMs available to the water resources community. Figure 2-10 shows the available stream hydrography coverage with the 1st order streams shown in light blue, and the 2nd through 6th order streams in dark blue. The 12-Digit hydrologic Unit Code (HUC) boundaries are also shown in Figure 2-10, which was the starting point for the spatial resolution for the watershed model.

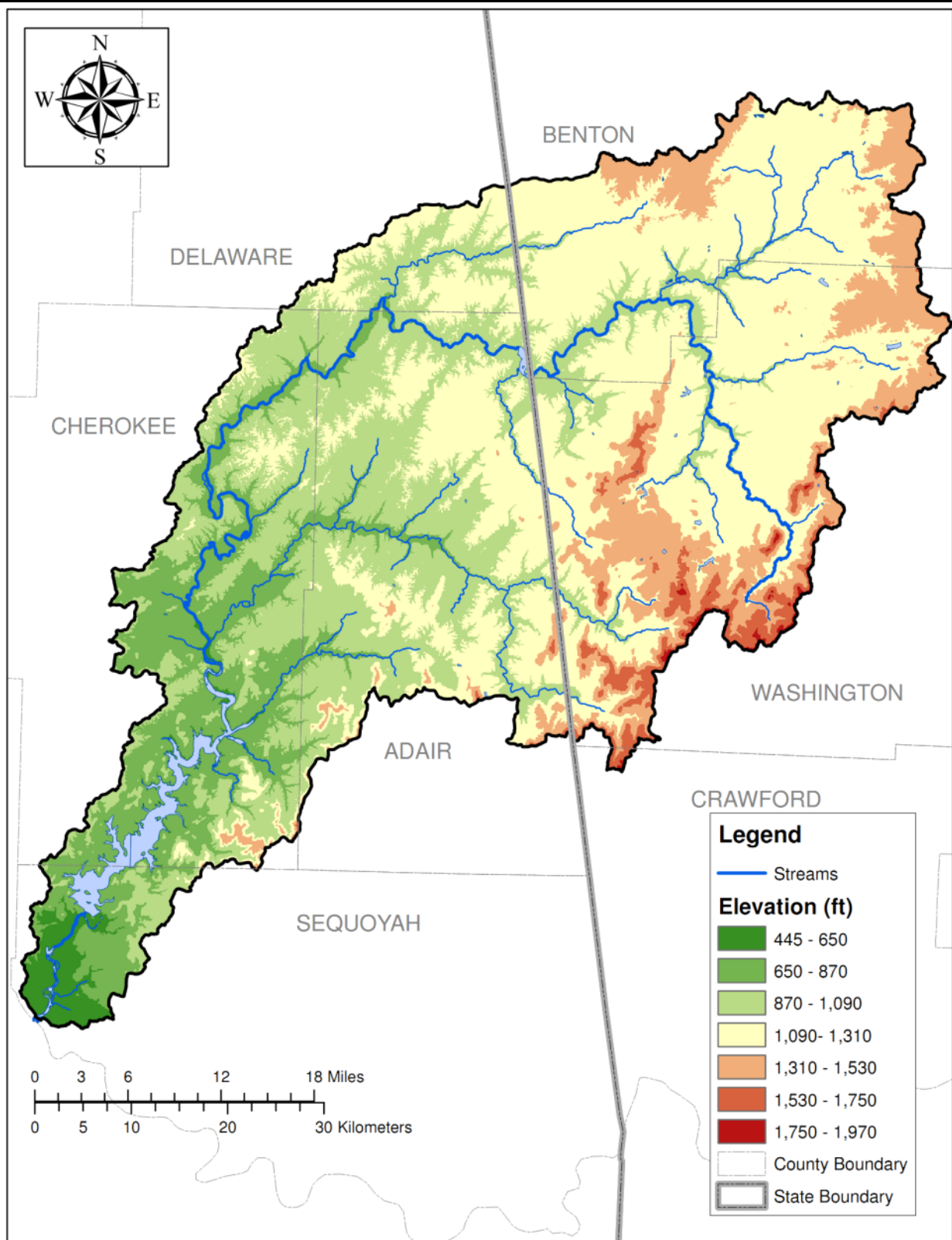


Figure 2-9 Derived from a 10-Meter DEM from the USGS Seamless Server

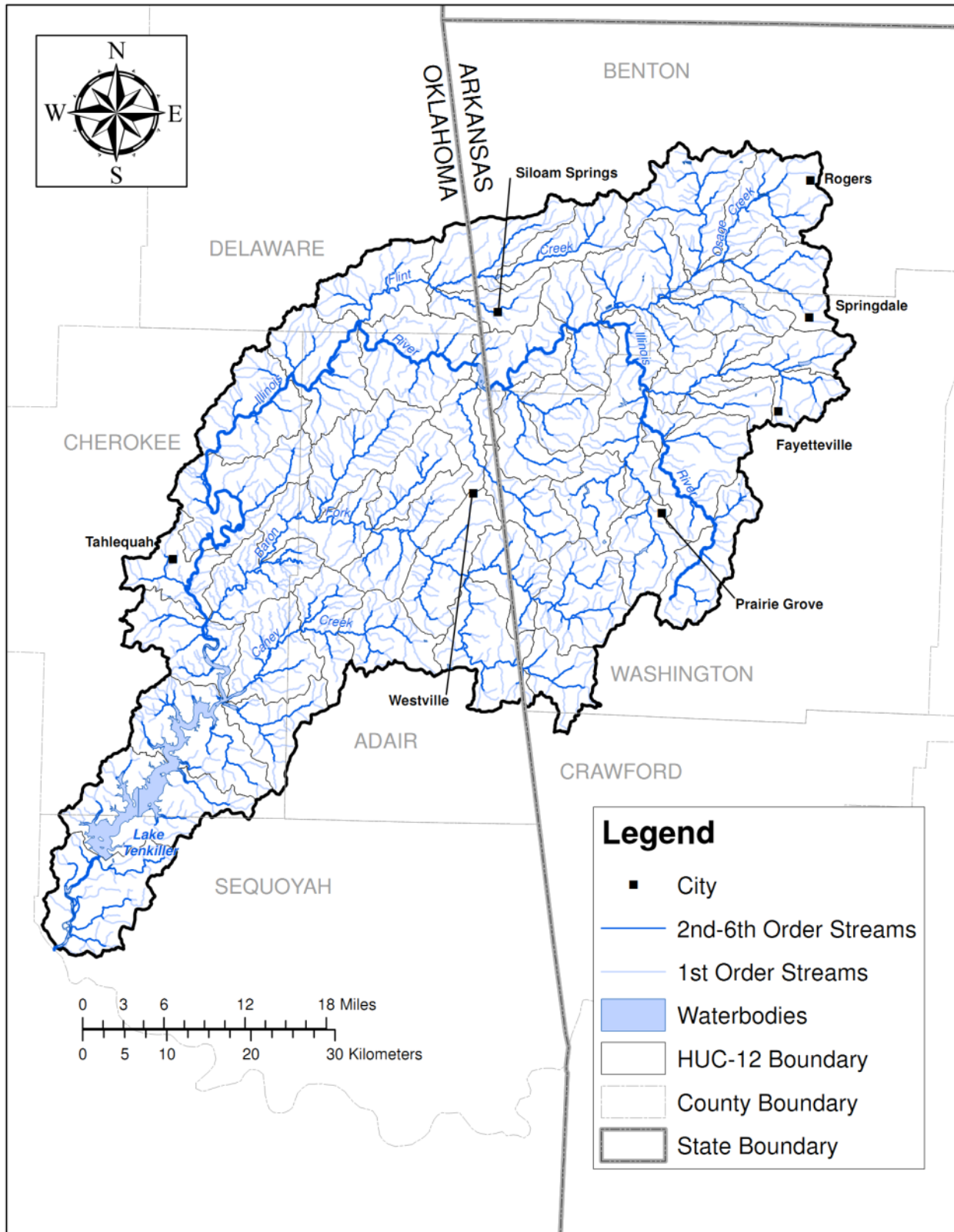


Figure 2-10 Stream Hydrography Coverage for the IRW from NHDPlus

2.5.3 Land Use

Land use, or land cover, data is a critical factor in modeling complex multi-land use watersheds as it provides the detailed characterization of the potentially primary source of pollutants entering the streams and rivers as nonpoint source contributions. In addition the land use distribution has a major determining impact on the hydrologic response of the watershed.

As discussed in the Data Report, a number of sources of land use data were investigated but, at that time, no single, consistent coverage, spanning both States, existed for the entire IRW other than the 2001 NLCD. Fortunately, in early 2011, the 2006 NLCD data was released and provided the consistent recent coverage needed covering both States, and applicable to a relatively recent time period with significant available water quality data. Table 2-9 lists the land use categories and distributions for the 1992, 2002, and 2006 NLCD, while Table 2-10 shows the correspondence between the NLCD categories and the model categories. **Error! Reference source not found.** shows and compares the spatial distribution of the NLCD categories for the 2001 and 2006 data layers.

Both Table 2-9 and Table 2-10 are color-coded to identify likely groupings of land uses with similar characteristics, with dark green showing forest categories, light brown for grasslands and shrub/scrub, pink for urban developed categories, etc. Comparing the category distributions for the three different time periods indicates the following:

1. There are some obvious inconsistencies between 1992 and the more recent 2001 and 2006 distributions, most likely due to differences in classifications within categories. For example, there is a big increase in grassland/herbaceous from 1991 to 2001, and a comparable decrease in cultivate cropland. Although cropland likely did decrease, the amount of the decrease indicates a classification issue.
2. Forest distributions between 1992 and 2001 also show a big jump in deciduous and decreases in both evergreens and mixed categories. However, the differences between 2001 and 2006 are relatively small and in the expected directions.
3. Developed land shows a decrease in the high and medium intensity categories, and then a big jump in the developed open space category, most likely due to a classification change. The changes in developed categories between 2001 and 2006 are more consistency and in the expected direction.
4. Overall, the land use distributions for 2001 and 2006 shown in Table 2-9 appear to be consistent, with modest changes and in the expected direction.

Based on this review of the NLCD data, the coverages for 2001 and 2006 appeared to be the most consistent and reliable, representative land use data layers for use in modeling the IRW. The Data Report also noted the availability of the USDA-NASS Cropland Data Layer (CDL) as a potential source of recent land use data, and digital orthophotos available from the State of Oklahoma. In addition, since the Data Report was submitted, land use coverages for the Arkansas portion of the IRW were obtained from the University of Arkansas Center for Advanced Spatial Technologies (CAST) for a number of years from 2003 to 2009. All of these additional land use data layers were available for refinements or adjustments to the NLCD coverage, as needed, for use in the watershed modeling.

Table 2-10 lists the 15 NLCD land use categories and their percentages for both 2001 and 2006, along with the aggregation of these categories into the eight categories that are simulated

by the watershed model; the Open Water category is listed in Table 3.2 but its area is included in the model as the surface area of streams and lakes. The practice of aggregating GIS land use categories for modeling is common in watershed modeling, depending on study objectives and details of the GIS layers. Small percentages of a land use category, such as evergreen and mixed forests in Table 2-10, are lumped with the dominant category, with similar land use/land cover characteristics for modeling, such as deciduous forests in Table 2-10. It is often difficult to distinguish and quantify model parameter values for such similar categories with only slightly different characteristics. In a similar manner, grasslands, shrub/scrub and barren are combined into one category, and the wetland categories are combined into another. Since projecting the impacts of future urbanization is a common use of watershed models, the developed categories are mostly left intact. One exception is combining the medium and high intensity classes since these are often small fractions of the total area, and the difference between them is arbitrary in many cases.

Table 2-9 Distribution of NLCD Land Use for 1992, 2001, and 2006

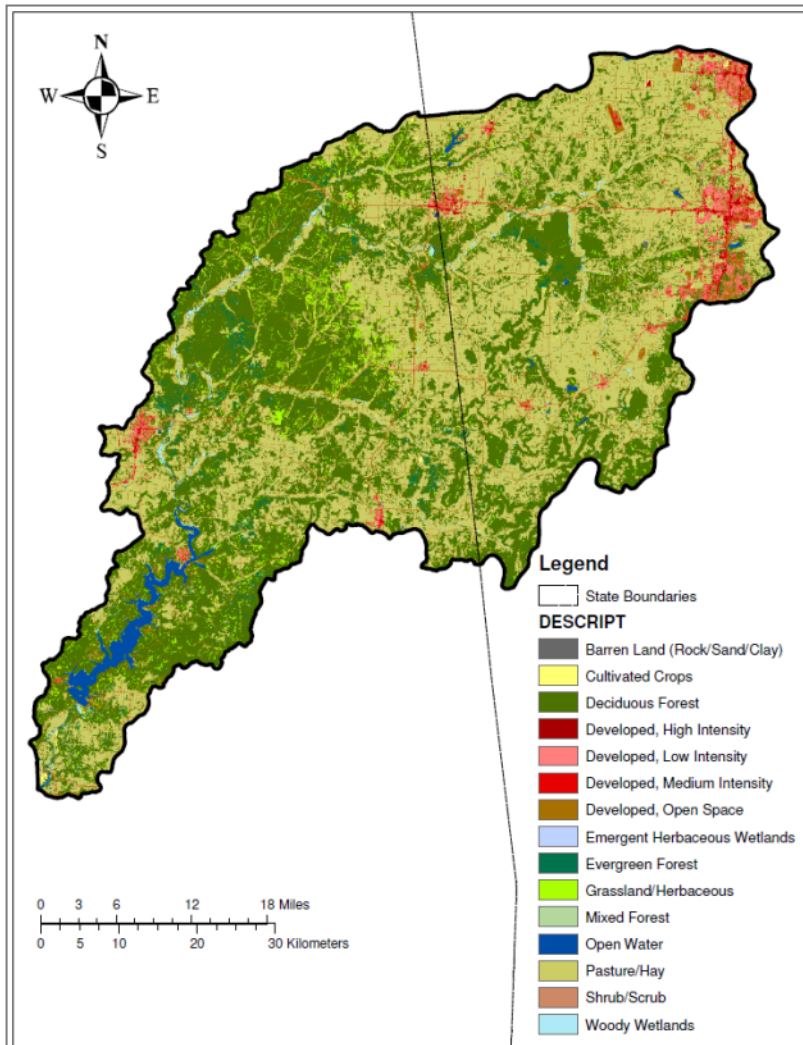
Description	1992		2001-v2		2006	
	Area (Sq. Mi.)	% Land Use	Area (Sq. Mi.)	% Land Use	Area (Sq. Mi.)	% Land Use
Deciduous Forest	555.98	33.63	684.66	41.40	679.64	41.11
Evergreen Forest	33.96	2.05	19.79	1.20	19.62	1.19
Mixed Forest	114.88	6.95	8.14	0.49	8.09	0.49
Pasture/Hay	769.13	46.52	693.31	41.92	679.15	41.08
Grassland/Herbaceous	0.21	0.01	56.38	3.41	60.05	3.63
Shrub/Scrub	13.56	0.82	7.69	0.46	8.27	0.50
Barren land (rock/sand/clay)	3.30	0.20	1.86	0.11	3.20	0.19
Developed, Open Space	7.50	0.45	92.85	5.61	97.99	5.93
Developed, Low Intensity	28.66	1.73	35.66	2.16	39.93	2.41
Developed, Medium Intensity	13.69	0.83	12.23	0.74	15.22	0.92
Developed, High Intensity	12.34	0.75	4.76	0.29	5.73	0.35
Woody Wetlands	5.04	0.31	9.75	0.59	9.73	0.59
Emergent Herbaceous Wetlands	1.63	0.10	0.12	0.01	0.12	0.01
Cultivated Crops	61.14	3.70	2.55	0.15	2.45	0.15
Open Water	32.34	1.96	24.13	1.46	24.15	1.46
Total	1653.35	100.00	1653.87	100.00	1653.35	100.00

Table 2-10 Aggregation of NLCD Land Use to Model Categories

NLCD Class (2001, 2006)	2001 Percent	2006 Percent	Aggregated Model Categories	2001 Percent	2006 Percent
Deciduous Forest	41.40%	41.11%	Forest	43.09%	42.78%
Evergreen Forest	1.20%	1.19%			
Mixed Forest	0.49%	0.49%			
Pasture/Hay	41.92%	41.08%	Pasture/Hay	41.92%	41.08%
Grassland/Herbaceous	3.41%	3.63%	Grass/Shrub/Barren	3.99%	4.33%
Shrub/Scrub	0.47%	0.50%			
Barren Land (Rock/Sand/Clay)	0.11%	0.19%			
Developed, Open Space	5.61%	5.93%	Developed, Open Space	5.61%	5.93%
Developed, Low Intensity	2.16%	2.42%	Developed, Low Intensity	2.16%	2.42%
Developed, Medium Intensity	0.74%	0.92%	Developed, Medium/High Intensity (includes Commercial/Industrial)	1.03%	1.27%
Developed, High Intensity	0.29%	0.35%			
Woody Wetlands	0.59%	0.59%	Wetlands	0.60%	0.60%
Emergent Herbaceous Wetlands	0.01%	0.01%			
Cultivated Crops	0.15%	0.15%	Cultivated Crops	0.15%	0.15%
Open Water	1.46%	1.46%	Open Water**	1.46%	1.46%
Totals	100%	100%	Totals	100%	100%

** - Open Water modeled as a water surface (stream/lake), not a land component

2001 NLCD



2006 NLCD

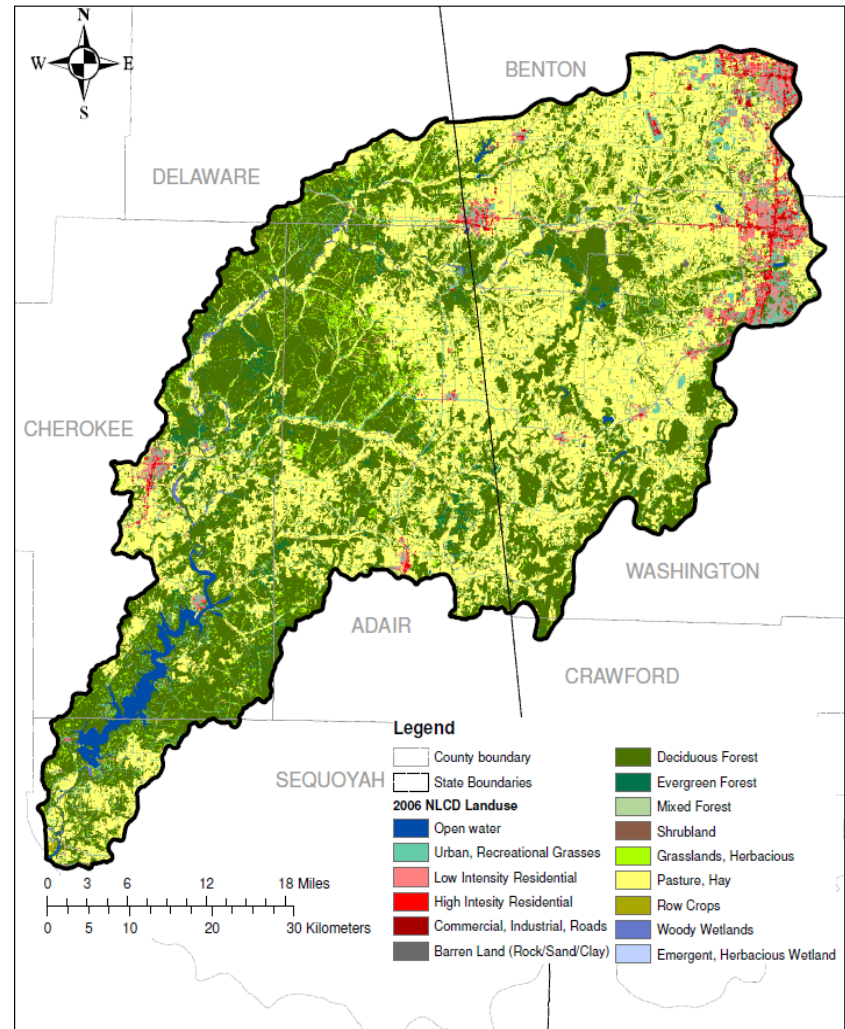


Figure 2-11 National Land Cover Data (NLCD) for 2001 and 2006

Effective Impervious Area

Effective Impervious Area, or EIA, is important to accurately represent in watershed models because of its impact on the hydrologic processes occurring in urban environments. The term “effective” implies that the impervious region is directly connected to a local hydraulic conveyance system (e.g., gutter, curb drain, storm sewer, open channel, or river) and the resulting overland flow will not run onto pervious areas and, therefore, will not have the opportunity to infiltrate along its respective overland flow path before reaching a stream or waterbody.

The EIA for the IRW will be represented using the NLCD 2001 v2 and NLCD 2006, as described above, but with specific focus on the Percent Imperviousness grid layers from those coverages. However, the NLCD Percent Imperviousness grids represent total impervious area (TIA), and it is important to address the distinction, and difference between TIA and EIA. EIA is always less than or equal to TIA.

For the IRW, the process for estimating the EIA for each land use involves first calculating the TIA of each developed urban land use category by overlaying the land use data over the impervious area grid, thus computing the impervious area (i.e., TIA) within each developed land use category. A summary of the results for the IRW, and for both the NLCD 2001 v2 and NLCD 2006 are shown in Table 2-11.

Table 2-11 Total Impervious Areas (TIA) and Percent Imperviousness of Each Urban Land Use for NLCD 2001 v2, and NLCD 2006, and Calculation of EIA

Land use Category	NLCD 2001		NLCD 2006		Average		EIA/TIA Ratio, %	Estimated EIA, %
	Impervious Area (ac)	TIA, %	Impervious Area (ac)	TIA, %	Total	TIA, %		
Developed, Open Space	4,051	6.8	4,268	6.8	4,160	6.8	30	2
Developed, Low Intensity	6,953	30.5	7,785	30.5	7,369	30.5	45	14
Developed, Medium Intensity	4409	56.4	5309	54.5	4,859	55.5	55	30
Developed, High Intensity	2454	80.5	2844	77.9	2,649	79.2	80	63
Total	17,867	19.2	20,206	19.9	19,037	19.6		

In order to convert these TIA values to the EIA values needed for use in the HSPF model, we used data and studies presented by Laenen (1980, 1983), as reported by Sutherland (1995). Sutherland (1995) also describes a number of methods and formulas for calculating EIA from TIA, using equations such as the following:

$$EIA = 0.1(TIA)^{1.5} \quad 2.1$$

The equations provided by Sutherland however, are not distinguished, or defined separately, for individual urban land use categories. Therefore, using the Sutherland EIA-TIA curves, we estimated the EIA/TIA ratio for each of the developed urban land use categories for the IRW, based on their TIA values in Table 2-11, and then used these ratios to calculate the Estimated EIA for each developed land use category.

The last two columns of Table 2-11 show the EIA/TIA ratios and the resulting 'Estimated EIA Percent' value (last column) for each developed category. The final step was to calculate a weighted value for our combined 'High/Medium Intensity' category, using an assumed distribution of 70% Medium Intensity and 30% High Intensity uses; this produced a weighted EIA value of 40% for the combined category. Table 2-12 shows the final EIA values assigned for the urban developed land use categories defined in the model for the IRW.

Table 2-12 Effective Impervious Area Percentage in Developed Land Use Classes in the IRW

Urban Land Use Category	EIA, %
Developed, Open Space	2
Developed, Low Intensity	14
Developed, Medium and High Intensity	40

These same EIA values will be used for 2006 NLCD land uses as well. During the BASINS UCI (Users Control Input) generation process, these EIA percentages are multiplied by the area of each corresponding developed NLCD category to compute the areas of the developed IMPLND and PERLND model categories. The model setup plug-in for HSPF in BASINS 4.0 allows entry of this data through the user interface.

These EIA values are reasonable and consistent with past HSPF applications performed by AQUA TERRA, and the calibration effort did not uncover or demonstrate a need to revise or adjust these values. These values assigned by land use category, and this approach, provide the added benefit of being able to estimate EIA values for future land use changes and scenarios related to urban growth and development.

2.5.4 Soils Data

Soils data is used to characterize the infiltration and soil moisture capacity characteristics of the watershed soils, along with the erodibility parameters for soil erosion. SSURGO (Soil Survey Spatial and Tabular Data) soils data for the IRW were downloaded from the USDA/NRCS Data Gateway site (<http://soildatamart.nrcs.usda.gov/>). SSURGO depicts information about the kinds and distribution of soils on the landscape. This dataset is a digital soil survey and generally is the most detailed level of soil geographic data developed by the National Cooperative Soil Survey. This dataset consists of georeferenced digital map data, computerized tabular attribute data, and associated metadata.

The properties of this dataset of interest in this watershed modeling study are: soil description, slope gradient, water table depth, flooding frequency, available water storage, hydrologic group, and hydric group. Spatial data on the SCS Hydrologic Soil Groups (HSG) were obtained and used to generate a map of the spatial distribution of these properties, shown in Figure 2-12. The HSG B, C, and D distributions by subwatershed will be used as a basis for model parameterization related to infiltration and soil moisture capacity values in the model.

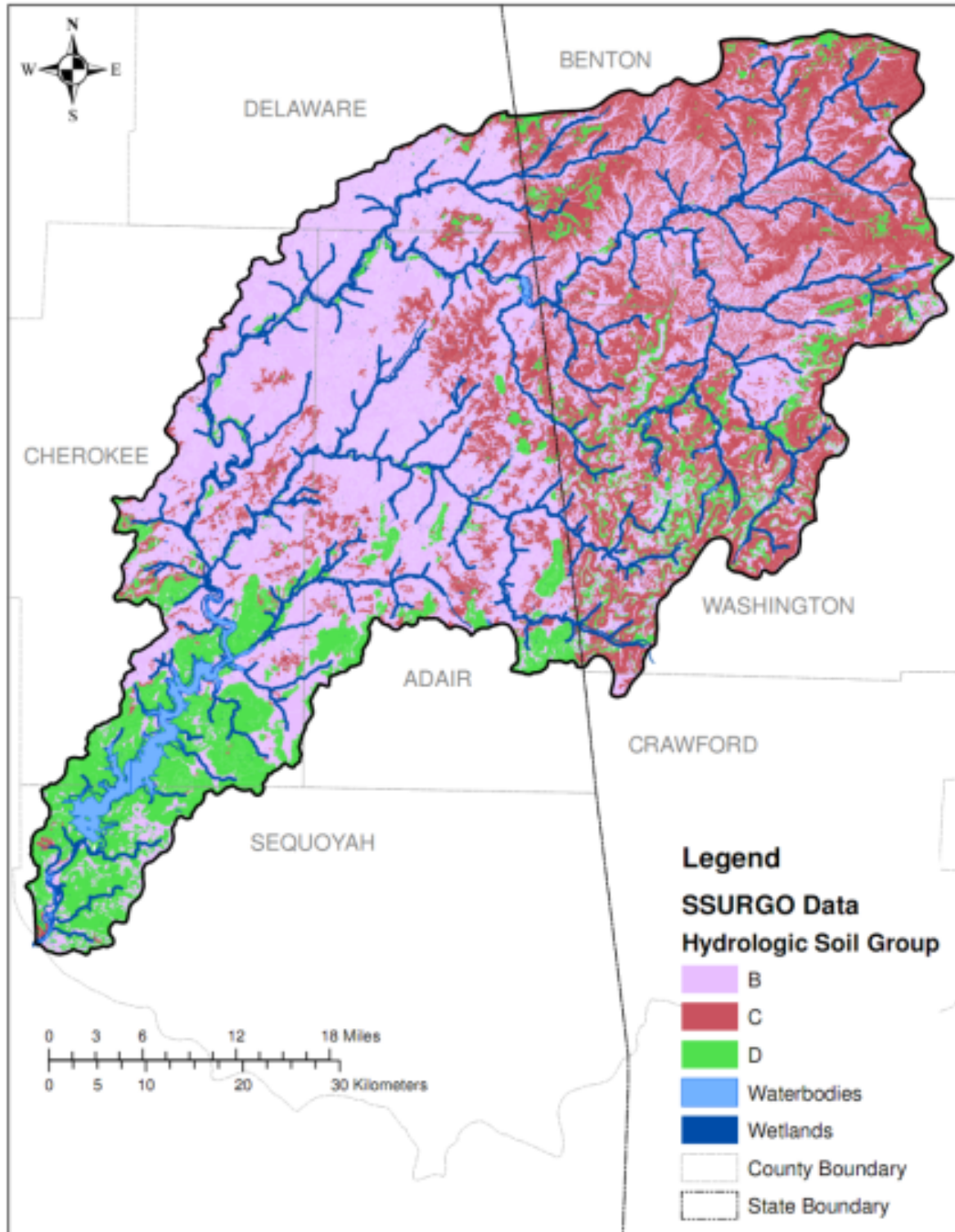


Figure 2-12 Distribution of NRCS Hydrologic Soil Groups for the IRW

Channel Characteristics

The river channel network in the Illinois River Watershed is the major pathway by which flow, sediment and contaminants are transported from the watershed to the Lake Tenkiller. As such, it is important to accurately represent or characterize the channel system in the HSPF model of the watershed. The river reach segmentation considered river travel time, riverbed slope continuity, cross section and morphologic changes, and entry points of major tributaries. When partitioning the channel segments, additional considerations included the Arkansas-Oklahoma state line, the USGS stream gage locations, Total Maximum Daily Load (TMDL) stream segments, and PCS (Permit Compliance System) facilities.

Although not a strict GIS type data layer, channel characteristics are needed to help define routing and stage-discharge behavior, bed composition for sediment, carbon, and nutrients, and bed/water column interactions related to temperature, benthic oxygen demand, nutrient fluxes, and benthic algal mass. Since they need to be defined spatially throughout the stream system, they will require information from as many sites as possible, and then assumptions will be needed to extend the parameterization to the rest of the stream segments.

Many of the USGS gage sites have cross section data available. These data consist of actual measured cross sections, and at some sites where no cross sections have been provided, idealized cross sections can be developed from available data. The USGS has multiple measurements of streamflow, stream width, and cross sectional area that have been made over a period of years, available online (<http://nwis.waterdata.usgs.gov/nwis/measurements/>). These data have been obtained and are being utilized for the corresponding stream reaches. However, that still leaves many portions of the stream system without localized physical measurements. Alternatively, this information can be developed from existing flood insurance studies with models used for calculating flood inundation levels (e.g. HEC-RAS). Lacking detailed physical data, geomorphic relationships between drainage area and channel width and depth values are sometimes used, but they are approximate and can lead to misleading stage-discharge relationships. Thus, actual cross section data at various points in the stream system are preferred.

Stream bed characteristics are also needed for setup of the instream sediment transport modeling, and for representing the bed/water column interactions for nutrients. Bed storages for sediment, including particle size distributions, and for nutrients provide the basis for both starting conditions and the potential magnitude of bed contributions to the water column.

Citations and data provided by M. Derichsweiler (personal communication, email dated 18 February 2010) included information on pebble counts for Battle Branch and Baron Fork (dated 1998), and the a paper by Harmel, Haan, & Dutnell (1999) identifies median bed particle diameters (D_{50}) for 36 sites along the Illinois River mainstem, as part of study on bank erosion and riparian vegetation impacts. As part of the court case, Grip (2008, 2009) performed aerial photography and analyses to study and define meander conditions and patterns for the Illinois River mainstem, and to estimate bank erosion contributions to the sediment load entering Lake Tenkiller. His data include hundreds of cross section measurements, with channel bottom, bank, and floodplain elevations that may be helpful for channel characterization. The Oklahoma Conservation Commission published two 319(h) reports (OCC, 2007) on water quality monitoring and analysis that included measurements of stream channel parameters (bank slopes, channel widths, bottom substrates, etc.) and streambank erosion potential. These studies focused largely on Peacheater and Tyner Creeks.

Haggard and Soerens (2006) discuss bed phosphorus releases from a small breached impoundment, the former Lake Frances, near the OK/AR state line. They present some bed information and phosphorus release estimates that will help to include these processes in the modeling. Sediment bed data for phosphorus is also reported for selected Ozark catchments (Haggard et al., 2007).

Hydraulic Characterization of River and Reservoir Segments

As part of the stream segmentation, the stream segments were analyzed to define their hydraulic behavior and characteristics, along with the tributary areas of the land use categories that drain to them. Within the channel module (RCHRES) of HSPF, the stream hydraulic behavior of each waterbody (stream/river or reservoir) is represented by a hydraulic function table, called an FTABLE, which defines the flow rate, surface area, and volume as a function of the water depth. In order to develop an FTABLE, the waterbody geometric and hydraulic properties (e.g., slope, cross-section, Manning's n) must be defined using data or estimated values. Once the geometry and hydraulic properties have been defined, it is possible to develop the FTABLE as a function of the depth of water (i.e., stage) at the outlet. The method used to develop FTABLEs for streams and rivers in the IRW involves using a single cross-section at the outlet (endpoint) of the reach, applying Manning's equation to calculate flow rate for a given depth, and then assuming the channel to be prismatic (i.e., constant cross-section and bottom slope) along its length, to calculate the corresponding surface area and volume; in some cases, multiple cross sections are utilized, if available to improve the representation of volume and surface area in long reaches.

The initial set of FTABLEs for the streams and rivers within the Illinois River Watershed were developed using this method, but with adjustments where USGS rating curves are available. The cross sections for the reaches are a mixture of: 1) measured cross sections from the USGS, 2) inferred cross sections developed from multiple measurements of flow/width/cross sectional area, and 3) simple prismatic cross sections developed from regional geomorphic relationships. At locations where a rating curve has been developed by the USGS, we merged the cross section with the rating curve to obtain a more accurate discharge representation. The following examples illustrate the FTABLE development at locations where (1) a cross section is available, and (2) where the geomorphic relationships are used.

The cross section shown in Figure 2-13 was measured at a riffle on Osage Creek, and is considered representative of the reach in subbasin 302. A trapezoid was fitted to this cross-section, and dimensions were estimated as follows: top width = 62', bottom width = 26', and bankfull height = 3.8'. The floodplain adjacent to the stream was characterized using Google Earth™. A line perpendicular to the stream was drawn at three locations for each stream reach to estimate the average floodplain slope: close to the upstream end, at the center, and the downstream end. Google Earth provides an elevation profile of the line and using these elevation profiles, floodplain slopes on both sides of the channel were computed, along with the distance from the stream. Roughness values (Manning's n) for the stream (range of 0.031 - 0.045) and the flood plain (range of 0.05 - 0.10) were estimated based on site photographs, Google Earth imagery and expert guidance. The FTABLEs were constructed using Manning's Equation, an assumed trapezoidal channel, and a trapezoidal floodplain.

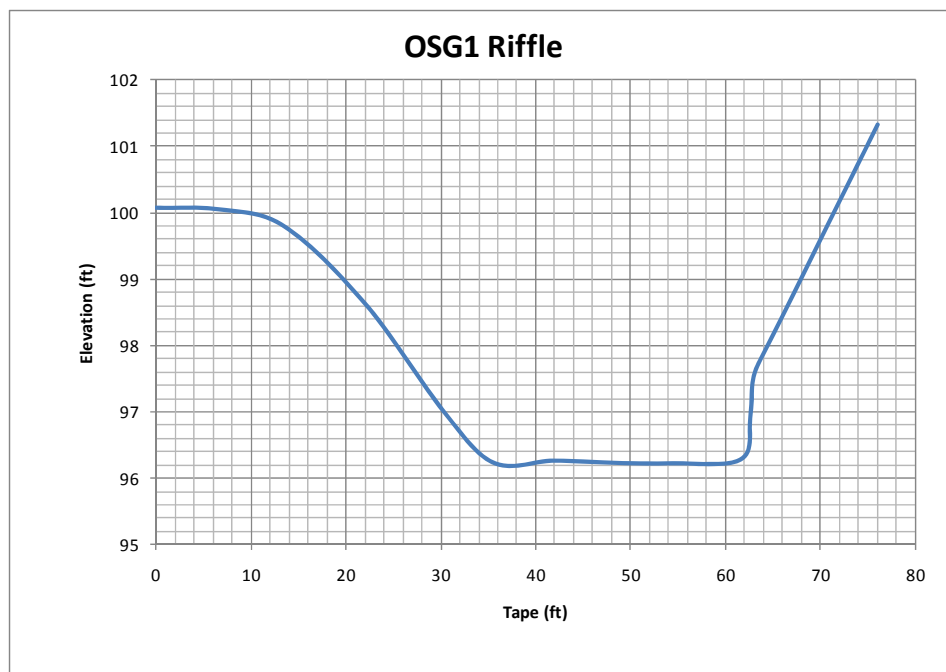


Figure 2-13 The cross-section of a riffle at site OSG1

At the locations where cross-section data were not available, bankfull width, bankfull depth, and channel depth were estimated as a function of drainage area using regional geomorphic equations (Equations 1 - 3). These equations were developed based on data available for 20 locations in the Illinois River Watershed (USGS field data, and Marty Matlock's research). These equations are different than the regional curve equations proposed by Dutnell (2000); although they are similar in form, Dutnell represented the channel cross-section as rectangular.

$$BW = 3.89DA^{0.48} \quad 1$$

$$BnkW = 30.69DA^{0.31} \quad 2$$

$$BD = 2.31DA^{0.22} \quad 3$$

where

BW = channel bottom width in feet

$BnkW$ = bankfull width in feet

BD = bankfull depth in feet

DA = drainage area in square miles

The remaining hydraulic characteristics of the stream (length, slope, floodplain slopes, and Manning's roughness coefficients) were estimated as explained earlier for reach 302. Example FTABLEs for reach 302 (developed with cross-section data), and 312 (developed with regional curve equation, drainage area 20.7 mi²) are shown in Table 2-13.

There are several small reservoirs and lakes such as Lake Wedington, SWEPCO Lake, and Lake Frances that are the defining reaches in their subbasins. FTABLEs for these lakes were derived from available stage-surface area data and stage-volume data, plus outlet data that defined their releases.

Table 2-13 Example FTABLEs for Reaches 302 and 312

FTABLE	302				
ROWS	COLS				***
17	4				***
	Depth	Surface Area	Volume	Discharge	***
	(ft)	(ac)	(ac-ft)	(cfs)	***
	0.0	0.0	0.0	0.0	
	0.3	12.0	9.3	11.0	
	0.6	25.1	19.6	35.8	
	1.0	37.3	30.9	72.0	
	1.3	40.5	43.2	119.2	
	1.6	43.7	56.6	177.2	
	1.9	46.9	70.9	246.3	
	2.5	53.3	102.7	418.6	
	3.2	59.7	138.5	638.5	
	3.8	66.1	178.3	908.9	
	5.1	128.8	301.8	1770.9	
	6.3	191.4	504.5	3020.9	
	7.6	254.0	786.6	4758.9	
	8.9	316.7	1148.1	7068.9	
	10.1	379.3	1588.8	10027.8	
	11.4	441.9	2108.9	13706.8	
	12.7	504.6	2708.4	18173.7	
END FTABLE	302				
FTABLE	312				
ROWS	COLS				***
17	4				***
	Depth	Surface Area	Volume	Discharge	***
	(ft)	(ac)	(ac-ft)	(cfs)	***
	0.0	0.0	0.0	0.0	
	0.4	9.9	5.6	8.7	
	0.8	14.8	12.7	29.6	
	1.1	24.8	21.2	62.2	
	1.5	28.7	31.2	107.4	
	1.9	32.6	42.7	166.2	
	2.3	36.6	55.6	239.6	
	3.0	44.4	86.0	434.4	
	3.8	52.3	122.3	700.2	
	4.5	60.2	164.4	1044.6	
	6.0	102.9	286.6	2243.5	
	7.5	145.6	472.9	4083.9	
	9.0	188.3	723.1	6743.4	
	10.5	231.0	1037.4	10372.7	
	12.0	273.7	1415.6	15108.6	
	13.5	316.4	1857.9	21078.7	
	15.0	359.1	2364.2	28403.5	
END FTABLE	312				

2.5.5 Final Segmentation

As noted at the beginning of this section, whenever any watershed model is set up and applied to a watershed, the entire study area must undergo a process sometimes referred to as 'segmentation'. The purpose of watershed segmentation is to divide the study area into individual land and channel segments, or pieces, that are assumed to demonstrate relatively homogenous hydrologic/hydraulic and water quality behavior.

Based on the GIS data layers discussed in this section, the proposed Final Segmentation for the IRW is shown in Figure 2-14.

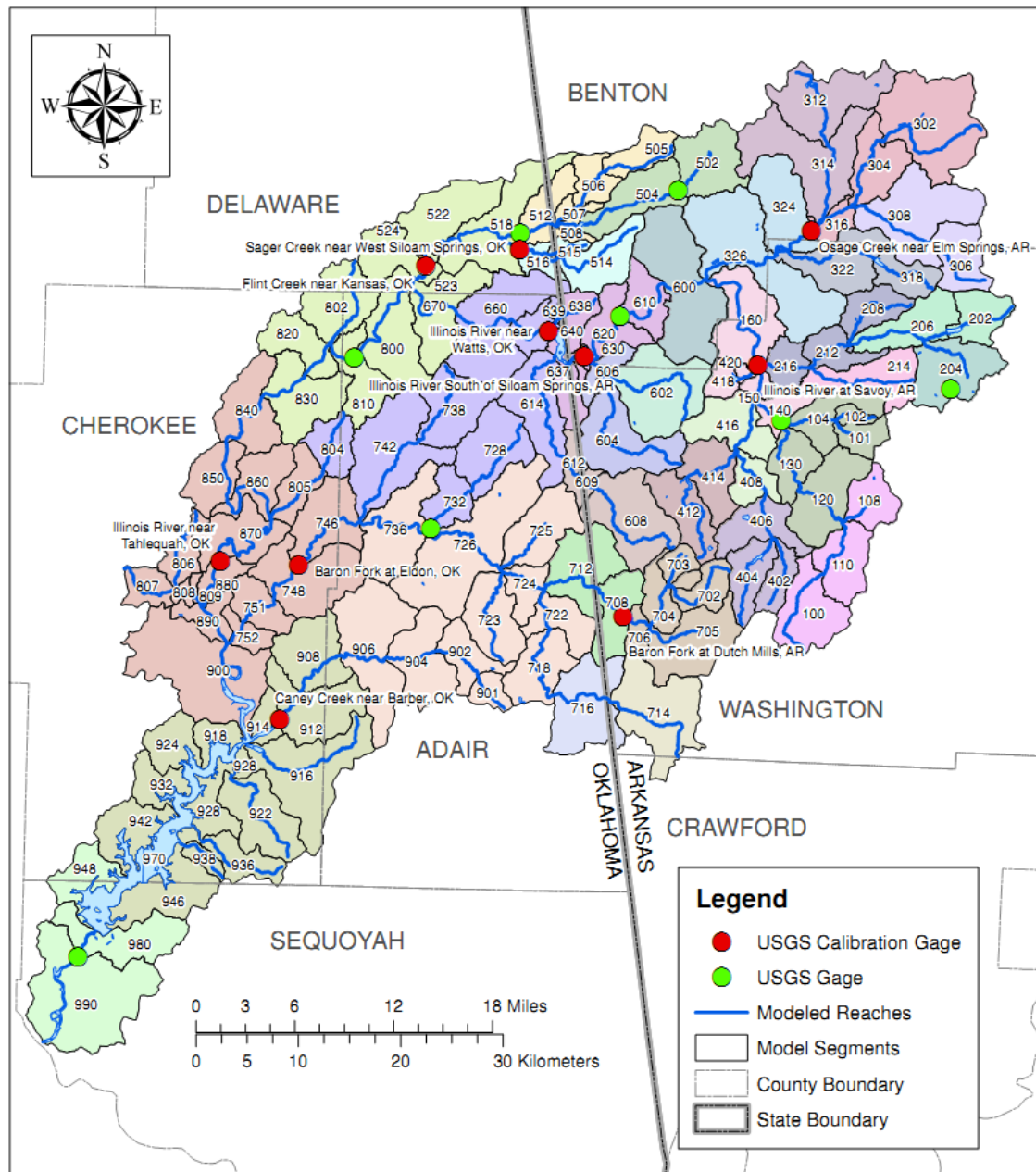


Figure 2-14 Final Segmentation of the IRW

Table 2-14 lists the stream reach characteristics with the reach number and name, along with the length, slope, downstream reach, and local drainage area.

The segmentation process started with the 12-digit HUC boundaries as the basic spatial units for the study. These were then overlaid with the NHD+ hydrography down to 2nd-3rd order streams. The 12-digit HUC boundaries were then adjusted to match reach endpoints at the various USGS gage sites, the AR/OK state line, the endpoints of the impaired segments on each State's 303d list, and the identified major point source dischargers. Some further subdivisions were made where stream segments were judged to be too long, and to allow finer spatial representation of the main stem and selected tributaries. We then solicited suggestions for further subdivisions from State agency representatives and local experts, before arriving at the Final Segmentation proposed in Figure 2-14. This Final Segmentation incorporates the results of those comments.

The reach numbers were assigned to correspond to the subbasin numbers. The numbering scheme is related to the original 12-digit HUC watersheds, and is arranged with lower upstream numbers and higher downstream numbers. Illinois River mainstem reaches have numbers that end with 0, and the hundreds digit corresponds to the original 12-digit HUC. The most upstream reach is 110, Lake Tenkiller is 970, and the most downstream reach is 990. Tributaries also have the same hundreds digit as the original HUC12 watersheds, and are numbered so that they flow downstream to higher reach/segment numbers. All mainstream and tributary stream reaches have the same number as the land segment that they drain.

This segmentation process resulted in 133 model subbasins (or segments) and 126 stream reaches.

Table 2-14 IRW Stream Reach Characteristics

Subbasin/ Reach Number	Stream Name/Location	Length (miles)	% Slope	Downstream Reach/Segment	Drainage Area (sq. mi.)
100	Illinois River	6.69	1.45	110	16.0
101	Farmington Creek	1.35	1.63	104	5.5
102	Goose Creek	2.85	0.24	104	2.2
104	Goose Creek	3.69	0.20	140	17.7
108	Hickory Creek	2.63	0.84	120	8.6
110	Illinois River	4.43	0.77	120	28.4
120	Illinois River	4.62	0.74	130	54.0
130	Illinois River near Viney Grove, AR (USGS gage 07194760)	5.02	0.31	140	63.2
140	Illinois River	2.69	0.28	150	86.4
150	Illinois River at Savoy, AR	2.76	0.27	160	167.5
160	Illinois River	8.91	1.29	600	262.8
202	Clear Creek	4.65	1.07	206	9.2
204	Mud Creek	4.56	0.36	206	16.8
206	Clear Creek	6.89	0.80	212	39.4
208	Little Wildcat Creek	6.18	0.15	212	8.7
212	Clear Creek	3.31	0.15	216	55.5
214	Hamestring Creek	7.32	0.25	216	14.8
216	Clear Creek	3.48	0.56	160	76.9
302	Osage Creek	8.80	0.67	304	29.9
304	Osage Creek	5.71	0.44	316	42.2
306	Spring Creek	4.94	0.48	308	11.3
308	Spring Creek	6.04	0.22	316	36.6

Environmental Protection Agency Regions 6
 Illinois River Watershed Nutrient Model and Tenkiller Ferry Lake EFDC Water Quality Model

Subbasin/ Reach Number	Stream Name/Location	Length (miles)	% Slope	Downstream Reach/Segment	Drainage Area (sq. mi.)
312	Little Osage Creek	6.39	0.46	314	20.7
314	Little Osage Creek	5.82	1.83	316	46.8
316	Osage Creek near Elm Springs, AR (USGS gage 07195000)	3.07	0.24	324	129.9
318	Brush Creek	4.68	0.68	322	7.7
322	Brush Creek	7.76	0.42	326	23.7
324	Osage Creek	3.54	0.29	326	146.4
326	Osage Creek	6.09	0.52	600	206.3
402	Muddy Fork	4.69	0.45	406	6.4
404	Blair Creek	6.54	0.24	406	9.7
406	Muddy Fork	3.24	0.91	408	27.8
408	Muddy Fork	3.98	0.31	416	34.7
412	Moore's Creek	7.01	0.02	414	12.4
414	Moore's Creek	4.59	0.46	416	24.5
416	Muddy Fork	3.96	0.39	150	73.3
418	Lake Wedington	0.78	0.21	420	3.9
420	Lake Wedington Outlet Stream	1.46	0.24	150	4.9
502	Flint Creek at Springtown, AR (USGS gage 07195800)	3.68	1.07	504	14.9
504	Flint Creek	7.46	0.14	508	29.3
505	Little Flint Creek	5.12	0.10	506	7.6
506	SWEPCO Lake	3.14	0.35	507	14.1
507	Little Flint Creek	1.85	0.15	512	16.4
508	Flint Creek	1.47	0.09	512	31.3
512	Flint Creek near West Siloam Springs, OK (USGS gage 07195855)	2.59	0.11	518	56.6
514	Sager Creek	6.80	0.57	516	13.0
515	Sager Creek Tributary	2.73	0.29	516	1.9
516	Sager Creek near West Siloam Springs, OK (USGS gage 07195865)	3.42	0.24	518	19.1
518	Flint Creek	7.84	2.76	522	98.3
522	Flint Creek	1.94	0.27	523	114.9
523	Flint Creek near Kansas, OK	0.76	0.24	524	115.7
524	Flint Creek	1.58	0.26	800	126.6
600	Illinois River	3.12	0.58	610	499.7
602	Wedington Creek	9.10	0.35	606	23.3
604	Cincinnati Creek	10.91	0.48	606	20.5
606	Cincinnati Creek	1.29	0.14	630	48.3
608	Ballard Creek	8.62	0.09	609	21.7
609	Ballard Creek	1.55	0.06	612	23.3
610	Illinois River at Hwy. 16 near Siloam Springs, AR (USGS gage 07195400)	4.98	0.42	620	508.9
612	Ballard Creek	1.70	0.24	614	27.6
614	Ballard Creek	8.93	0.38	637	45.5
620	Illinois River	4.47	0.50	630	519.0
630	Illinois River South of Siloam Springs, AR (USGS gage 07195430)	0.54	0.77	635	567.7
635	Illinois River – AR/OK Stateline	1.07	0.49	637	569.1
637	Illinois River	2.89	0.21	640	623.2
638	East Beaver Creek	2.40	0.23	639	4.9
639	East Beaver Creek	1.43	0.36	640	6.1
640	Illinois River near Watts, OK (USGS gage 07195500), Lake Francis Reach	0.48	0.24	650	629.5

Environmental Protection Agency Regions 6

Illinois River Watershed Nutrient Model and Tenkiller Ferry Lake EFDC Water Quality Model

Subbasin/ Reach Number	Stream Name/Location	Length (miles)	% Slope	Downstream Reach/Segment	Drainage Area (sq. mi.)
650	Illinois River	3.34	0.12	660	635.0
660	Illinois River	4.90	0.18	670	662.6
670	Illinois River	5.17	0.27	800	679.5
702	Jordan Creek	5.98	0.40	704	7.0
703	Bush Creek	2.31	0.33	704	3.8
704	Jordan Creek	3.18	0.17	706	19.3
705	Fly Creek	5.11	0.37	706	18.1
706	Baron Fork at Dutch Mills, AR (USGS gage 07196900)	2.17	0.51	708	41.1
708	Baron Fork	2.94	1.20	712	52.4
712	Baron Fork	4.19	0.13	724	69.4
714	Evansville Creek	7.36	0.13	716	24.3
716	Evansville Creek	4.47	0.12	718	45.1
718	Evansville Creek	6.05	1.01	722	58.4
722	Evansville Creek	2.98	0.63	724	67.8
723	Peavine Creek	7.23	0.16	726	14.4
724	Baron Fork	3.15	0.35	726	143.9
725	Shell Branch	4.49	0.68	726	15.1
726	Baron Fork	6.60	0.44	736	209.9
728	Peacheater Creek	6.13	0.35	732	16.6
732	Peacheater Creek at Christie, OK (USGS gage 07196973)	4.09	0.61	736	25.1
736	Baron Fork	5.96	1.45	746	254.2
738	Tyner Creek	6.53	0.65	742	15.4
742	Tyner Creek	7.34	0.27	746	41.8
746	Baron Fork at Eldon, OK (USGS gage 07197000)	6.34	1.18	748	311.6
748	Baron Fork	3.21	0.57	751	332.8
751	Baron Fork	3.74	0.24	752	341.3
752	Baron Fork	1.84	0.77	900	345.8
800	Illinois River at Chewey, OK (USGS gage 07196090)	7.01	0.41	810	824.7
802	Black Fox Springs	6.29	0.09	820	16.0
804	Dumpling Hollow	4.19	0.08	805	8.5
805	Dumpling Hollow	5.18	0.08	870	16.7
806	Tahlequah Creek	6.22	0.05	808	6.7
807	Ross Branch	4.56	0.04	808	6.1
808	Tahlequah Creek	1.11	0.46	809	14.2
809	Tahlequah Creek	0.75	1.55	890	15.1
810	Illinois River	2.85	0.20	820	836.6
820	Illinois River	2.79	0.86	830	863.3
830	Illinois River	3.43	2.22	840	880.7
840	Illinois River	4.89	1.15	850	896.4
850	Illinois River	3.69	3.87	860	907.2
860	Illinois River	6.25	4.58	870	918.7
870	Illinois River near Tahlequah, OK (USGS gage 07196500)	8.83	1.44	880	949.5
880	Illinois River	4.39	2.67	890	954.7
890	Illinois River	3.06	2.44	900	975.9
900	Illinois River	9.46	1.14	970	1359.3
901	Caney Creek	2.75	0.86	902	4.2
902	Caney Creek	3.64	1.81	904	13.1
904	Caney Creek	3.42	1.22	906	29.5
906	Caney Creek	3.87	0.13	908	56.7
908	Caney Creek	4.03	0.16	912	72.4
912	Caney Creek near Barber, OK (USGS gage 07197360)	2.68	2.25	914	90.2

Subbasin/ Reach Number	Stream Name/Location	Length (miles)	% Slope	Downstream Reach/Segment	Drainage Area (sq. mi.)
914	Caney Creek	2.25	0.70	970	94.6
916	Dry Creek	10.14	0.69	970	27.6
918	Local Drainage to Lake Tenkiller	1.46	0.22	970	4.8
922	Elk Creek	8.33	0.44	970	20.3
924	Local Drainage to Lake Tenkiller	2.09	0.49	970	8.5
928	Local Drainage to Lake Tenkiller	1.07	1.15	970	6.1
932	Local Drainage to Lake Tenkiller	1.31	1.07	970	7.4
936	Terrapin Creek	6.42	0.86	970	10.0
938	Chicken Creek	3.59	0.16	970	2.8
942	Local Drainage to Lake Tenkiller	1.96	0.44	970	11.7
946	Local Drainage to Lake Tenkiller	2.10	1.63	970	16.5
948	Local Drainage to Lake Tenkiller	1.65	0.83	970	9.7
970	Lake Tenkiller	36.61	0.95	980	1598.5
980	Illinois River	2.21	1.69	990	1614.6
990	Illinois River	6.96		-999	1653.4

2.6 Calibration and Validation of the IRW Model

2.6.1 Calibration and Validation Time Periods

Selection of time periods for model calibration and validation depends on a number of factors, including the availability of data for model operations, land use data for model setup, climate variability, and observed data for model-data comparisons. The principal time series data needed for hydrologic and water quality calibration – rainfall, evaporation, air temperature, wind speed, dew point temperature, cloud cover, solar radiation, observed flow, and water quality observations – indicates that long-term simulations are possible at a number of the USGS and AWRC gages within the IRW, spanning the time period covering the early 1990s through 2009. Quality Assurance and Quality Control (QA/QC) procedures followed throughout the effort, in accordance with the Project QAPP, are discussed in Appendix F.

Precipitation and meteorologic data are a fundamental necessity for model execution, and those data must span the entire simulation period, covering both calibration and validation periods. Partial periods of record, while not ideal, can still be used for consistency checks as part of the calibration and validation process. Land use data are available as snapshots in time, and partially control the selection process as it is preferable to have the land use data at the approximate mid-point of each period, calibration and validation, so that it provides a reasonable representation of conditions throughout each period.

Climate variability is considered once the potential time periods are identified, so that both calibration and validation are performed over a range of climate conditions, including a reasonable balance of wet and dry periods. Finally, the observed data for both flow and water quality exert the primary influence on the selection as the data must be available for performing the model-data comparisons for both components of the model application process.

As discussed in Section 2, the available precipitation and meteorologic data provide an adequate coverage of the watershed for the time period extending from about 1994 through 2009. Prior to 1994, the limitation is primarily related to the availability of hourly precipitation and meteorologic data other than air temperature and evaporation; the OK Mesonet network did not start until 1994 and the AWOS sites started in 1995.

The NLCD land use coverages are for 1992, 2001, and 2006. However, the 1992 data shows considerable inconsistencies as compared to the coverages for the other two dates.

The climate variability is most often assessed by analyzing annual rainfall records. Figure 2-15 shows the annual rainfall data from 1980 to 2009 for Fayetteville, Kansas 2 NE, and Odell 2N. The years 2002-2007 were dryer than normal at Fayetteville, but the same period at Odell included only 3 dry years compared to 3 wet years, and at the Kansas gage only 1 wet year occurred during that 6-year period. In general, the 1990s decade appears to be about normal, or slightly wetter than normal, whereas the decade of the 2000s is generally a little dryer than normal.

Based on these considerations, our selection of the calibration and validation periods is as follows:

- Calibration: WY 2001-2009
- Validation: WY 1992-2000.



Figure 2-15 Annual Rainfall Data for Fayetteville, Kansas, and Odell for 1980-2009

Our rationale for this selection is as follows:

- a. The most complete data for water quality calibration occurs during the period from about 2003 to 2009; thus, we selected the most recent time period for calibration. It is a general truism that model calibration should be performed for the period with the ‘best’ and most complete data coverage. In addition, calibration on the most recent time period, establishes a solid foundation for projecting impacts and changes for future conditions and potential scenarios.
- b. We extended the calibration period back to 2001 to include a more even balance of wet and dry years.
- c. The NLCD 2006 coverage will be used for the calibration period, and the NLCD 2001 coverage will be used for validation. We chose the 2001 coverage over the 1992 coverage due to the inconsistencies in classifications noted in Section 3.3. Although the 2001 NLCD land use coverage is just outside the validation period, it still is expected to provide a good representation of conditions for the 1992-2000 time period.
- d. We extended the validation period back to 1992 in spite of the limitations on hourly precipitation data noted above. We still have three hourly stations prior to 1994.

Table 2-15 shows the gage sites with flow and water quality data in the IRW. The highlighted sites are those 10 sites selected for model calibration and validation, with the green sites indicating the AR gages, the yellow sites indicating OK gages, and the pink sites indicating the border sites above and below the AR/OK state line. The highlighted gages are those generally with the longest and most recent period of data. Note that the Sager Creek gage is actually located in OK, but the majority of the watershed is in AR.

Table 2-15 IRW Gage Stations for Watershed Model Calibration and Validation

Location	Gage Station	Water Quality		Tributary Area (mi ²)	Elevation (ft)
Illinois River near Tahlequah, OK	7196500	8/23/1955	12/15/2009	959	664
Baron Fork at Eldon, OK	7197000	5/7/1958	12/14/2009	307	701
Baron Fork at Dutch Mills, AR	7196900	3/17/1959	8/25/2009	41	986
Illinois River near Watts, OK	7195500	9/12/1955	10/26/2009	635	894
Illinois River near Viney Grove, AR	7194760	9/6/1978	7/19/2007	81	1051
Illinois River at Savoy, AR	7194800	9/11/1968	8/25/2009	167	1019
Osage Creek near Elm Springs, AR	7195000	9/10/1951	8/25/2009	130	1052
Illinois River at Hwy. 16 near Siloam Springs AR	7195400	9/8/1978	9/20/1994	509	1170
Illinois River South of Siloam Springs, AR	7195430	10/3/1972	8/25/2009	575	909
Flint Creek at Springtown, AR	7195800	10/15/1975	7/1/1996	14	1173
Flint Creek near West Siloam Springs, OK	7195855	7/11/1979	8/28/1996	60	954
Sager Creek near West Siloam Springs, OK	7195865	5/24/1991	10/21/2009	19	960
Flint Creek near Kansas, OK	7196000	9/7/1955	10/26/2009	110	855
Peacheater Creek at Christie, OK	7196973	8/6/1991	5/16/1995	25	802
Caney Creek near Barber, OK	7197360	8/25/1997	10/27/2009	90	368
Illinois River at Chewey, OK	7196090	7/16/1996	10/27/2009	825	820
Illinois River near Gore, OK	7198000	4/12/1940	8/16/1995	1626	468

Pink – Border Stations; Green – AR Station; Yellow – OK Stations.

2.6.2 Hydrology Calibration/Validation Procedures and Results

Calibration of the IRW model was an iterative process of making parameter changes, running the model and producing comparisons of simulated and observed values, and interpreting the results. This process occurs first for the hydrology portions of the model, followed by the water quality portions. The procedures have been well established over the past 30 years as described in the HSPF Application Guide (Donigian et al., 1984) and summarized by Donigian (2002). The hydrologic calibration process is greatly facilitated with the use of the HSPEXP, an expert system for hydrologic calibration, specifically designed for use with HSPF, developed under contract for the USGS (Lumb, McCammon, and Kittle, 1994). This package gives calibration advice, such as which model parameters to adjust and/or input to check, based on predetermined rules, and allows the user to interactively modify the HSPF Users Control Input (UCI) files, make model runs, examine statistics, and generate a variety of comparison plots. HSPEXP still has some limitations, such as 'how much' to change a parameter and relative differences among land uses, which requires professional modeling experience and judgment. The post-processing capabilities of GenScn (e.g., listings, plots, statistics, etc.) (Kittle et al., 1998) are also used extensively during the calibration/validation effort. Software linkages to HSPEXP and selected GenScn capabilities are available through BASINS 4.0. Most recently, BASINS 4.0 scripting capabilities are used extensively to provide the HSPEXP analyses and additional summary statistics, in addition to plots and tables needed for calibration. These scripts were used extensively in the IRW calibration efforts.

Calibration of HSPF to represent the hydrology of the IRW is an iterative trial-and-error process. Simulated results are compared with recorded data for the entire calibration period, including both wet and dry conditions, to see how well the simulation represents the hydrologic response observed under a range of climatic conditions. By iteratively adjusting specific calibration parameter values, within accepted and physically-based ranges, the simulation results are changed until an acceptable comparison of simulation and recorded data is achieved.

The standard HSPF hydrologic calibration is divided into four phases:

- **Establish an annual water balance.** This consists of comparing the total annual simulated and observed flow (in inches), and is governed primarily by the input rainfall and evaporation and the parameters LZSN (lower zone nominal storage), LZETP (lower zone ET parameter), and INFILT (infiltration index).
- **Adjust low flow/high flow distribution.** This is generally done by adjusting the groundwater or baseflow, because it is the easiest to identify in low flow periods. Comparisons of mean daily flow are utilized, and the primary parameters involved are INFILT, AGWRC (groundwater recession), and BASETP (baseflow ET index).
- **Adjust stormflow/hydrograph shape.** The stormflow, which is compared in the form of short time step (1 hour) hydrographs, is largely composed of surface runoff and interflow. Adjustments are made with the UZSN (upper zone storage), INTFW (interflow parameter), IRC (interflow recession), and the overland flow parameters (LSUR, NSUR, and SLSUR). INFILT also can be used for minor adjustments.
- **Make seasonal adjustments.** Differences in the simulated and observed total flow over summer and winter are compared to see if runoff needs to be shifted from one season to another. These adjustments are generally accomplished by using seasonal (monthly variable) values for the parameters CEPSC (vegetal interception), LZETP, UZSN. Adjustments to KVARY (variable groundwater recession) and BASETP are also used.

The procedures and parameter adjustments involved in these phases are more completely described in Donigian et al. (1984), and the HSPF hydrologic calibration expert system (HSPEXP) (Lumb, McCammon, and Kittle, 1994).

The same model-data comparisons are performed for both the calibration and validation periods. The specific comparisons of simulated and observed values include:

- Annual and monthly runoff volumes (inches)
- Daily time series of flow (cfs)
- Storm event periods, e.g. hourly values (cfs)
- Flow frequency (flow duration) curves (cfs)

In addition to the above comparisons, the water balance components (input and simulated) are reviewed. This effort involves displaying model results for individual land uses, and for the entire watershed, for the following water balance components:

- Precipitation
- Total Runoff (sum of following components)
 - Overland flow
 - Interflow
 - Baseflow

- Potential Evapotranspiration
- Total Actual Evapotranspiration (ET) (sum of following components)
 - Interception ET
 - Upper zone ET
 - Lower zone ET
 - Baseflow ET
 - Active groundwater ET

- Deep Groundwater Recharge/Losses

Although observed values are not available for each of the water balance components listed above, the average annual values must be consistent with expected values for the region, as impacted by the individual land use categories. This is a separate consistency, or reality, check with data independent of the modeling (except for precipitation) to insure that land use categories and the overall water balance reflect local conditions.

Table 2-16 lists general calibration/validation tolerances or targets that have been provided to model users as part of HSPF training workshops over the past 10 years (e.g. Donigian, 2000). The values in the table attempt to provide some general guidance, in terms of the percent mean errors or differences between simulated and observed values, so that users can gauge what level of agreement or accuracy (i.e. very good, good, fair) may be expected from the model application.

The caveats at the bottom of the table indicate that the tolerance ranges should be applied to **mean** values and that individual events or observations may show larger differences and still be acceptable. In addition, the level of agreement to be expected depends on many site and application-specific conditions, including the data quality, purpose of the study, available

resources, and available alternative assessment procedures that could meet the study objectives.

Table 2-16 General Calibration/Validation Targets or Tolerances for HSPF Applications (Donigian, 2000)

	% Difference Between Simulated and Recorded Values		
	Very Good	Good	Fair
Hydrology/Flow	< 10	10 - 15	15 - 25
Sediment	< 20	20 - 30	30 - 45
Water Temperature	< 7	8 - 12	13 - 18
Water Quality/Nutrients	< 15	15 - 25	25 - 35
Pesticides/Toxics	< 20	20 - 30	30 - 40

CAVEATS: Relevant to monthly and annual values; storm peaks may differ more
 Quality and detail of input and calibration data
 Purpose of model application
 Availability of alternative assessment procedures
 Resource availability (i.e. time, money, personnel)

Figure 2-16 provides value ranges for both correlation coefficients (R) and coefficient of determination (R²) for assessing model performance for both daily and monthly flows. The figure shows the range of values that may be appropriate for judging how well the model is performing based on the daily and monthly simulation results. As shown, the ranges for daily values are lower to reflect the difficulties in exactly duplicating the timing of flows, given the uncertainties in the timing of model inputs, mainly precipitation.

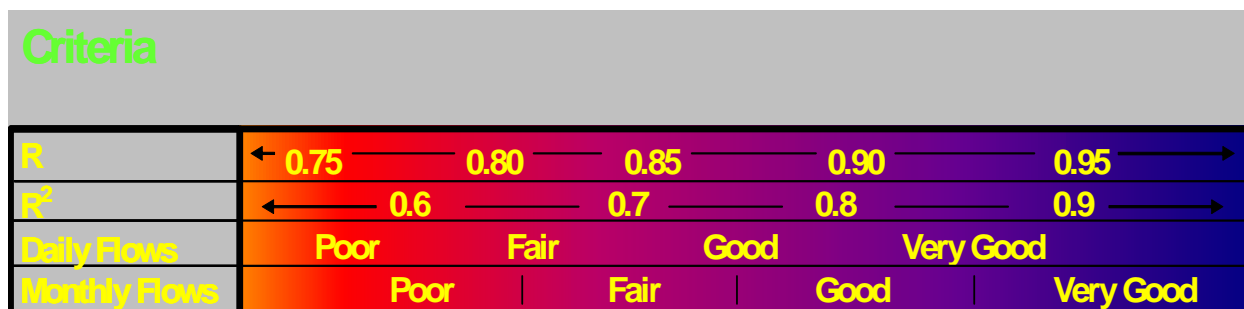


Figure 2-16 R and R² Value Ranges for Model Performance

Given the uncertain state-of-the-art in model performance criteria, the inherent errors in input and observed data, and the approximate nature of model formulations, **absolute** criteria for watershed model acceptance or rejection are not generally considered appropriate by most modeling professionals. And yet, most decision makers want definitive answers to the questions – “How accurate is the model?”, “Is the model good enough for this evaluation?”.

Consequently, for the IRW modeling effort, we have proposed that the targets and tolerance ranges for ‘Daily’ flows should correspond, at a minimum, to a ‘Fair to Good’ agreement, and

those for ‘**Monthly**’ flows should correspond to ‘**Good to Very Good**’ agreement for calibration. For the validation comparisons, we expect some decrease in model performance due to less dense gage coverage during for that time period. Thus we expect the validation results to correspond to the ‘**Fair to Good**’ ranges for both daily and monthly flows.

For any watershed modeling effort, the level of expected agreement is tempered by the complexities of the hydrologic system, the quality of the available precipitation and flow data, and the available information to help characterize the watershed and quantify the human impacts on water-related activities. These tolerances would be applied to comparisons of simulated and observed mean flows, annual runoff volumes, mean monthly and seasonal runoff volumes, and daily flow duration curves. Larger deviations would be expected for individual storm events and flood peaks in both space and time. The values shown above have been derived primarily from HSPF experience and selected past efforts on model performance criteria.

Flow Calibration and Validation Results

Complete flow calibration and validation results for all ten calibration sites (listed in Table 2-15 and shown in Figure 2-14) are provided in Appendix A. These results consist of a summary statistics table for all sites, and annual volumes and percent error table for each site, followed by flow duration and daily time series plots (arithmetic and log) for each site. Appendix A first presents the results for calibration and then validation.

Table 2-17 shows the calibration and validation summary statistics for all sites, while Tables 4.4 and 4.5 show the annual volume comparisons at the Stateline (Illinois River South of Siloam Springs – Reach 630) and at Tahlequah (Illinois River near Tahlequah OK – Reach 870), respectively.

Figure 2-17 and Figure 2-18 show the daily flow duration comparisons at Stateline and Tahlequah for calibration and validation periods respectively. Figure 2-19 and Figure 2-20 show the daily time series comparisons at the same sites for calibration and validation periods respectively. These results are extracted from Appendix A for ease of discussion herein.

Review of these results, compared to criteria in Table 2-16 and Figure 2-16, indicate the following:

- a. Annual flow comparison shows a Very Good or better calibration, with all the calibration volume errors less than 10%. The validation volume errors are higher, as is expected, with all the errors within 14%, except for Caney Creek which is an outlier at 40% error.
- b. The Monthly R2 and NSE (Nash-Sutcliff Efficiency) measures are consistently comparable, and are in the range of 0.65 to 0.91 (average of 0.80), corresponding to a Fair to Very Good range. The lowest values are primarily at one or two sites, which are commonly the smallest calibration sites (e.g., Sager Creek and Baron Fork at Dutch Mills). The smaller the site, the more it is impacted by errors in representative rainfall; more discussion is provided below.
- c. The Calibration Daily R2 values are consistently lower, as is expected, with an average value of 0.63, and a range of 0.50 to 0.78. This corresponds to a Poor/Fair to Good rating.
- d. The Annual Flow Volumes in Tables 4.4 and 4.5 (for Stateline and Tahlequah), and those in Appendix A, show a wide range in year-to-year differences, with the year 2006

especially problematic, usually over-simulated, for a number of the sites. Year 2006 was the second year of an extreme drought which may have contributed to the issues.

- e. The biggest challenge during the calibration was the occurrence of 'phantom' events in the NEXRAD data, showing daily rainfall totals of 10 to 20 inches or more, numerous times during the calibration period. An analysis of the NWS and Mesonet gages for their entire period of record, in both AR and OK, from about 1980 to 2010 identified only a single event with 8 inches of rainfall as the maximum daily observed during that period. Consequently, a number of the 'phantom' events were reviewed and compared to surrounding rainfall amounts, and their extreme values were adjusted accordingly, in order to minimize their impacts on the calibration. Similar efforts during the validation period were limited to two or three of the largest events with discrepancies, and it was obvious that additional phantom events existed. Available time and resources precluded a more extensive effort, and it was clear that the remaining issues likely impacted the accuracy of the validation as reflected in the statistics.

The flow-duration curves (Figure 2-17 and Figure 2-18) are one of the primary metrics for judging acceptance of model results, as they demonstrate the behavior of the model throughout the entire range of flows on the contributing watershed.

Figure 2-17 and Figure 2-18 show the flow duration curves for the Illinois River at the Stateline and Tahlequah, for both calibration and validation. It is clear that the calibration does a very good job of reproducing the observed flow duration curve at both sites, and a similar level of agreement is shown for the validation curves (Figure 2-18). In fact, for the Tahlequah site, the validation curve might be considered slightly better than the calibration curve, as the curves are almost indistinguishable for all flows above about 200 cfs.

- f. Not all the sites demonstrate such good agreement for the flow duration curves, as evidenced by other curves in Appendix A. It is common, especially for smaller sites, to show differences at low flows, high flows, or both; both of these extremes are also impacted by the accuracy of the measured flows at these extremes, which are common problems for flow gaging issues. Of the 10 calibration sites, the biggest differences in the calibration and validation flow duration curves appear to be at Illinois River at Savoie, Osage Creek near Elm Springs, Sager Creek near West Siloam Springs, and Caney Creek near Barber OK. It is likely that 'phantom' events contributed to some of the differences at these sites.

In summary, the model results show a Fair to Good overall calibration and validation, and in some cases (i.e., sites) a Very Good simulation, confirming that the overall model should provide a sound basis for subsequent water quality simulations. A number of sites could be further improved through additional analyses and assessment of the input rainfall data, and further calibration efforts might be warranted at selected sites if the model is used in any future efforts at the local scale to support watershed management efforts by either AR or OK.

Table 2-17 Calibration (top) and Validation (bottom) Summary Statistics

Reach	Calibration Statistics Name	Annual Flow (in)			Daily		Monthly		Daily Peaks % Diff	NSE	
		Sim	Obs	% Vol error	R	R ²	R	R ²		Daily	Monthly
150	Illinois River at Savoy, AR	14.59	13.77	5.97	0.81	0.65	0.91	0.83	-8.96	0.63	0.83
316	Osage Creek near Elm Springs, AR	18.64	17.07	9.18	0.77	0.59	0.88	0.77	0.72	0.48	0.74
516	Sager Creek near West Siloam Springs, OK	18.13	18.03	0.56	0.71	0.50	0.81	0.65	-12.84	0.40	0.65
523	Flint Creek near Kansas, OK	12.75	12.28	3.78	0.79	0.62	0.89	0.80	3.45	0.57	0.79
630	Illinois River South of Siloam Springs, AR	14.13	14.07	0.43	0.83	0.69	0.91	0.83	-8.44	0.67	0.82
640	Illinois River near Watts, OK	13.76	13.60	1.18	0.81	0.66	0.92	0.85	-3.48	0.63	0.84
706	Baron Fork at Dutch Mills, AR	14.81	15.10	-1.89	0.75	0.57	0.84	0.70	-8.46	0.49	0.69
746	Baron Fork at Eldon, OK	14.10	13.69	3.01	0.88	0.78	0.95	0.91	-6.91	0.78	0.91
870	Illinois River near Tahlequah, OK	13.57	13.74	-1.27	0.77	0.60	0.95	0.90	-11.77	0.58	0.88
912	Caney Creek near Barber, OK	14.20	13.18	7.70	0.79	0.62	0.90	0.81	4.44	0.57	0.80
Mean Values		14.87	14.45	2.87	0.79	0.63	0.90	0.80	-5.22	0.58	0.80

Reach	Validation Statistics Name	record starts	Annual Flow (in)			Daily		Monthly		Daily Peaks % Diff	NSE	
			Sim	Obs	% Vol error	R	R ²	R	R ²		Daily	Monthly
150	Illinois River at Savoy, AR	1996	13.64	14.40	-5.29	0.67	0.45	0.86	0.74	-22.63	0.29	0.73
316	Osage Creek near Elm Springs, AR	1996	17.85	15.86	12.55	0.71	0.50	0.89	0.79	-3.61	0.14	0.69
516	Sager Creek near West Siloam Springs, OK	1997	19.63	17.22	13.99	0.48	0.23	0.61	0.37	-34.63	0.00	0.31
523	Flint Creek near Kansas, OK	1993	16.75	15.34	9.18	0.67	0.44	0.84	0.71	-8.85	0.29	0.69
630	Illinois River South of Siloam Springs, AR	1996	13.43	14.95	-10.19	0.77	0.59	0.91	0.82	-16.46	0.57	0.81
640	Illinois River near Watts, OK	1992	16.79	16.30	2.97	0.78	0.62	0.90	0.81	18.45	0.46	0.80
706	Baron Fork at Dutch Mills, AR	1992	18.65	18.48	0.90	0.42	0.18	0.73	0.53	-0.71	-0.29	0.47
746	Baron Fork at Eldon, OK	1992	18.13	18.43	-1.65	0.85	0.73	0.93	0.87	-6.47	0.72	0.87
870	Illinois River near Tahlequah, OK	1992	16.40	16.20	1.24	0.75	0.57	0.91	0.84	-1.99	0.51	0.84
912	Caney Creek near Barber, OK	1998	20.52	14.71	39.52	0.83	0.69	0.93	0.87	59.18	0.32	0.74
Mean Values			17.18	16.19	6.10	0.69	0.50	0.85	0.73	-1.77	0.30	0.69

Table 2-18 Annual Flow Volumes in Inches for the Illinois River South of Siloam Springs (Reach 630) for the Calibration (top) and Validation (bottom) Periods

Year	Precipitation (in)	Simulated Flow (in)	Observed Flow (in)	Residual (in)	Percent Error
2001	47.60	15.46	14.23	1.22	8.60%
2002	41.70	14.85	14.24	0.61	4.30%
2003	35.70	8.70	7.32	1.37	18.73%
2004	45.87	16.65	15.13	1.52	10.06%
2005	30.25	10.26	10.42	-0.16	-1.50%
2006	46.26	11.23	6.92	4.31	62.36%
2007	34.04	9.83	10.42	-0.58	-5.57%
2008	53.43	20.79	26.09	-5.30	-20.31%
2009	54.27	19.36	21.83	-2.47	-11.32%
Mean	43.24	14.13	14.07	0.06	0.42%

Year	Precipitation (in)	Simulated Flow (in)	Observed Flow (in)	Residual (in)	Percent Error
1996	28.60	6.08	8.38	-2.31	-27.45%
1997	44.77	15.84	18.64	-2.80	-15.02%
1998	43.87	16.55	15.52	1.04	6.64%
1999	51.59	18.62	18.51	0.11	0.59%
2000	36.05	10.05	13.71	-3.66	-26.70%
Mean	40.98	13.43	14.95	-1.52	-10.19%

Table 2-19 Annual Flow Volumes in Inches for the Illinois River near Tahlequah (Reach 870) for the Calibration (top) and Validation (bottom) Periods

Year	Precipitation (in)	Simulated Flow (in)	Observed Flow (in)	Residual (in)	Percent Error
2001	46.01	13.42	14.77	-1.35	-9.17%
2002	41.06	13.01	12.16	0.84	6.94%
2003	36.20	7.91	6.83	1.07	15.72%
2004	48.19	16.86	16.59	0.27	1.63%
2005	31.14	9.69	10.20	-0.50	-4.93%
2006	45.11	9.44	6.12	3.32	54.15%
2007	36.57	10.01	10.52	-0.51	-4.85%
2008	56.93	22.93	26.36	-3.43	-13.02%
2009	53.81	18.84	20.11	-1.27	-6.33%
Mean	43.89	13.57	13.74	-0.17	-1.25%

Year	Precipitation (in)	Simulated Flow (in)	Observed Flow (in)	Residual (in)	Percent Error
1992	53.95	17.35	17.30	0.05	0.29%
1993	60.35	27.36	25.03	2.32	9.31%
1994	48.92	17.58	15.32	2.26	14.75%
1995	43.39	16.54	16.05	0.49	3.05%
1996	40.54	11.74	13.44	-1.70	-12.65%
1997	42.74	11.77	11.82	-0.05	-0.42%
1998	44.73	15.71	14.92	0.78	5.29%
1999	43.62	16.01	16.34	-0.33	-2.02%
2000	45.98	13.50	15.53	-2.02	-13.07%
Mean	47.14	16.40	16.19	0.20	1.24%

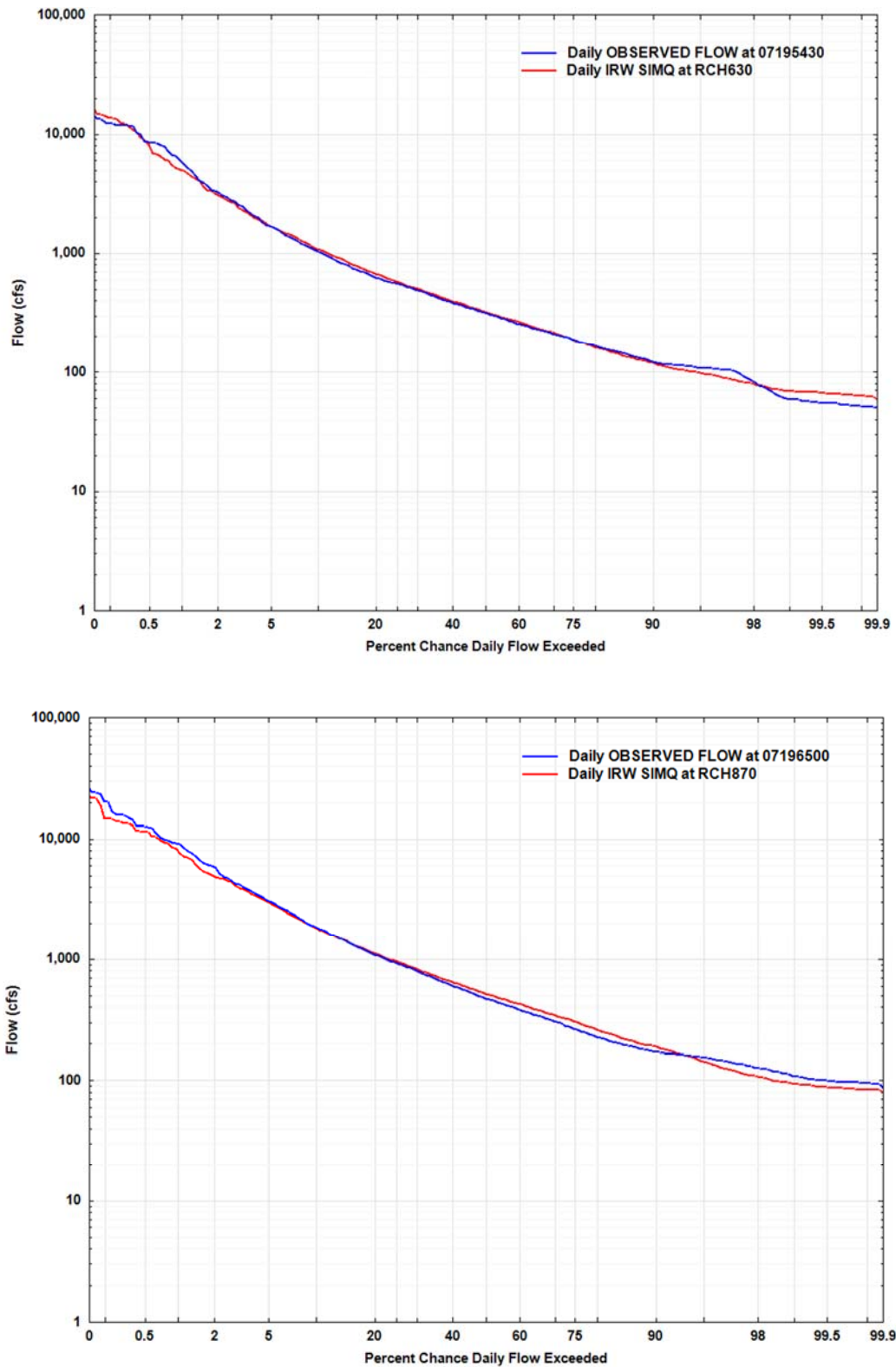


Figure 2-17 Daily Flow Duration Comparisons for the State Line (Reach 630) and Tahlequah (Reach 870) for the Calibration Period

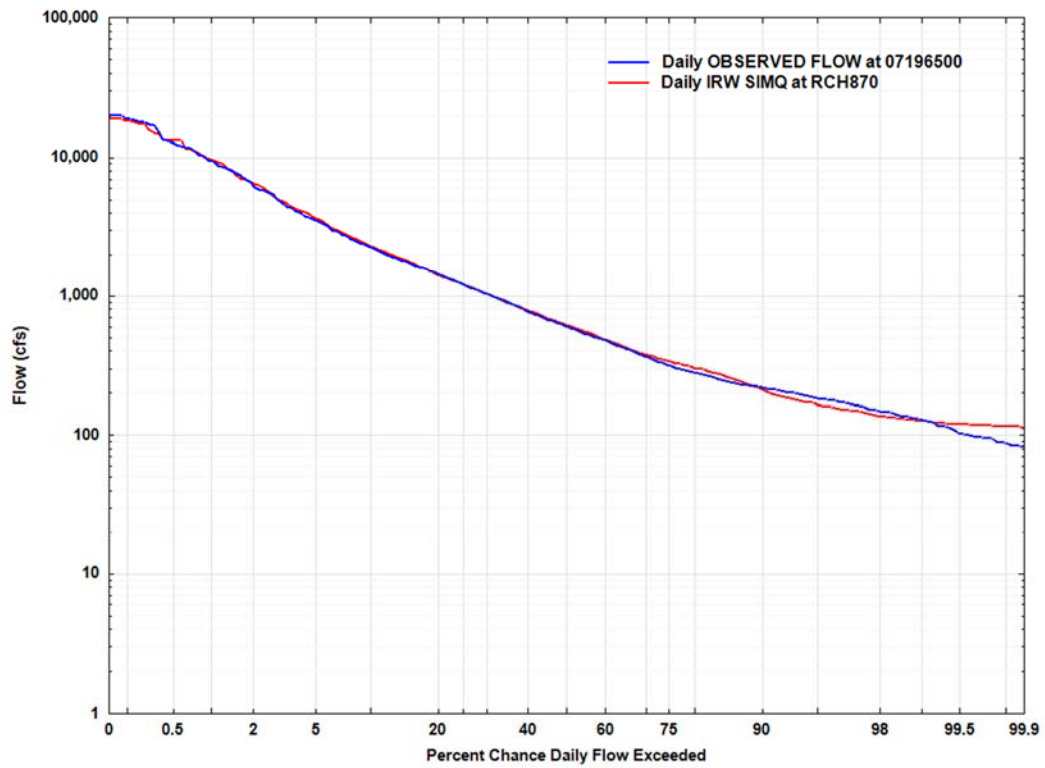
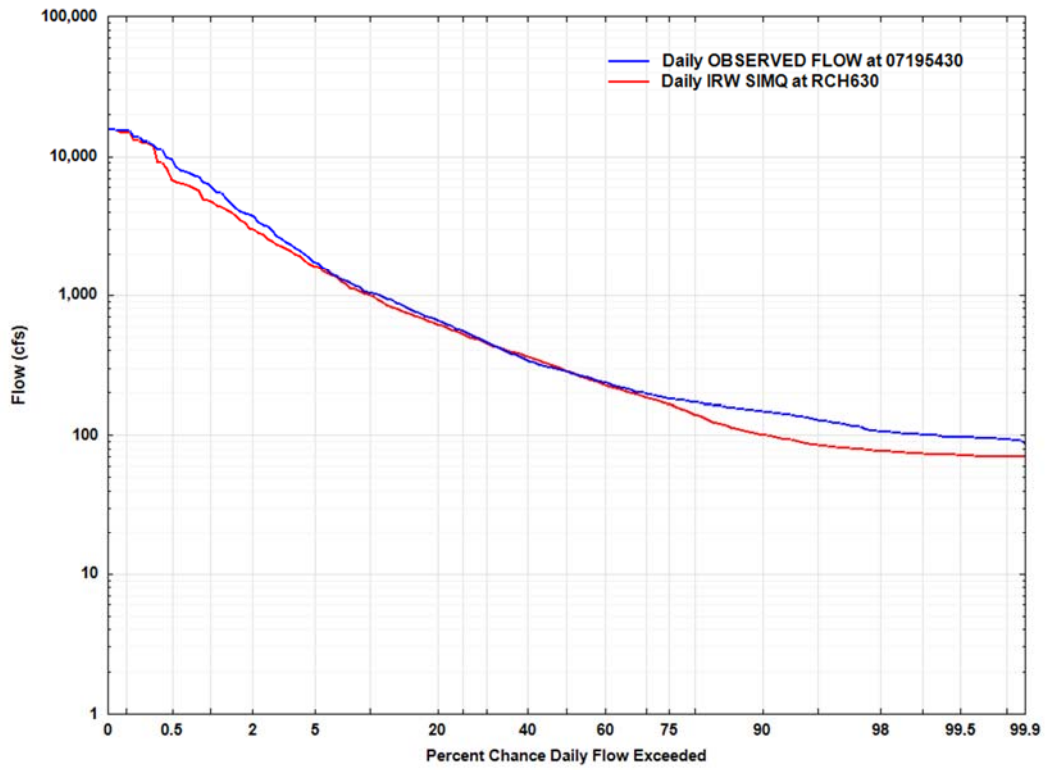


Figure 2-18 Daily Flow Duration Comparisons for the State Line (Reach 630) and Tahlequah (Reach 870) for the Validation Period

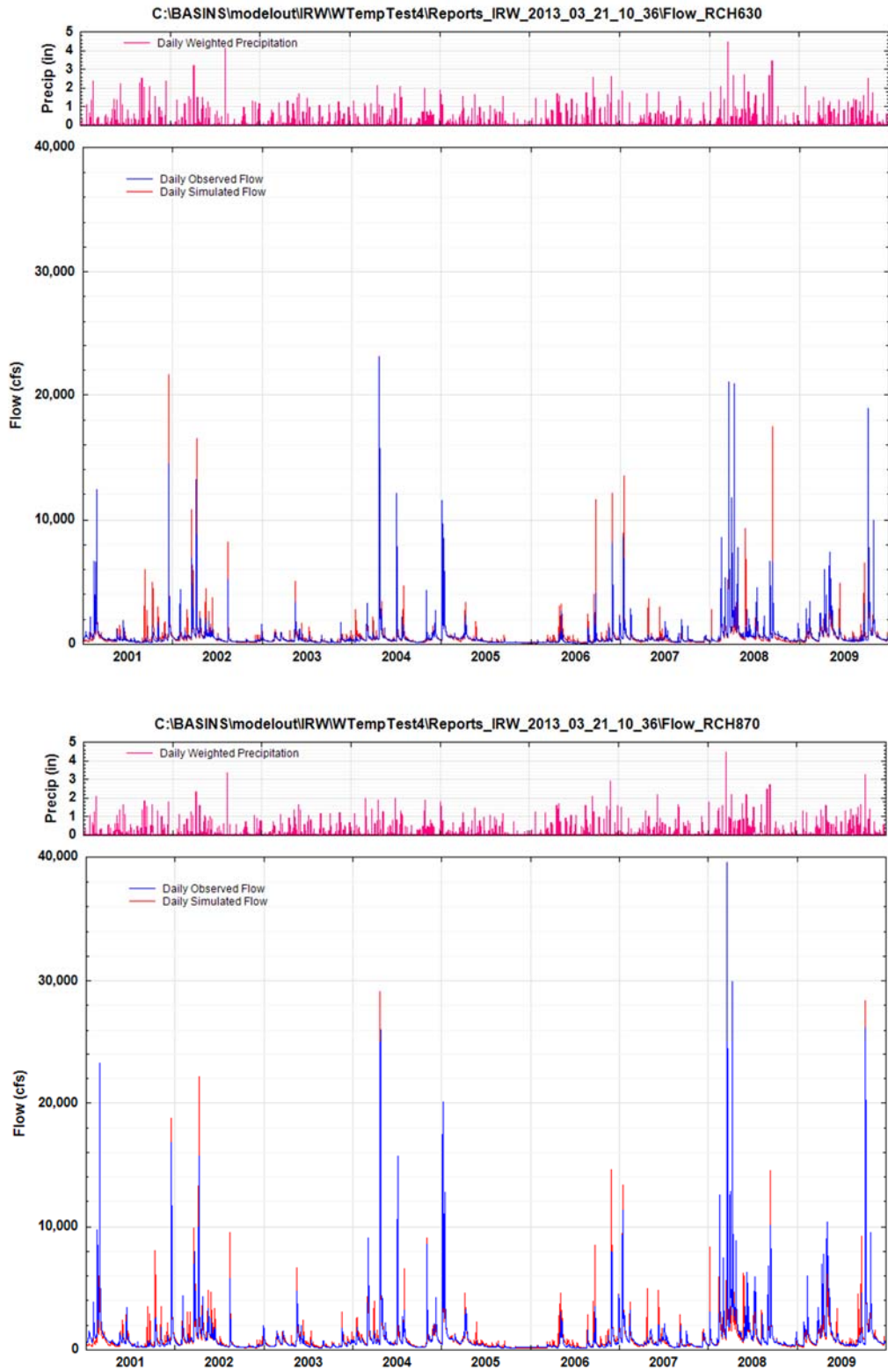


Figure 2-19 Daily Flow Time Series Comparisons for the State Line (Reach 630) and Tahlequah (Reach 870) for the Calibration Period

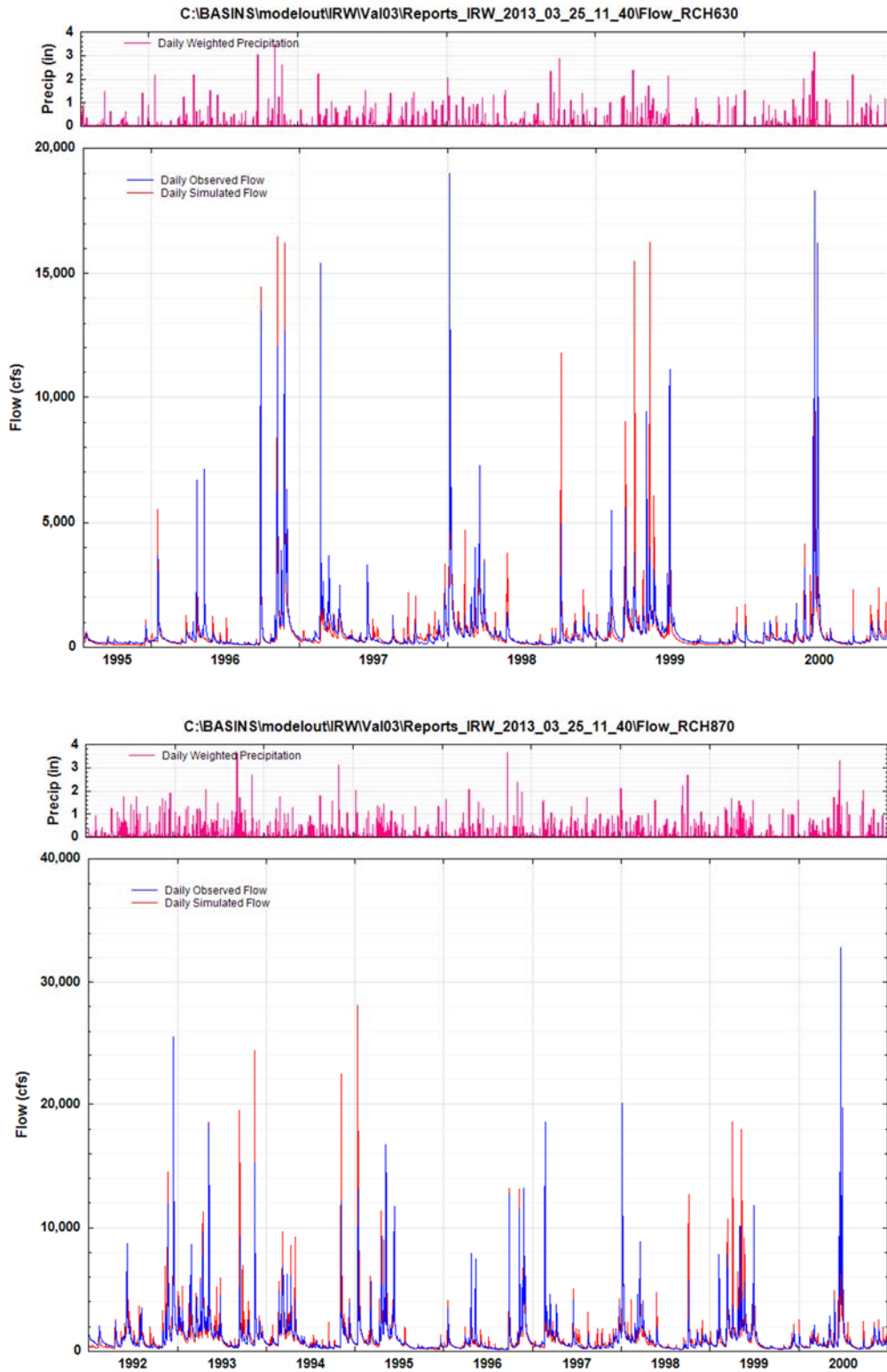


Figure 2-20 Daily Flow Time Series Comparisons for the State Line (Reach 630) and Tahlequah (Reach 870) for the Validation Period

2.6.3 Water Quality and Sediment Calibration Procedures and Comparisons

Water quality calibration is an iterative process; the model predictions are the integrated result of all the assumptions used in developing the model input and representing the modeled sources and processes. Differences in model predictions and observations require the model user to re-evaluate these assumptions, in terms of both the estimated model input and parameters, and consider the accuracy and uncertainty in the observations. At the current time, water quality calibration is more an art than a science, especially for comprehensive simulations of nonpoint, point, and atmospheric sources, and their impacts on instream water quality.

The following steps were performed at each of the calibration stations, following the hydrologic calibration and validation, and after the completion of input development for point source, atmospheric, and other contributions:

- A. Estimate all model parameters, including land use specific accumulation and depletion/removal rates, washoff rates, and subsurface concentrations
- B. Tabulate, analyze, and compare simulated annual nonpoint loading rates with the expected range of nonpoint loadings from each land use (and each constituent) and adjust loading parameters when necessary
- C. Calibrate instream water temperature to observed data
- D. Compare simulated and observed instream concentrations at each of the calibration stations, and compare simulated and estimated loads where available
- E. Analyze the results of comparisons in steps B, C, and D to determine appropriate instream and/or nonpoint parameter adjustments needed until model performance targets are achieved

The essence of watershed water quality calibration is to obtain acceptable agreement of observed and simulated concentrations (i.e. within defined criteria or targets), while maintaining the instream water quality parameters within physically realistic bounds, and the nonpoint loading rates within the expected ranges from the literature. The nonpoint loading rates, sometimes referred to as 'export coefficients' are highly variable, with value ranges sometimes up to an order of magnitude, depending on local and site conditions of soils, slopes, topography, climate, etc.

Sediment and Water Temperature Calibration Results

As noted above, water quality calibration begins with calibration of the nonpoint loading rates to available data and expected, or 'target', loading rates which will vary by location within the watershed (i.e., soils, slope, land cover) and land use. Sediment calibration follows analogous procedures in that target sediment loading rates are developed and used to guide the sediment loading rate calibration, as defined in Step B (above). Below we describe Steps B, C, and D as they apply to the sediment calibration, followed by the water temperature calibration and validation. Appendix B presents the complete sediment calibration results, while Appendix C presents the water temperature calibration and validation results.

Sediment Loading Rate Calibration

Development of sediment target loading rates is the first step following initial sediment model parameterization. In most cases, model users must rely on prior and nearby model applications or any available small site monitoring that may be applicable to the watershed being modeled. There are calculation procedures available to help develop target rates as a function of land use and land cover, such as the USDA Universal Soil Loss Equation (USLE) and other estimation

techniques (see Donigian and Love (2003) for discussion and guidance). These rates will vary by soils, slope, land cover, land use, etc), as noted above, but rates are so highly variable that we are normally only able to estimate a range of rates by land use. During calibration the sediment erosion model parameters are adjusted to produce the final rates within the target range, while producing TSS concentrations, and any available loading data, within the range of the observations. In most case, the only observations will be instream TSS concentrations, so the calibration procedure involves adjustments to both the loading rates and instream sediment transport parameters, until overall agreement is reached. Table 2-20 presents the final sediment loading rates resulting from this iterative calibration effort, by land use category across the top, and by meteorologic segment (yellow highlighted numbers and blue station designations, in the first two columns). Along the bottom of the table is the mean, maximum, and minimum rates across the IRW, and the high and low 'Target Rates' by land use are shown in the final two rows.

Table 2-20 demonstrates a significant range in sediment loading rates across the IRW even within a single land use category. This is primarily due to both slope and precipitation variations. These ranges are generally consistent with the target ranges but occasionally will fall outside the target range. Overall, the rates are consistent with available information on sediment loading and past modeling studies in the Midwest.

Instream Sediment Calibration Results

Sediment, or TSS (Total Suspended Solids), is often considered the most difficult and challenging water quality constituents to model. Lack of adequate sediment data, especially during storm events, lack of bed characterization data which has a major influence on the model results, and lack of sediment particle size information for both bed materials and storm samples all contribute to the difficulties in accurately simulating TSS. For these reasons, and others, simulated and observed TSS values are commonly displayed with a logarithmic scale, demonstrating the wide range in values commonly observed. In Figure 2-21 through Figure 2-24, we provide TSS model results for selected sites showing both the arithmetic scale (top graph) and the log scale (bottom graph) to demonstrate the visual differences when assessing model results. Complete results for all calibration sites are provided in Appendix B (separate document).

Figure 2-21 and Figure 2-22 show TSS model comparisons for Osage Creek and Ballard Creek, respectively; note that Ballard Creek was not one of our flow calibration sites as it is not a USGS site and does not have a continuous flow record. Data for Ballard Creek were provided by Brian Haggard at AWRC. Figure 2-23 and Figure 2-24 show TSS model comparisons for the Stateline (Reach 630) and Tahlequah (Reach 870), respectively; for the Stateline (Illinois River south of Siloam Springs, USGS gage 07196900) data were provide by both USGS (blue dots) and AWRC (green dots).

In reviewing these Sediment/TSS results, the calibration objective is usually to attempt to match the range of concentrations in the observed data and the general pattern and magnitude of observed TSS data for both storm and non-storm periods; it is usually difficult, if not impossible to force the model to match or approximate each of the observed data points. In addition to these comparisons, the sediment calibration also involves analyzing each stream reach for the behavior and composition of the sediment bed to ensure proper behavior; that includes identifying stream sections where bank erosion is known to occur and adjusting reach parameters so that those losses are represented, and maintaining stable or depositional behavior in other reaches based on observations and literature information. Table 2-21Table 2-20 shows the instream sediment balance we review as part of the calibration to ensure that all the individual reaches are behaving appropriately, and as expected, based on available

information. The balance involves checking each reach simulation, from upstream to downstream in sequence for each tributary and mainstem reach, and assessing the nonpoint and point contributions, the degree of deposition and scour, especially in reaches known to experience bed/bank erosion, the degree of erosion and deposition, and the calculated trapping efficiencies. If individual reaches produce anomalous behavior, parameters are adjusted and the simulation is repeated.

Table 2-20 Annual Sediment Loading Rates (tons/acre/year) for the IRW

Land Use Code	Land Use Name	PERLND										IMPLND		
		1	2	3	4	5	6	7	8	9	10	6	7	8
		Forest	Pasture1 / Litter	Pasture2	Pasture3	Grass/Shrub/Barren	Developed, Open	Developed, Low	Developed, Med/High	Wetlands	Cropland	Developed, Open	Developed, Low	Developed, Med/High
20	PCP_18	0.118	0.521	0.874	1.022	0.688	0.399	0.428	0.581	0.036	2.118	0.138	0.198	0.310
40	PCP_24	0.070	0.591	0.754	0.731	0.610	0.247	0.283	0.396	0.014	1.351	0.134	0.191	0.294
60	PCP_26	0.119	0.640	0.772	0.854	0.779	0.280	0.329	0.477	0.019	1.669	0.137	0.196	0.304
80	Stillwell 5 NNW	0.075	0.480	0.527	0.431	0.479	0.207	0.259	0.328	0.001	0.927	0.124	0.180	0.279
100	PCP_11	0.120	0.577	0.570	0.659	0.653	0.213	0.251	0.362	0.003	1.895	0.136	0.195	0.297
120	PCP_06	0.007	0.225	0.226	0.264	0.406	0.160	0.186	0.269	0.002	0.582	0.132	0.186	0.283
140	Westville	0.048	0.464	0.457	0.505	0.510	0.167	0.202	0.296	0.001	0.879	0.122	0.176	0.270
160	PCP_12	0.064	0.387	0.384	0.447	0.510	0.154	0.180	0.259	0.001	1.270	0.135	0.194	0.298
180	PCP_17	0.071	0.379	0.381	0.441	0.528	0.196	0.233	0.334	0.004	1.622	0.134	0.193	0.297
200	PCP_09	0.006	0.193	0.198	0.232	0.343	0.142	0.164	0.234	0.002	0.733	0.129	0.185	0.285
220	PCP_07	0.008	0.215	0.220	0.257	0.365	0.150	0.177	0.253	0.001	0.773	0.129	0.185	0.281
240	PCP_21	0.008	0.311	0.317	0.348	0.394	0.167	0.195	0.281	0.001	0.731	0.131	0.188	0.291
260	PCP_16	0.004	0.237	0.237	0.306	0.394	0.130	0.156	0.226	0.002	0.513	0.133	0.191	0.292
280	PCP_14	0.055	0.339	0.389	0.429	0.562	0.190	0.223	0.321	0.005	1.393	0.134	0.195	0.303
300	PCP_05	0.005	0.162	0.169	0.197	0.311	0.115	0.137	0.195	0.001	0.417	0.133	0.191	0.295
320	Cookson	0.063	0.635	0.678	0.553	0.521	0.217	0.261	0.331	0.003	1.487	0.123	0.177	0.279
340	PCP_10	0.010	0.305	0.313	0.359	0.413	0.181	0.212	0.308	0.003	0.929	0.131	0.188	0.288
360	PCP_23	0.052	0.487	0.499	0.549	0.515	0.255	0.287	0.405	0.013	1.110	0.130	0.188	0.291
380	PCP_22	0.023	0.164	0.250	0.239	0.399	0.128	0.189	0.208	0.001	0.634	0.133	0.192	0.295
400	PCP_08	0.087	0.653	0.751	0.816	0.727	0.254	0.302	0.430	0.014	1.495	0.134	0.191	0.292
420	PCP_15	0.126	0.527	0.569	0.559	0.526	0.189	0.223	0.323	0.006	1.280	0.134	0.192	0.291
440	PCP_02	0.019	0.205	0.274	0.239	0.329	0.116	0.138	0.199	0.001	0.476	0.133	0.190	0.290
460	PCP_00	0.051	0.242	0.360	0.342	0.615	0.172	0.254	0.281	0.004	1.178	0.137	0.199	0.310
480	PCP_03	0.027	0.272	0.426	0.403	0.697	0.218	0.322	0.356	0.002	0.945	0.138	0.200	0.311
500	PCP_19	0.006	0.169	0.203	0.201	0.310	0.127	0.151	0.218	0.001	0.649	0.136	0.196	0.302
520	PCP_04	0.122	0.589	0.716	0.800	0.568	0.217	0.256	0.368	0.011	1.340	0.136	0.195	0.302
540	PCP_10	0.018	0.188	0.230	0.230	0.278	0.110	0.129	0.185	0.010	0.521	0.133	0.192	0.295
560	Kansas 2 NE	0.050	0.385	0.447	0.434	0.514	0.169	0.198	0.283	0.001	0.954	0.137	0.198	0.309
580	PCP_13	0.013	0.200	0.241	0.240	0.364	0.131	0.153	0.219	0.006	0.563	0.136	0.195	0.297
600	PCP_01	0.042	0.421	0.488	0.480	0.448	0.172	0.205	0.291	0.002	1.084	0.132	0.188	0.287
620	Tahlequah	0.021	0.284	0.321	0.310	0.399	0.100	0.119	0.170	0.000	0.754	0.126	0.180	0.273
640	Webbers	0.048	0.281	0.294	0.295	0.232	0.082	0.096	0.138	0.004	0.940	0.126	0.179	0.274
660	Odell 2N	0.132	0.731	0.745	0.776	0.628	0.187	0.221	0.304	0.019	1.875	0.136	0.198	0.305
	Mean	0.051	0.378	0.433	0.453	0.485	0.180	0.216	0.298	0.006	1.063	0.132	0.190	0.293
	Max	0.132	0.731	0.874	1.022	0.779	0.399	0.428	0.581	0.036	2.118	0.138	0.200	0.311
	Min	0.004	0.162	0.169	0.197	0.232	0.082	0.096	0.138	0.000	0.417	0.122	0.176	0.270
	Target Rates (low)	0.05	0.50	0.50	0.50	0.30	0.15	0.15	0.25	0.00	1.00	0.05	0.10	0.20
	Target Rates (high)	0.15	1.50	1.50	1.50	1.00	0.30	0.30	0.50	0.01	3.00	0.25	0.50	0.50

With these issues in mind, our review of these results (and those included in Appendix B), indicates the following:

- a. The Osage Creek simulation in Figure 2-21 is a good example of the impact of limited observed data. For most of the simulation period, through 2006, the data are limited to bi-monthly monitoring often during low flow periods. During this time, the model simulates storm events with high concentrations up to 1,000 mg/l or more, whereas the observations are all 100 mg/l or less. When more frequent monitoring, including storm events, started in 2007, the observations show a wider range of concentrations with peaks reaching 800 to 1,000 mg/l (with a single observation up to 2,000 mg/l), demonstrating much better agreement with the simulated values. This supports the contention that the simulation for the earlier period, 2001 to 2006, is likely a better representation of expected TSS concentrations and behavior than the observations during that time period.
- b. The bottom plot in Figure 2-21 with a log scale also demonstrates the high variability in both the model and the data, and supports the contention that the simulation is an overall good representation for Osage Creek. The model results span the entire range of the observed data when more frequent samples, including storm events, are collected, and the model shows the same extreme variability with day-to-day dynamic swings of almost 3 orders of magnitude. These results are clearly a good representation of the sediment behavior in the watershed.
- c. Ballard Creek, in Figure 2-22, demonstrates very similar behavior as Osage Creek although observed peaks are all less than 1,000 mg/l. Considering the high flows simulated in 2002, the simulated peak of about 1,400 mg/l is realistic, given the lack of observed data that year.
- d. The TSS simulations for the Stateline (Figure 2-23) and Tahlequah (Figure 2-24) are consistent with the available observed data and with the simulations at the other sites. The model provides a good representation of TSS data at both of these sites, and most of the other calibration sites as presented in Appendix B.

Note that sediment validation was intended as part of the water quality validation; however, the lack of litter and nutrient application data during the validation period precluded that effort. If historic data is made available for the earlier 1992-2000 validation period, it is recommended that sediment and water quality validation efforts be implemented, if resources allow.

With the sediment calibration results included in Appendix B and discussed in this section, the IRW model provides a good representation of the sediment/TSS behavior within the IRW and a sound basis for the subsequent water quality calibration.

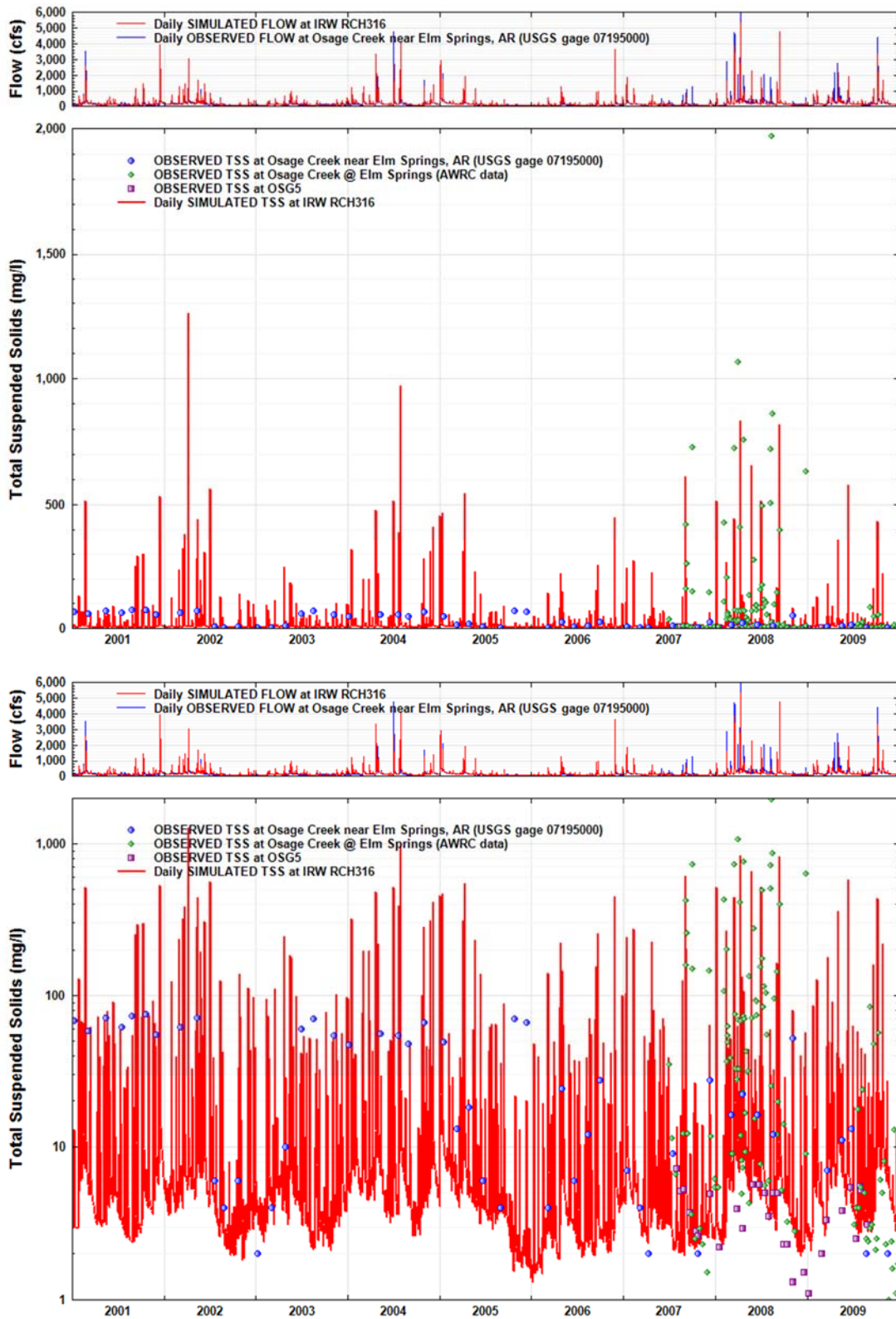


Figure 2-21 Sediment Calibration Plots for Osage Creek (Reach 316)

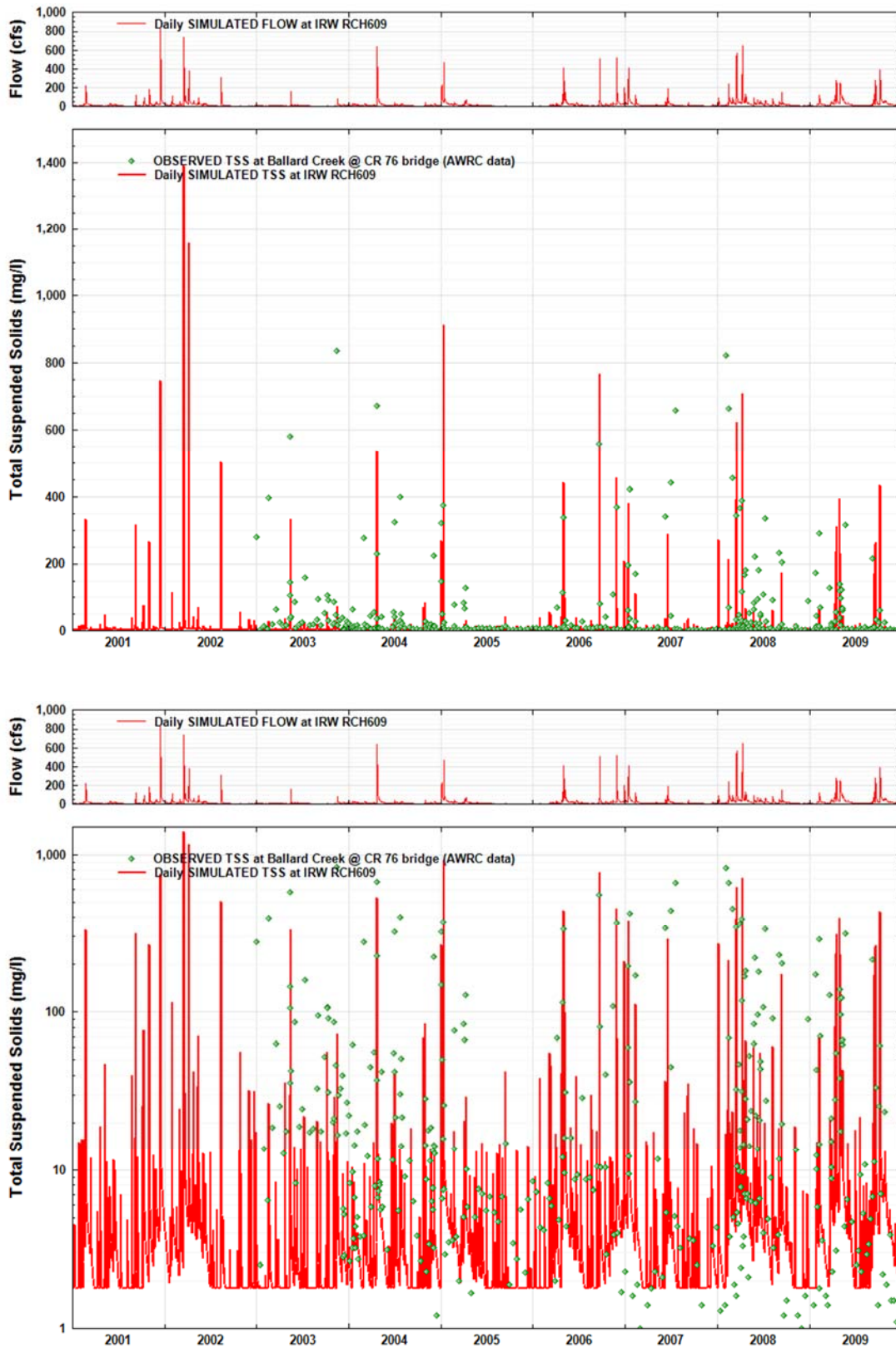


Figure 2-22 Sediment Calibration Plots for Ballard Creek (Reach 609)

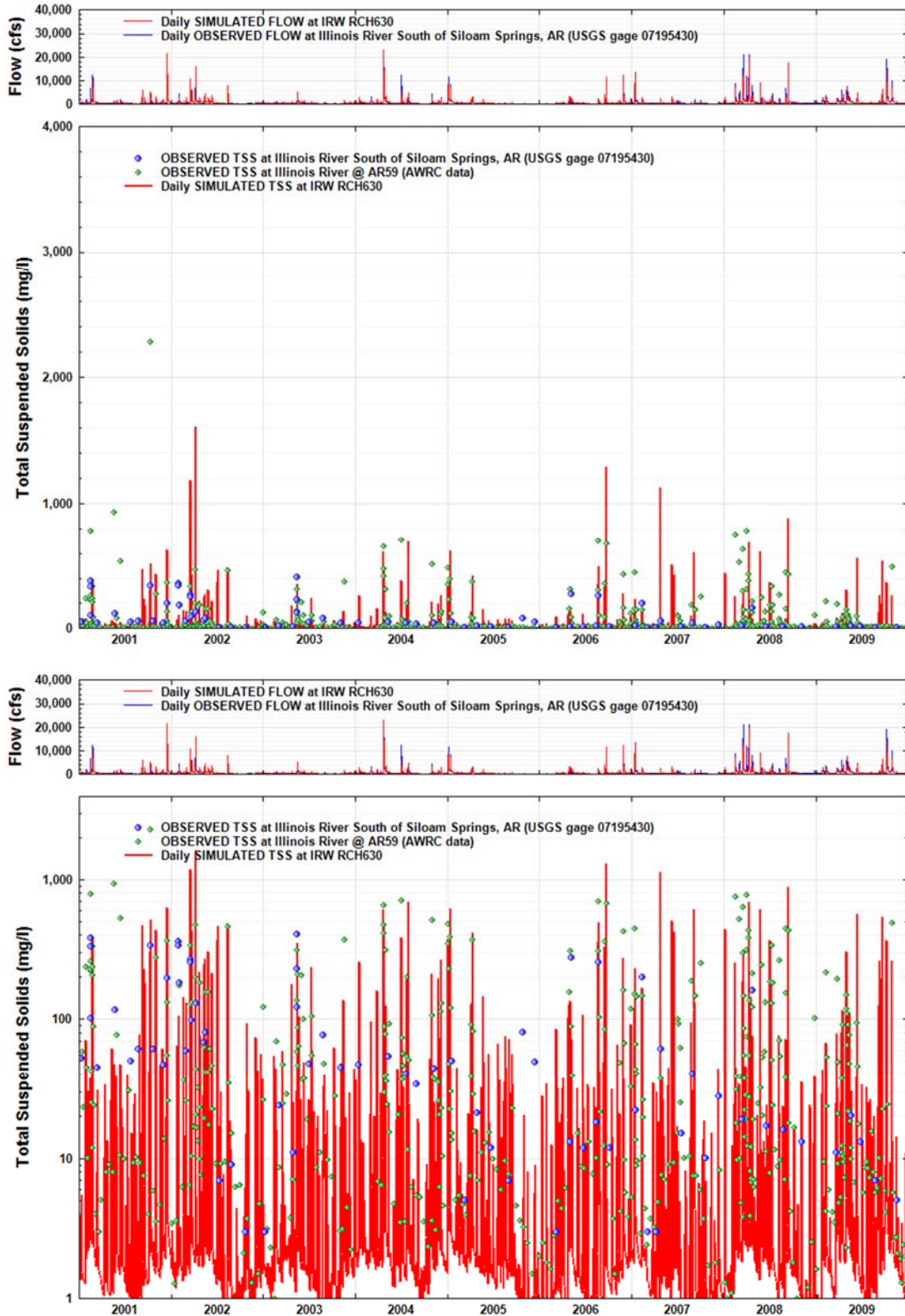


Figure 2-23 Sediment Calibration Plots for Illinois River south of Siloam Springs (Reach 630)

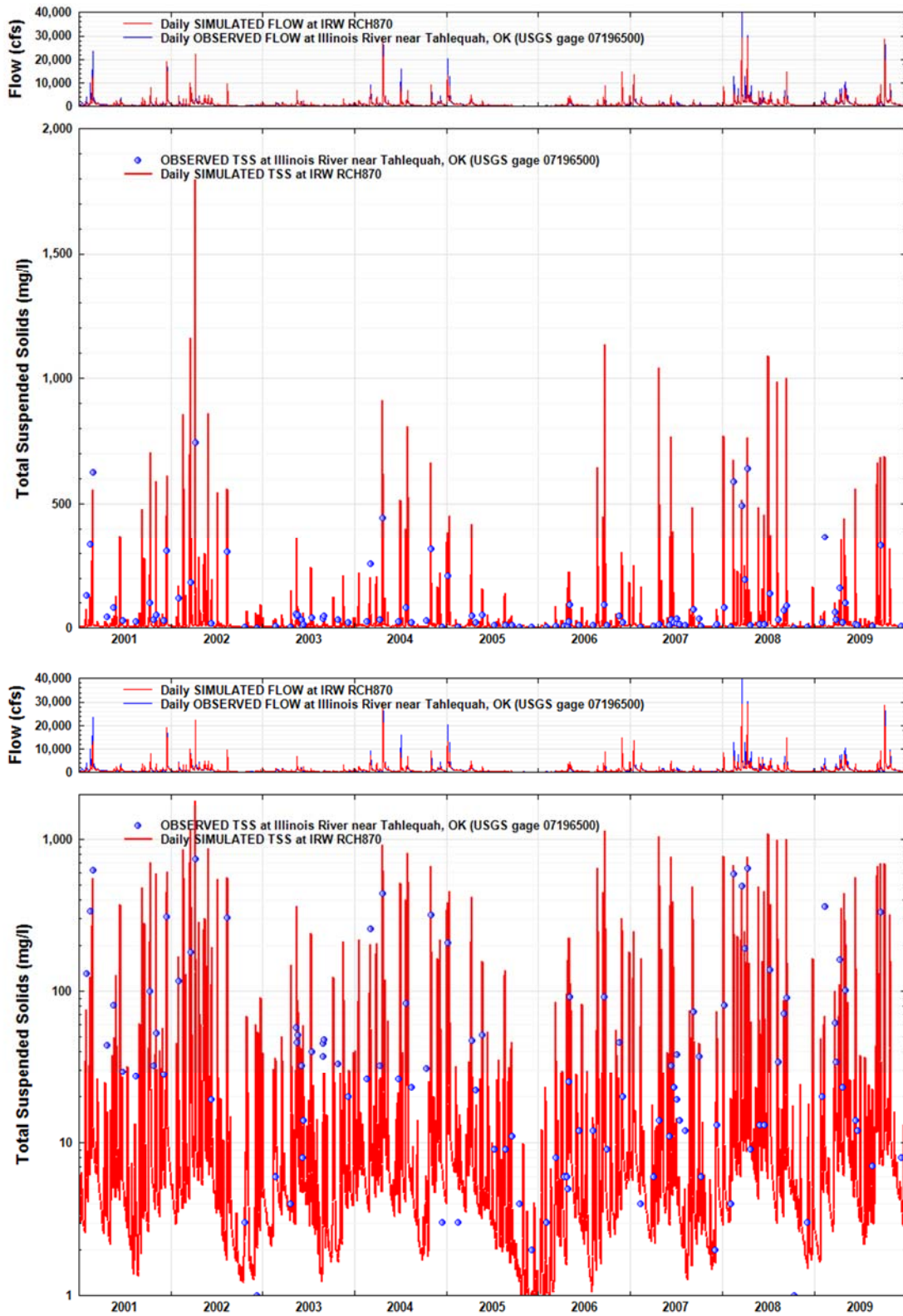


Figure 2-24 Sediment Calibration Plots for Illinois River near Tahlequah (Reach 870)

Table 2-21 Instream Reach Sediment Balance for IRW

Reach Segment	Nonpoint (tons)	Point Source (tons)	Upstream In (tons)	Total Inflow (tons)	Outflow (tons)	Dep(+)/Scour(-) (tons)	Cumulative Total (tons)	Cumulative Trapping (%)	Reach Trapping (%)
RCHRES 100 - Illinois River	4,147	0	0	4,147	4,457	-311	4,147	-7.5	-7.5
RCHRES 101 - Farmington Creek	810	0	0	810	865	-55	810	-6.8	-6.8
RCHRES 102 - Goose Creek	474	1	0	475	527	-52	475	-10.9	-10.9
RCHRES 104 - Goose Creek	2,047	0	1,393	3,439	3,537	-97	3,332	-6.1	-2.8
RCHRES 108 - Hickory Creek	2,399	0	0	2,399	2,557	-158	2,399	-6.6	-6.6
RCHRES 110 - Illinois River	3,413	0	4,457	7,870	7,930	-60	7,559	-4.9	-0.8
RCHRES 120 - Illinois River	3,063	0	10,487	13,550	13,560	-9	13,022	-4.1	-0.1
RCHRES 130 - Illinois River	1,973	0	13,560	15,532	15,653	-121	14,994	-4.4	-0.8
RCHRES 140 - Illinois River	793	0	19,190	19,982	19,622	360	19,119	-2.6	1.8
RCHRES 150 - Illinois River	388	0	39,608	39,996	39,469	527	37,148	-6.3	1.3
RCHRES 160 - Illinois River	2,082	0	51,399	53,480	52,662	819	50,128	-5.1	1.5
RCHRES 202 - Clear Creek	1,490	0	0	1,490	1,614	-124	1,490	-8.3	-8.3
RCHRES 204 - Mud Creek	3,152	19	0	3,171	3,439	-268	3,171	-8.5	-8.5
RCHRES 206 - Clear Creek	1,709	0	5,053	6,761	6,949	-188	6,370	-9.1	-2.8
RCHRES 208 - Little Wildcat Creek	1,261	0	0	1,261	1,403	-142	1,261	-11.2	-11.2
RCHRES 212 - Clear Creek	803	0	8,351	9,155	9,127	27	8,434	-8.2	0.3
RCHRES 214 - Hamestrung Creek	1,990	0	0	1,990	2,314	-324	1,990	-16.3	-16.3
RCHRES 216 - Clear Creek	475	0	11,441	11,916	11,930	-14	10,898	-9.5	-0.1
RCHRES 302 - Osage Creek	4,863	0	0	4,863	6,419	-1,556	4,863	-32.0	-32.0
RCHRES 304 - Osage Creek	1,900	44	6,419	8,363	9,359	-996	6,807	-37.5	-11.9
RCHRES 306 - Spring Creek	1,332	0	0	1,332	2,042	-710	1,332	-53.3	-53.3
RCHRES 308 - Spring Creek	2,845	72	2,042	4,959	5,838	-879	4,249	-37.4	-17.7
RCHRES 312 - Little Osage Creek	4,016	0	0	4,016	5,169	-1,153	4,016	-28.7	-28.7
RCHRES 314 - Little Osage Creek	4,831	0	5,169	10,000	10,364	-364	8,846	-17.2	-3.6
RCHRES 316 - Osage Creek	581	0	25,561	26,143	27,697	-1,555	20,484	-35.2	-6.0
RCHRES 318 - Brush Creek	830	0	0	830	1,089	-259	830	-31.2	-31.2
RCHRES 322 - Brush Creek	1,618	0	1,089	2,707	3,275	-568	2,448	-33.8	-21.0
RCHRES 324 - Osage Creek	1,828	0	27,697	29,525	28,354	1,171	22,312	-27.1	4.0
RCHRES 326 - Osage Creek	3,581	0	31,629	35,210	34,842	368	28,340	-22.9	1.0
RCHRES 402 - Muddy Fork	1,298	0	0	1,298	1,518	-220	1,298	-17.0	-17.0
RCHRES 404 - Blair Creek	1,856	0	0	1,856	2,613	-756	1,856	-40.8	-40.8
RCHRES 406 - Muddy Fork	2,784	0	4,131	6,914	6,874	40	5,938	-15.8	0.6
RCHRES 408 - Muddy Fork	1,577	4	6,874	8,455	8,852	-397	7,518	-17.7	-4.7
RCHRES 412 - Moores Creek	3,257	0	0	3,257	4,108	-851	3,257	-26.1	-26.1
RCHRES 414 - Moores Creek	3,667	0	4,108	7,775	8,141	-366	6,924	-17.6	-4.7
RCHRES 416 - Muddy Fork	2,771	0	16,993	19,764	19,513	251	17,213	-13.4	1.3
RCHRES 418 - STREAM 418	336	0	0	336	350	-13	336	-4.0	-4.0
RCHRES 420 - STREAM 420	91	0	350	441	473	-32	428	-10.6	-7.2
RCHRES 502 - Flint Creek	1,603	0	0	1,603	1,769	-167	1,603	-10.4	-10.4
RCHRES 504 - Flint Creek	1,469	0	1,769	3,238	3,520	-282	3,072	-14.6	-8.7
RCHRES 505 - Little Flint Creek	1,795	0	0	1,795	1,923	-127	1,795	-7.1	-7.1
RCHRES 506 - SWEPCO Lake	1,300	8	1,923	3,231	2,923	308	3,104	5.8	9.5
RCHRES 507 - Little Flint Creek	387	0	2,923	3,310	3,368	-58	3,491	3.5	-1.8
RCHRES 508 - Flint Creek	372	0	3,520	3,892	3,706	186	3,443	-7.6	4.8
RCHRES 512 - Flint Creek	1,596	0	7,074	8,670	8,689	-19	8,530	-1.9	-0.2
RCHRES 514 - Sager Creek	4,075	0	0	4,075	4,372	-297	4,075	-7.3	-7.3
RCHRES 515 - STREAM 515	604	0	0	604	644	-40	604	-6.6	-6.6
RCHRES 516 - Sager Creek	968	41	5,016	6,025	5,741	284	5,688	-0.9	4.7
RCHRES 518 - Flint Creek	3,471	0	14,430	17,900	17,900	0	17,688	-1.2	0.0
RCHRES 522 - Flint Creek	2,664	0	17,900	20,564	20,086	478	20,352	1.3	2.3
RCHRES 523 - Flint Creek	91	0	20,086	20,177	20,292	-115	20,444	0.7	-0.6
RCHRES 524 - Flint Creek	930	0	20,292	21,222	21,138	85	21,374	1.1	0.4
RCHRES 600 - Illinois River	2,209	0	87,504	89,713	87,567	2,146	80,676	-8.5	2.4
RCHRES 602 - Weddington Creek	2,322	0	0	2,322	2,596	-274	2,322	-11.8	-11.8
RCHRES 604 - Cincinnati Creek	2,045	0	0	2,045	2,288	-243	2,045	-11.9	-11.9
RCHRES 606 - Cincinnati Creek	510	0	4,884	5,394	5,333	61	4,877	-9.4	1.1
RCHRES 608 - Ballard Creek	2,334	0	0	2,334	3,177	-843	2,334	-36.1	-36.1
RCHRES 609 - Ballard Creek	201	0	3,177	3,379	3,497	-118	2,536	-37.9	-3.5
RCHRES 610 - Illinois River	548	0	87,567	88,116	88,577	-461	81,225	-9.1	-0.5
RCHRES 612 - Ballard Creek	566	0	3,497	4,063	4,105	-41	3,102	-32.3	-1.0

Table 2-21 (continued)

Reach Segment	Nonpoint (tons)	Point Source (tons)	Upstream In (tons)	Total Inflow (tons)	Outflow (tons)	Dep(+)/Scour(-) (tons)	Cumulative Total (tons)	Cumulative Trapping (%)	Reach Trapping (%)
RCHRES 614 - Ballard Creek	3,589	0	4,105	7,693	8,463	-770	6,691	-26.5	-10.0
RCHRES 620 - Illinois River	707	0	88,577	89,283	88,240	1,043	81,931	-7.7	1.2
RCHRES 630 - Illinois River	30	0	93,573	93,603	92,924	679	86,838	-7.0	0.7
RCHRES 635 - Illinois River	99	0	92,924	93,023	92,116	907	86,937	-6.0	1.0
RCHRES 637 - Illinois River	510	0	100,580	101,090	100,340	753	94,137	-6.6	0.8
RCHRES 638 - STREAM 638	233	0	0	233	264	-31	233	-13.5	-13.5
RCHRES 639 - STREAM 639	163	0	264	427	437	-10	396	-10.5	-2.4
RCHRES 640 - Illinois River	35	0	100,770	100,680	101,450	-765	94,444	-7.4	-0.8
RCHRES 650 - Illinois River	905	0	101,450	102,350	102,380	-23	95,349	-7.4	0.0
RCHRES 660 - Illinois River	5,172	0	102,380	107,550	113,640	-6,086	100,520	-13.1	-5.7
RCHRES 670 - Illinois River	2,010	0	113,640	115,650	112,900	2,748	102,530	-10.1	2.4
RCHRES 702 - Jordan Creek	2,037	0	0	2,037	2,169	-132	2,037	-6.5	-6.5
RCHRES 703 - Bush Creek	1,149	3	0	1,152	1,204	-52	1,152	-4.5	-4.5
RCHRES 704 - Jordan Creek	2,375	0	3,372	5,747	5,880	-133	5,564	-5.7	-2.3
RCHRES 705 - Fly Creek	5,393	0	0	5,393	5,602	-209	5,393	-3.9	-3.9
RCHRES 706 - Baron Fork	1,021	0	11,482	12,504	12,489	15	11,978	-4.3	0.1
RCHRES 708 - Baron Fork	3,039	0	12,489	15,528	15,719	-191	15,016	-4.7	-1.2
RCHRES 712 - Baron Fork	4,463	0	15,719	20,182	20,292	-110	19,479	-4.2	-0.6
RCHRES 714 - Evansville Creek	4,209	0	0	4,209	4,412	-203	4,209	-4.8	-4.8
RCHRES 716 - Evansville Creek	6,125	0	4,412	10,537	10,684	-147	10,333	-3.4	-1.4
RCHRES 718 - Evansville Creek	2,247	0	10,684	12,931	12,944	-13	12,581	-2.9	-0.1
RCHRES 722 - Evansville Creek	1,471	0	12,944	14,414	14,175	239	14,051	-0.9	1.7
RCHRES 723 - Peavine Creek	2,701	0	0	2,700	2,836	-136	2,700	-5.0	-5.0
RCHRES 724 - Baron Fork	1,296	0	34,467	35,763	35,582	181	34,827	-2.2	0.5
RCHRES 725 - Shell Branch	3,222	4	0	3,226	3,239	-13	3,226	-0.4	-0.4
RCHRES 726 - Baron Fork	6,243	0	41,658	47,900	48,525	-625	46,996	-3.3	-1.3
RCHRES 728 - Peacheater Creek	3,630	0	0	3,630	3,830	-201	3,630	-5.5	-5.5
RCHRES 732 - Peacheater Creek	958	0	3,830	4,788	4,878	-90	4,587	-6.3	-1.9
RCHRES 736 - Baron Fork	2,041	0	53,403	55,444	58,387	-2,943	53,623	-8.9	-5.3
RCHRES 738 - Tyner Creek	3,217	0	0	3,217	3,440	-223	3,217	-6.9	-6.9
RCHRES 742 - Tyner Creek	2,738	0	3,440	6,177	6,395	-217	5,954	-7.4	-3.5
RCHRES 746 - Baron Fork	1,085	0	64,781	65,866	64,903	963	60,662	-7.0	1.5
RCHRES 748 - Baron Fork	2,408	0	64,903	67,311	66,591	720	63,070	-5.6	1.1
RCHRES 751 - Baron Fork	810	0	66,591	67,401	67,046	355	63,880	-5.0	0.5
RCHRES 752 - Baron Fork	334	0	67,046	67,380	66,559	821	64,214	-3.7	1.2
RCHRES 800 - Illinois River	2,171	0	134,040	136,210	136,030	172	126,080	-7.9	0.1
RCHRES 802 - Black Fox Springs	1,469	0	0	1,469	1,612	-143	1,469	-9.7	-9.7
RCHRES 804 - Dumpling Hollow	625	0	0	625	684	-59	625	-9.5	-9.5
RCHRES 805 - Dumpling Hollow	362	0	684	1,046	1,111	-65	986	-12.6	-6.2
RCHRES 806 - Tahlequah Creek	731	0	0	731	865	-134	731	-18.4	-18.4
RCHRES 807 - Ross Branch	881	0	0	881	1,011	-129	881	-14.7	-14.7
RCHRES 808 - Tahlequah Creek	129	0	1,876	2,004	1,978	27	1,741	-13.6	1.3
RCHRES 809 - Tahlequah Creek	76	12	1,978	2,066	2,089	-23	1,829	-14.2	-1.1
RCHRES 810 - Illinois River	1,136	0	136,030	137,170	137,660	-491	127,210	-8.2	-0.4
RCHRES 820 - Illinois River	1,131	0	139,270	140,400	141,210	-808	129,810	-8.8	-0.6
RCHRES 830 - Illinois River	1,567	0	141,210	142,780	148,170	-5,393	131,380	-12.8	-3.8
RCHRES 840 - Illinois River	811	0	148,170	148,980	145,070	3,915	132,190	-9.7	2.6
RCHRES 850 - Illinois River	949	0	145,070	146,020	148,600	-2,583	133,140	-11.6	-1.8
RCHRES 860 - Illinois River	490	0	148,600	149,090	159,530	-10,445	133,630	-19.4	-7.0
RCHRES 870 - Illinois River	828	0	160,640	161,470	161,730	-262	135,440	-19.4	-0.2
RCHRES 880 - Illinois River	447	0	161,730	162,180	161,500	678	135,890	-18.9	0.4
RCHRES 890 - Illinois River	680	0	163,590	164,270	165,330	-1,054	138,400	-19.5	-0.6
RCHRES 900 - Illinois River	4,162	0	231,890	236,050	250,230	-14,183	206,770	-21.0	-6.0
RCHRES 901 - Caney Creek	869	0	0	869	1,103	-235	869	-27.0	-27.0
RCHRES 902 - Caney Creek	1,732	11	1,103	2,846	3,244	-398	2,611	-24.2	-14.0
RCHRES 904 - Caney Creek	2,820	0	3,244	6,064	6,629	-565	5,432	-22.0	-9.3
RCHRES 906 - Caney Creek	5,150	0	6,629	11,778	13,278	-1,500	10,581	-25.5	-12.7
RCHRES 908 - Caney Creek	3,782	0	13,278	17,059	17,816	-756	14,362	-24.0	-4.4
RCHRES 912 - Caney Creek	2,930	0	17,816	20,746	21,040	-294	17,293	-21.7	-1.4
RCHRES 914 - Caney Creek	593	0	21,040	21,633	19,283	2,351	17,886	-7.8	10.9
RCHRES 916 - Dry Creek	2,780	0	0	2,779	3,848	-1,068	2,779	-38.4	-38.4
RCHRES 922 - Elk Creek	1,793	0	0	1,793	2,369	-576	1,793	-32.1	-32.1
RCHRES 936 - Terrapin Creek	640	0	0	640	979	-339	640	-52.9	-52.9
RCHRES 938 - Chicken Creek	169	0	0	169	278	-109	169	-64.5	-64.5

Water Temperature Calibration and Validation Results

Water temperature is an environmental characteristic that impacts all the aquatic water quality processes. As such, it is an important variable to accurately represent. The energy balance calculations that are used to model water temperature with the HSPF stream reach module are well-established, and often produce very good to excellent simulations. Figures 4.11, 4.12, and 4.13 provide the water temperature calibration (top graphs) and validation (bottom graphs) results at the Illinois River at Savoy (Reach 150), the Stateline (Reach 630), and Tahlequah (Reach 870), respectively. Results for the other calibration sites are included in Appendix C.

It is clear from these three figures, and the others in Appendix C, that water temperature is well simulated by HSPF, and the high degree of agreement is essentially identical in both the calibration and validation periods. This supports our claim that the water temperature simulation has been validated. The model represents at a high degree of accuracy the seasonal patterns for water temperature at all the sites, in addition to the peak summer and low winter temperatures reflected in the observations. In a few select years, peak summer temperatures are occasionally under-simulated, but usually by 2 degrees F or less, and well within any estimate of variability or uncertainty in the observations.

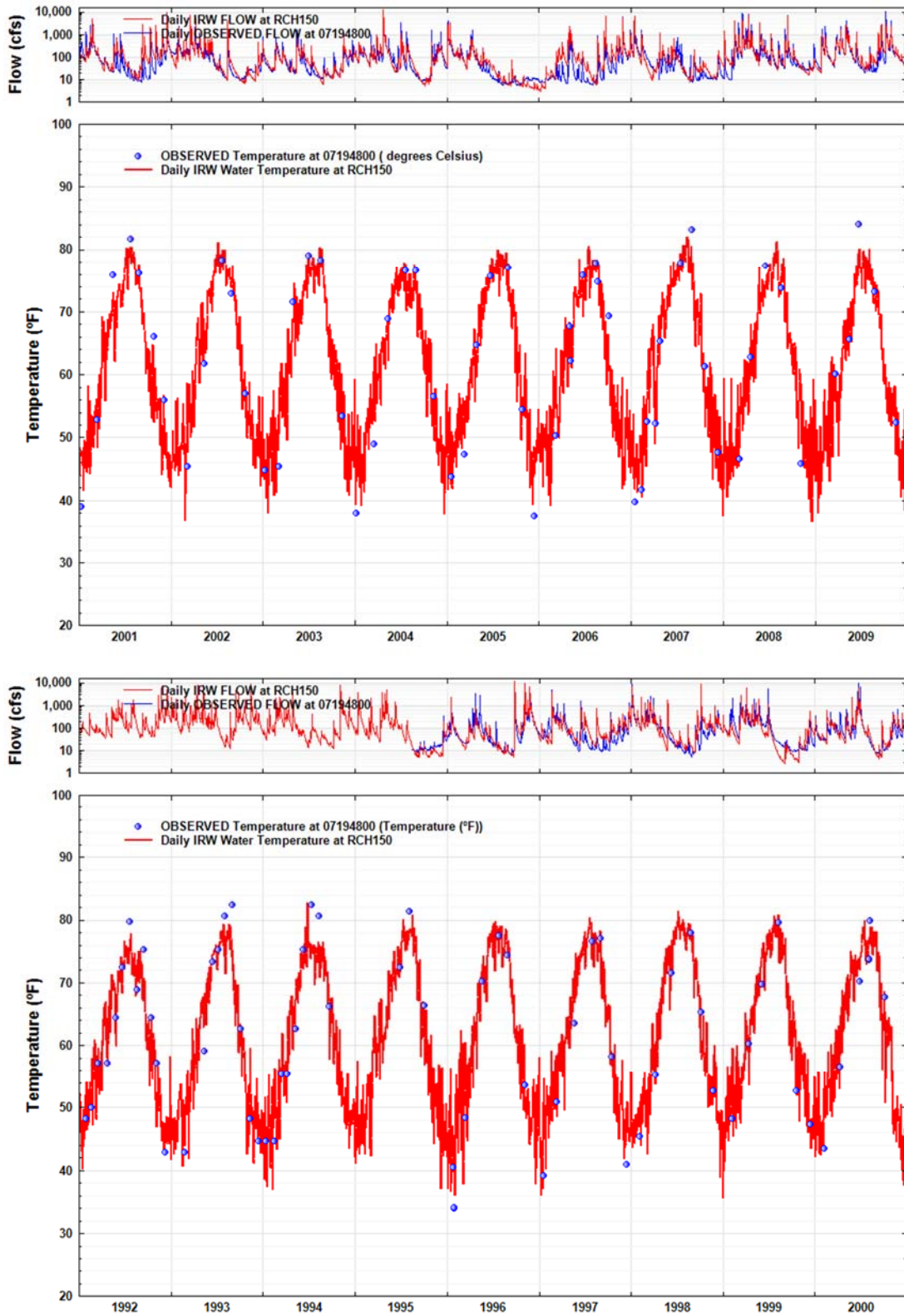


Figure 2-25 Water Temperatures Graphs for Illinois River at Savoy (Reach 150) for Calibration (top) and Validation (bottom) periods

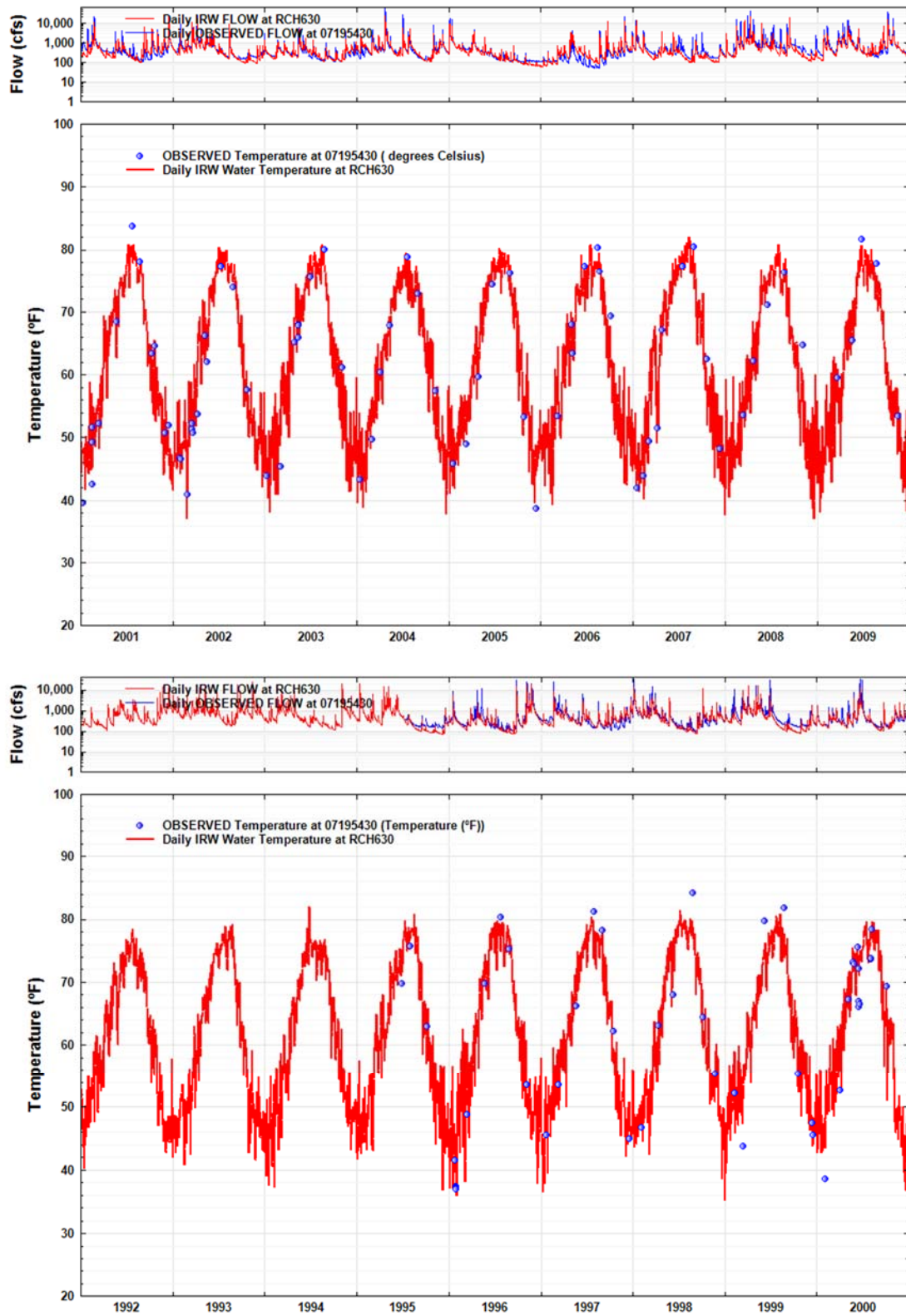


Figure 2-26 Water Temperatures Graphs for Illinois River South of Siloam Springs (Reach 630) for Calibration (top) and Validation (bottom) periods

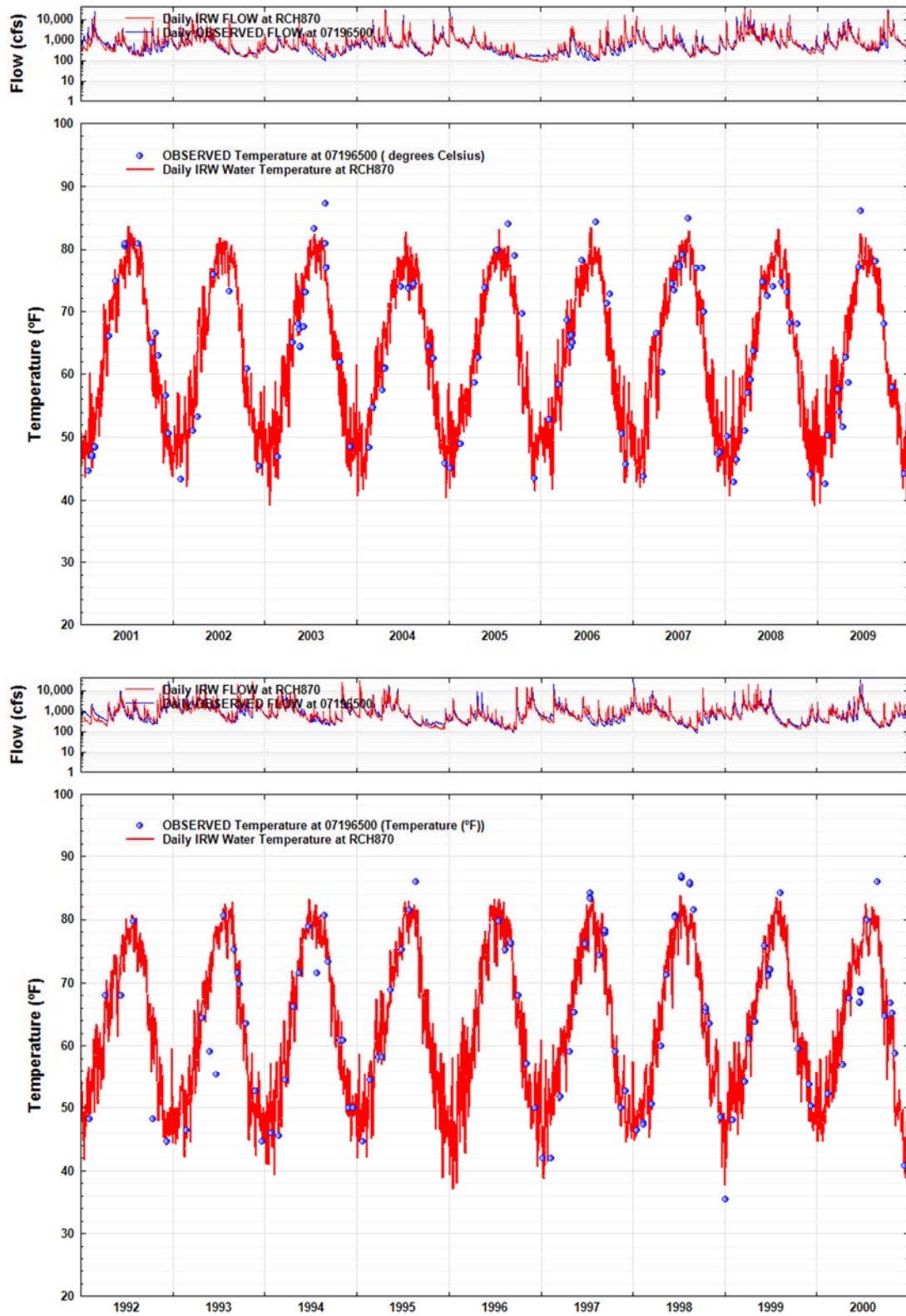


Figure 2-27 Water Temperatures Graphs for Illinois River near Tahlequah (Reach 870) for Calibration (top) and Validation (bottom) periods

2.6.4 Nonpoint Loading Calibration and Results

As noted earlier in Section 1.3, the nonpoint loading simulations in the IRW HSPF model are based on two separate procedures and modules within the HSPF code. All pasture areas, which receive fertilizer, manure and litter applications of nutrients, are represented by the AGCHEM module, while all the other land areas are represented by the simpler PQUAL routines (and IQUAL routines for impervious surfaces). This section describes the resulting loading rates for all nonpoint sources, as a function of land use categories, climate forcing functions, and land characteristics throughout the IRW. Section 4.4.1 discusses the PQUAL/IQUAL application to the non-pasture lands, while Section 4.4.2 specifically discusses the application of the AGCHEM module, its parameterization, and the resulting loading rates from all the pasture areas. Figure 2-28 shows the meteorologic segments of the IRW model which allows the model to use separate precipitation and other meteorologic data for areas throughout the watershed. As a result of the climate variation, along with soils, slope, and land use characteristics, the resulting nonpoint source loading rates calculated by the model vary throughout the watershed. A summary of the mean, minimum, and maximum annual nonpoint source rates by constituent and land use, calculated by the model in lbs/ac/yr, is listed in Table 2-22; a detailed listing for all 33 model segments (shown in Figure 2-28) is included in Appendix E.

PQUAL/IQUAL Application to Non-Litter Areas

For the PQUAL/IQUAL application for all the non-litter land areas, the calibration procedure involves adjusting pollutant accumulation and removal rates, and user-specified subsurface concentrations, while comparing the resulting loading rates and instream concentrations with available observed data. The goal is to obtain reasonable nonpoint source loading rates for each pollutant-land use combination, while producing an acceptable simulation of the corresponding instream concentrations.

Since direct observations of loading rates is often limited, and rarely available for most modeled watersheds, “target” ranges are developed from all available local, and possibly regional information on nonpoint source contributions. Table 2-23 shows the target ranges developed to guide the calibration for the IRW. These ranges were developed from modeling studies in Arkansas (Donigian et al., 2005; Donigian et al., 2009), Minnesota (Mishra et al., 2014), Iowa (Donigian et al., 1995a) and Maryland (Donigian et al., 1995b). Although this may seem like a disparate group of locations to guide this study in the IRW of AR and OK, the loading rates reflect a large range due to climate, soils, slope, land use, and nutrient input conditions. Based on experience with the model and specifically in all these locations, including the IRW, the ranges shown in Table 2-23 provide a reasonable comparison to judge acceptability of the nonpoint rates for the IRW. The goal is to maintain the majority of the loading rates within the target ranges, and allow for any specific local IRW conditions that may indicate a preference or need for values in the lower or upper portions of the range. Thus, the ranges are general guidance to assess the acceptability of nonpoint simulation, and not absolute limits.

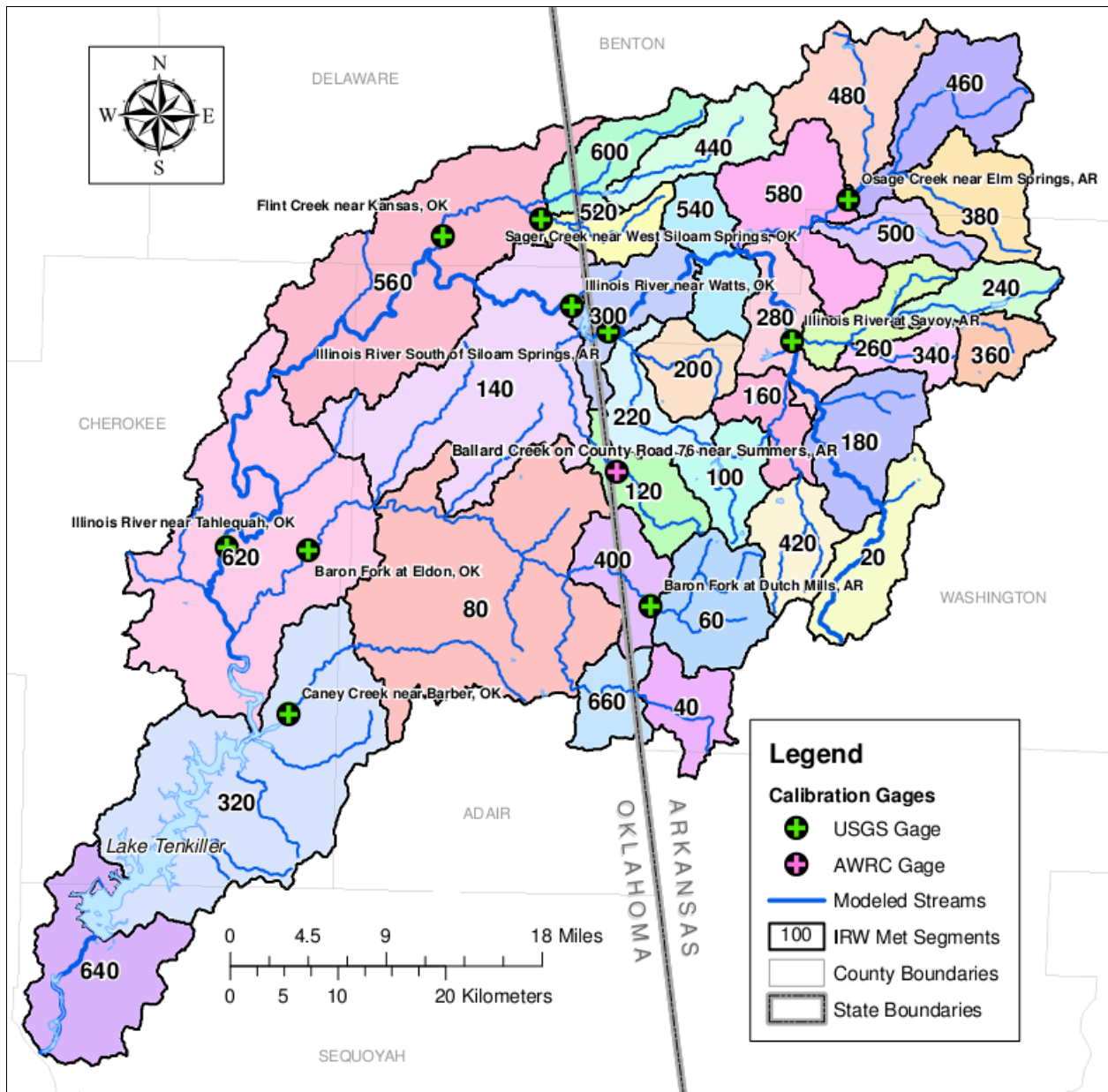


Figure 2-28 Meteorologic Segments for the IRW

Table 2-22 Modeled Nonpoint Source Loading Rates (lb/ac/yr) for the IRW

Land Uses		Pervious											Impervious		
Metric	Nonpoint Source Constituent	Forest	Pasture1	Pasture1 - Litter	Pasture2	Pasture3	Grass/ Shrub/ Barren	Developed, Open	Developed, Low	Developed, Med/High	Wetlands	Cropland	Developed, Open	Developed, Low	Developed, Med/High
Mean	BOD	2.50	15.73	22.73	17.92	18.61	7.28	7.75	9.98	13.43	1.99	31.06	9.88	14.11	16.23
	NO3	3.78	8.12	2.66	8.02	7.94	6.43	8.34	9.56	10.93	2.75	18.14	2.26	3.61	4.06
	NH3	0.17	0.47	0.36	0.48	0.49	0.53	0.80	0.80	0.79	0.10	0.74	0.48	0.76	0.86
	LabileOrgN	0.13	0.83	1.20	0.95	0.99	0.39	0.41	0.53	0.71	0.11	1.64	0.52	0.75	0.86
	RefractoryOrgN	0.30	1.25	1.81	1.42	1.48	0.87	0.93	1.20	1.61	0.24	3.73	1.19	1.69	1.95
	TN	4.38	10.67	6.04	10.88	10.90	8.23	10.48	12.08	14.04	3.20	24.26	4.44	6.81	7.73
	PO4	0.03	0.57	2.47	0.57	0.58	0.46	0.22	0.28	0.35	0.01	0.86	0.26	0.38	0.42
	LabileOrgP	0.02	0.12	0.17	0.13	0.14	0.05	0.06	0.07	0.10	0.01	0.23	0.07	0.10	0.12
	RefractoryOrgP	0.03	0.34	0.50	0.39	0.41	0.08	0.09	0.11	0.15	0.02	0.36	0.11	0.16	0.19
	TP	0.08	1.02	3.14	1.09	1.13	0.59	0.37	0.47	0.60	0.05	1.44	0.45	0.64	0.72
Min	BOD	1.52	6.18	6.35	6.52	7.57	5.10	5.58	7.19	9.76	0.96	19.88	9.60	13.70	15.76
	NO3	2.28	5.84	1.73	5.75	5.67	4.77	6.19	7.14	8.19	1.28	12.98	2.16	3.45	3.88
	NH3	0.06	0.23	0.18	0.23	0.22	0.29	0.50	0.50	0.50	0.04	0.38	0.47	0.74	0.84
	LabileOrgN	0.08	0.33	0.34	0.35	0.40	0.27	0.30	0.38	0.52	0.05	1.05	0.51	0.73	0.83
	RefractoryOrgN	0.18	0.49	0.50	0.52	0.60	0.61	0.67	0.86	1.17	0.12	2.39	1.15	1.64	1.89
	TN	2.63	6.94	2.77	6.96	6.99	6.06	7.77	8.99	10.47	1.48	16.83	4.29	6.57	7.45
	PO4	0.02	0.28	0.46	0.28	0.29	0.23	0.13	0.17	0.20	0.01	0.43	0.25	0.36	0.40
	LabileOrgP	0.01	0.05	0.05	0.05	0.06	0.04	0.04	0.05	0.07	0.01	0.15	0.07	0.10	0.12
	RefractoryOrgP	0.02	0.13	0.13	0.14	0.16	0.06	0.06	0.08	0.11	0.01	0.23	0.11	0.16	0.18
	TP	0.05	0.49	0.73	0.53	0.54	0.33	0.25	0.31	0.39	0.02	0.81	0.43	0.62	0.69
Max	BOD	4.86	33.12	60.41	35.85	40.87	9.68	10.71	13.55	17.75	3.70	46.72	10.71	15.30	17.60
	NO3	6.88	12.42	4.59	12.26	12.12	9.29	12.09	13.85	15.85	5.24	27.02	2.54	4.07	4.57
	NH3	0.48	1.38	1.10	1.43	1.42	0.91	1.19	1.19	1.18	0.26	1.44	0.51	0.81	0.92
	LabileOrgN	0.26	1.75	3.20	1.90	2.16	0.51	0.57	0.72	0.94	0.20	2.47	0.57	0.81	0.93
	RefractoryOrgN	0.58	2.63	4.80	2.85	3.25	1.16	1.29	1.63	2.13	0.44	5.61	1.29	1.84	2.11
	TN	8.12	18.18	13.68	18.13	18.12	11.87	15.05	17.29	20.03	6.10	36.54	4.91	7.52	8.53
	PO4	0.06	1.26	6.64	1.25	1.28	0.70	0.41	0.47	0.59	0.02	1.58	0.30	0.43	0.48
	LabileOrgP	0.04	0.24	0.44	0.26	0.30	0.07	0.08	0.10	0.13	0.03	0.34	0.08	0.11	0.13
	RefractoryOrgP	0.06	0.67	1.16	0.77	0.88	0.11	0.12	0.16	0.20	0.04	0.54	0.12	0.18	0.20
	TP	0.16	2.18	8.24	2.18	2.28	0.86	0.59	0.70	0.91	0.09	2.40	0.50	0.72	0.81

Table 2-23 “Target” Nonpoint Source Loadings Rates (lb/ac/yr) for the IRW

Constituent	Forest		Pasture*		Developed		Cropland		Impervious	
	Low	High	Low	High	Low	High	Low	High	Low	High
BOD/Organics	2	10	5	70	5	15	5	50	3	20
NO3	1	10	2	15	5	15	10	30	2	5
NH3	0.1	1.0	0.2	1.5	0.2	2.0	0.5	2.0	0.5	1.5
TN	2	8	2	25	5	20	10	50	3	10
PO4	0.02	0.10	0.2	2.0	0.1	1.0	0.3	2.0	0.2	0.7
TP	0.05	0.50	0.5	2.5	0.2	1.5	0.5	3.0	0.3	1.0

*excludes pasture receiving litter applications

Representing BOD and Organic Materials in Runoff Loadings

Runoff and erosion from the land transfers organic material from the land surface and soil to streams and other receiving waterbodies. Translating this organic material into the oxygen demand and organic-related species modeled by HSPF in the streams is accomplished by modeling a “generic” organic material on the land area (non-pasture categories), and defining it using the units of BOD, i.e., as oxygen demand. We refer to this as “BOD/Organics” in the model. It is important to note here that the pasture land category uses detailed agrichemical modules in HSPF in which organic nutrients are modeled more explicitly. The methodology for defining organic nutrient components in the nonpoint loading from pasture is described in a subsequent section, below.

The methodology for representing the generic organic material has historically been based on the “biomass” material that is modeled in the instream compartment (i.e., with the HSPF RCHRES module), with the assumption that this BOD/Organic material is 40% labile and 60% refractory, with the refractory material reflecting algal stoichiometry. The result is that the factor for converting the BOD/organic material simulated by the model to instream BOD is 0.4, and the remaining material (60%) is fractionated into refractory organic nutrients (i.e., N, P, C) based on the stoichiometric parameters that define the biomass material in HSPF. It has become common practice for modelers to adjust the factors somewhat during calibration on different watersheds following comparison of simulated and observed values. The factors used in the IRW model are based on this methodology, including some past adjustments.

Another methodology (Tetra Tech, 2002) that results in very similar factors is to assume the organic material is humic acid, and utilize typical stoichiometric ratios for humic acid to convert the material to specific organic nutrient species.

The factors utilized in the Illinois River model are shown below, and are compared with the values obtained from the original HSPF biomass approach (i.e., without adjustment) and the humic acid assumptions. In all three cases, the labile fraction is assumed to be 40%. The factors for BOD and refractory organics are included in the HSPF UCI file; the factors for the labile organic species are derived from the 40% labile fraction and the stoichiometric factors that define the BOD material in HSPF. The labile factors are shown here for completeness; they are not explicitly included in the HSPF UCI file because the labile organic nutrients are part of the BOD material.

Table 2-24 Comparison of Factors Converting Generic Organic Matter (BOD/Organics) from the Land to Organic Species in Streams

	<u>IRW Model</u>	<u>HSPF Biomass</u>	<u>Humic Acid</u>
BOD	0.40	0.40	0.40
Refractory Organic N:	0.048	0.032	0.041
Refractory Organic P:	0.0046	0.0044	0.0051
Refractory Organic C:	0.60	0.18	0.57
Labile Organic N	0.0212	0.0212	0.0212
Labile Organic P	0.00293	0.00293	0.00293
Labile Organic C	0.120	0.120	0.120

In summary, a generic organic material (BOD/Organics) is modeled on the non-pasture land areas, and the resulting loadings of oxygen depleting material, labile/reactive organic nutrients, and refractory/non-reactive organic nutrients to water bodies are defined by applying multiplication factors to the runoff of the BOD/Organic material.

Organic Material Originating on Pasture Land Areas

The agrichemical modules that are used to model pasture land in the Illinois River watershed explicitly model organic nitrogen and phosphorus. The modeled runoff of organic N is multiplied by 0.6 to generate refractory organic N loadings, using the assumption that 40% of the organics are labile. Refractory organic P loadings are generated by multiplying the calculated organic P runoff by 1.2, which includes the 60% refractory fraction plus an adjustment factor of 2 derived from calibration efforts. Since the agrichemical modules don't explicitly model organic carbon (or BOD), the refractory organic carbon loadings are generated by using organic N runoff as a surrogate, and adjusting it by the refractory fraction of 0.6 and converted to C using the stoichiometric factors from the HSPF biomass material.

BOD loadings from pasture are generated similarly to the refractory organic carbon; the organic N runoff is adjusted by the labile fraction (0.4) and converted to BOD using the stoichiometric factors from the HSPF biomass material. The resulting factors are summarized below. The BOD and refractory organics factors are included directly in the UCI file. The three labile organics factors are implicit in the BOD factor and the stoichiometric conversion factors from the HSPF biomass material; they are shown below for completeness:

BOD	=	7.555	x	Organic N Runoff
Refractory Organic N:	=	0.60	x	Organic N Runoff
Refractory Organic P:	=	1.20	x	Organic P Runoff
Refractory Organic C:	=	3.41	x	Organic N Runoff
Labile Organic N	=	0.400	x	Organic N Runoff
Labile Organic P	=	0.0553	x	Organic N Runoff
Labile Organic C	=	2.27	x	Organic N Runoff

These factors are used in developing the organics component loadings shown in Table 2-24 and Appendix E.

AGCHEM Calibration and Application for the Pasture areas

Since the HSPF agrichemical (AGCHEM) module simulates the complex soil and nutrient processes that occur on pasture lands, it also requires much more detailed input data to

characterize the soil compartment, the vegetation, and the nutrient inputs in terms of amounts applied, their timing and their methods of application. Consequently, the use of AGCHEM for the IRW pasture areas required analyses of the available soil and nutrient application data to develop appropriate input to the model consistent with the model representation of the nitrogen (N) and phosphorus (P) cycles. This section describes the model setup and input development, along with the overall calibration process.

In the IRW model, pasture is divided into four categories (listed below), all of which are simulated using the detailed HSPF AGCHEM modules for nitrogen (N) and phosphorus (P)

1. Pasture 1 (Litter) - low slope pasture (2.5%) with poultry litter applications
2. Pasture 1 (Non Litter) - low slope pasture without poultry litter applications
3. Pasture 2 - medium slope (>2.5 – 4.0%), no litter
4. Pasture 3 - higher slope pasture (>4.0%), no litter

N and P chemical species in litter are applied to category 1, along with manure from grazing animals. The other three categories are assumed to receive both fertilizer applications and manure as a result of grazing. The procedures for estimating the litter, fertilizer, and manure N and P applications, along with implementation of these applications within the model, are discussed below.

Manure

The manure applications are based on the IRW SWAT model application by Saraswat et al., (2010), and are based on estimated 2002 cattle populations and pasture areas; Saraswat estimated that 5.99 kg/ha/day (5.35 lb/ac/day) of manure are applied to all four pasture areas within the model. Manure is added to pasture every timestep during the grazing season from March 1 to November 30.

The manure was assumed to consist of an average of dairy and beef manure fractions from the parameter database used in the SWAT model: mineral N = 0.0085, mineral P = 0.0045, organic N = 0.0305, organicP = 0.005, NH₃-N/mineral N = 0.99, NH₃-N = 0.00842, NO₃-N = 0.000085

These fractions, plus the daily application amount were converted to the following nutrient application amounts in lbs/ac/day, and distributed between the surface soil layer (70%) and upper soil layer (30%):

NO₃-N = 0.000454 lb/ac/day
NH₃-N = 0.0450 lb/ac/day
OrgN = 0.163 lb/ac/day
PO₄-P = 0.0240 lb/ac/day
OrgP = 0.0267 lb/ac/day

The model implementation of manure applications utilized the 'atmospheric deposition' capability to account for these daily inputs. Each PERLND received a daily time series of atmospheric deposition for each species and each soil layer. The time series consists of zero values between Dec. 1 and Feb. 28, and values of 1.0 between March 1 and November 30. The above application amounts (distributed 70%/30% for the surface and upper zone soil layers) were used as multiplication factors to the time series. Internally the model converts the daily amounts to the timestep of the run, i.e., the daily values are divided by 24 and applied in each hour.

Fertilizer

N fertilizer was applied to all non-litter pasture at a rate of 79 lb/ac/yr, based on the assumptions used in the IRW model by Storm and Mittelstet (2014). The N was assumed to be ammonium-nitrate, 50% NH₃-N and 50% NO₃-N, and the applications were divided as follows; 30% in the surface soil layer and 70% in the upper layer. The applications were further divided in time. There was one application per month, with 4.2% of the application amount applied each month between October and March, and 12.5% applied each month between April and September. The fertilizer applications were implemented using the Special Actions method in HSPF.

Poultry Litter

The poultry litter nutrient applications were estimated primarily from data provided by the Arkansas Natural Resources Commission (ANRC, by E. Swaim and P. Fisk, multiple personal communications in 2011 through 2013) and the Oklahoma Department of Agriculture, Food and Forestry (ODAFF, Q. Pham) on litter generation, application, and export on both sides of the state line. While the OK data was provided for each 12-digit HUC, the AR data was almost exclusively for the entire IRW within AR. Only for 2009 to 2011 were litter application data provided by 12-digit HUC for the AR side, and they were overlain with the 12-digit HUC coverage and the 2009 spatial distribution was used for the entire calibration period. Further details are provided below.

Oklahoma Litter Data

The data provided for Oklahoma consists of an ODAFF database, "Poultry Waste Land Application Sites" map layer, also called "PltWasteApp". The database contains litter application amounts and application areas for individual application sites, in addition to other parameters related to the location and year of application.

The PltWasteApp database was summarized by extracting litter application amounts and areas by year (2001-2009) for each model meteorologic segment and subbasin (approximating 12-digit HUCs) in OK. (Note: OK litter applications in boundary met segments that are primarily in Arkansas were reassigned to the adjacent downstream Met segment in OK). Also, the application amounts for 2001 and 2002 were averaged and used for both years because the data for 2001 was deemed less reliable as the reporting program was in its initial year.

For each met segment, the average application area for 2001-2009 was computed; this area was assigned as the total area of application for each year, since the model does not allow changes in segment areas during a run. These areas are the areas of pasture category #1. The area of the pasture category #2 is equal to the total Low Slope pasture area minus the litter application area (category #1).

The litter application areas and the litter application amounts for each met segment were used to compute the litter application rate for each year; this rate is used to compute the individual nutrient input to soil layers in the Pasture Category #1 PERLNDs. It should be noted that some met segments had zero litter applied. We took this approach in order to maintain the correct total amount of litter applied each year, in spite of the fact that the actual application areas are changing each year.

Poultry litter is assumed to consist of the following nutrient species (applicable to the HSPF AGCHEM), derived from the University of Arkansas, Nutrient Analysis of Poultry Litter (FSA-9529), (Sharpley et al., 2009) and amounts in lbs per ton of litter:

NO3-N:	0.8 lbs
NH4-N:	7.7 lbs
Organic N:	53.5 lbs
PO4-P:	27.0 lbs (1.9 dissolved + 25.1 adsorbed)
Organic P:	3.0 lbs

The litter applications were implemented in the HSPF input using Special Actions. The amounts were split 70% in the surface soil layer and 30% in the upper layer. PO4 and NH4 were added to the corresponding adsorbed storage compartments within the AGCHEM simulation. The application was performed in five applications beginning March 1, and separated by 2 months. Therefore, the applications occurred on March 1, May 1, July 1, September 1, and November 1.

Arkansas Litter Data

The Arkansas litter data was obtained from Arkansas Natural Resources Commission (ANRC), and consisted of litter generation, storage, export, number of birds of each species, and the area available for application. The data were for each year between 2003 and 2011. However, the data were sums by watershed HUC, and the data provided for 2003-2008 were effectively the totals for the entire AR portion of the IRW. The data provided for 2009-2011 were totals by 12-digit HUCs, providing a spatial distribution of the applications consistent with the model subbasins within AR. We also received data for 2004 by 11-digit HUCs, but much of the data was aggregated so that it only divided the AR portion into 4 separate areas.

The application amounts and application areas were compiled by 12-digit HUC for the more detailed period of 2009-2011. These 12 digit HUC values were accumulated/assigned to the model met segments that contained the HUC, providing the spatial distribution needed for the AR portion of the IRW.

The total annual application areas were compiled for 2004-2011; an apparently erroneous area of 28,496 acres was omitted from 2005 data (after confirming the error with P. Fisk at ANRC). The average of these annual values was assumed to be the total area of application in AR for the model calibration period (2001-2009). The average application area for each met segment for the 2009-2011 period (computed in the previous step) was used to distribute the total annual application areas by met segment for the earlier years without the distribution detail. These areas are the areas of pasture category #1 in each met segment. The area of the pasture category #2 is equal to the total Low Slope pasture area minus the litter application area (category #1).

The total annual application amounts for the AR portion of the IRW were compiled from the original database for the years 2004-2009; the data for 2003 were suspect, and therefore assumed to be unreliable due to the start-up problems during the initial year. The 2009-2011 spatial distribution of litter application amounts by met segment (computed above) were used to compute the fraction of the total application for each met segment. These fractions were applied to the total application amount for each year 2004-2009 to compute the met segment application amounts for these years.

The litter application rates for 2004 and 2005 were averaged, and used for the earlier 2001-2003 period; this was based on anecdotal information indicating that AR poultry numbers and litter generation amounts for the 2001-2005 period were relatively stable.

The application areas and amounts by met segment were distributed to nutrient species and implemented in the model using Special Actions as described above for Oklahoma.

The resulting litter application amounts demonstrated some anomalous variations from year to year for selected segments, requiring further adjustments (mostly reductions) and some averaging across years as part of the calibration effort. Table 2-25 provides the final litter application amounts developed from the ANRC and ODAFF data but adjusted during the AGCHEM calibration (discussed further below).

AGCHEM Calibration

The initial parameterization of the AGCHEM module for the pasture lands was derived from previous AGCHEM applications in Iowa (Donigian et al., 1995a), Maryland (Donigian et al., 1995b), and the Chesapeake Bay Region (Donigian et al., 1998a). These prior efforts provided initial parameters values that were then adjusted for the IRW and subsequently through the calibration process. Calibration of the AGCHEM module is focused on developing expected nutrient balances for both N and P, adjusting the model process rates to reflect the expected nutrient balances, and comparing the nutrient runoff rates with the target rates. Nutrient balances for N and P, and for major land use categories, were developed as part of the Chesapeake Bay effort (see Donigian et al., 1998b), and adjusted for pasture conditions within the IRW. The major adjustments were related to the added P from the litter applications, the increase in TP runoff due to the litter applications, and associated changes in soil fluxes and storages.

Table 2-23 presents the target nonpoint source loading rates for the IRW HSPF application, but it does not include the expected rates for litter-applied pasture. Review of literature specific to AR and the general IRW environs indicates that maximum TP loading rates can be in the range of 4 to 8 lb/ac/yr for pastures receiving litter applications and livestock grazing (Romeis et al., 2011; Daniel et al., 2009; Sharpley, 2009). Consequently, we considered TP loading rates of 8 to 10 lb/ac/yr as maximum possible rates in our modeling.

Another consideration for modeling the litter-applied pasture is the level of P in the soil due to long-term over-application of P in many cases, which is well known to have a direct impact on the level of TP in runoff from these areas (Daniel et al, 2009). The common metric used for P levels in soils is the Soil Test Phosphorus (STP) that is also used by both states to monitor and regulate the allowable rates of litter applications. For our modeling, we adopted a similar approach to Storm and Mittelstet (2014) in their IRW SWAT model; we assigned P storages in the model based on STP values in their report displayed by HUC12 watersheds. We defined 4 levels of STP, as Low, Moderate, High and Very High values, corresponding to 1-100, 101-200, 201 – 400, and >400 lb P/ac. These values were assigned to the HSPF model surface and upper soil zone storages of PO₄-P as initial storage values.

Calibration of AGCHEM to expected nutrient balances involves a number of considerations. Below we discuss some of the issues and interacting effects that must be reviewed and adjusted to ensure proper behavior of the model to adequately represent the N and P nutrient cycles in soils. Table 2-26 is an example of the model-generated annual P balance for one specific litter-applied pasture segment (within met Segment 140 shown in Figure 2-28). Corresponding results are available for both N and P in the model backup documentation (provided to EPA Region 6), as the material is too voluminous to include in a report.

Table 2-25 Final Litter Application Rates (tons/acre/year) Used in the IRW HSPF Model

Met Segment	2001	2002	2003	2004	2005	2006	2007	2008	2009	Mean
20	0.59	0.59	0.59	0.62	0.94	0.94	0.94	0.94	0.38	0.73
40	1.12	1.12	1.12	1.16	1.25	1.25	1.25	1.25	1.25	1.20
60	0.92	0.92	0.92	0.96	1.17	1.17	1.17	1.17	0.58	1.00
80	0.38	0.44	0.74	0.27	1.05	1.05	1.05	1.05	1.05	0.79
100	0.64	0.64	0.64	0.67	1.02	1.02	1.02	1.02	0.41	0.79
120	0.73	0.73	0.73	0.76	1.16	1.16	1.16	1.16	0.46	0.90
140	1.35	1.35	1.35	0.82	1.37	1.47	0.62	0.55	0.53	1.05
160	1.52	1.52	1.52	2.03	2.03	2.03	2.03	2.03	2.03	1.86
180	0.67	0.67	0.67	0.70	1.06	1.06	1.06	1.06	0.42	0.82
200	0.87	0.87	0.87	0.90	1.38	1.38	1.38	1.38	0.55	1.06
220	0.45	0.45	0.45	0.47	0.43	1.13	1.03	0.27	0.28	0.55
240	0.32	0.32	0.32	0.34	0.31	0.81	0.74	0.19	0.20	0.39
260	0.26	0.26	0.26	0.27	0.25	0.66	0.60	0.15	0.16	0.32
280	0.25	0.25	0.25	0.27	0.24	0.64	0.58	0.15	0.16	0.31
300	0.07	0.07	0.07	0.08	0.07	0.18	0.16	0.04	0.05	0.09
320	0.35	0.69	0.75	0.38	1.25	0.89	1.11	1.11	1.11	0.85
340	1.11	1.11	1.11	1.16	1.41	1.41	1.41	1.41	0.70	1.20
360	0.00	0.00	0.00	0.00	0.00	0.00	0.00	0.00	0.00	0.00
380	1.03	1.03	1.03	1.07	1.15	1.15	1.15	1.15	1.15	1.10
400	0.73	0.73	0.73	0.76	1.15	1.15	1.15	1.15	0.46	0.89
420	0.67	0.67	0.67	0.70	1.07	1.07	1.07	1.07	0.42	0.82
440	0.34	0.34	0.34	0.35	0.32	0.85	0.77	0.20	0.21	0.41
460	0.00	0.00	0.00	0.00	0.00	0.00	0.00	0.00	0.00	0.00
480	0.94	0.94	0.94	0.98	1.20	1.20	1.20	1.20	0.60	1.02
500	0.83	0.83	0.83	0.86	1.32	1.32	1.32	1.32	0.52	1.02
520	0.26	0.26	0.26	0.27	0.25	0.66	0.59	0.15	0.16	0.32
540	0.17	0.17	0.17	0.17	0.16	0.42	0.38	0.10	0.10	0.20
560	1.19	1.19	1.19	1.19	1.19	1.19	0.92	1.03	0.60	1.07
580	0.36	0.36	0.36	0.38	0.35	0.91	0.83	0.21	0.23	0.44
600	0.32	0.32	0.32	0.33	0.30	0.80	0.72	0.19	0.20	0.39
620	1.17	1.17	1.17	1.17	1.12	1.15	0.31	1.46	1.27	1.11
640	0.00	0.00	0.74	0.18	1.29	1.29	1.29	1.29	1.29	0.82
660	1.24	1.24	1.24	1.24	1.19	1.19	1.19	1.19	1.29	1.22

Table 2-26 Sample AGCHEM Phosphorus Balance for Pasture-Litter for Met Segment 140

Total P Balance Report For P:152 (Pasture1-Litter) (lbs/ac)										
Date	Mean	2001	2002	2003	2004	2005	2006	2007	2008	2009
Phosphorus Loss (lb/ac)										
Surface	3.12	1.71	4.24	2.59	3.36	0.98	3.35	2.20	5.56	4.08
Interflow	0.59	0.09	0.20	0.36	0.43	0.27	1.31	0.70	1.16	0.80
Baseflow	0.01	0.01	0.01	0.01	0.01	0.01	0.01	0.01	0.02	0.02
Sediment	0.19	0.07	0.11	0.03	0.42	0.07	0.03	0.12	0.55	0.34
Total	3.91	1.88	4.55	2.99	4.22	1.34	4.69	3.03	7.28	5.24
Labile Org P from POORN	0.27	0.03	0.07	0.02	0.43	0.08	0.04	0.19	0.94	0.62
Refractory Org P from SEDP 1	0.69	0.08	0.18	0.06	1.17	0.22	0.11	0.51	2.40	1.52
Total P Loss	4.88	1.99	4.81	3.08	5.81	1.64	4.85	3.73	10.62	7.38
Plant P										
Surface	0.02	0.02	0.02	0.01	0.02	0.01	0.01	0.02	0.04	0.03
Upper	18.80	0.24	10.37	32.12	30.24	21.02	18.81	18.80	18.80	18.80
Lower	4.97	4.97	4.97	4.97	4.97	4.97	4.97	4.97	4.97	4.97
Groundwater	0.00	0.00	0.00	0.00	0.00	0.00	0.00	0.00	0.00	0.00
Total	23.79	5.22	15.36	37.10	35.22	25.99	23.78	23.79	23.82	23.80
P Storages (lb/ac)										
PO4-P Soln Storage										
Surface	0.00	0.00	0.00	0.00	0.00	0.00	0.00	0.00	0.00	0.00
Upper	0.23	0.00	0.37	0.28	0.09	0.02	0.74	0.21	0.19	0.16
Interflow	0.00	0.00	0.01	0.00	0.00	0.00	0.03	0.00	0.00	0.00
Lower	0.13	0.29	0.16	0.14	0.10	0.02	0.16	0.12	0.09	0.09
GW	0.00	0.00	0.00	0.00	0.00	0.00	0.00	0.00	0.00	0.00
Total	0.36	0.29	0.53	0.42	0.18	0.04	0.94	0.33	0.28	0.24
PO4-P Ads Storage										
Surface	23.97	22.13	23.16	23.35	22.82	30.69	22.16	23.79	23.70	23.90
Upper	202.89	181.32	205.75	204.89	200.42	211.21	211.13	205.63	203.05	202.60
Lower	113.97	117.76	115.44	114.39	112.83	111.30	114.61	114.08	113.08	112.24
GW	221.75	221.29	221.47	221.58	221.69	221.75	221.81	221.91	222.09	222.19
Total	562.58	542.51	565.83	564.20	557.77	574.95	569.71	565.41	561.93	560.94
ORGP Storage										
Surface	61.89	26.83	38.21	49.96	56.07	65.67	75.46	80.46	81.33	83.05
Upper	75.20	52.46	53.64	59.93	60.69	63.86	90.17	97.20	99.00	99.84
Lower	110.62	118.67	116.92	114.89	112.79	110.49	108.22	106.39	104.59	102.60
GW	80.00	80.00	80.00	80.00	80.00	80.00	80.00	80.00	80.00	80.00
Total	327.71	277.97	288.77	304.78	309.55	320.02	353.85	364.04	364.92	365.49
P FLUXES										
Manure Deposition (lb/a)										
PO4-P - Surface	4.62	4.62	4.62	4.62	4.62	4.62	4.62	4.62	4.62	4.62
ORGP - Surface	5.14	5.14	5.14	5.14	5.14	5.14	5.14	5.14	5.14	5.14
PO4-P - Upper	1.98	1.98	1.98	1.98	1.98	1.98	1.98	1.98	1.98	1.98
ORGP - Upper	2.20	2.20	2.20	2.20	2.20	2.20	2.20	2.20	2.20	2.20
Litter Applications (lb/a)										
PO4-P	28.23	36.45	36.45	36.45	22.14	36.99	39.69	16.74	14.85	14.31
ORGP	3.14	4.05	4.05	4.05	2.46	4.11	4.41	1.86	1.65	1.59
Other Fluxes (lb/ac)										
ORGP Mineralization										
Surface	3.68	1.09	1.70	2.46	3.65	3.06	4.20	3.99	6.69	6.32
Upper	10.23	0.95	4.00	8.96	8.64	10.19	12.60	15.28	15.76	15.71
Lower	2.66	2.85	2.81	2.77	2.72	2.66	2.61	2.56	2.52	2.47
Groundwater	0.00	0.00	0.00	0.00	0.00	0.00	0.00	0.00	0.00	0.00
Total	16.58	4.88	8.51	14.19	15.02	15.91	19.41	21.83	24.97	24.50
PO4-P Immobilization										
Surface	4.49	5.00	5.25	6.29	3.88	4.83	5.86	2.97	3.26	3.05
Upper	12.63	0.00	1.77	11.85	6.47	9.93	35.37	19.53	14.86	13.86
Lower	0.73	1.52	1.06	0.73	0.62	0.37	0.34	0.73	0.72	0.48
Groundwater	0.00	0.00	0.00	0.00	0.00	0.00	0.00	0.00	0.00	0.00
Total	17.85	6.52	8.08	18.87	10.97	15.12	41.57	23.23	18.84	17.40

- a. Nutrient balances for agricultural soils involve inputs, outputs, storages, and fluxes. The two largest are usually nutrient applications (as fertilizer, manure/litter, and atmospheric deposition) as inputs, and plant uptake as outputs. Thus, much of the calibration effort focuses on accurately representing these components of the nutrient balance.
- b. Most published nutrient balances (e.g., Donigian et al., 1998b) focus on the 'plant-available' components as they are the ones of major concern, both in terms of uptake by plants and aquatic biota, and in runoff. The organic forms are required to be included in a modeling framework, and they are shown in Table 2-25, but this is primarily needed to implement a mass-balance approach in the modeling.
- c. The runoff flux (as an output) is critical for watershed water quality issues, but it is usually a small fraction of the overall nutrient balance, for both N and P.
- d. Other fluxes, such as mineralization and immobilization (or fixation) can be important, and need to be evaluated along with the other fluxes.
- e. Storages, such as the PO₄-P storage which corresponds to the STP (surface and upper soil zones) need to be examined to ensure that they reflect expected behavior, such as increases from applications and mineralization, and decreases from plant uptake and immobilization. Storages that continually increase or decrease may indicate a need for additional calibration and/or re-assessment of other fluxes.

AGCHEM calibration often takes numerous iterations of simulation runs, generation of the nutrient balance results (like Table 2-26), review of those results, and then consideration of the impact of the runoff loads on instream water quality. Since the runoff rates are a small part of the overall nutrient balance, it may take many iterations to attain a reasonable runoff rate, while ensuring the corresponding nutrient inputs, outputs, fluxes, and storages are within proper limits. Once this is attained, then reviewing the instream water quality calibration (discussed below in Section 4.5) may lead to adjustments to the instream parameters until the results clearly indicate that the nonpoint source loading rates require further adjustment.

The final calibration is only attained after the nonpoint source rates are deemed to be reasonable, the AGCHEM nutrient balances and runoff rates are acceptable, and the instream comparison of observed data and the simulation values demonstrate acceptable agreement. The final nonpoint source rates shown in Table 2-23 and Appendix E were judged to meet these criteria at the conclusion of the instream water quality calibration discussed below.

2.6.5 Instream Water Quality Calibration Results

Calibration of the instream water quality parameters that control the aquatic processes, along with nutrient fate and transport, is normally the final step in the watershed water quality calibration process. However, given that the entire effort is often an iterative process, it is fairly common to re-iterate the component steps in the process with a need to re-examine the sediment and nonpoint source loading rates, and even sometimes the hydrologic calibration, in an attempt to improve flow simulations for time periods when data is available for the water quality calibration effort. In many cases, either under or over simulation of flows will have dramatic impacts on the calculated concentrations that are the focus of the calibration effort. This is especially true during extreme high flow, or low flow, conditions, such as those that occurred in 2005-2006, in the middle of the calibration period.

For the IRW water quality effort, the nonpoint source loading rates discussed above were initially calibrated to be within the general range of the expected 'target' rates, but then adjusted

as needed within the target ranges, depending on the differences observed in the concentrations of water quality constituents at the calibration gages. Figure 2-28 shows the 10 USGS calibration gages (many operated cooperatively with AWRC) where the hydrologic calibration was performed, and all these gages were also the focus of the water quality calibration. One additional gage for water quality was the Ballard Creek gage, operated by AWRC (Ballard Creek on County Road 76 near Summers, AR) as it had a wealth of nutrient data, including storm periods.

As noted in Section 2.4, the IRW model simulates the following constituents:

1. Flow/discharge
2. TSS
3. water temperature
4. DO
5. BOD ultimate, or total BOD
6. NO₃/NO₂, combined
7. NH₃/NH₄
8. Total N
9. PO₄
10. Total P
11. Phytoplankton as Chl a
12. Benthic algae (as biomass)

Flow/discharge, TSS, and water temperature were discussed in the previous sections. This section presents the results of modeling the remaining constituents. Figures 4.15 through 4.18 show the water quality calibration results for DO, TN, PO₄-P and TP for the Illinois River near the AR/OK Stateline (Model Reach 630, USGS Gage 17195430) and at the Illinois River near Tahlequah, OK (Model Reach 870, USGS 07196500). Appendix E includes a complete set of graphs for all the simulated water quality constituents for all 11 gages shown in Figure 2-28.

Water quality calibration, analogous to hydrologic calibration, follows an upstream to downstream approach to implement successive improvements in model results as we 'follow the water' from the smaller headwater creeks, to moderate streams, and ultimately to the major conveyance of the Illinois River. For the IRW, this approach started on the Baron Fork at Dutch Mills (Reach 706), Osage Creek near Elm Springs (Reach 316), Illinois River at Savoy (Reach 150), and as noted earlier, Ballard Creek on County Road 76 (Reach 609). As the upstream simulations demonstrated improvements, the focus moved downstream to the Illinois River south of Siloam Springs, AR (Reach 630), Illinois River near Watts, OK (Reach 640), Sager Creek near West Siloam Springs, OK (Reach 516) and Flint Creek near Kansas, OK (Reach 523). The concluding efforts focused on the Illinois River near Tahlequah, OK (Reach 870), Baron Fork at Eldon, OK (Reach 746), and Caney Creek near Barber, OK (Reach 912). As the calibration was concluded, the parameter values were extended to the areas around Lake Tenkiller that drain directly to the Lake.

Water quality calibration is significantly more complex than hydrologic or water temperature calibration efforts as the nutrient forms must be considered jointly during calibration due to their complex dependencies and interactions. Thus, time series plots of PO₄-P and TP must be considered and reviewed together, along with BOD/DO and algal processes, as these allow uptake of PO₄-P, while the oxidation of organic materials produces additional PO₄-P. Similarly, the nitrogen forms of NO₃-N and NH₄-N comprise part of the TN (along with Organic N), but they also directly interact through nitrification and denitrification mechanisms. The biotic

components of phytoplankton and benthic algae also consume these nutrients through respiration, and then serve as a source of organic material. A sound understanding of nutrient cycling in aquatic systems is a must for attempting calibration of dynamic streams and rivers.

For these reasons, our plots include all the relevant nutrient forms that comprise these N and P cycles in the aquatic system to provide a comprehensive view of how the model is simulating these variables. Due to the Oklahoma TP standard for scenic rivers, our major focus in this study was on the P components and sources. However, the interacting mechanisms with N noted above required the joint simulation of both N and P in this effort.

Review of the model results in Figure 2-29 through 4.18, and in Appendix E, provide the basis for our calibration assessment in the following statements:

- a. For the majority of the modeled constituents, the simulated values provide reasonable agreement with the observed data, especially when sufficient data is available for both storm and non-storm periods to support a valid calibration. For a modeling assessment, we define 'reasonable agreement' as comprised of three components:
 - i. The simulated values are within a factor of 2 of the observations, i.e., the majority of simulated daily concentration values are within 50% to 200% of the observations, and
 - ii. The simulated values demonstrate a range of values (low to high) comparable to the observations, and
 - iii. The pattern of the simulated daily time series is similar to the peaks and valleys of the observations, when the population of the observations is adequate to define an observable pattern, possibly seasonal pattern.
- b. The DO simulation shows a very good seasonal pattern consistent with the observed data, and the peaks and valleys are generally well represented. However, there are greater deviations in some years, and especially during the drought years of 2005-2006. Appendix E shows similar behavior to that shown in Figure 2-29 and 4.17; some sites show greater scatter, and others show lesser scatter than the results in these 2 figures, but the overall agreement is still reasonable.
- c. For the two major sites of concern, the IR south of Siloam Springs (Reach 630), and the IR near Tahlequah (Reach 870), the simulations demonstrate good overall agreement for most all of the constituents simulated. Overall, the P components are generally better simulated than the N components as P was the major focus of this study due to the OK scenic rivers standard based on TP.
- d. Our overall assessment of the water quality calibration is that the model demonstrates reasonable agreement with most observations for DO, TP, NO₃-N, Organic N, and TN for most of the calibration sites. The larger mainstem sites, such as IR at Savoy, Osage Creek, IR South of Siloam Springs, IR near Watts, Baron Fork at Eldon, and IR near Tahlequah definitely show better agreement than the smaller sites. This is also shown clearly on Baron Fork (see Appendices E.8 and E.9) where the downstream site at Eldon shows better agreement than the smaller upstream site near at Dutch Mills.

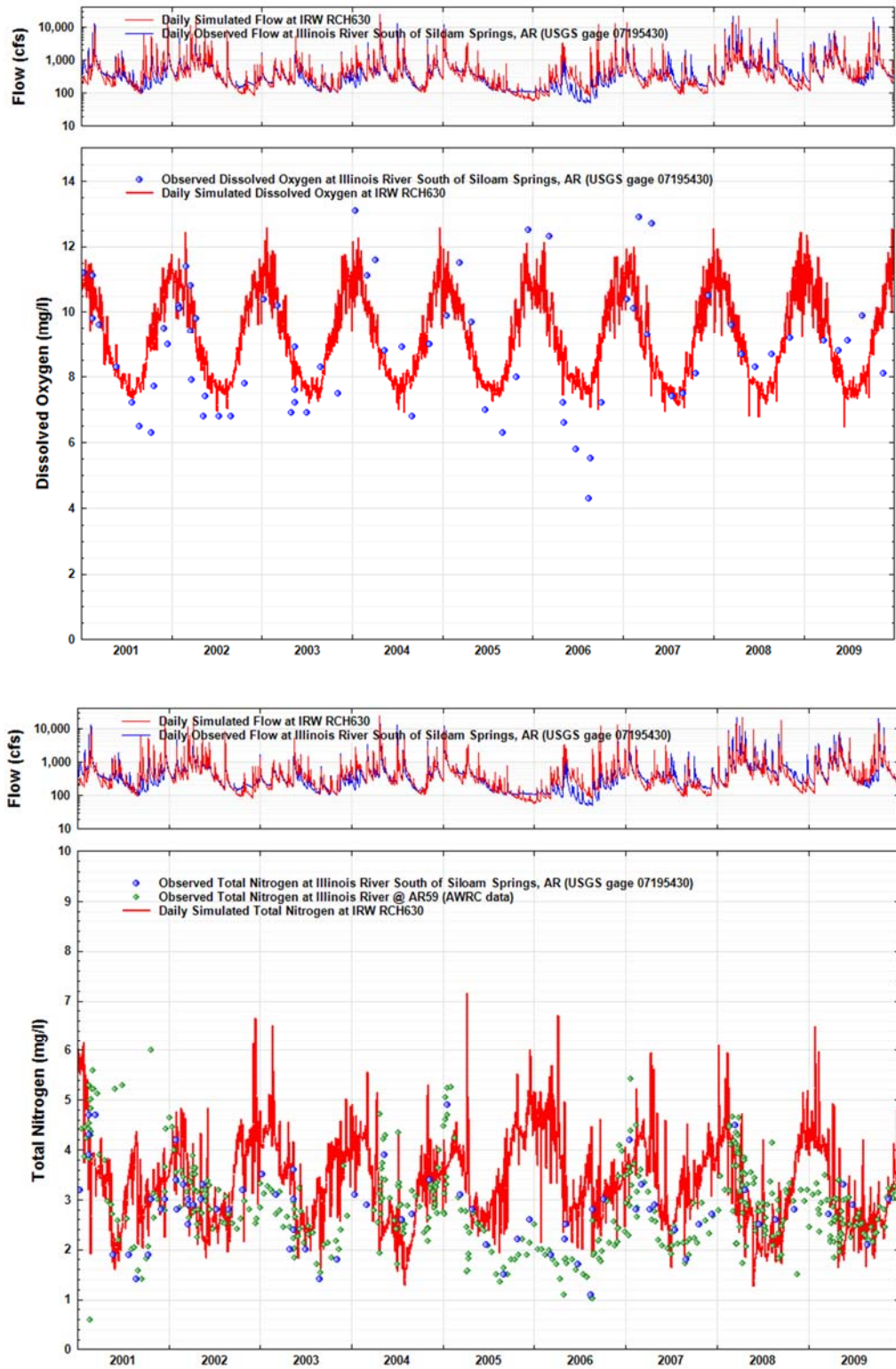


Figure 2-29 Simulated and Observed DO (top) and TN (bottom) at Illinois River below Siloam Springs, AR (Reach 630, USGS 07195430)

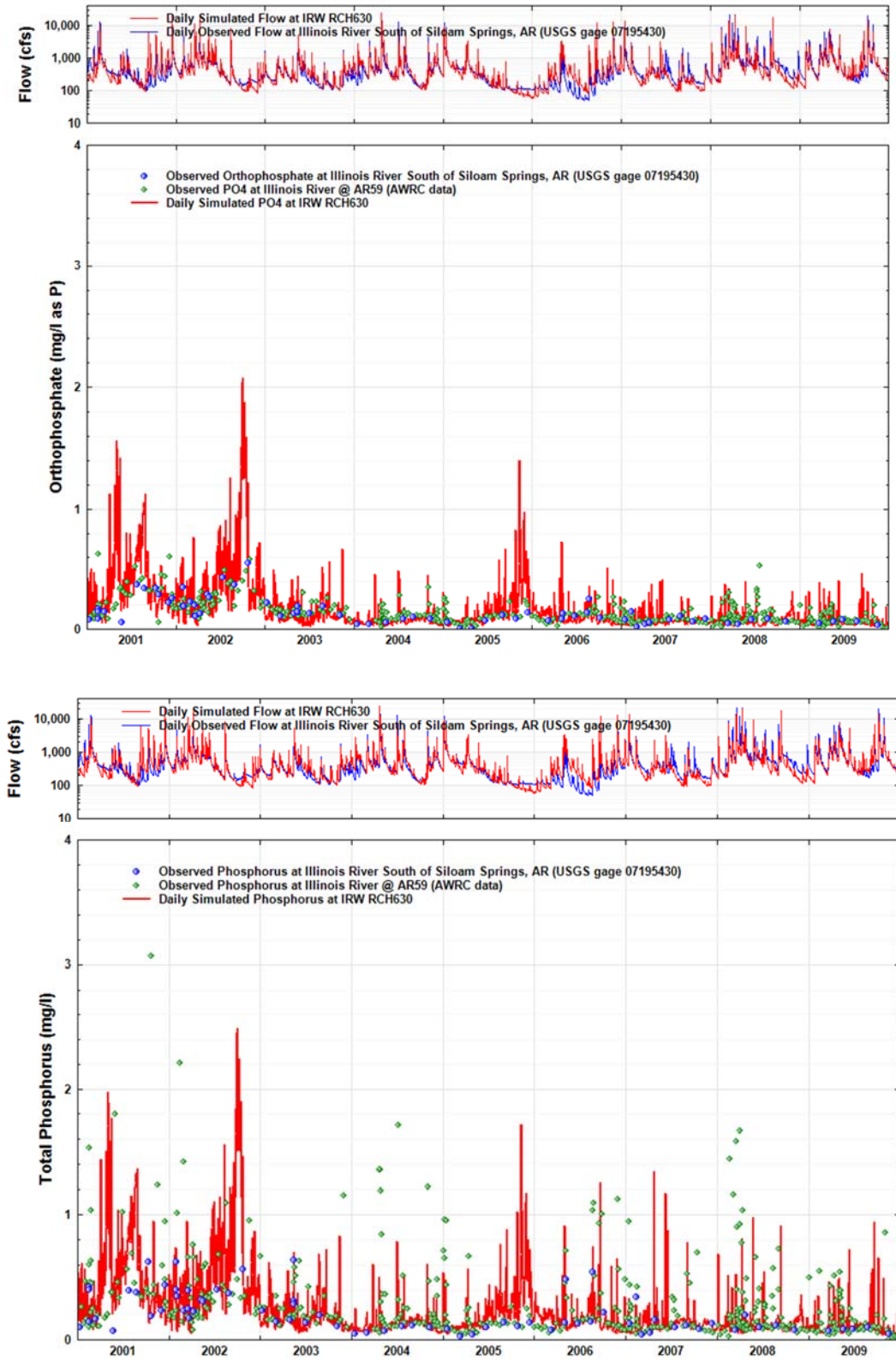


Figure 2-30 Simulated and Observed PO4-P (top) and TP (bottom) at Illinois River below Siloam Springs, AR (Reach 630, USGS 07195430)

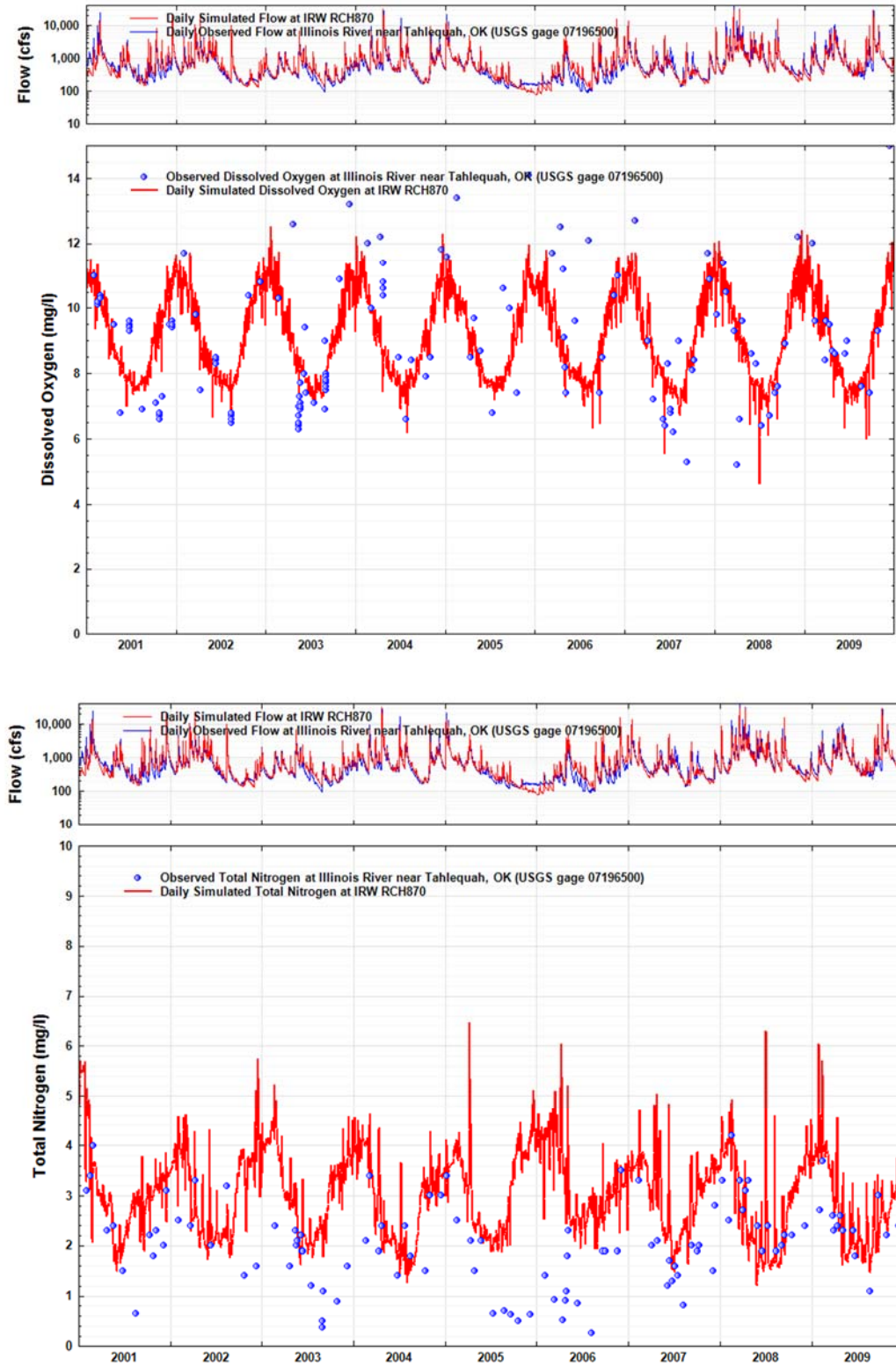


Figure 2-31 Simulated and Observed DO (top) and TN (bottom) at Illinois River near Tahlequah, OK (Reach 630, USGS 07196500)

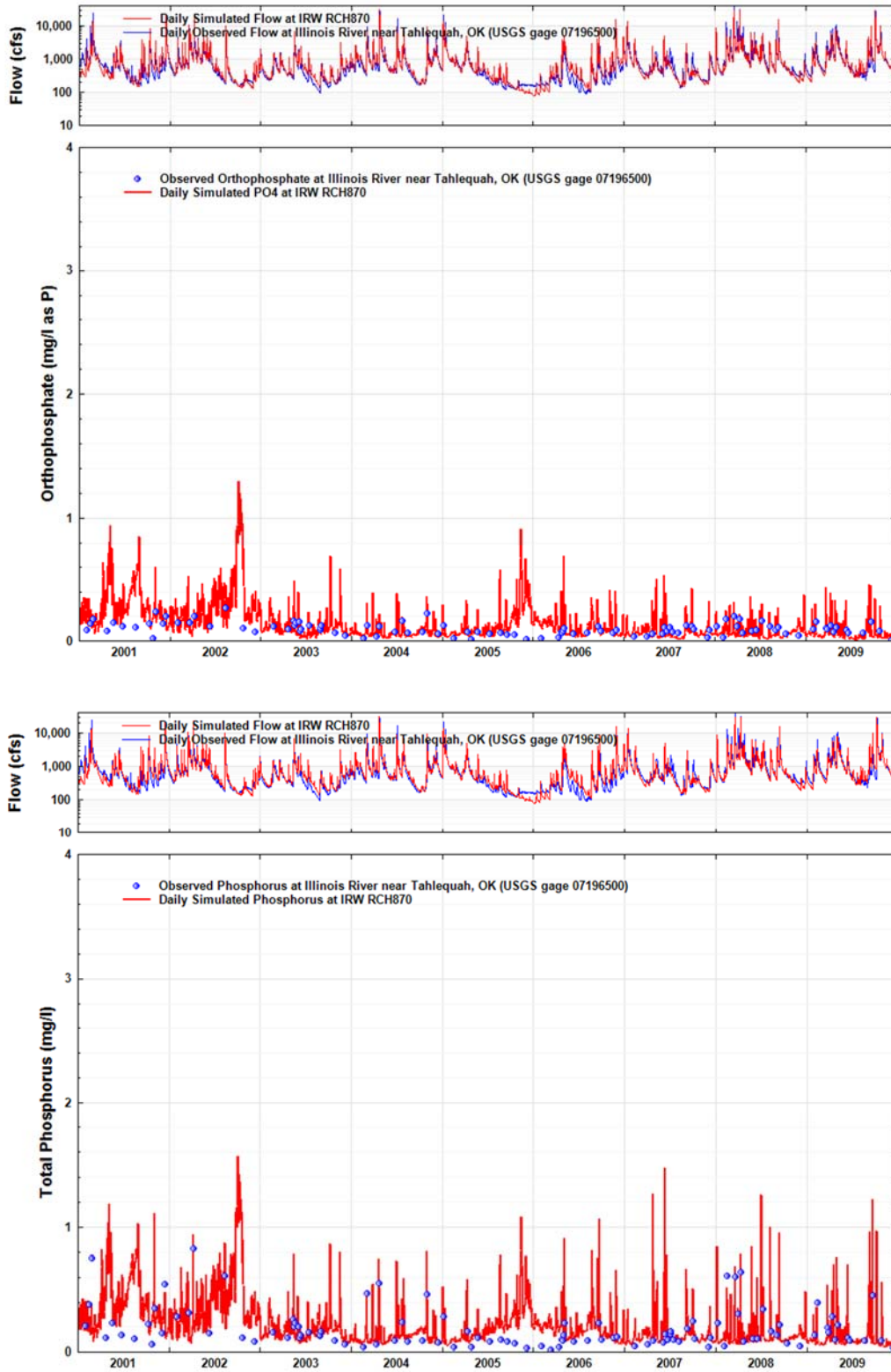


Figure 2-32 Simulated and Observed PO₄-P (top) and TP (bottom) at Illinois River near Tahlequah, OK (Reach 870, USGS 07196500)

- e. As discussed in Section 4.3.1, for a number of gage sites there are substantial differences in the amount and peak values of data collected during storm events versus non-storm periods. The TSS results for Osage Creek (Figure 2-21) demonstrate the significant difference in peak concentrations for samples collected during normal bimonthly sampling for much of the period from 2001 to 2006, versus those data for storm periods collected from 2007 to 2009. Similar patterns are seen for PO₄-P, TP, and NH₄-N at other sites. The result is that calibrating to only non-storm data will likely lead to the model under-estimating concentrations and loads. Consequently, our calibration efforts focused more on the data periods when storm data had been collected. Also, this is a primary rationale for our 'reasonable agreement' criteria of between 50% and 200% of observations.
- f. The drought conditions in 2005-06 had a major impact on model results, causing significant over-estimation of nutrient forms, especially both P and N forms and DO. Part of the cause is the under simulation of flow during that drought which contributed to the over-estimation for many concentrations.
- g. The results in Appendix E show that there are problems for certain constituents, at selected sites, such as NH₄-N and PO₄-P at a number of the smaller watershed sites. Each of these could benefit from further investigation and calibration efforts that would quantify the sources and their contributions in these smaller watersheds, and then evaluate appropriate means of reduction to attain improved agreement. Ballard Creek (Reach 609) is such a site as it demonstrates nutrient behavior somewhat different (usually higher concentrations) than most of the other small headwaters watersheds, and it has an impressive compilation of nutrient data during the calibration period, both storm and non-storm periods. Our early calibration work focused on Ballard Creek, but its high nutrient concentrations were not entirely consistent with the other small watershed sites.

In summary, the overall water quality calibration for the IRW demonstrates overall reasonable agreement with the majority of the observed data, especially for the IR mainstem sites, and for the two major sites of concern, at the AR/OK state line and at Tahlequah. Greater differences between observed data and simulated values are seen at the smaller headwater watershed sites, and further investigation and calibration efforts are recommended. Also, due to lack of historic litter and nutrient application data, water quality validation was not possible.

2.7 TP and TN Loading and Load Allocation Analyses

This section presents and discusses the TP and TN loading results at the AR/OK stateline and at Tahlequah, and load allocation analyses at selected major sites within the IRW. The load analyses in Section 5.1 further supports the model calibration by comparing the model-predicted loads with other load estimates derived from the observed data, while the load allocation in Section 5.2 provides an analysis of the relative sources of TP and TN as represented in the model. This allocation analyses is the type of source information needed for assessment of load reduction scenarios and subsequent TMDL development.

2.7.1 Loading Analyses at AR/OK Stateline and Tahlequah

Different methods and sources were used for the loading values developed for the AR/OK stateline and for the IR near Tahlequah, OK. The AWRC provided loading estimates for the IR South of Siloam Springs, AR (Reach 630, USGS 07195400) for the period from 1997 through 2008 (B. Haggards, Personal Communication on 5/26/10) based on their data collection and

analysis efforts (e.g., see Haggard (2010), and Massey and Haggard (2010) as an example of annual reports). For 2009, AQUA TERRA used the AWRC data and performed the same calculations to develop the loading values, and confirmed the numbers with AWRC. Figure 2-33 shows the scatterplot of log-transformed monthly loads (TP at top, and TN at bottom) between the HSPF simulated and the AWRC-calculated monthly loads (labeled as 'Observed' in Figure 2-33); log transformations are commonly used for nutrient loads due to their high variability. The R^2 values of 0.66 for TP and 0.63 for TN are considered reasonable, especially since these are within 20% of the flow calibration and validation R^2 values. There is considerable scatter in the plots but a reasonable correlation is evident.

For the IR near Tahlequah (Reach 870, USGS 07196500), the data collection frequency was considerably less than at the Stateline, and load estimates were not available from any agency. Consequently, we selected a USGS program called LOADEST as a technique for load estimation.

Rating curves were developed for the Stateline based on daily loads computed by Brian Haggard. The Figure 2-35 shown below provide those results for TP and TN at Reach 630, just upstream of the Stateline. The results show good consistency between the modeled and observed values for most of the range of the observed flows. For the TN plot the lower values appear to be slightly over-simulated below about 500 cfs.

LOAD ESTimator (LOADEST) is a software program designed to estimate the loadings of constituents in streams based on discrete samples of constituent concentrations and observed streamflow (Runkel and Cohn, 2004). The program develops a regression model using the observed data, and additional data variables specified by the user. The regression model is then used to estimate loads over a user-specified time interval. The program also calculates, mean load estimates, standard errors, and 95% confidence intervals on a monthly, seasonal, or annual basis.

Three statistical estimation methods are used for calibration and estimation of loads. The Adjusted Maximum Likelihood Estimation (AMLE) and Maximum Likelihood Estimation (MLE) methods are appropriate when the residuals (i.e., differences between observed and calculated values) are normally distributed. AMLE is appropriate when the calibration data contains censored data (i.e., when observed values are less than a laboratory detection limit). If there are no censored data, then AMLE and MLE give the same results. Least Absolute Deviation (LAD) is used when residuals are not normally distributed.

LOADEST includes several predefined models that specify the form of the regression equation. The user can either preselect the model based on specific knowledge of the system being modeled, or let LOADEST select the best model from the set of predefined models. For this study, LOADEST was allowed to select the best regression model to estimate TN and TP loads. LOADEST provides several useful statistics, like concentration bias, partial concentration ratio, and Nash-Sutcliffe efficiency index for load and concentration estimation following the calibration and estimation.

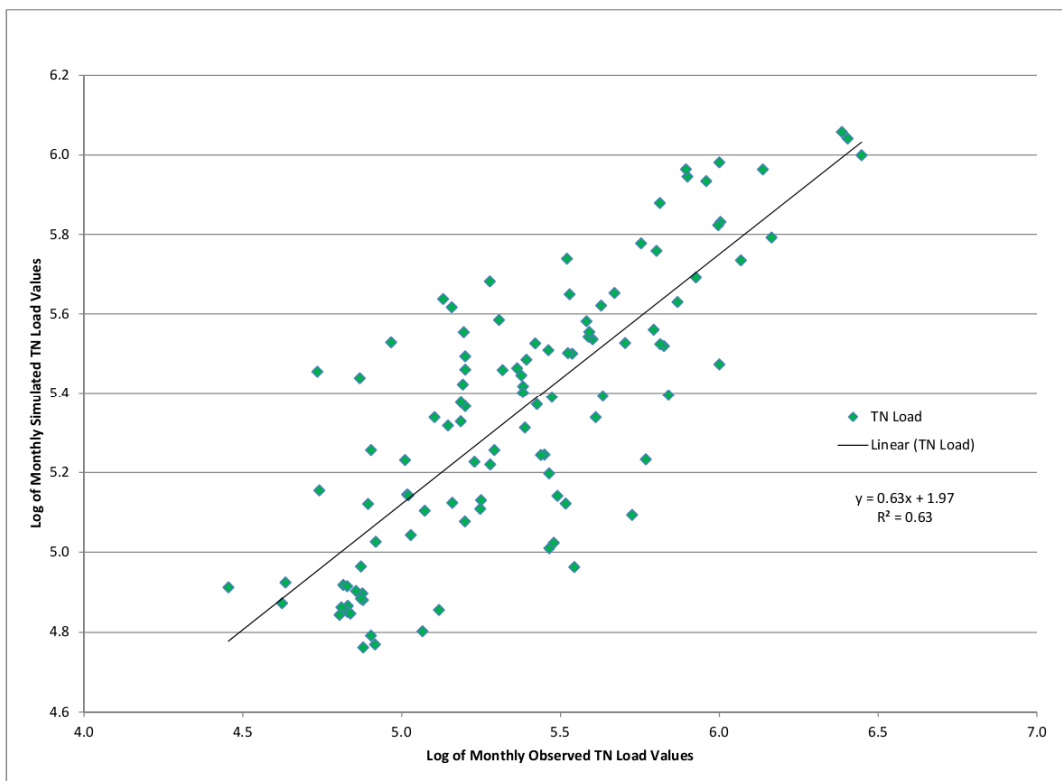
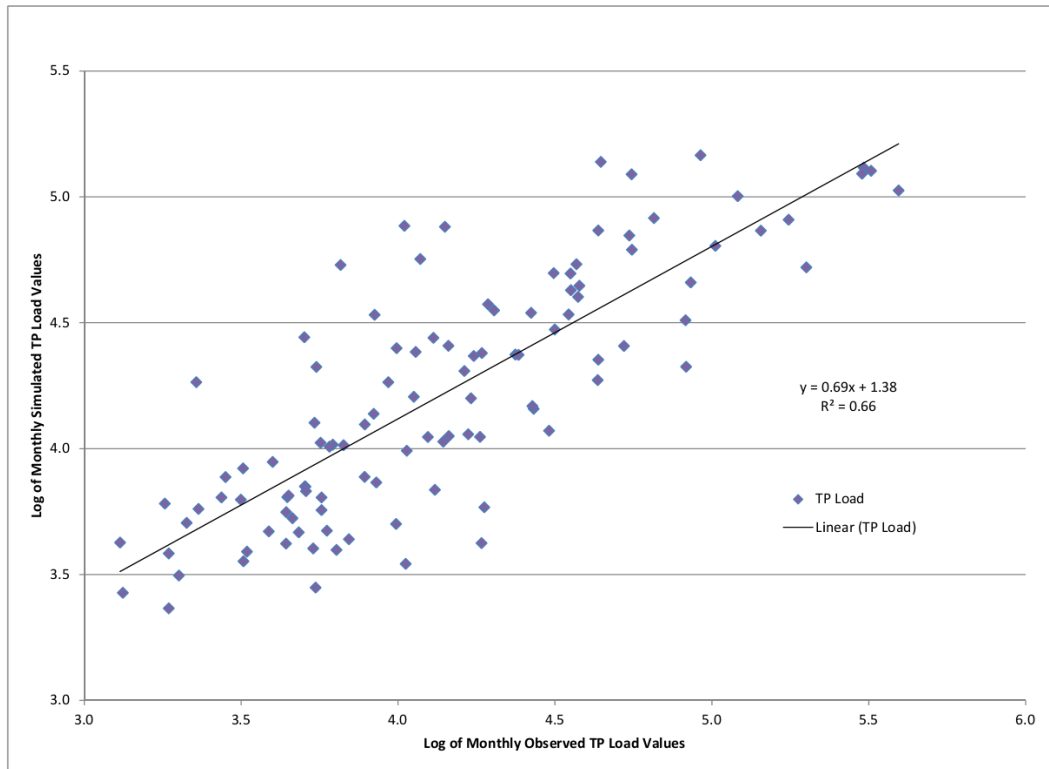


Figure 2-33 Scatterplots of TP (top) and TN (bottom) Monthly Loads at the IR South of Siloam Springs, AR (RCH630)

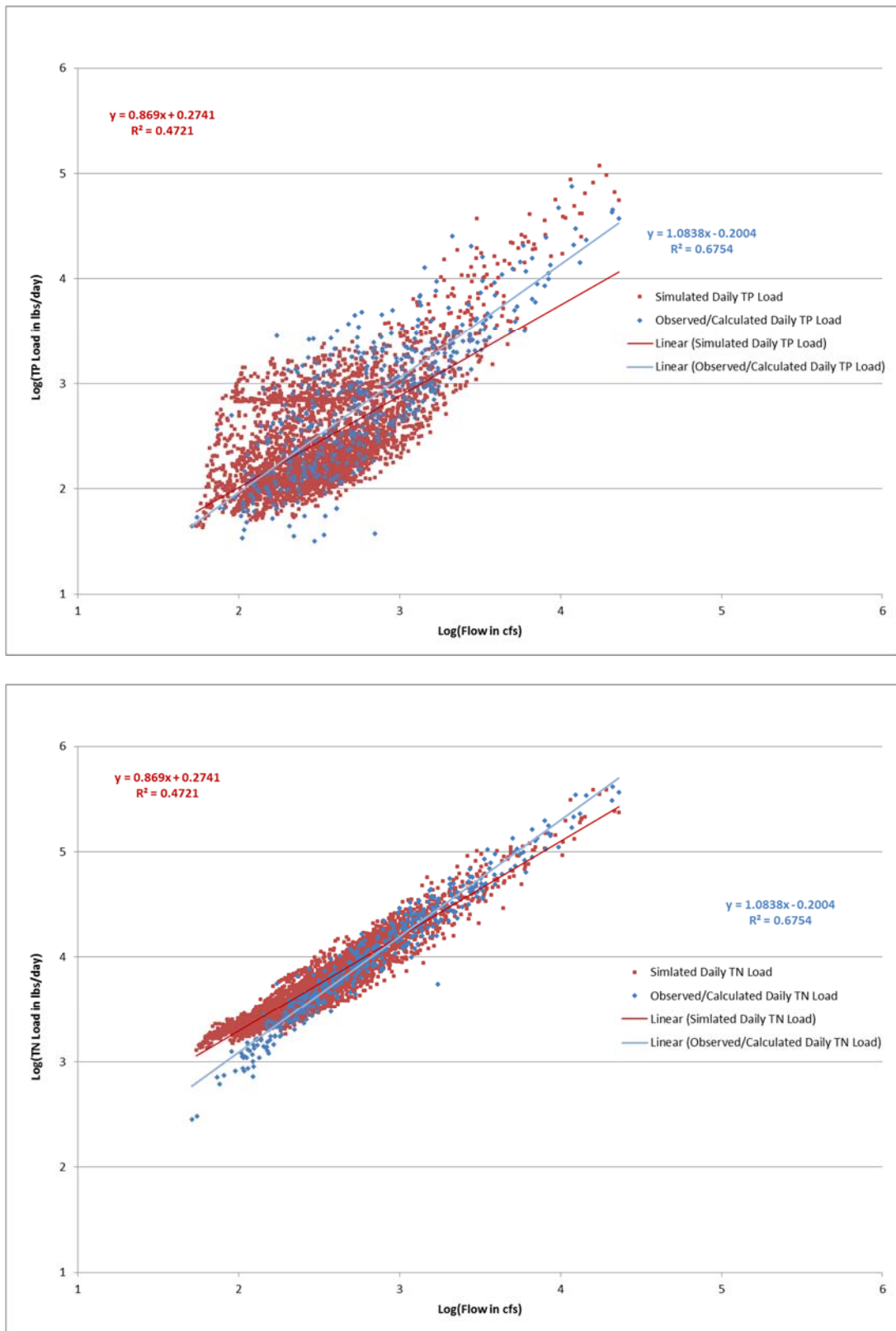


Figure 2-34 Flow and load rating curves of TP (top) and TN (bottom) at the IR South of Siloam Springs, AR (RCH630)

The LOADEST analysis was performed using data for the Illinois River near Tahlequah. Approximately 110 grab samples of TN and TP concentration and continuous daily streamflow were available at the gage for the IRW model calibration period of 2001-2009. The discrete observed TN and TP values were provided to LOADEST along with the complete time series of observed flow for the calibration period. LOADEST was allowed to select the best regression model for each of the constituents.

The LOADEST estimation results are reported from the MLE method, as there were no censored data, and the residuals were normally distributed. The summary statistics suggest that the LOADEST model provides reasonable estimates of TN and TP load (Table 2-27); however, TP may be overestimated by LOADEST since the Partial Concentration Ratio is greater than 1 (Table 2-27).

Table 2-27 LOADEST Summary Statistics for TP and TN loads at the Illinois River near Tahlequah (RCH870)

Constituent	Bias Percentage¹	Partial Concentration Ratio²	Nash-Sutcliffe Efficiency Index³
Total Nitrogen	-2.26	0.98	0.95
Total Phosphorus	15.02	1.15	0.86

¹Positive values suggest overestimation and vice-versa. Model should not be used if + or – bias exceeds 25%.

²Values >1 indicate overestimation, and vice-versa.

³Value of 1 means a perfect fit to observed data, 0 means that the model estimates are as accurate as the mean of the observed data, and <0 means that the observed mean is a better estimate than the model estimate.

The load estimates of TN and TP from LOADEST were compared with the load estimates from the corresponding reach (RCH870) of the HSPF model of the IRW (Table 2-28)). The HSPF model generally estimated higher TN and TP loads than LOADEST; however, the results from the two models were similar for much of the simulation period. To compare the results from the models, the monthly loadings were plotted (Figure 2-33 for TP and Figure 2-35 for TN) using log scales. The high correlation coefficients (0.9 for TN and 0.8 for TP) suggest that the two models demonstrate significant agreement. Comparison of the two plots also shows that there is considerably more scatter for TP than for TN, as might be expected since TP is more closely associated with TSS (and sediment), which demonstrates great variability often requiring display with logarithmic scales.

It should be noted that the LOADEST and HSPF models of the IRW are two different types of models; LOADEST is a statistical model, and HSPF is a continuous simulation model based on physical and empirical relationships approximating important watershed processes. The models should not be expected to produce the same results, but the comparison of the two models does increase confidence in the overall IRW modeling effort and results at Tahlequah.

Table 2-28 Annual Loadings of TN and TP (tons/year) by LOADEST and the HSPF IRW model at the Illinois River near Tahlequah (RCH870)

Year	Total Nitrogen (tons/year)		Total Phosphorus (tons/year)	
	LOADEST Estimates (MLE)	HSPF Model Estimates	LOADEST Estimates (MLE)	HSPF Model Estimates
2001	2,752	2,645	280	316
2002	1,948	2,619	171	376
2003	873	1,680	56	117
2004	2,733	3,133	349	287
2005	1,886	2,181	149	139
2006	853	2,014	55	226
2007	1,700	2,211	86	156
2008	4,630	4,250	498	513
2009	3,484	3,646	289	355
Average	2,318	2,709	215	276

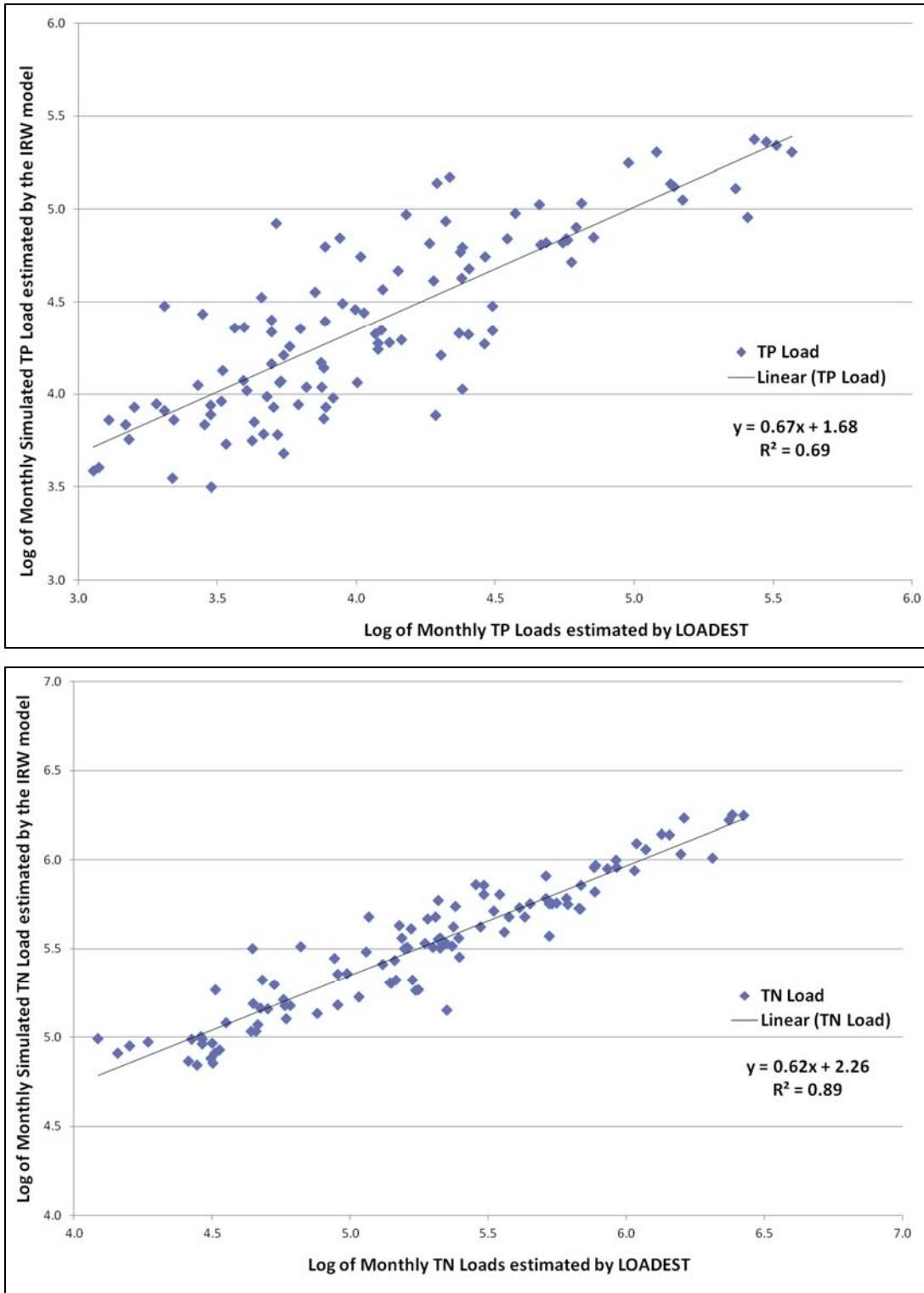


Figure 2-35 Comparison of Monthly Loading (lbs/mo) of TP (top) and TN (bottom) estimated with LOADEST and the HSPF IRW model at the Illinois River near Tahlequah (RCH870)

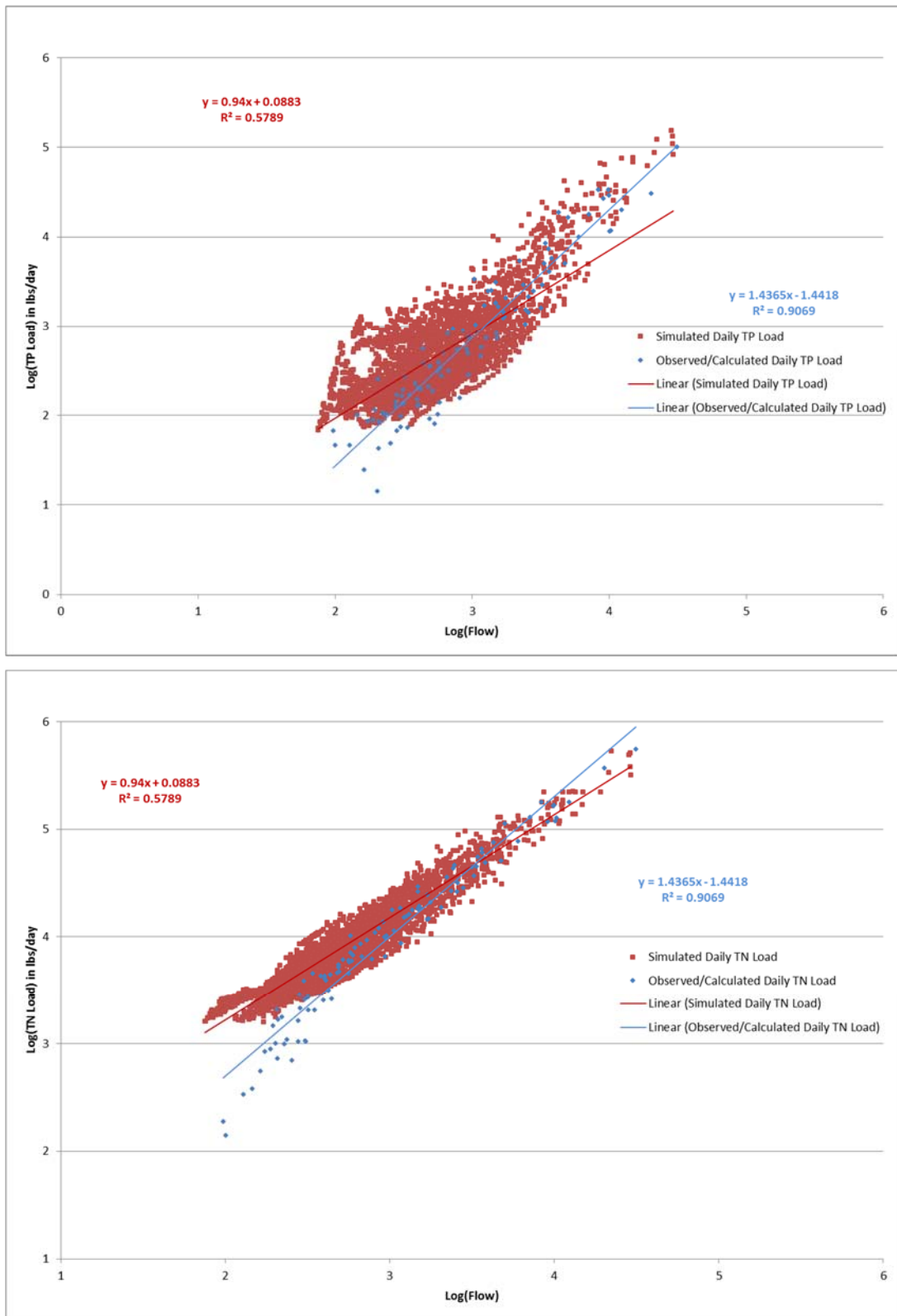


Figure 2-36 Flow and load rating curves of TP (top) and TN (bottom) at the Illinois River near Tahlequah (RCH870)

2.7.2 Load Allocation at AR/OK Stateline and Tahlequah

Load allocation is the process of performing calculations with the model output in order to determine how much of the constituent load at any point (stream reach) is derived from each of the constituent sources in the drainage area above that point. Thus it provides a calculation, and division, of the total load into its contributing sources, and thereby identifies the dominant contributors to constituent concentrations and loads at that point in the watershed. The calculations are performed from upstream to downstream within in each tributary so that all land uses and point sources are included, and any instream gains/losses are also considered. In this way, load reduction and TMDL development can identify which sources to target to most effectively reduce loads and meet water quality standards.

Table 2-29 and Table 2-30 provide the results of the load allocation analyses for TP and TN, respectively, for seven key locations within the IRW. These include the upstream IR calibration sites at Savoy AR (Reach 150), Osage Creek near Elm Springs AR (Reach 316), IR near Siloam Springs (Reach 630), and the actual AR/OK stateline (Reach 635) which is about one mile downstream of the Stateline gage. The last 3 sites in these tables are the most downstream gages on the IR (Reach 870), Baron Fork (Reach 746), and Caney Creek (Reach 912) that contribute directly to Lake Tenkiller.

Each of these tables contain two displays: the top display shows the absolute numbers (in pounds/year) of the nutrient loads (either TP or TN) from each source, including both land-based nonpoint sources and point sources, stream gains and losses, and selected subtotals and totals. The bottom display shows the percent contribution from each source at each reach, with total percentages shown at the far right.

Review of the information in Table 2-29 and Table 2-30 provides a wealth of insight into the source contributions within the IRW, as follows:

- a. Pasture is the dominant nonpoint source for both TP and TN, with about 20% to more than 80% of TP from all pasture areas, and 40% to 65% of TN (from summing the percent pasture contributions). Also, for TN forest is the other major source. Pasture and forest each represent slightly more than 40% of the land areas of the IRW.
- b. Only in the Osage Creek watershed (Reach 316), with its urbanized uplands (and associated STPs) do point sources exceed the nonpoint contributions; for TP, 60% is from point sources and 40% from nonpoint and other sources. For TN, the numbers are about reversed, with 30% from point sources and almost 70% from nonpoint.
- c. At the AR/OK Stateline, the annual TP load is about 356,000 pounds, and the annual TN load is about 3.6 Million pounds. The split is about 30%/70% for TP for point/nonpoint, and about 17%/83% for TN point/nonpoint.
- d. Urbanized and developed areas contribute less than 2-4% of the TP in most cases, and up to 6-9% of TN in some areas. Although these contributions are small watershed-wide, they can and often do have significant impacts at smaller scales.

Although the percent load contributions in these tables are precise numbers, they are the result of many assumptions in the model and the model application procedures (discussed above). So these numbers should be considered as 'best estimates', and the percent contributions might vary as much as $\pm 20\%$. Also, it should be noted that the Pasture1-Litter segment also includes grazing animal manure applications. As a result, the litter applications represent 60% of the TP and 40% of the TN applied, so these adjustments should be applied to the numbers in Tables 5.3 and 5.4 for those segment contributions.

Table 2-29 Load Allocation for TP for Selected Reaches within the IRW

Nonpoint and Point sources loading of Total P (lbs) after applying the gains/losses in the stream																					
Allocation Point	Total Point Source Loading of TP (lbs)	Total Nonpoint Source Loading of TP (lbs)	Total Gain (+) from stream scour (lbs)	% Gain (+) from stream scour	Sources												Total Point Source	Total Nonpoint Source	Gains from Channel Scour	Diversions & Minor Gains/losses	Total (PS + NPS + Channel Gain)
					Forest	Pasture1	Pasture1-Litter	Pasture2	Pasture3	Grass/Shrub/Barren	Developed, Open	Developed, Low	Developed, Med/High	Wetlands	Cropland						
RCH 150	5,491	100,503	3,438	3.2%	3,810	23,436	26,804	13,186	28,010	1,075	2,454	781	253	28	304	5,469	100,143	3,438	10	109,059	
RCH 316	93,949	52,659	6,906	4.7%	813	13,376	3,293	4,420	15,080	685	4,730	5,713	4,269	7	274	93,949	52,659	6,906	14	153,529	
RCH 630	103,930	244,263	11,863	3.4%	7,901	47,165	56,798	24,900	72,200	3,094	11,444	9,957	6,956	77	722	102,634	241,214	11,863	33	355,745	
RCH 635	103,930	244,603	11,863	3.4%	7,912	47,257	56,773	24,914	72,204	3,098	11,451	9,947	6,949	78	722	102,527	241,304	11,863	33	355,727	
RCH 746	2,857	163,480	5,903	3.5%	9,928	33,737	35,854	22,282	48,938	8,013	3,359	251	60	33	168	2,843	162,622	5,903	16	171,383	
RCH 870	135,836	394,649	36,904	7.0%	18,197	85,618	96,928	38,450	99,852	12,173	15,292	11,089	7,727	191	1,107	132,510	386,623	36,904	-3,304	552,733	
RCH 912	2,257	46,108	2,862	5.9%	2,531	12,905	4,015	7,449	16,607	988	1,027	302	198	3	82	2,257	46,108	2,862	5	51,232	
Percentage of loadings of TP from each source after reduction factor is applied																					
Allocation Point	Sources														Total Point Source	Total Nonpoint Source	Gains from Channel Scour	Diversions & Minor Gains/losses	Total (PS + NPS + Channel Gain)		
	Forest	Pasture1	Pasture1-Litter	Pasture2	Pasture3	Grass/Shrub/Barren	Developed, Open	Developed, Low	Developed, Med/High	Wetlands	Cropland										
RCH 150	3.5	21.5	24.6	12.1	25.7	1.0	2.3	0.7	0.2	0.0	0.3	5.0	91.8	3.2	0.0	100.00					
RCH 316	0.5	8.7	2.1	2.9	9.8	0.4	3.1	3.7	2.8	0.0	0.2	61.2	34.3	4.5	0.0	100.00					
RCH 630	2.2	13.3	16.0	7.0	20.3	0.9	3.2	2.8	2.0	0.0	0.2	28.9	67.8	3.3	0.0	100.00					
RCH 635	2.2	13.3	16.0	7.0	20.3	0.9	3.2	2.8	2.0	0.0	0.2	28.8	67.8	3.3	0.0	100.00					
RCH 746	5.8	19.7	20.9	13.0	28.6	4.7	2.0	0.1	0.0	0.0	0.1	1.7	94.9	3.4	0.0	100.00					
RCH 870	3.3	15.5	17.5	7.0	18.1	2.2	2.8	2.0	1.4	0.0	0.2	24.0	69.9	6.7	-0.6	100.00					
RCH 912	4.9	25.2	7.8	14.5	32.4	1.9	2.0	0.6	0.4	0.0	0.2	4.4	90.0	5.6	0.0	100.00					

Table 2-30 Load Allocation for TN for Selected Reaches within the IRW

Nonpoint and Point sources loading of Total N (lbs) after applying the gains/losses in the stream																				
Allocation Point	Total Point Source Loading of TN (lbs)	Total Nonpoint Source Loading of TN (lbs)	Atm. Dep. on water (lbs)	Total Gain (+)/ Loss (-) in the stream (lbs)	% Gain (+)/ Loss (-) in the stream	Forest	Pasture1	Pasture1-Litter	Pasture2	Pasture3	Grass/Shrub/Barren	Developed, Open	Developed, Low	Developed, Med/High	Wetlands	Cropland	Total Point Source	Total Nonpoint Source	Diversions & Minor Gains/losses	Total
RCH 150	30,759	972,127	32	-4,840	-0.5%	210,426	248,952	43,007	125,820	232,360	13,862	64,504	17,848	4,549	1,895	4,321	30,505	967,543	120	998,168
RCH 316	480,530	1,005,542	30	-12,281	-0.8%	45,241	255,212	6,609	72,806	257,788	9,071	134,538	130,125	80,685	444	4,680	476,590	997,200	168	1,473,958
RCH 630	610,468	3,053,254	146	-49,109	-1.3%	443,651	626,737	108,022	282,550	822,441	43,399	318,302	225,779	127,280	5,012	11,649	599,796	3,014,823	476	3,615,095
RCH 635	610,468	3,058,343	149	-50,080	-1.4%	444,594	628,328	108,103	282,957	823,118	43,515	318,805	225,736	127,246	5,057	11,646	599,635	3,019,103	479	3,619,216
RCH 746	14,868	1,696,905	73	-12,542	-0.7%	519,203	290,699	66,484	187,292	405,728	110,723	92,650	5,589	1,055	2,095	3,040	14,667	1,684,559	223	1,699,449
RCH 870	732,435	4,869,605	375	-137,356	-2.5%	1,023,887	1,005,827	190,599	414,927	1,090,350	178,289	430,103	250,343	139,576	12,107	18,652	709,303	4,754,658	-47,352	5,416,609
RCH 912	19,441	510,038	12	-2,779	-0.5%	128,561	110,887	8,478	62,122	143,470	14,167	27,950	6,654	3,481	194	1,531	19,202	507,495	58	526,755

Percentage of loadings of TN from each source after reduction factor is applied																
Allocation Point	Forest	Pasture1	Pasture1-Litter	Pasture2	Pasture3	Grass/Shrub/Barren	Developed, Open	Developed, Low	Developed, Med/High	Wetlands	Cropland	Total Point Source	Total Nonpoint Source	Diversions & Minor Gains/losses	Total	
RCH 150	21.08	24.94	4.31	12.61	23.28	1.39	6.46	1.79	0.46	0.19	0.43	3.06	96.93	0.01	100.00	
RCH 316	3.07	17.31	0.45	4.94	17.49	0.62	9.13	8.83	5.47	0.03	0.32	32.33	67.65	0.01	100.00	
RCH 630	12.27	17.34	2.99	7.82	22.75	1.20	8.80	6.25	3.52	0.14	0.32	16.59	83.40	0.01	100.00	
RCH 635	12.28	17.36	2.99	7.82	22.74	1.20	8.81	6.24	3.52	0.14	0.32	16.57	83.42	0.01	100.00	
RCH 746	30.55	17.11	3.91	11.02	23.87	6.52	5.45	0.33	0.06	0.12	0.18	0.86	99.12	0.01	100.00	
RCH 870	18.90	18.57	3.52	7.66	20.13	3.29	7.94	4.62	2.58	0.22	0.34	13.09	87.78	-0.87	100.00	
RCH 912	24.41	21.05	1.61	11.79	27.24	2.69	5.31	1.26	0.66	0.04	0.29	3.65	96.34	0.01	100.00	

Section 3 Tenkiller Ferry Lake EFDC Water Quality Model Analysis

3.1 Overview of the EFDC Model

The Environmental Fluid Dynamics Code (EFDC) is a general-purpose surface water modeling package for simulating three-dimensional (3-D) circulation, mass transport, sediments and biogeochemical processes in surface waters including rivers, lakes, estuaries, reservoirs, nearshore and continental shelf-scale coastal systems. The EFDC model was originally developed at the Virginia Institute of Marine Science for estuarine and coastal applications (Hamrick, 1992; 1996). Over the past decade, the US Environmental Protection Agency (EPA) has continued to support its development, and EFDC is now part of a family of public domain surface water models recommended by EPA to support water quality investigations including TMDL studies. In addition to state of the art hydrodynamics with salinity, water temperature and dye tracer simulation capabilities, EFDC can also simulate cohesive and non-cohesive sediment transport, the transport and fate of toxic contaminants in the water and sediment bed, and water quality interactions that include dissolved oxygen, nutrients, organic carbon, algae and bacteria. A state of the art sediment diagenesis model (Di Toro, 2001) is internally coupled with the water quality model (Park et al., 2000). Special enhancements to the hydrodynamic code, such as vegetation resistance, drying and wetting, hydraulic structure representation, wave-current boundary layer interaction, and wave-induced currents, allow refined modeling of tidal systems, wetland and marsh systems, controlled-flow systems, and near-shore wave-induced currents and sediment transport. The EFDC code has been extensively tested, documented and used in more than 100 surface water modeling studies (Ji, 2008). The EFDC model is currently used by university, government, engineering and environmental consulting organizations worldwide.

Dynamic Solutions, LLC (DSLCC), has developed a version of the EFDC code that streamlines the modeling process and provides links to DSLCC's pre- and post-processing software tool EFDC_Explorer7 (Craig, 2013). The DSLCC version of the EFDC code is open source and DSLCC coordinates with EPA to provide ongoing updates and enhancements to both DSLCC's version of EFDC as well as the version of the EFDC code provided by EPA.

3.2 Model Simulation Period

The EFDC model simulation period is 1 January 2005 through 31 December 2006. There are more observed water quality data available in year 2006; therefore, the Tenkiller Ferry Lake EFDC model is calibrated for the period of 1 January 2006 through 31 December 2006 and validated for the period of 1 January 2005 through 31 December 2005.

The modeled constituents in the Tenkiller Ferry Lake EFDC model are given below.

- Stage
- Water temperature
- Total suspended solids (TSS)
- Nitrogen (TN, organic N, TKN, NO₂+NO₃, NH₃/NH₄)
- Phosphorus (TP, organic P, Ortho-Phosphate)
- Total organic carbon (TOC)
- Phytoplankton (as Chl-a)
- Dissolved oxygen (DO)

3.3 Grid Development

The previously developed lake model consisted of 195 horizontal cells. In this current project, the grid resolution of the lake model has been made finer to resolve technical issues related to grid resolution identified in the previous study (DSLCC, 2006). Grid resolution has been increased in the Forebay areas of the lake where bathymetry is characterized by steep bottom slopes. This refinement of the previous grid should reduce numerical diffusion errors caused by the sigma vertical layers. Grid resolution has also been increased in the upper riverine part of the reservoir and transition zone where the previous grid represented a laterally averaged channel. Figure 3-1 shows a plan view map of the updated 1,443 horizontal cells that has been developed for the current model for Lake Tenkiller. Sixteen (16) even thickness vertical sigma layers are used to represent vertical spatial resolution.

3.4 Shoreline and Bathymetry

In the previous EFDC model for the lake, bottom elevation data was digitized from historical USGS quadrangle maps that represented the topography of the area before construction of the dam in the early 1950s (DSLCC, 2006). Detailed contemporary bathymetric data is now available from a 2005 survey that was conducted to support the collection of sediment cores (Fisher, 2008; Fisher et al., 2009) and the development of a laterally-averaged hydrodynamic and water quality model of Lake Tenkiller (Wells et al., 2008). The new refined lake model grid (Figure 3-1) has been updated with the bathymetry data collected in 2005. The shoreline of the lake is defined by the normal pool elevation of 632.0 ft (192.63 m). The comparison of stage-volume relationship is shown in Figure 3-2 and the stage-volume relation used in EFDC model matches very well with the observed stage-volume relationship.

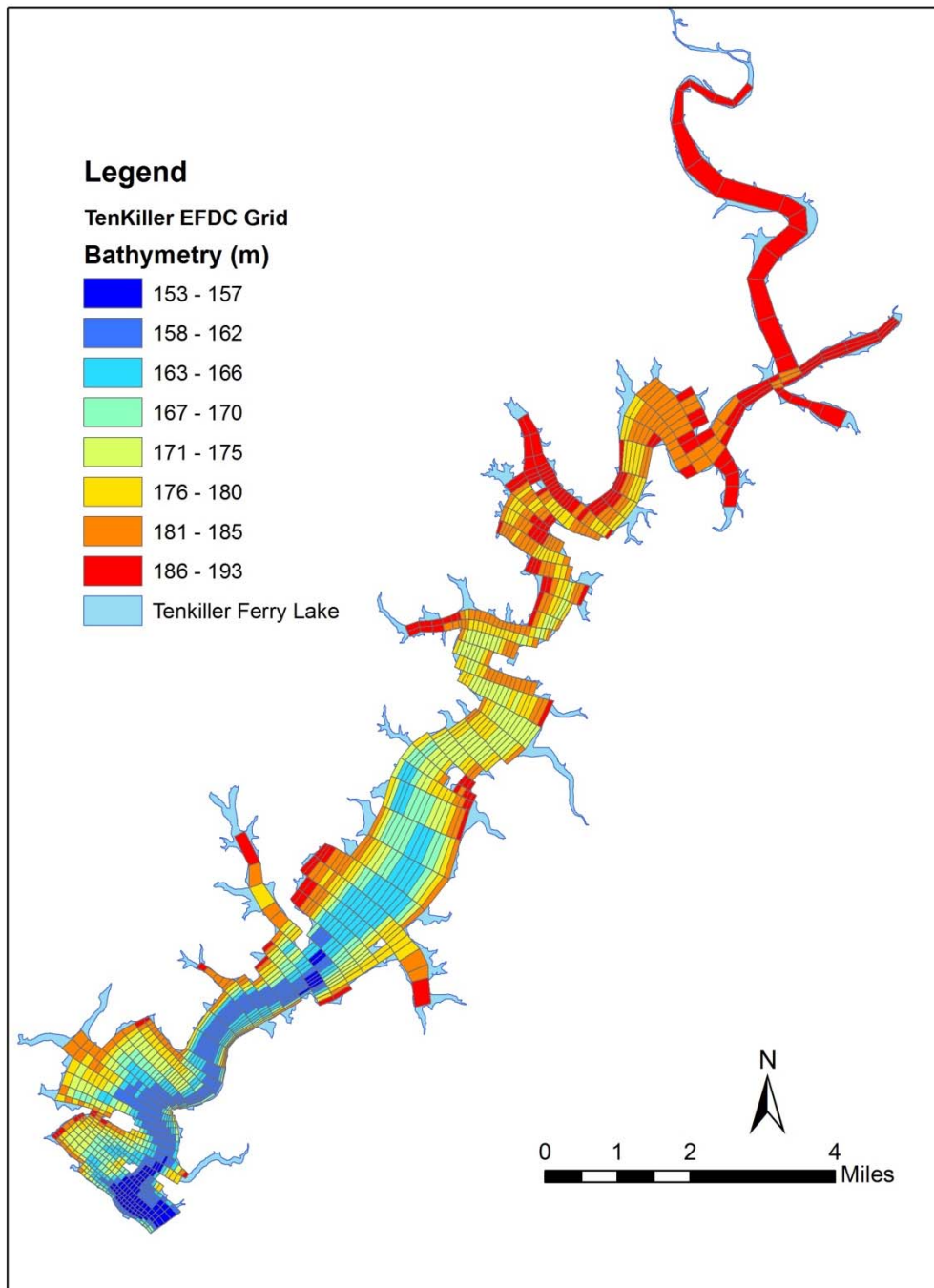


Figure 3-1. Modeling Domain of the Tenkiller Ferry Lake EFDC

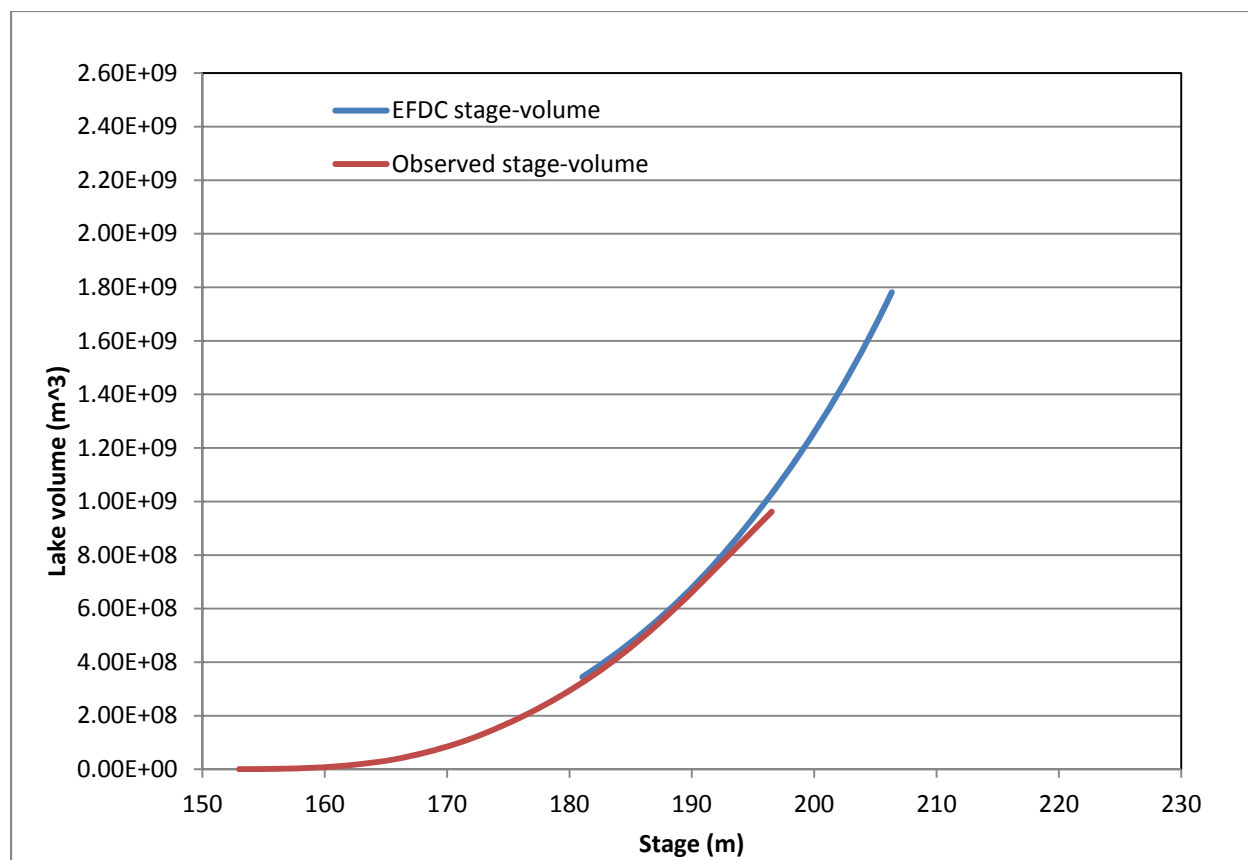


Figure 3-2. Tenkiller Ferry Lake Stage and Storage Volume. Comparison of Observed Data and EFDC Model

3.5 Meteorological Data

Meteorological data used in EFDC includes rainfall, wind speed and direction, relative humidity, atmospheric pressure, cloud cover, solar radiation, and air temperature. These data are used to calculate the atmospheric impact on water temperature and physical transport processes in the system. The data are also used to calculate evapotranspiration in the model domain. The station used in the EFDC model to describe atmospheric forcing is MESONET station COOK, and its location east of the lake can be seen in Figure 3-3. Meteorological data was compiled to represent the two year period (2005-2006) selected for EFDC lake model calibration and validation.

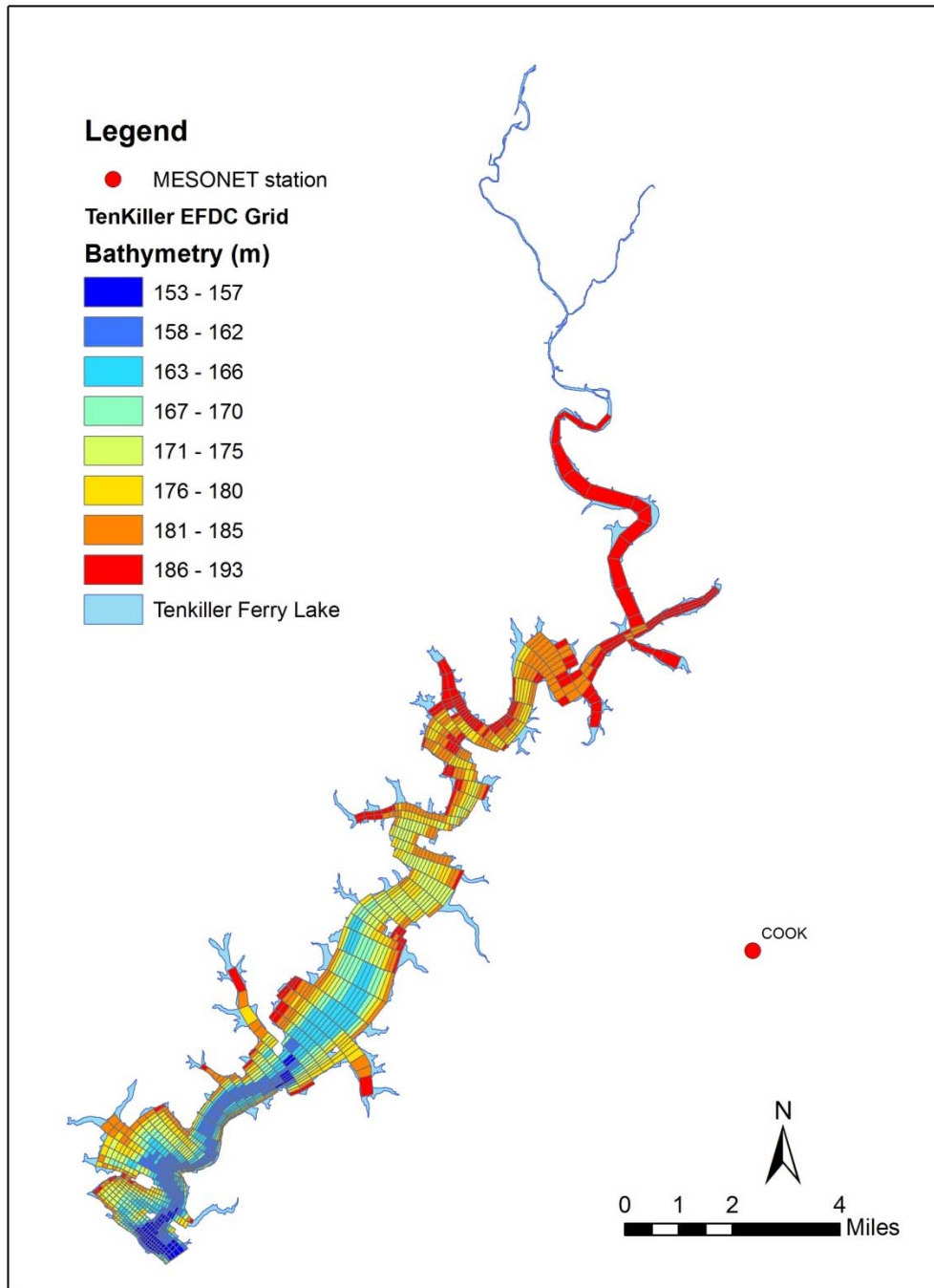


Figure 3-3. Location of the MESONET station COOK

3.6 Boundary Conditions

Boundary conditions for EFDC must be specified for flow boundary conditions to define external inflows of water and mass loading into the EFDC model domain. Flow boundary datasets required for input to EFDC include time series of flow, water temperature, suspended solids and water quality constituents to define mass loading inputs to a waterbody. Flow boundary data was compiled to represent the two year period (2005-2006) selected for EFDC lake model calibration and validation.

The Tenkiller Ferry Lake model was developed with sixteen (16) flow boundaries to define water coming into the lake from the HSPF watershed model, one (1) flow boundary to define releases of water at the dam, and one (1) flow boundary to define a flow balance to account for water removed from the lake by water supply and other unaccounted flows such as leakage from the dam. Table 3-1 lists the eighteen (18) model flow boundary indexes with the number of EFDC cells assigned for the boundary and the HSPF_ID corresponding to that location.

External flow boundary conditions from the HSPF model were assigned to grid cells based on physical location and the specific boundary condition represented in the lake model (Figure 3-4). Simulated streamflow and runoff, water temperature, suspended solids, organic carbon, nutrients, dissolved oxygen and algae biomass records provided by the HSPF model were used to assign flow boundaries for seven (7) tributaries and nine (9) NPS catchments for input to the lake model. More detailed information can be found in Section 3.7 (HSPF-EFDC Linkage). Figure 3-4 shows the HSPF watershed model locations that provided the flow and water quality data for input to the lake model.

Flow release records at the dam (designated by the USACE as Station TENO2 shown in Figure 5-1) are maintained by the USACE. The water supply withdrawals from Tenkiller Ferry Lake were not available; therefore, a flow balance was estimated using all inflows including all HSPF simulated watershed flows, and rainfall, and all outflows including evaporation and flow releases at the dam. A flow balance was computed to ensure that the EFDC model simulated lake stage matched the observed lake stage which in turn ensures that the physical representation of lake surface area, volume, and residence time is accurate. The flow balance adjustment ensures that water temperature and water quality conditions could be simulated and calibrated without the uncertainty associated with a discrepancy between observed and modeled lake stage and volume.

The methodology used to develop the flow balance is accepted practice for developing hydrodynamic models of reservoirs (Cole and Wells, 2008; Green, 2013). A flow balance for the Lake Tenkiller model is needed to account for the known variance of flow measurements provided by the USGS, unknown inflows, and unknown outflows such as leakage identified by the US Army Corp of Engineers at the dam and unknown water withdrawals for local water supply systems served by Lake Tenkiller. On a daily average basis, the volume accounted for by the flow balance represented less than 0.1%, of the average volume of the lake during 2005-2006. When flow balance water is withdrawn from the lake, the mass of nutrients removed from the lake will correspond to the local nutrient concentration simulated at lake locations assigned for the flow balance. Since flow balance withdrawals will export water with nutrient concentrations that may, or may not, be lower than watershed inflow concentrations, and the flow balance volume over the simulation period is relatively small, the flow balance is not expected to impact the overall water quality simulation for Lake Tenkiller.

Table 3-1. Tenkiller Ferry Lake EFDC Model Flow Boundaries and Data Source

BC	Boundary Group ID	NAME	Data	Cells
1	Dam Release	Dam release	Outflow	3
2	Subbasin 946	Unknown	HSPF NPS catchment	2
3	Subbasin 948	Unknown	HSPF NPS catchment	2
4	Subbasin 942	Unknown	HSPF NPS catchment	2
5	Subbasin 938	Chicken Creek	HSPF tributary	1
6	Subbasin 936	Unknown	HSPF tributary	1
7	Subbasin 928	Unknown	HSPF NPS catchment	2
8	Subbasin 922	Unknown	HSPF tributary	1
9	Subbasin 916	Dry Creek	HSPF tributary	1
10	Subbasin 932	Unknown	HSPF NPS catchment	1
11	Subbasin 924	Unknown	HSPF NPS catchment	1
12	Subbasin 918	Unknown	HSPF NPS catchment	1
13	Subbasin 912	Unknown	HSPF tributary	1
14	Subbasin 914	Caney Creek	HSPF NPS catchment	1
15	Subbasin 752	Baron Fork	HSPF tributary	1
16	Subbasin 890	Unknown	HSPF tributary	1
17	Subbasin 900	Illinois River	HSPF NPS catchment	2
18	Balance Flow		Estimated	4

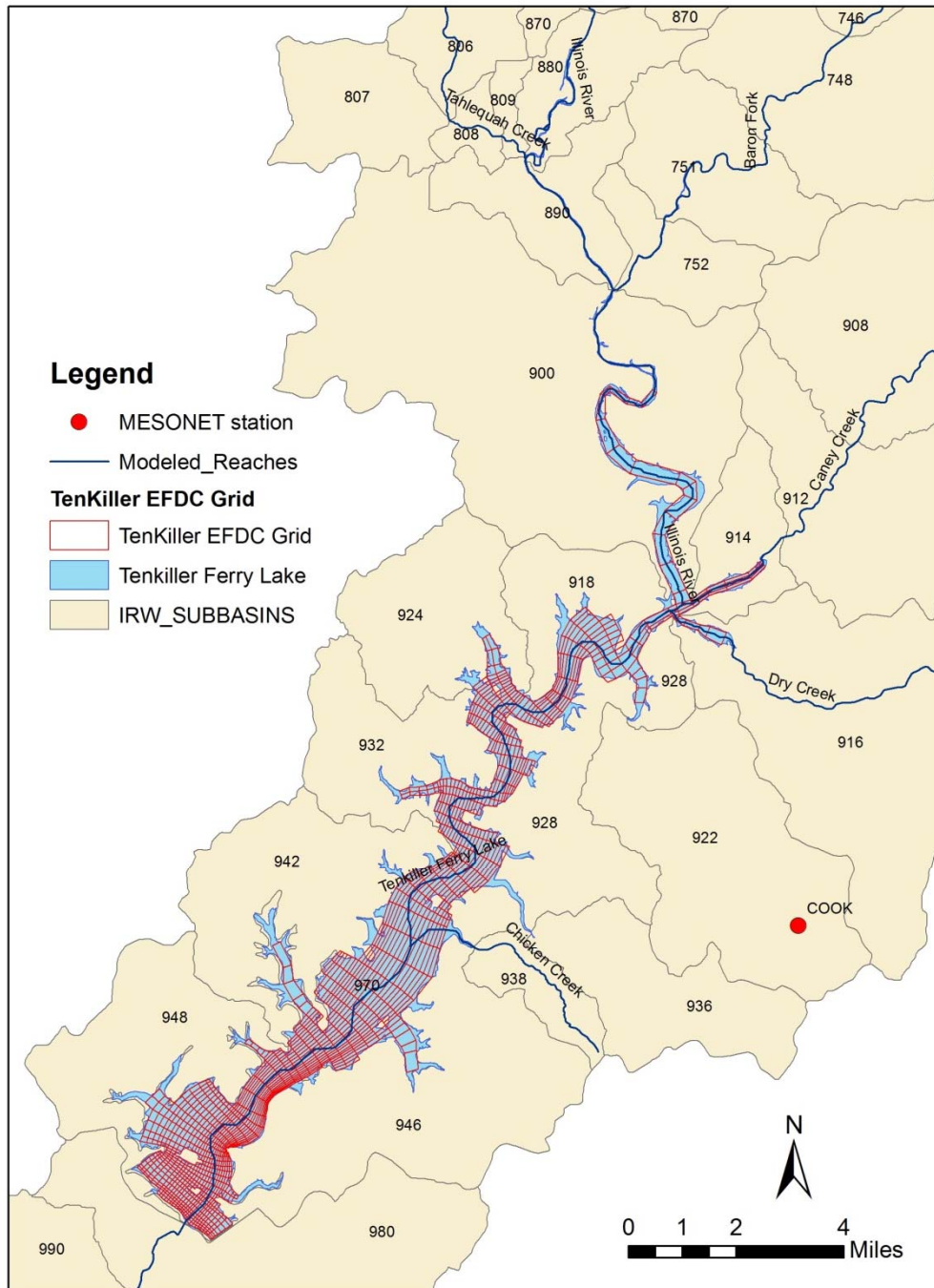


Figure 3-4. HSPF tributary and catchment locations

3.7 HSPF-EFDC Linkage

For the Tenkiller Ferry Lake model, streamflow and pollutant loading data were obtained from the HSPF model developed to represent runoff over the drainage area to the lake. Sub-watersheds of the HSPF model, defined by reaches where flow and pollutant loads are routed through a one-dimensional reach network, simulate flow and water quality concentrations at fixed downstream outlet locations. Sub-watersheds not defined by an in-stream reach simulate water volume and constituent loads as distributed NPS runoff over the drainage area of the sub-watershed. The HSPF sub-watersheds defined as in-stream reaches (TRIB) and distributed catchments (NPS) that provide external flow and loads to the lake are listed in Table 3-2.

The HSPF watershed model was setup for model calibration and validation to represent hydrologic and watershed runoff conditions over the long-term period from 1992-2009. As described in Section 3.5 (Meteorological Data) and Section 3.6 (Boundary Conditions), the EFDC lake model was setup to represent a two-year period (2005-2006) for model calibration (2006) and model validation (2005). The HSPF watershed model results simulated for 2005-2006 were extracted and linked for input to the EFDC lake model.

State variables of the HSPF watershed model developed for the Tenkiller Ferry Lake project are listed in Table 3-2. State variable units are identified for in-stream reaches (TRIB) and distributed catchments (NPS).

Table 3-2. HSPF State Variables and Units for the Tenkiller Ferry Lake Watershed Model

HSPF State Variable	Name	Units	Units
HYDROLOGY		TRIB	NPS
Streamflow; NPS Runoff	FLOW	cfs	cf/hr
Water Temperature	WTEM	Deg-F	Deg-F
SEDIMENT TRANSPORT			
Inorganic Total Suspended Solids	TSS	mg/L	tons/hr
WATER QUALITY			
Algae biomass (as Chl-a)	PHYT	mg/L	lbs/hr
CBOD	CBOD	mg/L	lbs/hr
Refractory Organic Carbon	TORC	mg/L	lbs/hr
Refractory Organic Phosphorus	TORP	mg/L	lbs/hr
Total Phosphate	PO4	mg/L	lbs/hr
Total Phosphorus	TP	mg/L	lbs/hr
Refractory Organic Nitrogen	TORN	mg/L	lbs/hr
Ammonia+Ammonium-Nitrogen	NH3+NH4	mg/L	lbs/hr
Nitrate+Nitrite-Nitrogen	NO2+NO3	mg/L	lbs/hr
Total Nitrogen	TN	mg/L	lbs/hr
Dissolved Oxygen	DOX	mg/L	lbs/hr

The functional relationships used to link the HSPF results for input to the EFDC model are listed in Table 3-3. The HSPF-EFDC linkage of flow, water temperature, suspended solids, phosphate, ammonia, nitrate and dissolved oxygen is straightforward and only requires conversion of some of the HSPF units to EFDC units. HSPF-EFDC linkage of algae and organic matter requires transformations as described below.

Table 3-3. HSPF-EFDC Linkage

EFDC HYDRODYNAMICS & SEDIMENT TRANSPORT	Units	HSPF-EFDC Linkage
Flow	cms	HSPF Streamflow; Runoff
Water Temperature	C	HSPF Water Temperature (WTEM)
Inorganic Cohesive Solids	mg/L	HSPF TSS
EFDC WATER QUALITY		
Bluegreen Algae	mg/L	HSPF PHYT Biomass * C/Chl * F_BG
Diatoms Algae	mg/L	HSPF PHYT Biomass * C/Chl * F_D
Green Algae	mg/L	HSPF PHYT Biomass * C/Chl * F_G
Refractory Particulate Org Carbon	mg/L	HSPF (CBOD/(CVBO/CDW) + ORC)* F_R
Labile Particulate Org Carbon	mg/L	HSPF (CBOD/(CVBO/CDW) + ORC)* F_L
Diss Org Carbon	mg/L	HSPF (CBOD/(CVBO/CDW) + ORC)* F_D
Refractory Particulate Org Phosphorus	mg/L	HSPF (CBOD/(CVBO/CDW) *P/C + ORP)* F_R
Labile Particulate Org Phosphorus	mg/L	HSPF (CBOD/(CVBO/CDW) *P/C + ORP)* F_L
Diss Org Phosphorus	mg/L	HSPF (CBOD/(CVBO/CDW)*P/C + ORP)* F_D
Total Phosphate	mg/L	HSPF PO4
Refractory Particulate Org Nitrogen	mg/L	HSPF (CBOD/(CVBO/CDW)*N/C + ORN)* F_R
Labile Particulate Org Nitrogen	mg/L	HSPF (CBOD/(CVBO/CDW)*N/C + ORN)* F_L
Diss Org Nitrogen	mg/L	HSPF (CBOD/(CVBO/CDW)*N/C + ORN)* F_D
Ammonium Nitrogen	mg/L	HSPF NH3+NH4
Nitrate+Nitrite Nitrogen	mg/L	HSPF NO2+NO3
Chemical Oxygen Demand	mg/L	HSPF n/a COD=0
Dissolved Oxygen	mg/L	HSPF DOX

HSPF represents algae as a single assemblage with output units for the Tenkiller Ferry Lake project as mg Chl/L. A C/Chl ratio of 0.025 mg C/ug Chl is assigned to convert the HSPF results for chlorophyll biomass to organic carbon for input to EFDC. This ratio was also used by Wells et al. (2008) for the development, calibration, and validation of a CE-QUAL-W2 model of the Tenkiller Ferry Lake. The Tenkiller Ferry Lake EFDC model was developed to simulate three algae groups: cyanobacteria, diatom, and green algae. The fraction assigned to cyanobacteria (F_C), diatoms (F_D), and blue green (F_BG) algae was 0.27, 0.51, and 0.22, respectively. These fraction numbers were developed based on the CDM collected data during 2005 to 2007.

Labile HSPF CBOD and refractory HSPF organic carbon (ORC), organic phosphorus (ORP), and organic nitrogen (ORN) are added as shown in the HSPF-EFDC linkage in Table 3-3 to derive non-living TOC, TOP and TON for input to the EFDC model. HSPF derived TOC, TOP and TON is then split for input to EFDC as refractory, labile and dissolved components of total organic matter using the fractions given in Table 3-4. Parameter values for assignment of the splits of TOC, TOP and TON (Table 3-4) are taken from the CE-QUAL-W2 modeling study of the Tenkiller Ferry Lake (Wells et al., 2008).

CBOD is represented as ultimate CBOD in the HSPF model. The stoichiometric ratio for oxygen: dry weight of biomass (CVBO) has a value of CVBO=1.98 mg O₂/mg-DW and the ratio of carbon: dry weight (CDW) is 0.49 mg C/mg-DW. The parameter values used to convert CBOD to an equivalent organic carbon basis are taken from the parameter values assigned for the HSPF model. The stoichiometric ratios for Phosphorus to Carbon and Nitrogen to Carbon are based on Redfield ratios where C/P = 41.1 mg C/mg-P and C/N = 5.7 mg C/mg-N (Di Toro 2001).

Table 3-4. Refractory, Labile and Dissolved Splits for Organic Matter

	Refractory F_R	Labile F_L	Dissolved F_D
	RPOM	LPOM	DOM
TOC	0.25	0.25	0.5
TOP	0.25	0.25	0.5
TON	0.25	0.25	0.5

Section 4 Water Quality and Sediment Flux Model

4.1 Water Quality Model

For the Tenkiller Lake Ferry EFDC model, the water quality model is internally coupled with the hydrodynamic model, a sediment transport model and a sediment diagenesis model. The hydrodynamic model describes circulation and physical transport processes including turbulent mixing and water column stratification during the summer months. The sediment transport model describes the water column distribution of inorganic cohesive particles resulting from transport, deposition, and resuspension processes. The sediment diagenesis model describes the coupling of particulate organic matter deposition from the water column to the sediment bed, decomposition of organic matter in the bed, and the exchange of nutrients and dissolved oxygen across the sediment-water interface.

State variables of the EFDC hydrodynamic model (water temperature) and sediment transport model (inorganic suspended solids) are internally coupled with the EFDC water quality model. State variables of the EFDC water quality model include algae; organic carbon, inorganic phosphorus (orthophosphate), organic phosphorus; inorganic nitrogen (ammonium and nitrite + nitrate), organic nitrogen; chemical oxygen demand (COD) and dissolved oxygen. The state variables represented in the Tenkiller Ferry Lake hydrodynamic and water quality model are listed in Table 4-1.

The EFDC water quality model is based on the kinetic processes developed for the Chesapeake Bay model (Cercio and Cole, 1995; Cercio et al., 2002). An overview of the source and sink terms for each state variable is presented in this section. The details of the state variable equations and kinetic terms for each state variable are presented in Park et al. (1995), Hamrick (2007) and Ji (2008). Tables listing the calibrated values of selected water quality model parameters and coefficients are presented in **Appendix H**.

Table 4-1. EFDC State Variables

	EFDC State Variable		EFDC UNITS	Used in Model
	Flow	FLOW	cms	Yes
	Water_Temperature	TEM	Deg-C	Yes
	Salinity	SAL	ppt	No
	Cohesive Suspended Solids	COH	mg/L	Yes
	Non-cohesive Suspended Solids	NONCOH	mg/L	No
1	BlueGreen_Algae	CHC	mgC/L	Yes
2	Diatoms_Algae	CHD	mgC/L	Yes
3	Green_Algae	CHG	mgC/L	Yes
4	Refractory_Part particulate_Org_C	RPOC	mgC/L	Yes
5	Labile_Part particulate_Org_C	LPOC	mgC/L	Yes
6	Diss_Org_C	DOC	mgC/L	Yes
7	Refractory_Part particulate_Org_P	RPOP	mgP/L	Yes

	EFDC State Variable		EFDC UNITS	Used in Model
8	Labile_Part particulate_Org_P	LPOP	mgP/L	Yes
9	Diss_Org_P	DOP	mgP/L	Yes
10	Total_PhosphatePO4	TPO4	mgP/L	Yes
11	Refractory_Part particulate_Org_N	RPON	mgN/L	Yes
12	Labile_Part particulate_Org_N	LPON	mgN/L	Yes
13	Diss_Org_N	DON	mgN/L	Yes
14	Ammonium_N	NH4	mgN/L	Yes
15	Nitrate+Nitrite_N	NO3	mgN/L	Yes
16	Particulate-Biogenic_Silica	PBSI	mgSi/L	No
17	Available_Silica	SI	mgSi/L	Yes
18	Chemical_Oxy_Demand	COD	mg/L	Yes
19	Dissolved_Oxygen	OXY	mgO2/L	Yes
20	Total_Active_Metal	TAM	mg/L	No
21	Fecal_Coliform_Bacteria	FCB	# /100mL	No

Suspended Solids

Suspended solids in the EFDC model can be differentiated by size classes of cohesive and non-cohesive solids. For the Tenkiller Ferry Lake model, suspended solids are represented as a single size class of cohesive particles. Cohesive suspended solids are included in the model to account for the inorganic solids component of light attenuation in the water column. Since cohesive particles derived from silts and clays are characterized by a small particle diameter (< 62 microns) and a low settling velocity, cohesive particles can remain suspended in the water column for long periods of time and contribute to light attenuation that can influence algae production. Non-cohesive particles, consisting of fine to coarse size sands, by contrast, are characterized by much larger particles (> 62 microns) with rapid settling velocities that quickly remove any resuspended non-cohesive particles from the water column.

The key processes that control the distribution of cohesive particles are transport in the water column, flocculation and settling, deposition to the sediment bed, consolidation within the bed, and resuspension or erosion of the sediment bed. In the EFDC model for Tenkiller Ferry Lake, cohesive settling is defined by a constant settling velocity that is determined by model calibration. Deposition and erosion are controlled by the assignment of critical stresses for deposition and erosion and the bottom layer velocity and shear stress computed by the hydrodynamic model. The critical stress for erosion is typically defined with a factor of 1.2 times the critical deposition stress (Ji, 2008). Initial critical stresses for deposition and erosion of cohesive particles are taken from parameter values defined by Ji (2008) for a sediment transport model of Lake Okeechobee and then adjusted during model calibration. Parameter values for deposition and erosion assigned for the calibration of cohesive solids are summarized in

Table 4-2.

Table 4-2. EFDC Model Parameter Values for Cohesive Solids

Variable	Value	Description	Units
SDEN	3.774E-07	Sediment Specific Volume	m ³ /g
SSG	2.65	Sediment Specific Gravity	--
WSEDO	4.0E-06	Constant Sediment Settling Velocity	m/s
TAUD	8.00E-04	Critical Stress for Deposition	(m/s) ²
WRSPO	1.00E-03	Reference Surface Erosion Rate	g/m ² /s
TAUR	5.00E-06	Critical Stress for Erosion	(m/s) ²

The units of (m/s)² shown in

Table 4-2 for critical shear stress for deposition and erosion are not typical for sediment transport literature. The units assigned for the EFDC model are derived by normalizing the units typically measured for shear stress (e.g., dynes/cm²) by a water density of 1000 kg/m³. A critical shear stress for erosion of 0.16 dynes/cm² is thus assigned for input to EFDC with a value of 1.6e-05 (m/s)² by multiplying the shear stress of 0.16 dynes/cm² by a factor of 1.0e-04 since 1 dyne is defined as 1 g-cm/sec².

Algae

Phytoplankton in the EFDC model can be represented by three different functional groups of algae as (1) blue-green cyanobacteria; (2) diatoms; and (3) green chlorophytes. The distribution fraction among cyanobacteria, diatom, and green algae of the Tenkiller Ferry Lake EFDC model was developed based on the CDM collected data during 2005 to 2007.

Kinetic processes represented for algae include photosynthetic production, basal metabolism (respiration and excretion), settling and predation. Photosynthetic production is described by a growth rate that is functionally dependent on a maximum growth rate, water temperature, the availability of sunlight at the surface, light extinction in the water column, the optimum light level for growth, and half-saturation dependent nutrient limitation by either nitrogen or phosphorus. Growth and basal metabolism are temperature dependent processes while settling and predation losses are assigned as constant parameter values.

In a reservoir like Tenkiller Ferry Lake, spatial gradients controlled by biogeochemical processes are characterized by typical riverine, transition and lacustrine zones (Cooke et al., 2011). For the Tenkiller Ferry Lake EFDC model, six zones were used to represent the spatial variations in algae kinetics (Figure 4-1). Other kinetic coefficients determined for calibration of the algae model are presented in **Appendix H**.

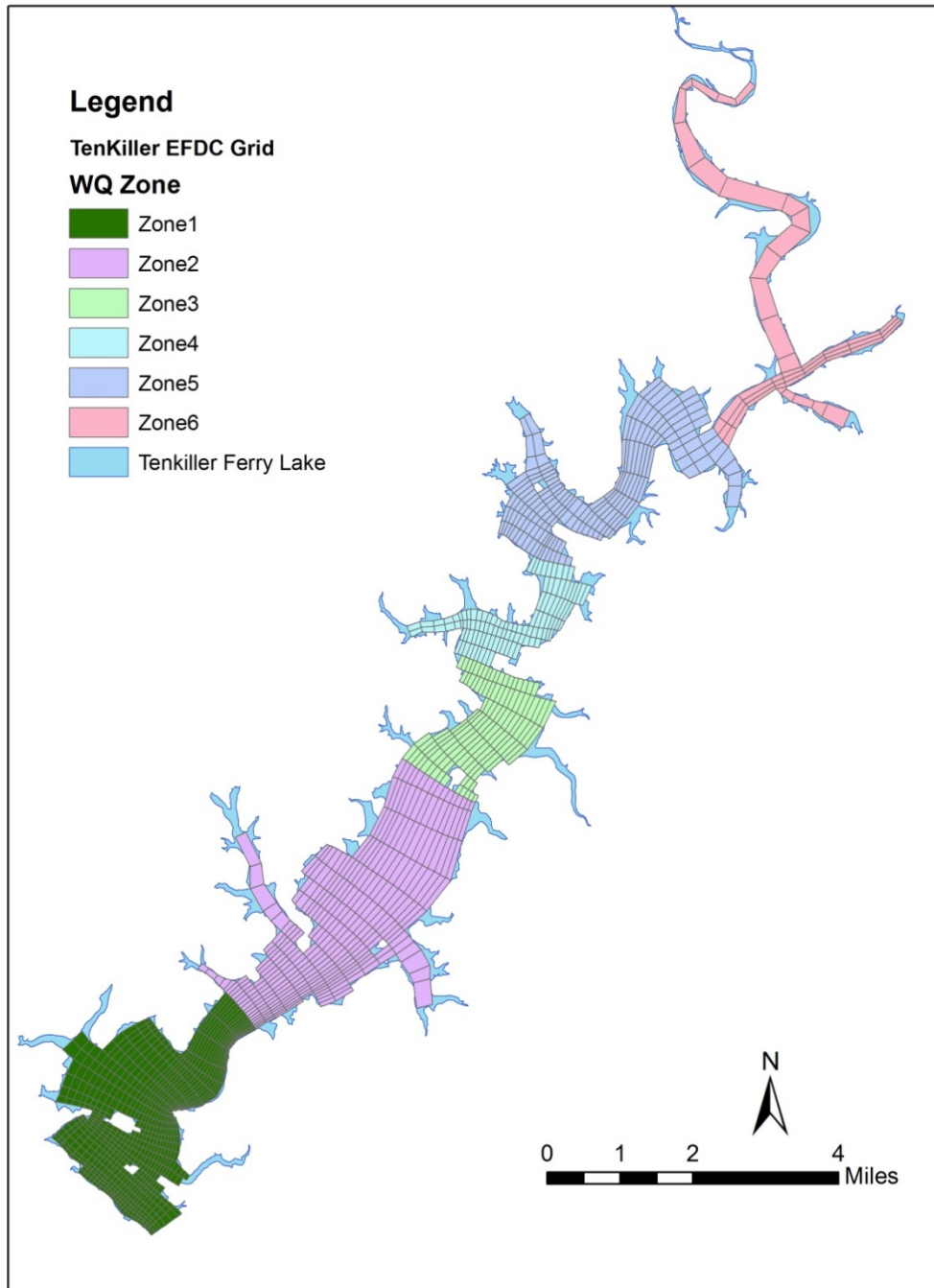


Figure 4-1. Spatial water quality kinetic zones defined for Tenkiller Ferry Lake

Organic Carbon

Total organic carbon is represented in the model with three state variables as dissolved organic carbon (DOC) and refractory and labile particulate organic carbon (RPOC and LPOC). The time scale for decomposition of particulate organic matter (POM) is used to differentiate refractory and labile POM with labile matter decomposing rapidly (weeks to months) while decay of

refractory POM takes much longer (years). Although DOC is not termed “labile”, DOC is considered to react with a rapid time scale for decomposition (weeks to months).

Kinetic processes represented in the model for particulate organic carbon (POC) include algal predation, dissolution of RPOC and LPOC to DOC, and settling. Kinetic processes for DOC include sources from algal excretion and predation and dissolution of POC and losses from decomposition and denitrification. With the exception of settling of POC, all the kinetic reaction processes are temperature dependent.

Phosphorus

Total organic phosphorus is represented in the model with three state variables as dissolved organic phosphorus (DOP) and refractory and labile particulate organic phosphorus (RPOP and LPOP). As with organic carbon, the time scale for decomposition of particulate organic matter (POM) is used to differentiate refractory and labile POP. Kinetic processes represented in the model for POP include algal metabolism, predation, dissolution of RPOP and LPOP to DOP, and settling. Kinetic processes for DOP include sources from algal metabolism and predation and dissolution of POP to DOP with losses of DOP from mineralization to phosphate. With the exception of settling of POP, the kinetic reaction processes are temperature dependent.

Inorganic phosphorus is represented as single state variable for total phosphate which accounts for both the dissolved and sorbed forms of phosphate. Adsorption and desorption of phosphate is defined on the basis of equilibrium partitioning using an assigned phosphate partition coefficient for suspended solids. Kinetic terms for total phosphate include sources from algal metabolism and predation and mineralization from DOP. Losses for phosphate include settling of the sorbed fraction of total phosphate and uptake by phytoplankton growth. Depending on the concentration gradient between the bottom water column and sediment bed porewater phosphate, the sediment-water interface can serve as either a source or a loss term for phosphate in the water column. With the exception of the partition coefficient and the settling of sorbed phosphate, the kinetic reaction processes for phosphate are temperature dependent.

Nitrogen

Total organic nitrogen is represented in the model with three state variables as dissolved organic nitrogen (DON) and refractory and labile particulate organic nitrogen (RPON and LPON). As with organic carbon, the time scale for decomposition of particulate organic matter (POM) is used to differentiate refractory and labile PON. Kinetic processes represented in the model for PON include algal metabolism, predation, dissolution of RPON and LPON to DON, and settling. Kinetic processes for DON include sources from algal metabolism and predation, dissolution of PON to DON and losses of DON from mineralization of PON to ammonium. With the exception of settling of PON, the kinetic reaction processes are temperature dependent.

Inorganic nitrogen (ammonia, nitrite and nitrate) is represented by two state variables as (1) ammonia and (2) nitrite+nitrate. Kinetic terms for ammonia include sources from algal metabolism and predation and mineralization from DON. Losses for ammonia include bacterially mediated transformation to nitrite and nitrate by nitrification and uptake by phytoplankton growth. Depending on the concentration gradient between the bottom water column and sediment bed porewater ammonia, the sediment-water interface can serve as either a source or a loss term for ammonia in the water column. The kinetic reaction processes for ammonia are temperature dependent. Since the time scale for conversion of nitrite to nitrate is

very rapid, nitrite and nitrate are combined as a single state variable representing the sum of these two forms of nitrogen. Kinetic terms for nitrite/nitrate include sources from nitrification from ammonia to nitrite and nitrate. Losses include uptake by phytoplankton growth and denitrification to nitrogen gas. Depending on the concentration gradient between the bottom water column and sediment bed porewater nitrite/nitrate, the sediment-water interface can serve as either a source or a loss term for nitrite/nitrate in the water column. The kinetic reaction processes for nitrite/nitrate are temperature dependent.

Chemical Oxygen Demand (COD)

In the EFDC water quality model, chemical oxygen demand (COD) represents the concentration of reduced substances that can be oxidized through inorganic processes. The principal source of COD in freshwater is methane released from oxidation of organic carbon in the sediment bed across the sediment-water interface. Since sediment bed decomposition is accounted for in the coupled sediment diagenesis model, the only source of COD to the water column is the flux of methane across the sediment-water interface. Sources from the open water boundaries and upstream flow boundaries are set to zero for COD. The loss term in the water column is defined by a temperature dependent first order oxidation rate.

Dissolved Oxygen

Dissolved oxygen is a key state variable in the water quality model since several kinetic processes interact with, and can be controlled by, dissolved oxygen. Kinetic processes represented in the oxygen model include sources from atmospheric reaeration in the surface layer and algal photosynthetic production. Kinetic loss terms include algal respiration, nitrification, decomposition of DOC, oxidation of COD, and bottom layer consumption of oxygen from sediment oxygen demand. Sediment oxygen demand is coupled with particulate organic carbon deposition from the water column and is computed internally in the sediment flux model. The kinetic reaction processes for dissolved oxygen are all temperature dependent.

Kinetic Coefficients

Most of the water quality parameters and coefficients needed by the EFDC water quality model were initialized with default values as indicated in the user's manual (Park, et.al., 1995; Hamrick, 2007). These default values are, in general, the same as the parameter values determined for the Chesapeake Bay model (Cercio and Cole, 1995). Models developed for Lake Washington (Arhonditsis and Brett, 2005) and the tributaries of Chesapeake Bay (Cercio et al., 2002) also provided several of the kinetic coefficients needed for the EFDC water quality model. Kinetic coefficients and model parameters were adjusted, as needed, within ranges reported in the literature, during model calibration to obtain the most reasonable agreement between observed and simulated water quality concentrations such as suspended solids, algal biomass, organic carbon, dissolved oxygen and nutrients. A large body of literature is available from numerous advanced modeling studies developed over the past decade to provide information on reported ranges of parameter values that can be assigned for site-specific modeling projects (see Ji, 2008; Park et al, 1995; Hamrick, 2007; Dynamic Solutions, 2012). Kinetic coefficients and model parameters assigned for the water quality model as either global or spatial zone dependent parameters for the Tenkiller Ferry Lake model are listed in **Appendix H**.

Atmospheric Deposition

Atmospheric deposition is represented in the EFDC model with separate source terms for dry deposition and wet deposition. Dry deposition is defined by a constant mass flux rate (as g/m²-day) for a constituent that settles as dust or is deposited on a dry surface during a period of no precipitation. Wet deposition is defined by a constant concentration (as mg/L) of a constituent in rainfall and the time series of precipitation assigned for input to the hydrodynamic model. For the Tenkiller Ferry Lake, wet and dry deposition data (Table 4-3) was assigned as the average of annual data from 2005-2006 for ammonia and nitrate from the National Atmospheric Deposition Program (NADP) for Station AR27 (Fayetteville, Lat 36.1011; Lon -94.1737) and the Clean Air Status and Trends Network (CASTNET) Station CHE185 (Cherokee Nation, Lat 35.7507, Lon -94.67) (Figure 4-2). Since data was not available from the CASTNET and NADP sites for phosphate, dry deposition for phosphate was estimated using annual average ratios of N/P for atmospheric deposition of N and P reported for 6 sites located in Iowa (Anderson and Downing, 2006) and the ammonia and nitrate data obtained from the NADP and CASTNET data sources.

Table 4-3. Dry and Wet Atmospheric Deposition for Nutrients

Constituent	Dry	Wet	Data Source
	g/m ² -day	mg/L	
TPO4	7.786E-06	0.001	Anderson & Downing (2006), Table VII
NH4	1.143E-04	0.274	Dry (CASTNET, CHE185); Wet (NADP, AR27); average 2005-2005
NO3	3.205E-05	0.19	Dry (CASTNET, CHE185); Wet (NADP, AR27); average 2005-2006

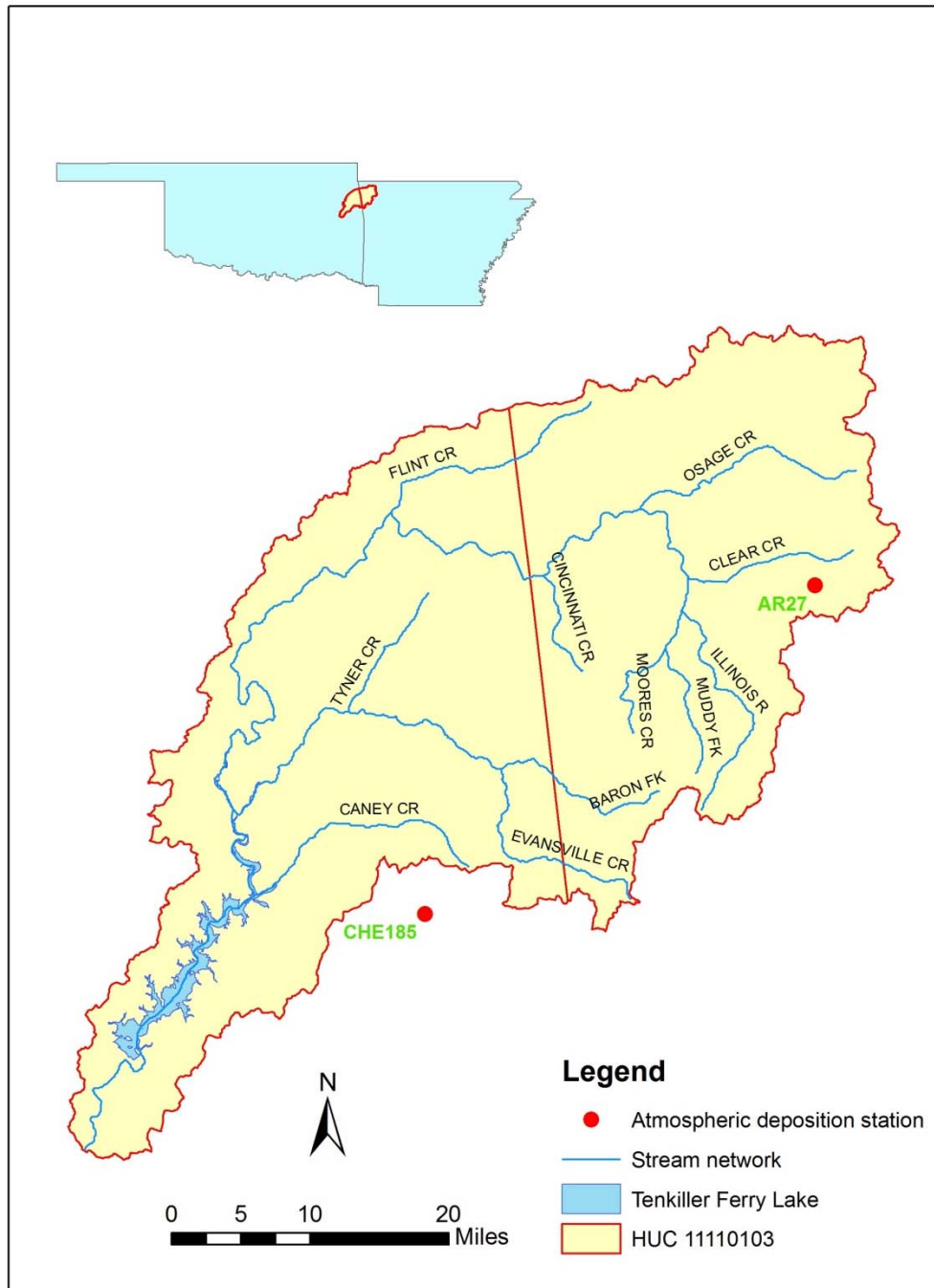


Figure 4-2. Location of the Atmospheric Deposition Monitoring Stations

4.2 Sediment Flux Model

The EFDC water quality model provides three options for defining the sediment-water interface fluxes for nutrients and dissolved oxygen. The options are: (1) externally forced spatially and temporally constant fluxes; (2) externally forced spatially and temporally variable fluxes; and (3) internally coupled fluxes simulated with the sediment diagenesis model. The water quality state variables that are controlled by diffusive exchange across the sediment-water interface include phosphate, ammonia, nitrate, silica, chemical oxygen demand and dissolved oxygen. The first two options require that the sediment fluxes be assigned as spatial/temporal forcing functions based on either observed site-specific data from field surveys or best estimates based on the literature and sediment bed characteristics. The first two options, although acceptable for model calibration against historical data sets, do not provide the cause-effect predictive capability that is needed to evaluate future water quality conditions that might result from implementation of pollutant load reductions from watershed runoff. The third option, activation of the sediment diagenesis model developed by Di Toro (2001), does provide the cause-effect predictive capability to evaluate how water quality conditions might change with implementation of alternative load reduction or management scenarios. For the Tenkiller Ferry Lake model, the third option was selected to implement the sediment diagenesis model so that load allocation scenarios could be evaluated to determine an appropriate load allocation for the Tenkiller Ferry Lake.

Living and non-living particulate organic carbon deposition, simulated in the EFDC water quality model, is internally coupled with the EFDC sediment diagenesis model. The sediment diagenesis model, based on the sediment flux model of Di Toro (2001), describes the decomposition of particulate organic matter in the sediment bed, the consumption of dissolved oxygen at the sediment-water interface (SOD) and the exchange of dissolved constituents (ammonia, nitrate, phosphate, silica, COD) across the sediment-water interface. State variables of the EFDC sediment flux model are sediment bed temperature, sediment bed particulate organic carbon (POC), particulate organic nitrogen (PON), particulate organic phosphorus (POP), porewater concentrations of phosphate, ammonia, nitrate, silica and sulfide/methane. The sediment diagenesis model computes sediment-water fluxes of chemical oxygen demand (COD), sediment oxygen demand (SOD), phosphate, ammonium, nitrate, and silica. The state variables modeled for the Tenkiller Ferry Lake sediment flux model listed in Table 4-4. An overview of the source and sink terms is presented with a description of each state variable group in this section. The details of the state variable equations, kinetic terms and numerical solution methods for the sediment diagenesis model are presented in Di Toro (2001), Park et al. (1995) and Ji (2008).

Table 4-4. EFDC Sediment Diagenesis Model State Variables

No.	Name	Bed Layer	Units	Activated
1	POC-G1	Layer-2	g/m ³	Yes
2	POC-G2	Layer-2	g/m ³	Yes
3	POC-G3	Layer-2	g/m ³	Yes
4	PON-G1	Layer-2	g/m ³	Yes
5	PON-G2	Layer-2	g/m ³	Yes
6	PON-G3	Layer-2	g/m ³	Yes
7	POP-G1	Layer-2	g/m ³	Yes
8	POP-G2	Layer-2	g/m ³	Yes
9	POP-G3	Layer-2	g/m ³	Yes
10	Partic-Biogenic-Silica	Layer-2	g/m ³	No
11	Sulfide/Methane	Layer-1	g/m ³	Yes
12	Sulfide/Methane	Layer-2	g/m ³	Yes
13	Ammonia-N	Layer-1	g/m ³	Yes
14	Ammonia-N	Layer-2	g/m ³	Yes
15	Nitrate-N	Layer-1	g/m ³	Yes
16	Nitrate-N	Layer-2	g/m ³	Yes
17	Phosphate-P	Layer-1	g/m ³	Yes
18	Phosphate-P	Layer-2	g/m ³	Yes
19	Available-Silica	Layer-1	g/m ³	No
20	Available-Silica	Layer-2	g/m ³	No
21	Ammonia-N-Flux		g/m ² -day	Yes
22	Nitrate-N-Flux		g/m ² -day	Yes
23	Phosphate-P-Flux		g/m ² -day	Yes
24	Silica Flux		g/m ² -day	Yes
25	SOD		g/m ² -day	Yes
26	COD Flux		g/m ² -day	Yes
27	Bed Temperature		Deg-C	Yes

Particulate Organic Matter

The sediment diagenesis model incorporates three key processes: (1) depositional flux of particulate organic matter (POM) from the water column to the sediment bed; (2) diagenesis or decomposition of POM in the sediment bed; and (3) the resulting fluxes of dissolved oxygen, chemical oxygen demand, sulfide/methane and nutrients across the sediment-water interface. Particulate organic matter is represented as carbon (POC), nitrogen (PON), and phosphorus (POP) stoichiometric equivalents based on carbon-to-dry weight and Redfield ratios for C/N, and C/P. In the water quality model, POM deposition describes the settling flux from the water column to the bed of non-living refractory and labile detrital matter and living algal biomass. In the sediment flux model, POM is split into three classes of reactivity. The labile fraction (POM-G1) is defined by the fastest reaction rate with a half-life on the order of 20 days. The refractory fraction (POM-G2) is defined by a slower reaction rate with a half-life of about 1 year. The inert

fraction (POM-G3) is non-reactive with negligible decay before ultimate burial into the deep inactive layer of the sediment bed.

The sediment flux model represents the sediment bed as a two layer system. The first layer is a very thin aerobic layer. The second layer is a thicker anaerobic active layer. The thickness of the aerobic layer, which is on the order of only a millimeter, is internally computed in the sediment flux model as a function of bottom layer dissolved oxygen concentration, the sediment oxygen demand rate and the diffusivity coefficient for dissolved oxygen. The thickness of the anaerobic active layer is assigned as a parameter for model setup. The depth of the anaerobic active layer, defined by the depth to which benthic organisms mix particles within a homogeneous bed layer, can range from ~5 to 15 cm (Ji, 2008). An active anaerobic layer thickness of ~10 cm has been determined from both theoretical considerations and field observations in estuaries (Di Toro, 2001). Any particle mass transported out of the active layer is not recycled back into the active layer since these particles are lost to deep burial out of the sediment bed.

The thickness of the active anaerobic layer controls the volume of the anaerobic layer, the amount of mass stored in the anaerobic layer and the long-term response of the sediment bed to changes in organic matter deposition from the water column. A relatively thin active layer will respond quickly to changes in watershed loading and water column deposition of particulate matter. Conversely, a thick active layer will respond slowly to changes in watershed loading and deposition of particulate materials from the water column to the bed. The rate, at which solutes stored in the anaerobic active layer are transported between the thin aerobic and thick anaerobic active layer, and potentially the overlying water column, is controlled by the mixing coefficients assigned as model parameters for particulate and dissolved substances. Anaerobic active layer thickness and diffusive mixing rates are considered to be adjustable parameters for model calibration to determine the most appropriate parameter values for each spatial zone. As documented in **Appendix I** an anaerobic layer thickness of 10 cm is assigned for each spatial zone of the sediment flux model

Since the surface aerobic sediment layer is very thin, the depositional flux from the overlying water column is assigned to the lower anaerobic active sediment layer where decomposition then occurs. The source term for the three “G” classes of POM is the depositional flux from the overlying water column to the sediment bed. The loss terms for POM are the temperature dependent decay (i.e., diagenesis) of POM and removal by burial from the aerobic (upper) to active anaerobic (lower) layers and from the anaerobic (lower) layer to deep burial out of the sediment bed model domain.

Dissolved Constituents

The decay or mineralization of POM results in the diagenetic production of dissolved constituents. The concentration gradients of ammonia, nitrate, phosphate, and sulfide/methane within the two porewater layers and between the surficial porewater layer 1 and the bottom layer of the water column control the sediment fluxes computed in the model. Mineralization of POP produces phosphate which is then subject to adsorption/desorption by linear partitioning with solids in the sediment bed. Diffusive exchange is controlled by the concentration gradient of dissolved constituents, the diffusion velocity, and the bed layer thickness. Other processes that govern the mass balance of dissolved materials in the sediment bed include burial, particle mixing and removal by kinetic reactions.

Ammonia and Nitrate

Ammonia is produced in layer 2 by temperature dependent decomposition of the reactive G1 and G2 classes of PON. Ammonia is nitrified to nitrate with a temperature and oxygen dependent process. The only source term for nitrate is nitrification in the surficial layer. Nitrate is removed from both layers by temperature dependent denitrification with the carbon required for this process supplied by organic carbon diagenesis. Nitrogen is lost from the sediment bed by the denitrification flux out of the sediments as nitrogen gas (N₂). The sediment-water fluxes of ammonia and nitrate to the overlying water column are then computed from the concentration gradients, the porewater diffusion coefficient and the thickness of the surficial bed layer.

Phosphate

Phosphate is produced by temperature dependent decomposition of the reactive G1 and G2 classes of particulate organic phosphorus in the lower layer 2 of the sediment bed. Since linear partitioning with solids is defined for phosphate, a fraction of total phosphate is computed as particulate phosphate and a fraction remains in the dissolved form. The partition coefficient for phosphate for the surficial layer 1 is functionally dependent on (a) the oxygen concentration in the overlying bottom layer of the water column based on the assignment of 2 mg/L as a critical concentration for oxygen that triggers the oxygen dependent process, (b) the magnitude of the partition coefficient assigned for the lower layer 2, and (c) an enhancement factor multiplier. There are no removal terms for phosphate in either of the two layers. The sediment-water flux of dissolved phosphate to the overlying water column is then computed from the concentration gradient, the porewater diffusion coefficient and the thickness of the surficial bed layer.

Methane/Sulfide

Sulfide is produced by temperature dependent decomposition of the reactive G1 and G2 classes of particulate organic carbon in the lower layer of the sediment bed. Sulfide is lost from the system by the organic carbon consumed by denitrification. Linear partitioning with solids is also defined for sulfide to account for the formation of iron sulfide. The sediment flux model accounts for three pathways for loss of sulfide from the sediment bed: (1) temperature dependent oxidation of sulfide; (2) aqueous flux of sulfide to the overlying water column; and (3) burial out of the model domain. If the overlying water column oxygen concentration is low then the sulfide that is not completely oxidized in the upper sediment layer can diffuse into the bottom layer of the water column. The aqueous flux of sulfide from the sediments is the source term for the flux of chemical oxygen demand (COD) from the sediment bed to the water column.

When sulfate is depleted, methane can be produced by carbon diagenesis and oxidation of methane then consumes oxygen. In saltwater systems, such as estuaries and coastal waters, sulfate is abundant and methane production and oxidation are not represented in the sediment flux model. In freshwater systems, such as Tenkiller Ferry Lake, sulfate is typically characterized by very low concentrations. In freshwater systems methane production and oxidation are represented in the sediment diagenesis model instead of sulfide production and oxidation.

Sediment Oxygen Demand

The sulfide/methane oxidation reactions in the surficial layer result in an oxygen flux to the sediment bed from the overlying water column. Sediment oxygen demand (SOD) includes the

carbonaceous oxygen demand (CSOD) from sulfide/methane oxidation and the nitrogenous oxygen demand (NSOD) from nitrification. The total SOD is computed as the sum of the carbonaceous and nitrogenous components of the oxygen flux.

Sediment Diagenesis Model Parameters and Kinetic Coefficients

The sediment diagenesis model requires the assignment of a large number of model parameters and kinetic coefficients. Based on the results of sediment flux models developed for estuaries, coastal systems and lakes, Di Toro (2001) has summarized parameter values used for diagenesis, sediment properties, mixing and kinetic coefficients for the different projects. The comparison of data assigned for several different projects shows the robustness of the sediment flux model since many of the parameter values and kinetic coefficients were essentially unchanged for model applications unless there was a site-specific reason that supported the use of a different value. The exception to this generality, however, is the extreme variation of the kinetic coefficients required to represent partitioning of phosphate in the upper and lower layers of the sediment bed and the benthic release of dissolved phosphate under anoxic conditions in the hypolimnion. Since the sediment flux model does not explicitly represent the chemical reactions and interactions that determine phosphate sorption, particularly under low oxygen conditions in the overlying water column when dissolved phosphate is released across the sediment-water interface, the sediment flux model coefficients that represent phosphate partitioning are parameters that were adjusted, as needed, to calibrate the model.

Kinetic coefficients and parameters of the sediment flux model were initially assigned based on the Chesapeake Bay Model (Cercio and Cole, 1995; Cercio et al., 2002) and the compilation of parameter values reported in Di Toro (2001). Selected coefficients, particularly the phosphate partitioning parameters, were adjusted, as needed, to achieve calibration of the water quality and sediment flux model. Kinetic coefficients and model parameters assigned for calibration of the sediment diagenesis model as either global or spatial zone dependent parameters for the Tenkiller Ferry Lake model are listed in **Appendix I**.

Initial Conditions for Sediment Diagenesis Model

The sediment diagenesis model requires specification of initial conditions for particulate organic matter content (as C, N, and P) and porewater concentrations of inorganic nutrients (as NH_4 , NO_3 , and PO_4). Sediment core data was available for Tenkiller Ferry Lake from special surveys conducted by CDM in August 2005 to provide data needed to support the development of the lake model. The locations of the sediment core data are shown in Figure 4-3. Station LKSED-01 and LKSED-02 represent the lacustrine zone of the lake. LKSED-03, LKSED-04, and LKSED-05 are located in the transition zone between riverine and lacustrine environment. The parameters analyzed included total nitrogen (TN), total phosphorus (TP), and total solids. The analyzed TP is available in both dry and wet weight with unit of mg/kg, but TN is only available in wet weight.

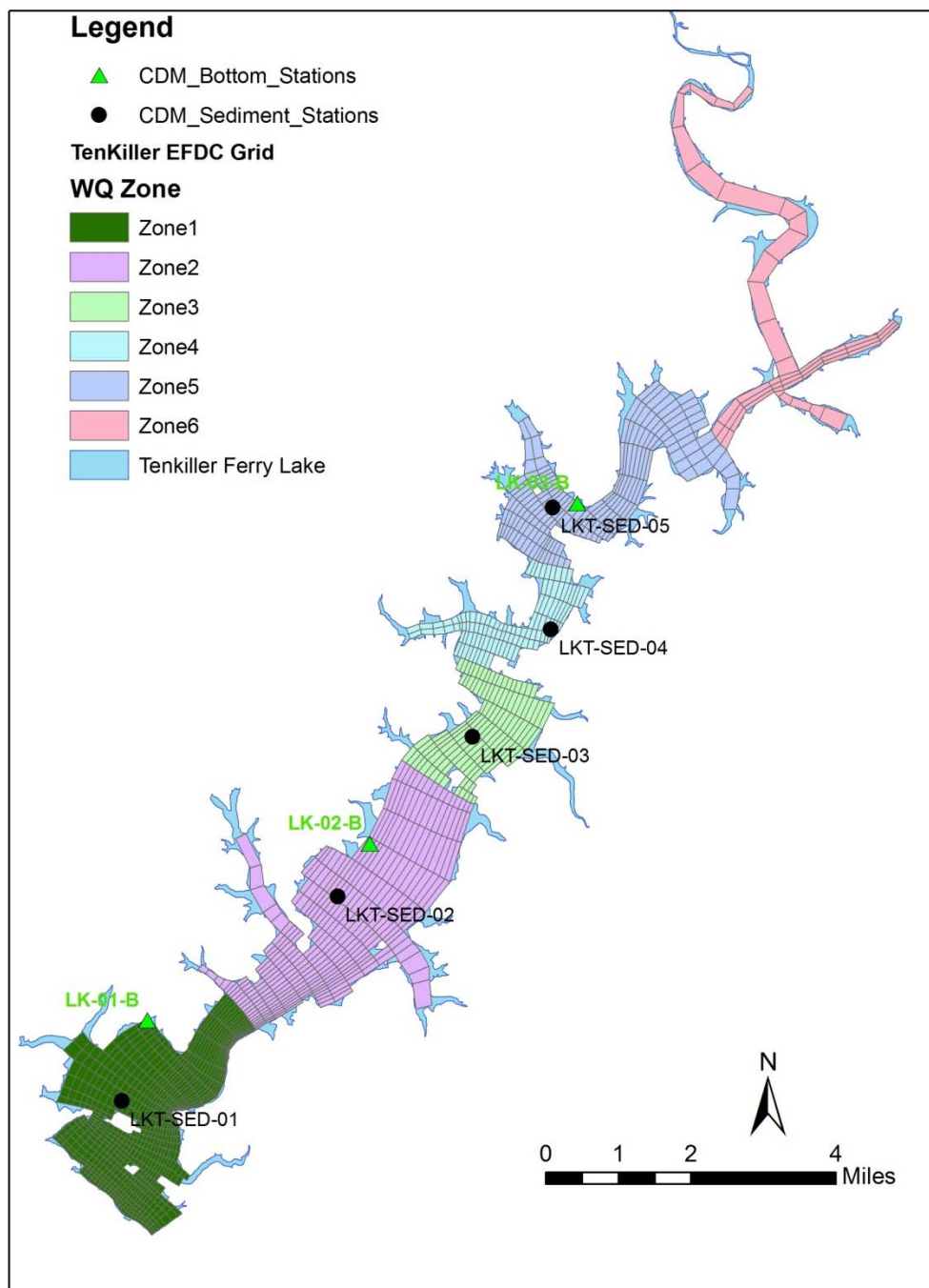


Figure 4-3. Location of the CDM Sediment Core and Shallow Benthic Stations

TN and TP dry weight content of the sediment bed, measured as mg/kg, was converted to bed concentration as g/m³ for input to the EFDC model based on solids density and porosity using the following relationship:

$$\text{Bed Concentration (g/m}^3\text{)} = \text{Bed Dry Weight (mg/kg)} \cdot (1 - \text{Porosity}) \cdot \text{Solids Density}$$

Measured TP in dry and wet weight was used to derive the solid density. Dry weight of TN was calculated using the derived solid density and porosity. Bed concentrations of TN and TP were then calculated using the above relationship.

CDM also collected the sediment bed data at three shallow benthic sites: LK-01-B, LK-02-B, and LK-03-B (Figure 4-3). The analyzed parameters included water soluble ammonium, water soluble nitrate, TN, water soluble phosphorus, and TP. The average ratio of TON:TN and TOP:TP at these stations were used to derive the TON and TOP data from these five CDM sediment core stations with the measured TN and TP data.

TOC measurements were not available from the special CDM monitoring program in the Tenkiller Ferry Lake. In the absence of site-specific data, TOC content of the sediment bed (was estimated from the TON data and a C:N ratio of 10 which was taken from sediment core data reported for a lake in Massachusetts (Kaushai and Binford, 1999) and is considered to be a typical C:N ratio for organic matter derived from terrestrial sources in a watershed. The G1, G2 and G3 reactive classes of TOC, TON and TOP was estimated for initial conditions using the following fractional splits:

$$G1: 1 / (1+10+100) = 0.00901;$$

$$G2: 10 / (1+10+100) = 0.09009$$

$$G3: 100 / (1+10+100) = 0.9009$$

A sample of the derived solid density, bulk density, TOP, and TPO4 for these five CDM sediment core stations is given in Table 4-5.

Table 4-6 summarizes how sediment bed data was assigned to water quality zones. Sediment bed data in zone 5 was used for Zone 6, where sediment bed data were not available.

Table 4-5. Sediment Phosphorus Data

						TOP:TP 0.98	TPO4:TP 0.02
	TP (mg/kg)	BulkDens (g/cm**3)	SolidsDens (g/cm**3)	Porosity	TP (g/m**3)	TOP (g/m**3)	TPO4 (g/m**3)
LKSED-1	1344.4	0.823	1.159	0.196	251.221	246.982	4.239
LKSED-2	933.4	0.765	1.236	0.288	277.693	273.006	4.686
LKSED-3	1023.6	0.767	1.177	0.274	254.825	250.525	4.300
LKSED-4	1222.5	0.815	0.892	0.174	231.129	227.229	3.900
LKSED-5	968.5	0.713	1.083	0.309	279.026	274.318	4.709

Table 4-6. Sediment Bed Data used for Water Quality Zones

WQ Zone	CDM Site	Sediment Bed Data Available	WQ Zone Based on
1	LKT-SED-01	Sediment Bed Data	LKT-SED-01
2	LKT-SED-02	Sediment Bed Data	LKT-SED-02
3	LKT-SED-03	Sediment Bed Data	LKT-SED-03
4	LKT-SED-04	Sediment Bed Data	LKT-SED-04
5	LKT-SED-05	Sediment Bed Data	LKT-SED-05
6	none	none	LKT-SED-05

Section 5 Calibration and Validation Stations

5.1 Stage Calibration and Validation Stations

The observed stage data in Tenkiller Ferry Lake is available at station TENO2 by the US Army Corps of Engineers Tulsa District. The location of station TENO2 is shown in Figure 5-1.

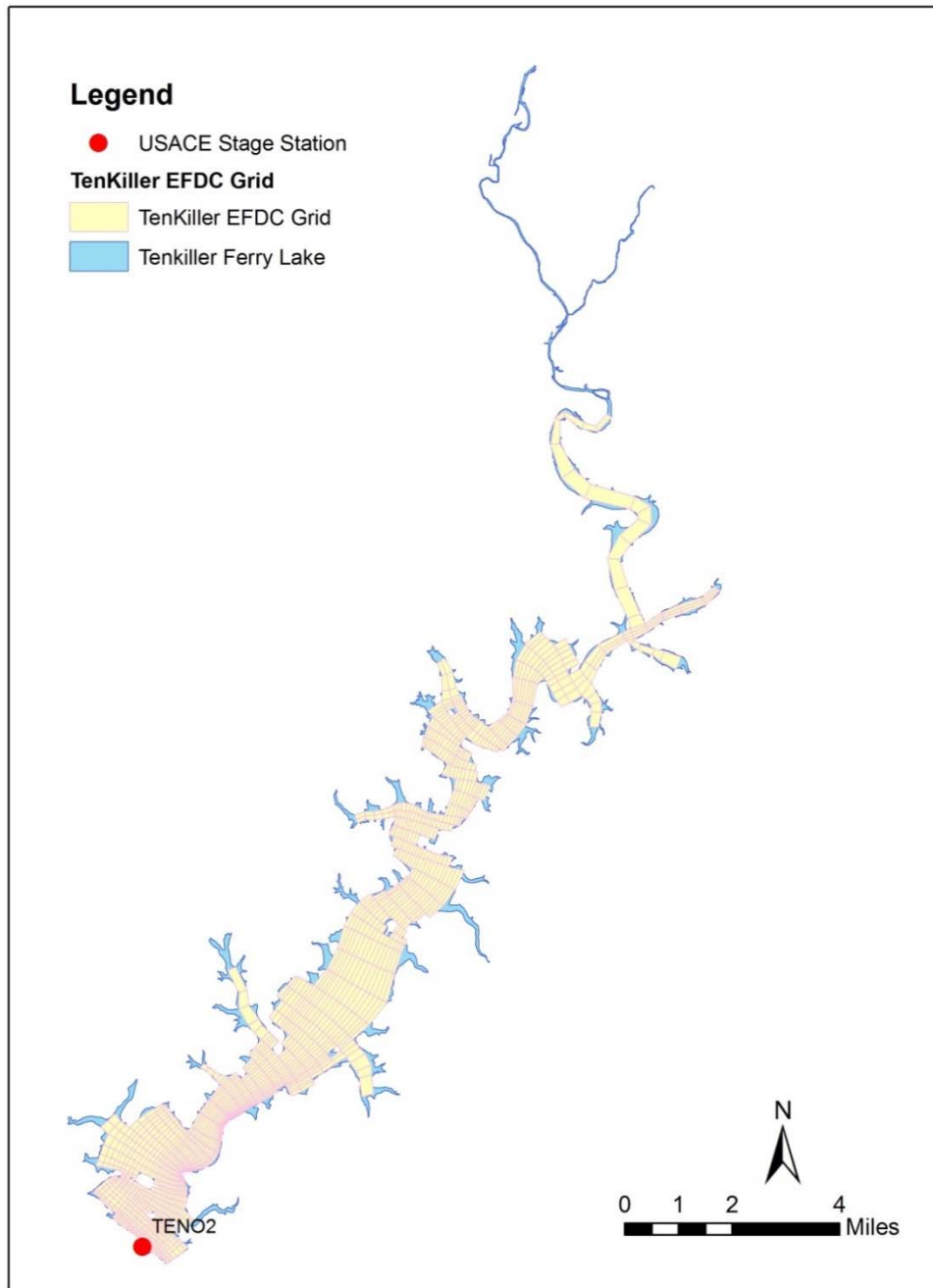


Figure 5-1. Location of the USACE Stage Monitoring Station TENO2

5.2 Water Quality Calibration Stations

The developed Tenkiller Ferry Lake EFDC water quality model was calibrated and validated at seven (7) OWRB stations and four (4) CDM stations. The detailed information can be found in Table 5-1 and Figure 5-2 and Figure 5-3.

There are very limited OWRB data to generate meaningful statistics, but there are enough CDM monitoring data for statistics comparison between the observed and simulated data. The CDM monitoring stations are spatially distributed in the lake: LK-01 represented the deep portion of the lake; LK-02 was located in the middle of the lake; LK-03 represented the upper portion of the lake; and LK-04 was in the transition zone between the riverine environment of the Illinois River and the lacustrine environment of Tenkiller Ferry Lake.

The quarterly OWRB monitoring surveys and the CDM sampling conducted during 2005-2006 were not designed to collect water quality data to evaluate the short-term impact of storm event inflow loading on lake water quality. All available station data from the OWRB and CDM surveys were used for the model calibration and validation years of 2005-2006. OWRB BUMP reports show that data was collected in Lake Tenkiller at quarterly intervals from 2001-2002; 2003-2004; 2005-2006; and 2011-2012.

Table 5-1. Calibration and Validation Stations for the Tenkiller Ferry Lake EFDC Model

Agency	Station ID	Station Name	Latitude	Longitude
OWRB	Site1	121700020020-01S	35.600017	-95.044628
OWRB	Site1	121700020020-01B	35.600017	-95.044628
OWRB	Site2	121700020020-02	35.674433	-94.976408
OWRB	Site3	121700020220-03	35.739050	-94.954261
OWRB	Site4	121700020220-04	35.755422	-94.905072
OWRB	Site5	121700020220-05	35.763844	-94.892400
OWRB	Site6	121700020220-06	35.766339	-94.887192
OWRB	Site7	121700020020-07	35.639381	-95.014631
CDM/USGS	LK-01		35.609700	-95.049450
CDM/USGS	LK-02		35.677420	-94.978780
CDM/USGS	LK-03		35.737160	-94.939280
CDM/USGS	LK-04		35.792078	-94.888507

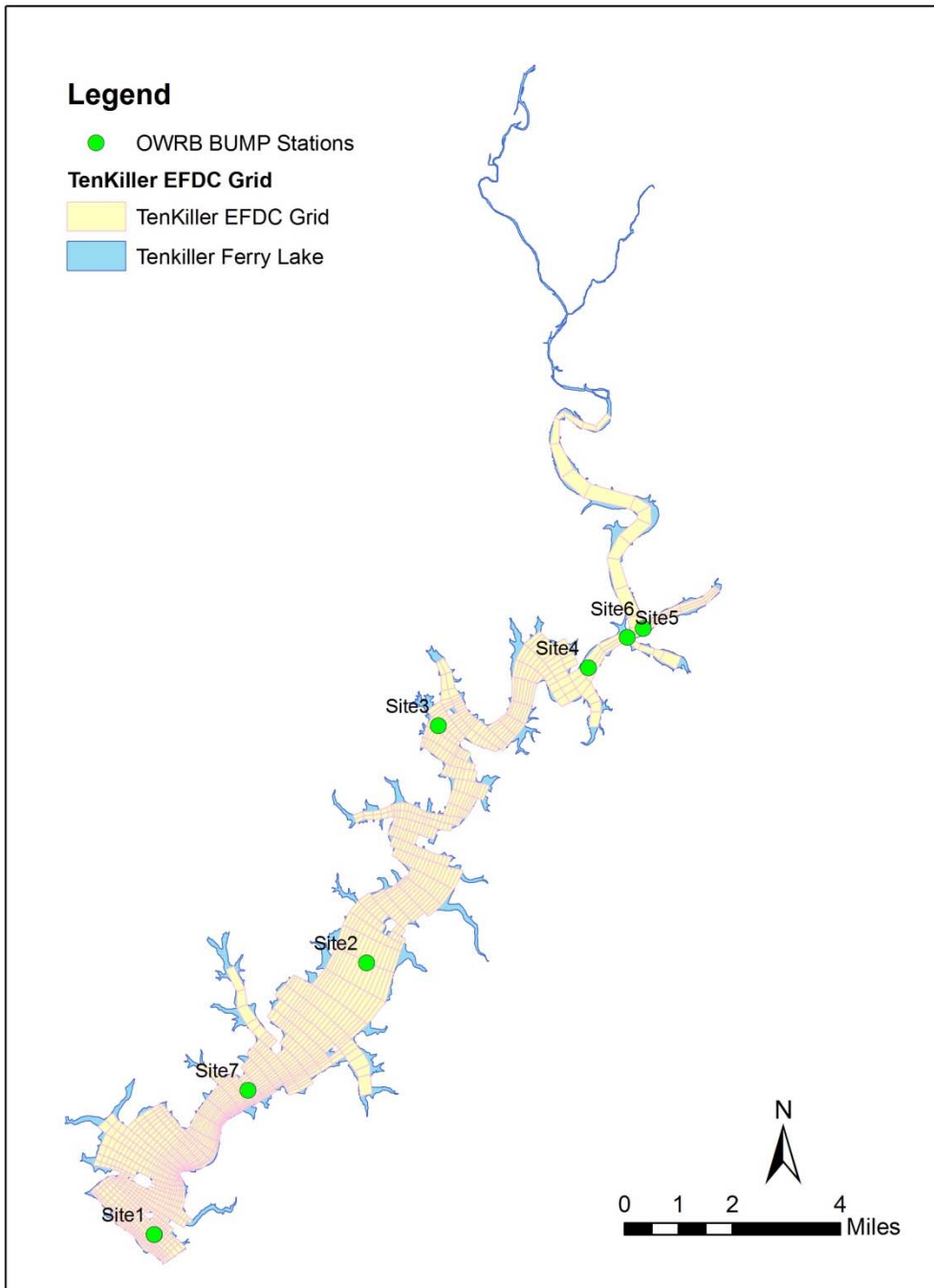


Figure 5-2. Location of the OWRB Monitoring Stations

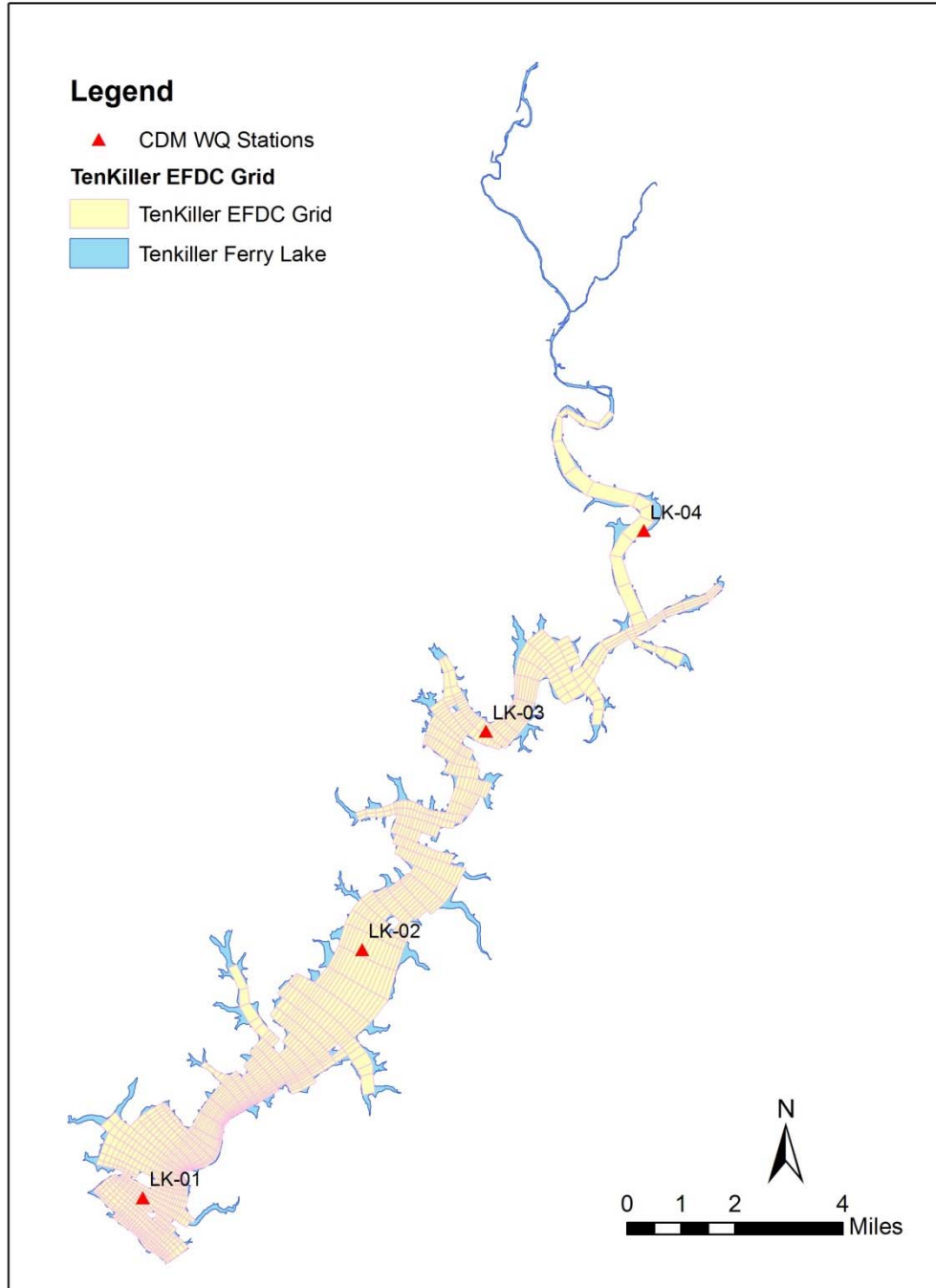


Figure 5-3. Location of the CDM/USGS Monitoring Stations

Section 6 Model Performance Statistics

6.1 Model Performance Statistics

Model performance is evaluated to determine the endpoint for model calibration using a “weight of evidence” approach that has been adopted for many modeling studies. The “weight of evidence” approach includes the following steps: (a) visual inspection of plots of model results compared to observed data sets (e.g., station time series); and (b) analysis of model-data performance statistics as (a) Root Mean Square (RMS) Error and (b) Relative RMS Error as described below. The “weight of evidence” approach recognizes that, as an approximation of a waterbody, perfect agreement between observed data and model results is not expected and is not specified as a performance criterion for the success of model calibration. Model performance statistics are used, not as absolute criteria for acceptance of the model, but rather, as guidelines to supplement the visual evaluation of model-data time series plots to determine the endpoint for calibration of the model. The “weight of evidence” approach used for this study thus acknowledges the approximate nature of the model and the inherent uncertainty in both input data and observed data.

The model-data model performance statistic selected for the calibration of the hydrodynamic and water quality model are the (a) Root Mean Square Error (RMSE) and the (b) Relative RMS Error. The RMSE has units defined by the units of each state variable of the model. The Relative RMS error, computed as the ratio of the RMSE to the observed range of each water quality constituent and expressed as a percentage, is also used as a statistic to characterize model performance (Blumberg et al., 1999; Ji, 2008). Since the Relative RMS error is expressed as a percentage, this performance measure provides a straightforward statistic to evaluate the agreement between model results and observations.

The RMS Error, also known as the Standard Error of the mean, can be used to determine the width of the confidence interval around model predictions. The 95% confidence interval for the model is approximately equal to the model result at each point in time “ $\pm 2 \times$ Standard Error”. Since the RMS Error and the Standard Error of the mean represent the same statistic, the 95% confidence interval for the model is determined as $\pm 2 \times$ the root-mean-squared error.

Observed station data has been processed to define time series for each station location for the surface layer and bottom layer of the water column. Observed data is assigned to a vertical layer based on surface water elevation, station bottom elevation and the total depth of the water column estimated for the sampling date/time. Station locations are overlaid on the model grid to define a set of discrete grid cells that correspond to each monitoring site for extraction of model results. For time series of model results extracted for each grid cell (station) and surface and bottom depth layer, the match of the model simulation time with date/time of observations for comparison to the model is defined by a time tolerance parameter of ± 1440 minutes. Model results are extracted for the set of model-data pairs if the model time is within the observed data date/time \pm time tolerance.

The equations for the RMSE and the Relative RMS Error are,

$$\text{RMSE} = \sqrt{\frac{1}{N} \sum (O - P)^2} \quad \text{Equation (1)}$$

$$\text{Relative RMS Error} = \frac{\text{RMSE}}{(O_{\text{range}})} \times 100 \quad \text{Equation (2)}$$

Where

N is the number of paired records of observed measurements and EFDC model results,

O is the observed water quality measurement,

P is the predicted EFDC model result, and

O_{range} is the range of observed data computed from the maximum and minimum values.

In evaluating the results obtained with the EFDC model, a Relative RMS Error performance measure of $\pm 20\%$ is adopted for evaluation of the comparison of the model predicted results and observed measurements of water surface elevation of the lake. For the hydrographic state variables simulated with the EFDC hydrodynamic model, a Relative RMS Error performance measure of $\pm 50\%$ is adopted for evaluation of the comparison of the predicted results and observed measurements for water temperature. For the water quality state variables simulated with the EFDC water quality model, a Relative RMS Error performance measure of $\pm 20\%$ is adopted for dissolved oxygen; $\pm 50\%$ for nutrients and suspended solids; and $\pm 100\%$ for algal biomass for the evaluation of the comparison of the predicted results and observed water quality measurements for model calibration. These targets for hydrodynamic, sediment transport and water quality model performance, defined for the overall composite statistic computed from the set of station-specific statistics, are consistent with the range of model performance targets recommended for the HSPF watershed model (Donigian, 2000).

Given the lack of a general consensus for defining quantitative model performance criteria, the inherent errors in input and observed data, and the approximate nature of model formulations, *absolute* criteria for model acceptance or rejection are not appropriate for studies such as the development of the lake model for Tenkiller Ferry Lake. The relative RMS errors presented above will be used as targets, but not as rigid criteria for rejection or acceptance of model results, for the performance evaluation of the calibration of the EFDC hydrodynamic and water quality model of Tenkiller Ferry Lake.

Section 7 Hydrodynamic Model Calibration and Validation

7.1 Lake Stage Calibration

The developed hydrodynamic model was calibrated for the time period of January 1, 2006 to December 31, 2006. Figure 7-1 shows the comparison of observed lake elevation at the USACE station TENO2 and simulated water surface elevation extracted from a grid cell at that location. Simulated lake elevation is in excellent agreement with the measured lake elevation for the entire calibration period from January 2006 through December 2006. The simulated average stage was 190.991 m, very close to the averaged observed stage of 190.985 m. The calculated RMS error was 0.029 m and the relative RMS error was 0.6% (Table 7-1). The summary of calculated statistics between observed and simulated water surface elevation for the calibration period is given in Table 7-1.

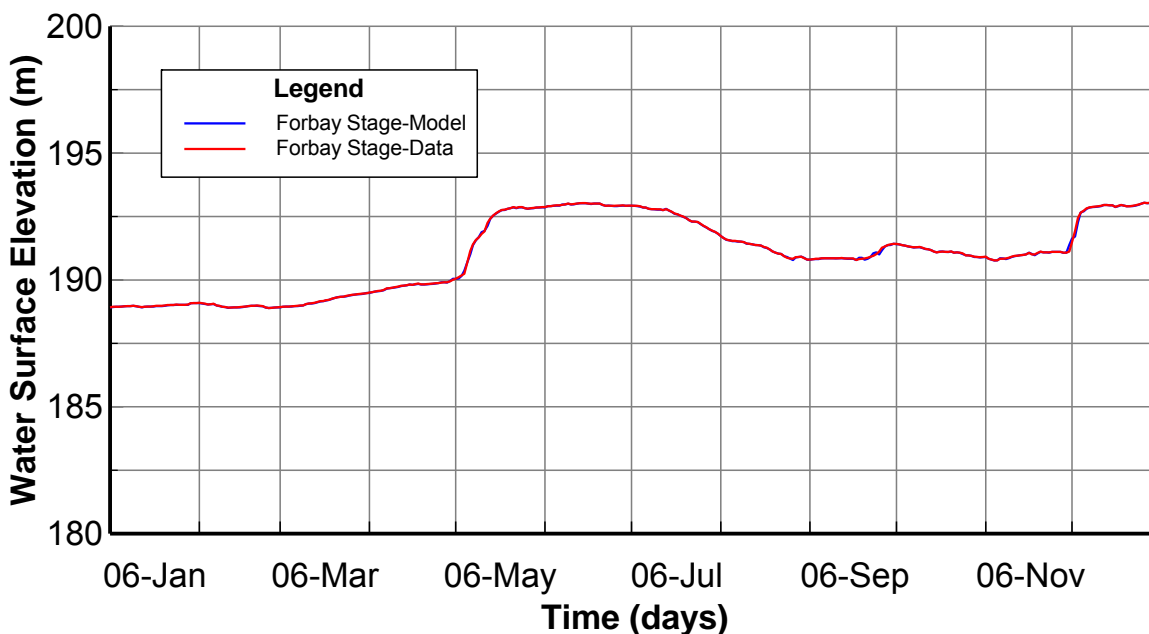


Figure 7-1. Comparison of Simulated and Observed Water Level during January 2006 to December 2006

Table 7-1. Summary Model Performance Statistics for Hydrodynamic Model of Tenkiller Ferry Lake Calibration and Validation Periods

Station ID	Parameter	Layer	Starting	Ending	# Pairs	RMS (m)	Rel RMS (%)	Data Average (m)	Model Average (m)
TENO2	Stage (m)	Surface	1/1/2006 0:00	12/31/2006 0:00	365	0.029	0.6	190.989	190.985
TENO2	Stage (m)	Surface	1/3/2005 0:00	12/31/2005 0:00	363	0.022	0.3	191.455	191.456

7.2 Lake Stage Validation

The developed Tenkiller Ferry Lake EFDC model was validated for the time period of January 1, 2005 to December 31, 2005. The validation plot of surface water elevation at UASCE station TENO2 is given in Figure 7-2. The summary of calculated statistics between observed and simulated water surface elevation for the validation period is given in Table 7-1. Simulated lake elevation is again in excellent agreement with the measured lake elevation for the entire validation period. The simulated average stage was 191.456 m, very close to the averaged observed stage of 191.455 m. The calculated RMS error was 0.022 m and the relative RMS error was 0.309% (Table 7-1).

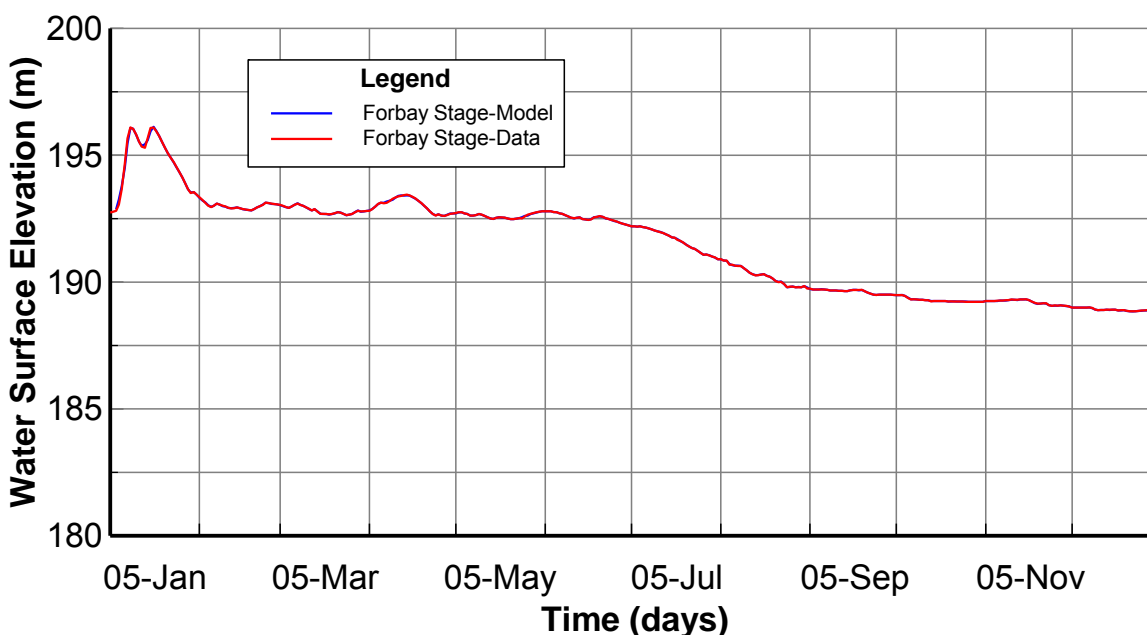


Figure 7-2. Comparison of Simulated and Observed Water Level during January 2005 to December 2005

The calculated relative RMS errors for both calibration and validation periods are well within in the defined model performance target of $\pm 20\%$; hence, the model results of water surface elevation are deemed to be acceptable.

7.3 Lake Hydraulic Residence Time Calibration and Validation

The Tenkiller Ferry Lake EFDC model was calibrated to data collected in 2006 (January 1-December 31) and then validated to data collected in 2005 (January 1-December 31). Estimates of hydraulic residence time for the whole lake are developed for 2005 and 2006 based on annual average inflow and lake volume. Modeled hydraulic residence time is compared to estimates of hydraulic residence time derived from USACE observations of annual average inflow and lake storage volume for 2005 and 2006.

The USACE Tulsa District maintains an archive of daily records of lake level, storage volume, release flow and inflow for Lake Tenkiller. The USACE provides inflow data to the lake derived from USGS gage measurements for the Illinois River at Tahlequah, OK; Baron Fork at Eldon, OK and Caney Creek at Gore, OK. Since the USGS gages do not directly measure streamflow entering the lake, the USACE provides adjusted inflow data (INFLOW ADJ) that accounts for the incremental increase of drainage area between the USGS gage locations and the inflow locations to the lake of the Illinois River, Baron Fork and Caney Creek.

The EFDC model relationship between lake stage and storage volume (Figure 3-2) is used with the simulated results for lake stage for 2005 (Figure 7-2) and 2006 (Figure 7-1) to determine lake storage volume for 2005 and 2006. Streamflow results from the HSPF watershed model were extracted for the lake inflow locations for the Illinois River, Baron Fork and Caney Creek to provide comparable records for modeled and observed streamflow data to estimate hydraulic residence time. Hydraulic residence time is estimated as the ratio of the lake storage volume and the inflow to the lake from the three streams.

Table 7-2 presents estimates of observed and modeled hydraulic residence time on an annual average basis for 2005 and 2006.

USACE records from 1997-2010 were used to estimate the long-term average hydraulic residence time of 0.58 years for the whole lake. Literature estimates of residence time for Lake Tenkiller ranging from 0.68 years (Nolen et al., 1989); 0.76 years (OWRB, 1996); and 0.7 years (Cooke et al., 2011) are consistent with the 1997-2010 estimate developed for this analysis.

For 2005, the observed residence time is estimated as 0.73 yr while for the low flow conditions of 2006, a longer observed residence time is estimated as 1.14 yr. The EFDC model results indicate a residence time of 0.87 yr for 2005 and 0.85 yr for 2006. Under the hydrologic conditions of 2005, the model results indicate a somewhat longer residence time (0.87 yr) than the observations (0.73 yr) with a relative error of 18.7% for the model. Under the low flow conditions of 2006, the relative error for the model is 25.7% with the model residence time (0.85 yr) shorter than the observed residence time (1.14 yr).

Table 7-2. Comparison of Observed and Simulated Whole Lake Hydraulic Residence Time: January-December

Jan-Dec	USACE Volume (Ac-ft)	IR+BF+CC USACE InflowAdj (cfs)	IR+BF+CC USACE InflowAdj (cf/yr)	Residence Time (yr)			
2005	608,861.7	1150.99	3.6298E+10	0.73			
2006	589,667.6	714.44	2.2531E+10	1.14			
1997-2010	654,426.2	1558.75	4.9157E+10	0.58			
Jan-Dec	EFDC Volume (Ac-ft)	IR+BF+CC HSPF Inflow (cfs)	IR+BF+CC HSPF Inflow (cf/yr)	EFDC Res Time (yr)	Obs-EFDC Rel Error Res Time (%)	Obs-HSPF Rel Error Inflow (%)	Obs-EFDC Rel Error Volume (%)
2005	585,000.6	931.30	2.9370E+10	0.87	-18.7%	23.6%	3.9%
2006	567,341.2	924.60	2.9158E+10	0.85	25.7%	-22.7%	3.8%

Cooke et al. (2011) derived residence time estimates for 2005 (2.41 yr) and 2006 (2.45 yr) based on USACE Tulsa District storage volume and inflow data for the half-year summer period from April through September. As shown in Table 7-3, the EFDC estimate for summer residence time in 2005 of 2.36 yr is very close to the observed 2005 estimate of 2.42 yr with only a 2.4% relative error for residence time and 1.5% error for streamflow. For summer 2006, however, the EFDC residence time estimate of 1.7 yr is lower than the observed estimate of 2.46 yr. The relative error for the residence time (30.9%) is consistent with the 28% relative error for summer streamflow where streamflow was significantly overestimated for the very dry hydrologic conditions of the summer months of 2006.

Table 7-3. Comparison of Observed and Simulated Whole Lake Hydraulic Residence Time: April-September

Half-Yr Apr-Sept	USACE Volume (Ac-ft)	IR+BF+CC USACE InflowAdj (cfs)	IR+BF+CC USACE InflowAdj (cf/half-yr)	Residence Time (yr)			
2005	612,979.9	699.45	1.1029E+10	2.42			
2006	613,192.2	688.31	1.0853E+10	2.46			
Half-Yr Apr-Sept	EFDC Volume (Ac-ft)	IR+BF+CC HSPF Inflow (cfs)	IR+BF+CC HSPF Inflow (cf/half-yr)	EFDC Res Time (yr)	Obs-EFDC Rel Error Res Time (%)	Obs-HSPF Rel Error Inflow (%)	Obs-EFDC Rel Error Volume (%)
2005	589,821.6	689.33	1.0869E+10	2.36	2.4%	1.5%	3.8%
2006	588,840.6	956.54	1.5083E+10	1.70	30.9%	-28.0%	4.0%

As shown in the tables, the relative error of ~4% for the estimate of model storage volume for the January-December and April-September periods of 2005 and 2006 shows very good comparison to the observed storage volume. The relative error for HSPF streamflow, however, of ~23% (Jan-Dec, 2005 and 2006) and 28% (Apr-Sept, 2006) clearly shows that the discrepancy in the EFDC model estimates of residence time can be attributed to discrepancies in the HSPF streamflow results particularly during the dry flow conditions of the summer of 2006.

Section 8 Water Quality Model Calibration and Validation

8.1 Introduction

Prior to model calibration, one-year model spin-up was conducted to eliminate the impact of initial water quality conditions on model results. Calibration of the lake model is demonstrated with model-data comparisons for water temperature, total suspended solids, dissolved oxygen, nutrients, total organic carbon, and algae biomass as station time series. Vertical profiles are presented for water temperature and dissolved oxygen. Observed data collected near the surface is compared to lake model results for the EFDC surface layer ($k=16$) and data collected near the bottom is compared to model results for the EFDC bottom layer ($k=1$). Station results are presented in this section to show model calibration for the selected stations in Tenkiller Ferry Lake. The location of these stations can be found in Figure 5-2 and Figure 5-3.

Over the calibration and validation periods (2005-2006), the observed data were very limited; in many cases the sample size of observed data for one individual year was less than 10. In particular, there were no ammonium data available for model validation. Hence, the summary statistics were provided for the simulation period of two complete years while the comparison plots were provided separately for calibration and validation periods. In the case that the sample size over the simulation period of two complete years is less than 5, the statistics are not provided.

As discussed in Section 8.8, the HSPF watershed model overestimated loading to the lake during a storm event that occurred in late April and May 2006. Observed data sets were filtered to remove the impact of the significant overestimate of watershed loading in late April and May 2006 on the lake model response and the calculation of model performance statistics based on paired observations and model results. Three sampling dates in May 2006 were removed from the observed data sets for computation of model performance statistics for TSS, chlorophyll a, TPO4 and TP. Observations were filtered for Station LK-03 because this station, located in the transition zone of the lake, showed the greatest lake response impact to the overestimate of watershed loading for the late April and May 2006 storm event.

8.2 Water Temperature Calibration and Validation

Procedures used to calibrate water temperature included: 1) check the linkage between HSPF and EFDC; 2) check the meteorological data to make sure the solar radiation data are in the reasonable range; and (3) adjust the key parameters within the reasonable ranges to best match the observed data. Through the model calibration process, it was found that the most important parameters for water temperature calibration were heat transfer coefficient between bed and water column, minimum fraction of solar radiation absorbed in the surface layer, vertical layer thickness distribution, and vertical eddy viscosity.

Modeled water temperature results are presented for comparison to the observed data for the surface layer ($k=16$) and bottom layer ($k=1$). Water temperature calibration plots at LK-01 and LK-03 are given in Figures 8-1 through 8-4. Water temperature validation plots at LK-01 and LK-03 are given in Figures 8-5 through 8-8. The summary statistics of water temperature are given in Table 8-1.

The comparisons of water temperature vertical profiles at LK-01 and LK-03 are given in Figures 8-9 and 8-10. The complete calibration and validation time series plots and vertical profiles for all monitoring stations are given in APPENDIX J through APPENDIX M.

As can be seen in these model-data plots, the model results for the surface and bottom layer are in fairly good agreement with the measured water temperature for both calibration and validation periods. At the surface layer of LK-03, the simulated data matched the observed temperature very well (Figures 8-7 and 8-11). However, the EFDC model underpredicted the bottom layer temperature in summer stratified conditions during the validation period, as shown in Figure 8-8.

The calculated RMS errors ranged from 0.937 °C at the surface layer of station LK-03 to 5.636 °C at the bottom layer of station LK-04 as shown in Table 8-1. The calculated relative RMS errors ranged from 4.5% at the surface layer of station LK-03 to 27.1% at the bottom layer of station LK-04. Considering the fact that the model results are within or close to the defined model performance target of $\pm 50\%$ for water temperature, the model results for water temperature are deemed to be acceptable.

Model results are extracted as “snapshots” for a time interval of the simulation that matches the observed date/time records for the survey profile. As can be seen in these model-data vertical profile plots, the model results are reasonably consistent with observed water temperature for well mixed winter conditions, but not as good for summer stratified conditions. The water temperature stratification simulated by EFDC in summer time is less than the observed data, which is caused by the artificial vertical numerical diffusion introduced by the sigma grid.

Table 8-1. Summary Statistics of Water Temperature (°C)

Station ID	Layer	Starting	Ending	# Pairs	RMS (°C)	Rel RMS (%)	Data Average (°C)	Model Average (°C)
LK-01	Layer 1	5/18/2005 12:25	9/26/2006 11:30	27	2.061	24.2	12.322	13.702
LK-01	Layer 16	5/18/2005 12:25	9/26/2006 11:30	27	1.987	10.1	25.199	23.731
LK-02	Layer 1	5/18/2005 9:33	9/26/2006 7:30	27	2.071	26.9	13.044	14.361
LK-02	Layer 16	5/18/2005 9:33	9/26/2006 7:30	27	0.95	4.7	25.131	25.185
LK-03	Layer 1	5/18/2005 14:34	9/26/2006 14:25	27	3.019	15.0	24.4	22.03
LK-03	Layer 16	5/18/2005 14:34	9/26/2006 14:25	27	0.937	4.5	26.191	26.543
LK-04	Layer 1	7/26/2005 16:40	9/26/2006 15:45	21	5.636	27.1	23.8	19.642
LK-04	Layer 16	7/26/2005 16:40	9/26/2006 15:45	21	1.088	5.2	25.812	26.191

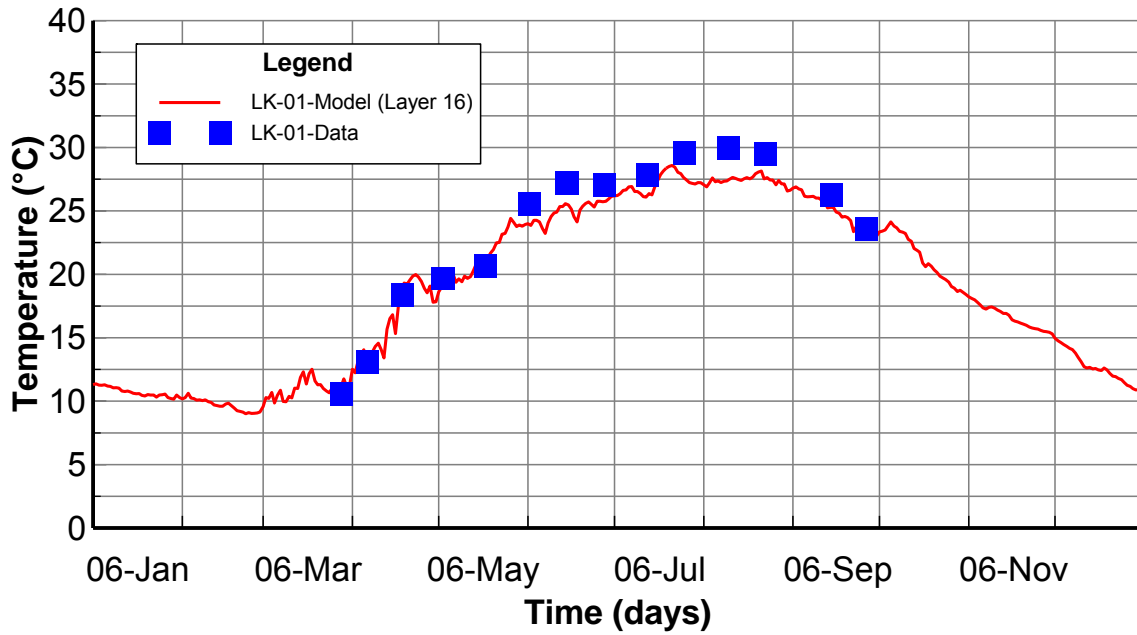


Figure 8-1. Surface Layer Water Temperature Calibration Plot at Station LK-01.

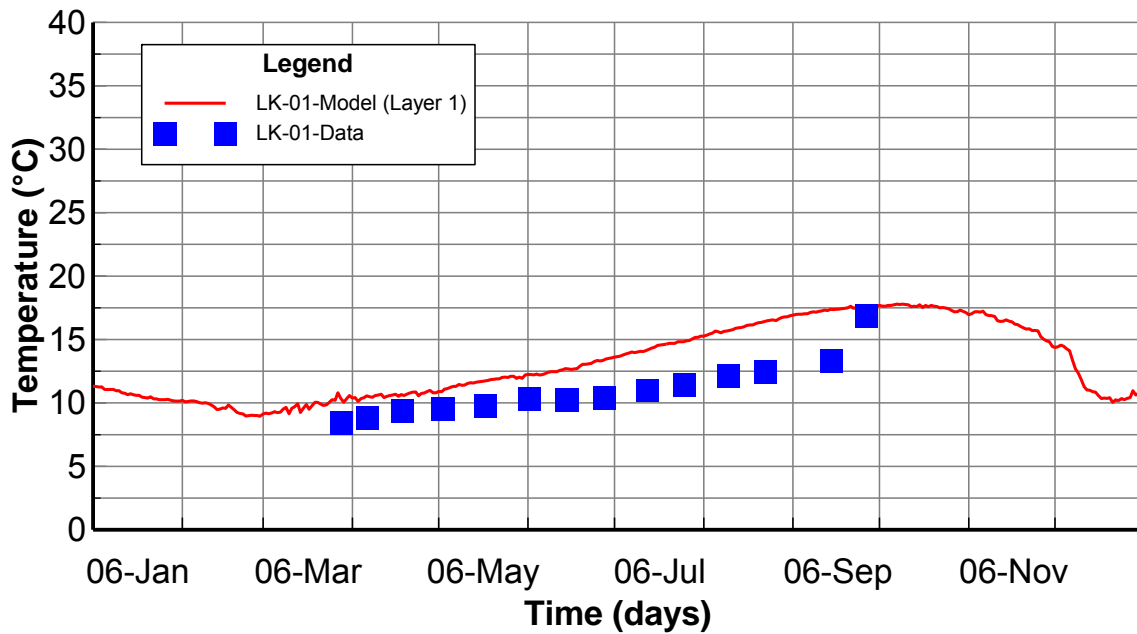


Figure 8-2. Bottom Layer Water Temperature Calibration Plot at Station LK-01.

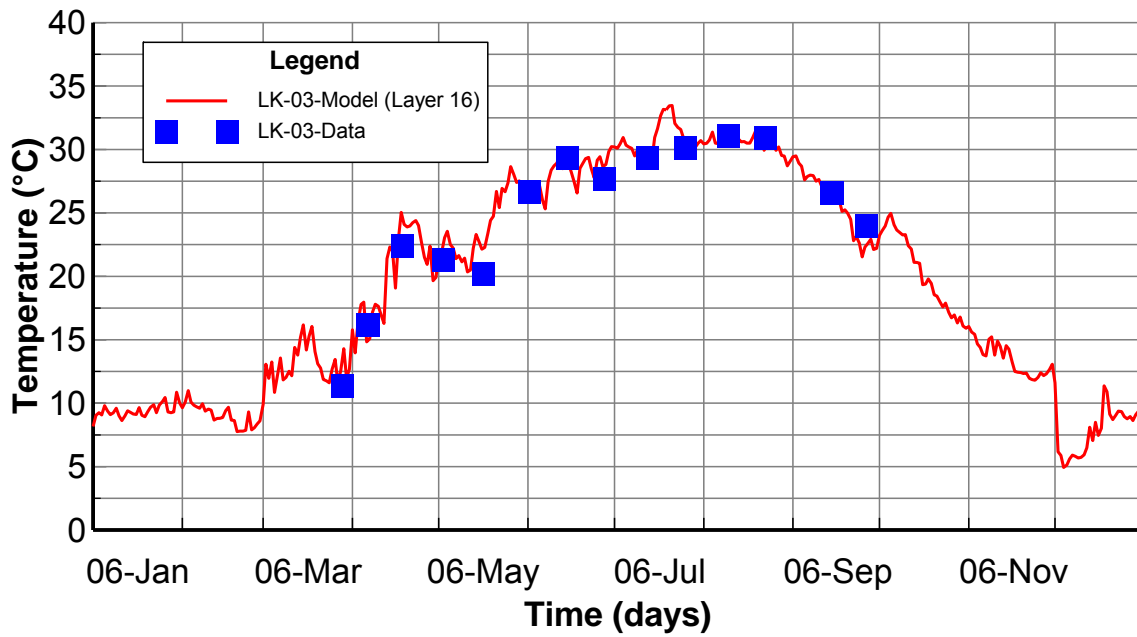


Figure 8-3. Surface Layer Water Temperature Calibration Plot at Station LK-03.

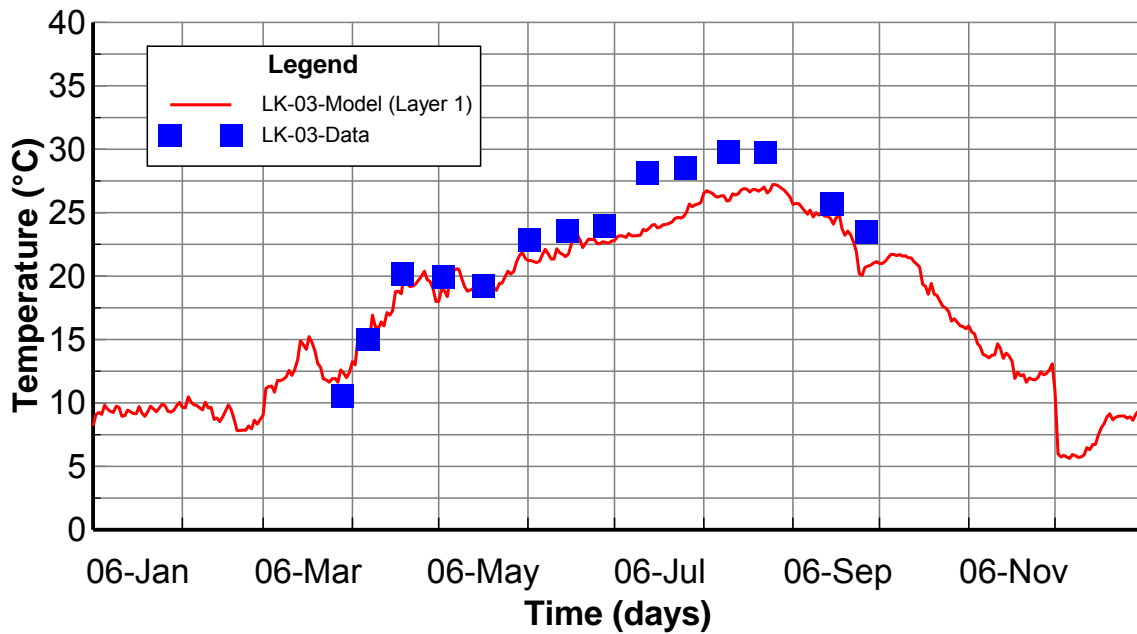


Figure 8-4. Bottom Layer Water Temperature Calibration Plot at Station LK-03.

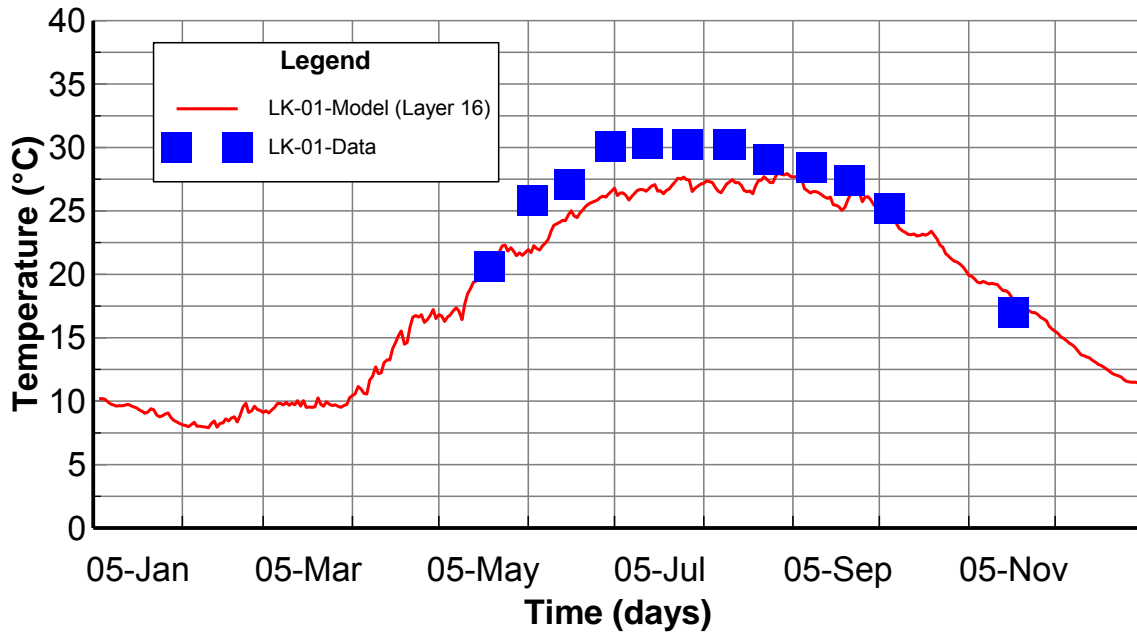


Figure 8-5. Surface Layer Water Temperature Validation Plot at Station LK-01

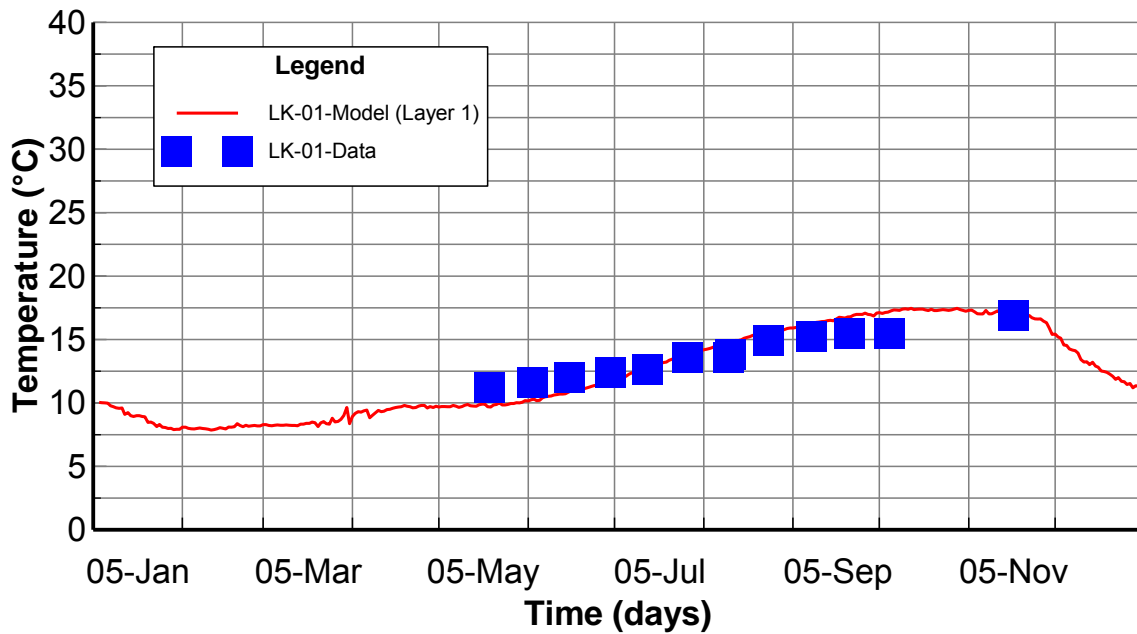


Figure 8-6. Bottom Layer Water Temperature Validation Plot at Station LK-01

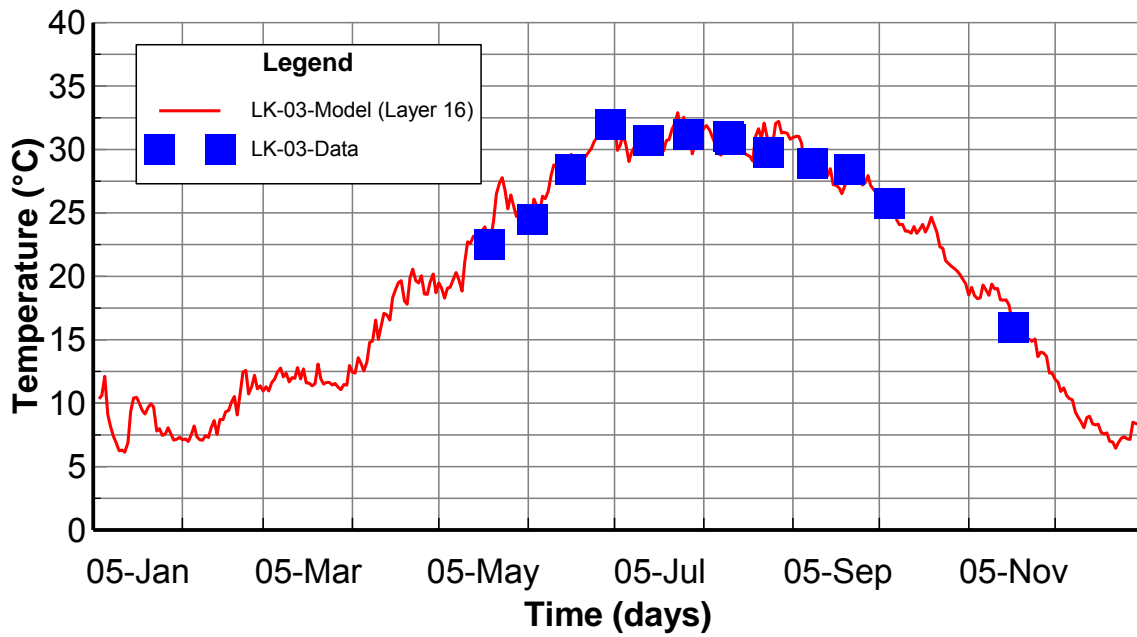


Figure 8-7. Surface Layer Water Temperature Validation Plot at Station LK-03

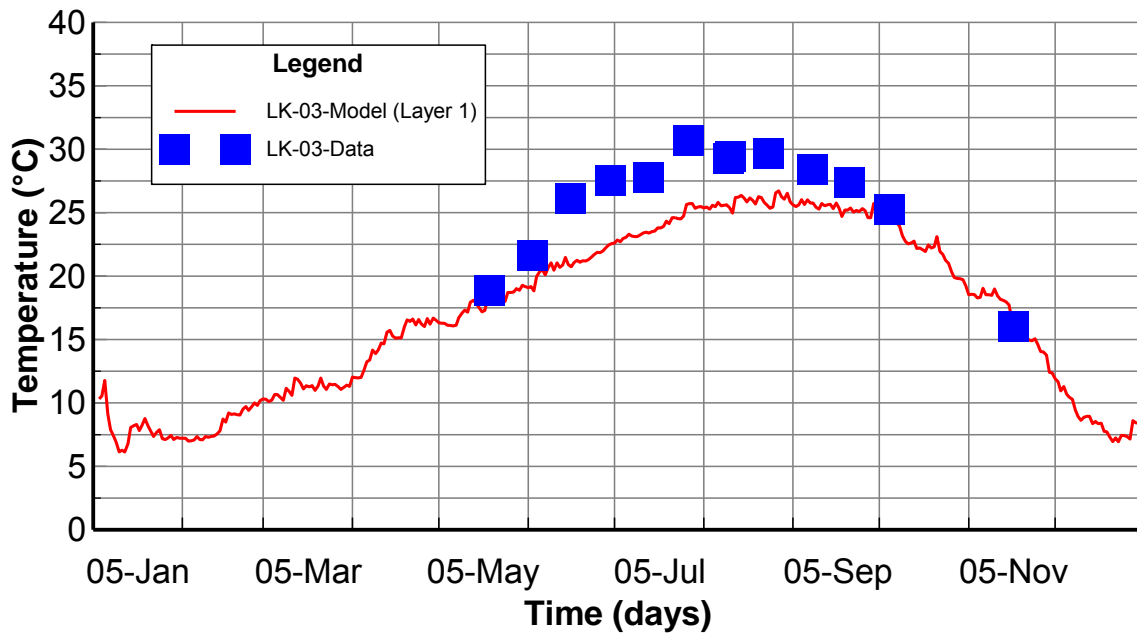


Figure 8-8. Bottom Layer Water Temperature Validation Plot at Station LK-03

TenKiller Hydrodynamic and Water Quality Model
Vertical Profiles: LK-01, Model Cell: 21, 12

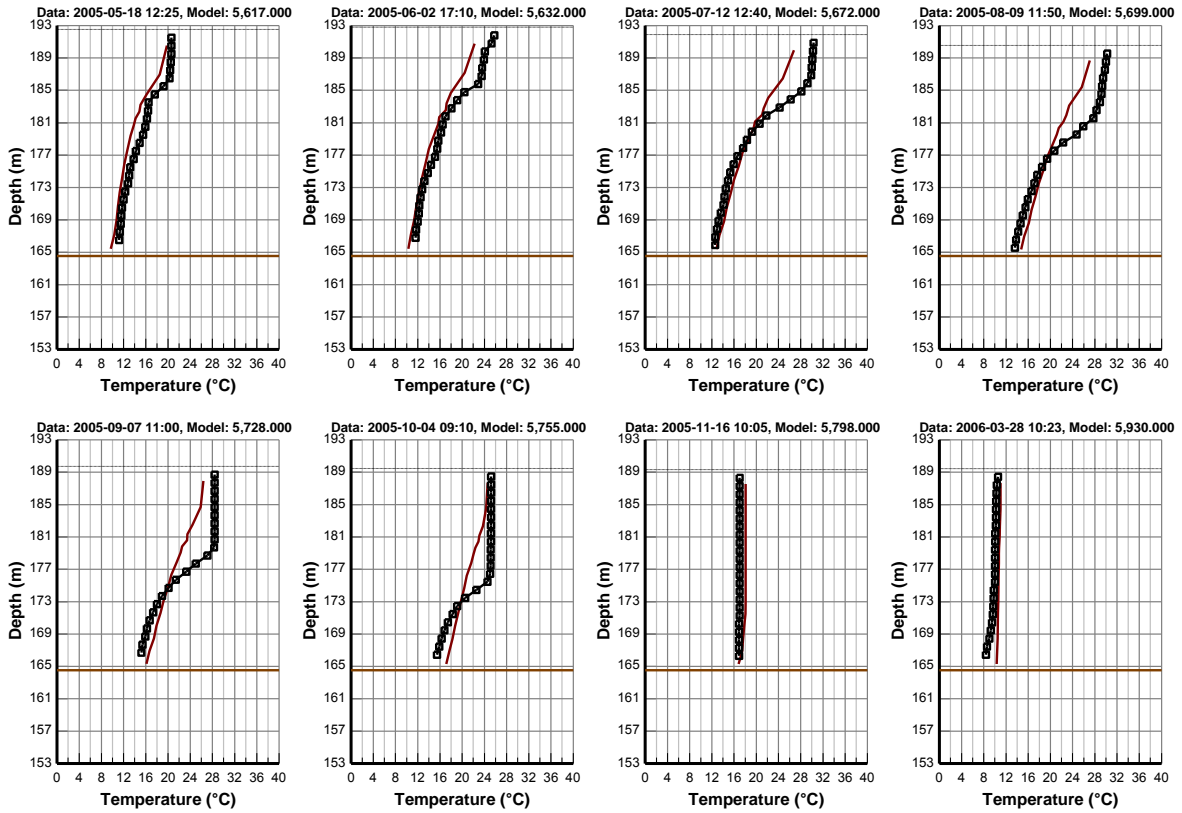


Figure 8-9. Water Temperature Vertical Profile Comparison Plot at Station LK-01 (5 May 2005 – 28 March 2006) (page 2-1)

TenKiller Hydrodynamic and Water Quality Model
Vertical Profiles: LK-01, Model Cell: 21, 12

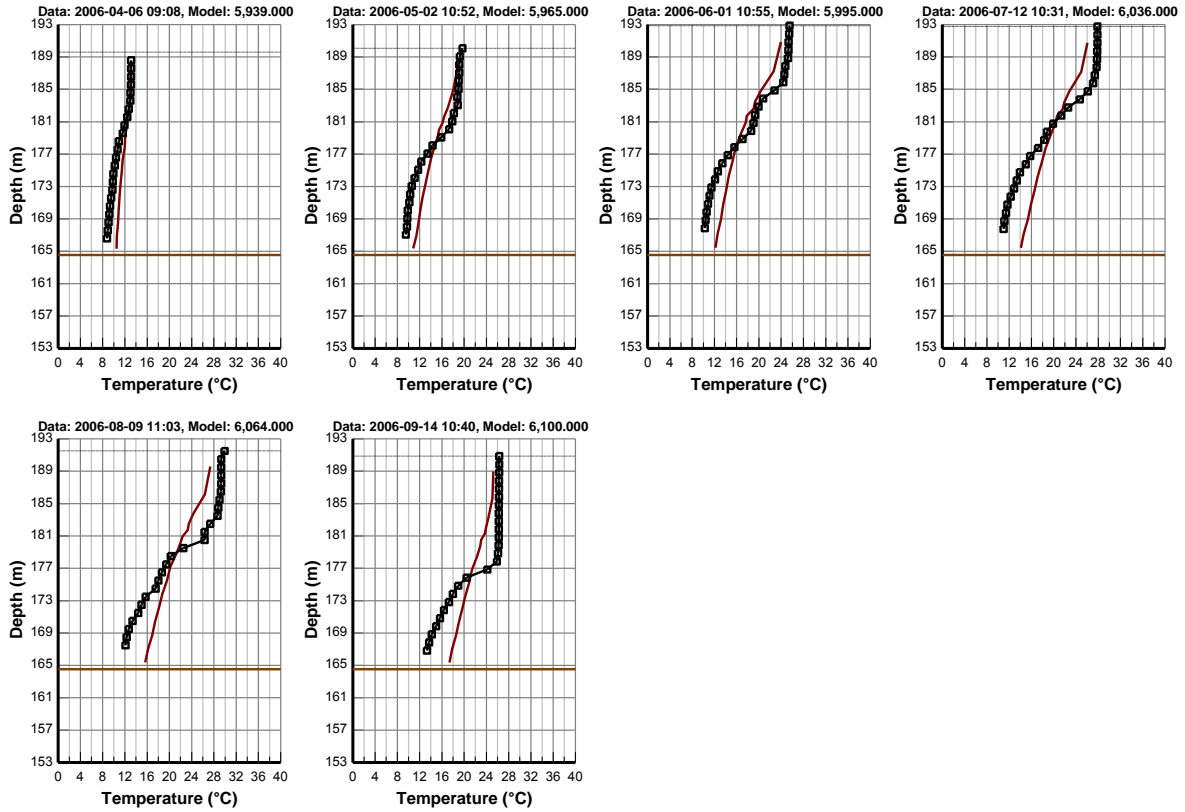


Figure 8-10. Water Temperature Vertical Profile Comparison Plot at Station LK-01 (6 April 2005 – 14 September 2006) (page 2-2)

TenKiller Hydrodynamic and Water Quality Model
Vertical Profiles: LK-03, Model Cell: 21, 69

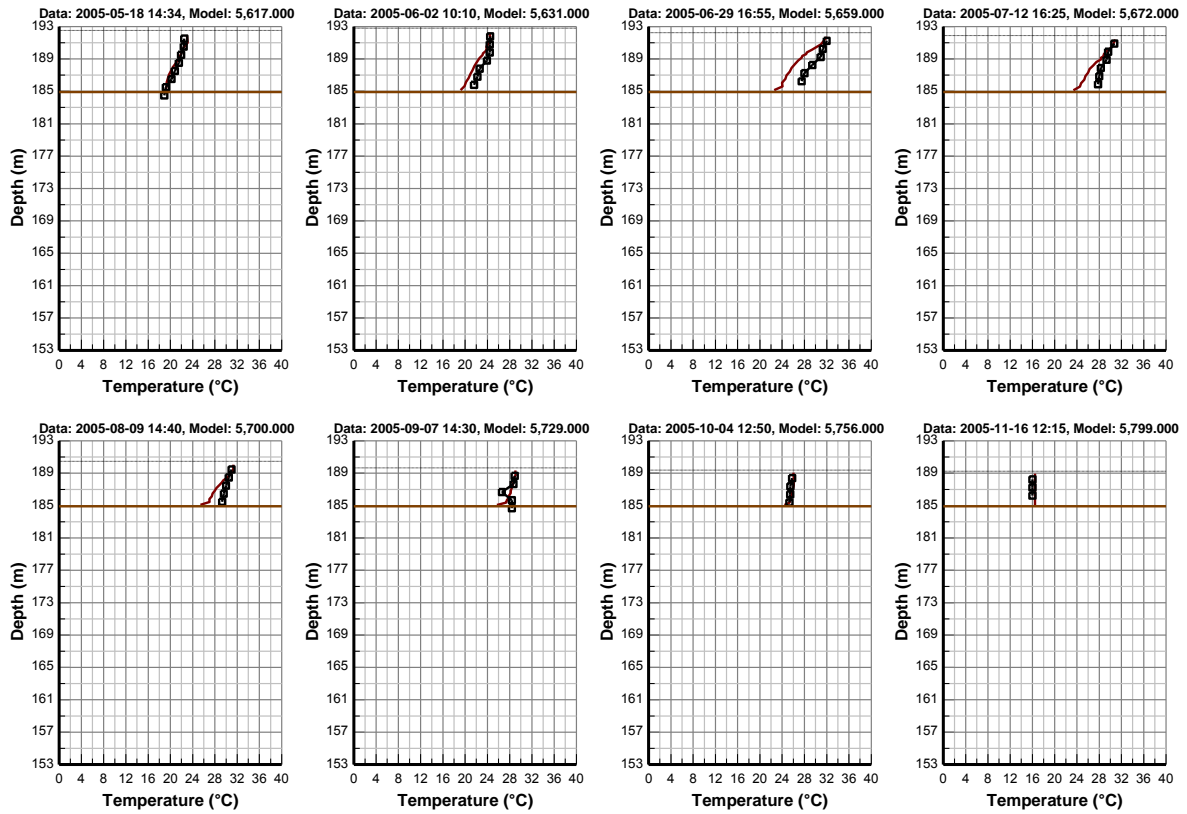


Figure 8-11. Water Temperature Vertical Profile Comparison Plot at Station LK-03 (18 May 2005 – 16 November 2005) (page 2-1)

TenKiller Hydrodynamic and Water Quality Model
Vertical Profiles: LK-03, Model Cell: 21, 69

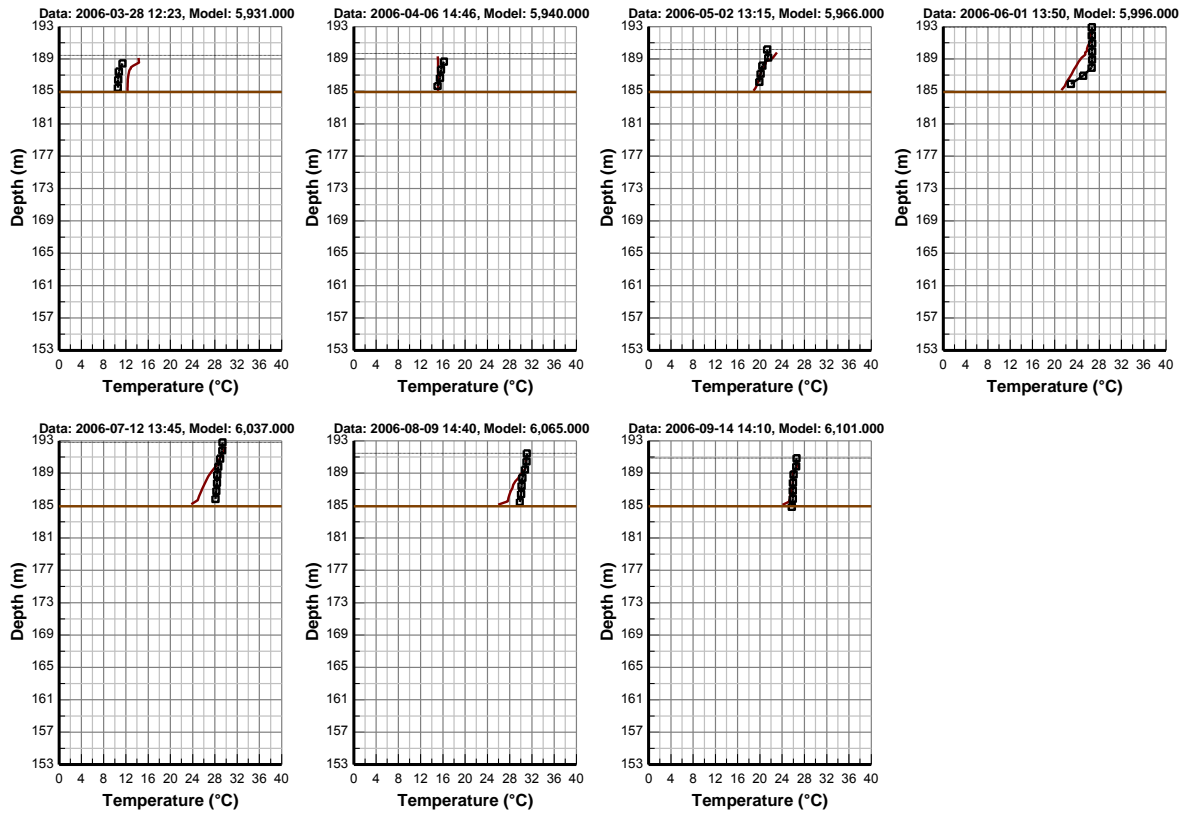


Figure 8-12. Water Temperature Vertical Profile Comparison Plot at Station LK-03 (28 March 2006 – 14 September 2006) (page 2-2)

8.3 Total Suspended Solids Calibration and Validation

Procedures used to calibrate total suspended solids included: 1) check the linkage between HSPF and EFDC to make sure that the setup of TSS boundary conditions for the Lake EFDC model is correct; and 2) adjust the key parameters within reasonable ranges to best match the observed data. Through the model calibration process, it was found that the most important parameters for TSS calibration were critical shear stress for deposition, critical shear stress for erosion, reference surface erosion rate, and settling velocity. At stations LK-03 and LK-04, the TSS boundary conditions from the watershed loads showed much more of an impact on model results than the EFDC sediment transport parameters.

Modeled TSS results are presented for comparison to the observed data for the surface layer ($k=16$) and bottom layer ($k=1$). Total suspended solids calibration plots at LK-01 and LK-03 are given in Figures 8-13 through 8-16. Total suspended solids validation plots at LK-01 and LK-03 are given in Figures 8-17 through 8-20. The summary statistics of total suspended solids are given in Table 8-2. The complete calibration and validation time series plots for all monitoring stations are given in APPENDIX J and APPENDIX K.

As can be seen in these model-data plots, the model results for the surface and bottom layer are in reasonable agreement with the measured TSS. The calculated relative RMS errors ranged from 38.3% at the surface layer of station LK-01 to 166% at the surface layer of station LK-03. In the bottom layer, the model results are close to the defined model performance target of $\pm 50\%$ for TSS except at the bottom layer of station LK-01 where the relative RMS error is 70% (Table 8-2). Overall, the composite model performance for the relative RMS error for TSS for the 4 stations is 77% ($n=180$ data pairs).

The purpose of the total suspended solids calibration is to simulate a reasonable amount of suspended solids in the water column to make sure that light extinction due to suspended solids is a reasonable representation of the effects of light attenuation on both water temperature and water clarity. Since water temperature is reasonably well simulated and the model results are close to the defined model performance target for TSS, the model results of TSS calibration are deemed to be acceptable.

Table 8-2. Summary Statistics of TSS (mg/l)

Station ID	Layer	Starting	Ending	# Pairs	RMS (mg/l)	Rel RMS (%)	Data Average (mg/l)	Model Average (mg/l)
LK-01	Layer 1	5/18/2005 12:58	9/26/2006 12:00	21	2.801	70.0	3.048	1.491
LK-01	Layer 16	5/18/2005 12:05	9/26/2006 12:00	25	2.68	38.3	2.7	0.526
LK-02	Layer 1	5/18/2005 10:19	9/26/2006 8:00	25	11.707	50.9	7.64	5.338
LK-02	Layer 16	5/18/2005 9:01	9/26/2006 8:00	24	3.701	61.8	3.048	2.19
LK-03	Layer 1	5/17/2005 15:22	8/9/2006 14:50	19	10.554	45.888	7.789	2.867
LK-03	Layer 16	5/17/2005 14:05	9/26/2006 14:40	31	14.970	166.331	5.484	3.640
LK-04	Layer 1	7/26/2005 16:40	9/26/2006 16:00	19	78.635	51.1	52.816	23.31
LK-04	Layer 16	7/26/2005 16:40	9/26/2006 16:00	20	30.003	91.0	17.1	9.911

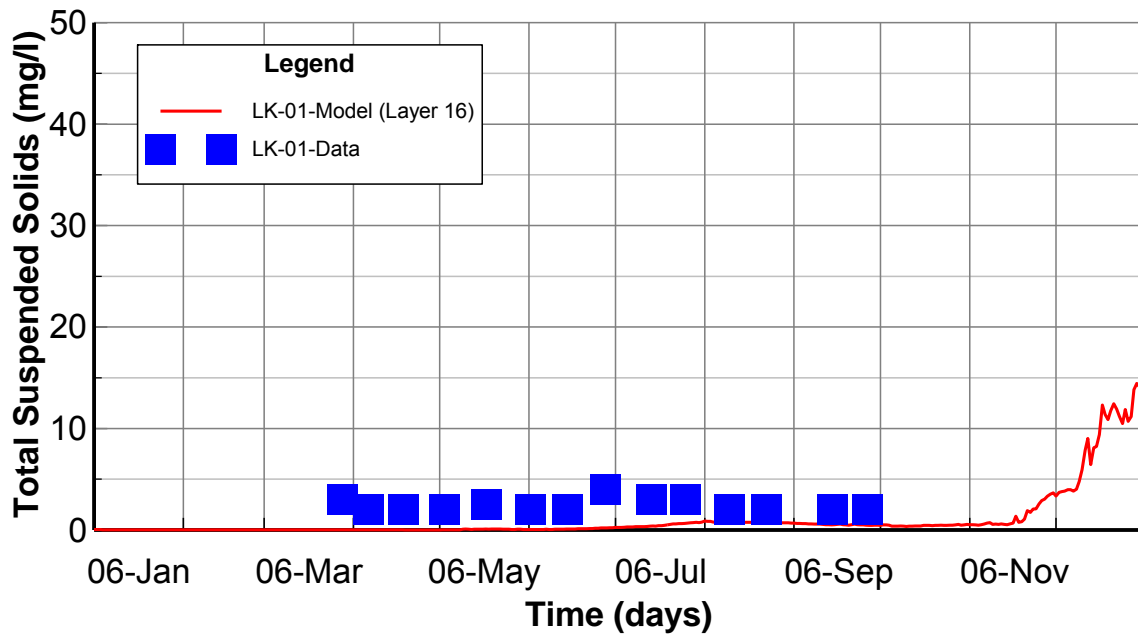


Figure 8-13. Surface Layer TSS Calibration Plot at Station LK-01.

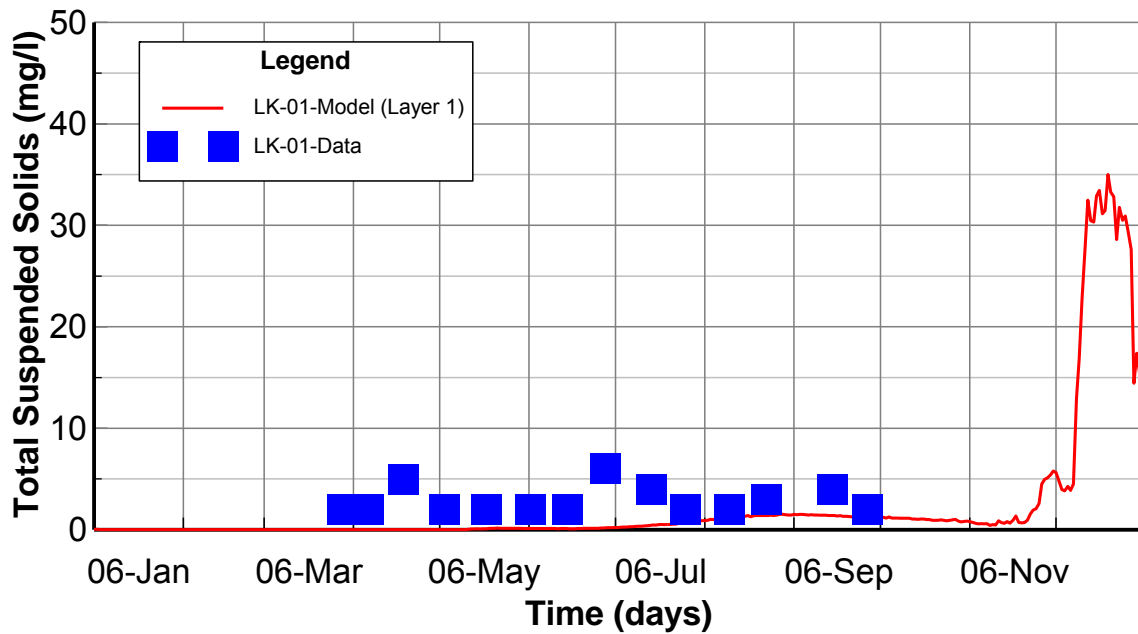


Figure 8-14. Bottom Layer TSS Calibration Plot at Station LK-01.

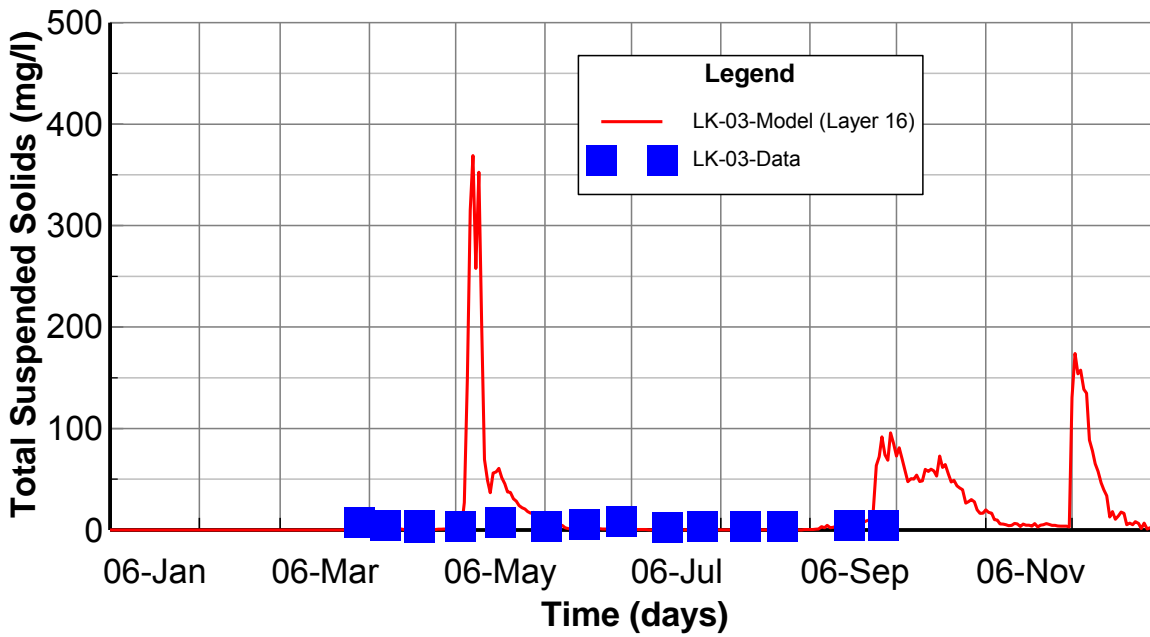


Figure 8-15. Surface Layer TSS Calibration Plot at Station LK-03.

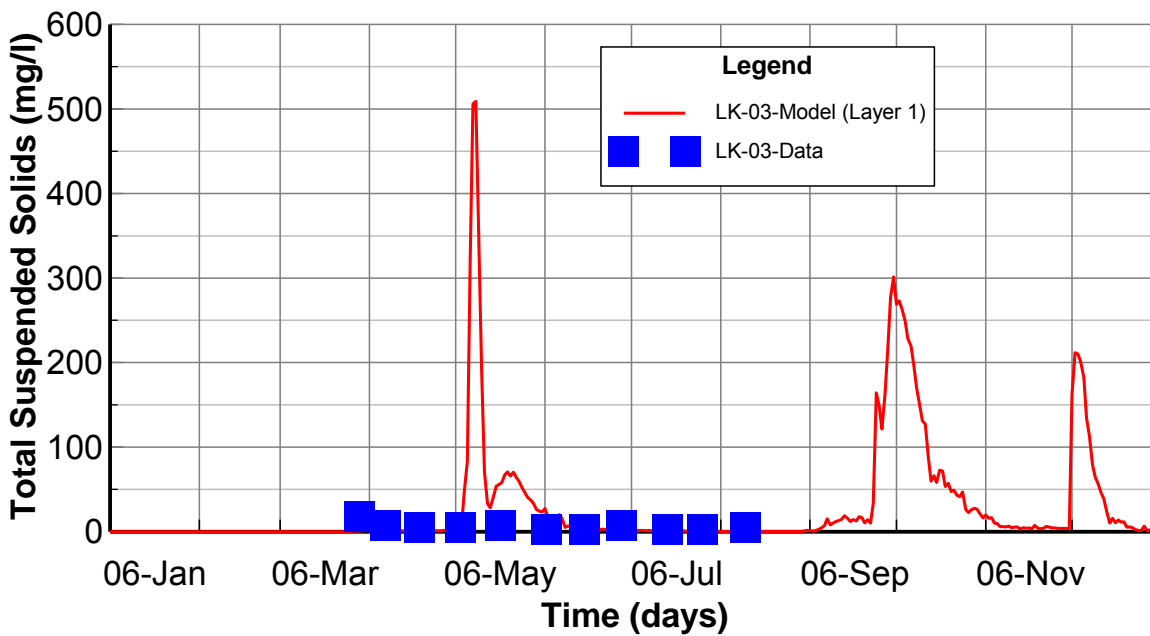


Figure 8-16. Bottom Layer TSS Calibration Plot at Station LK-03.

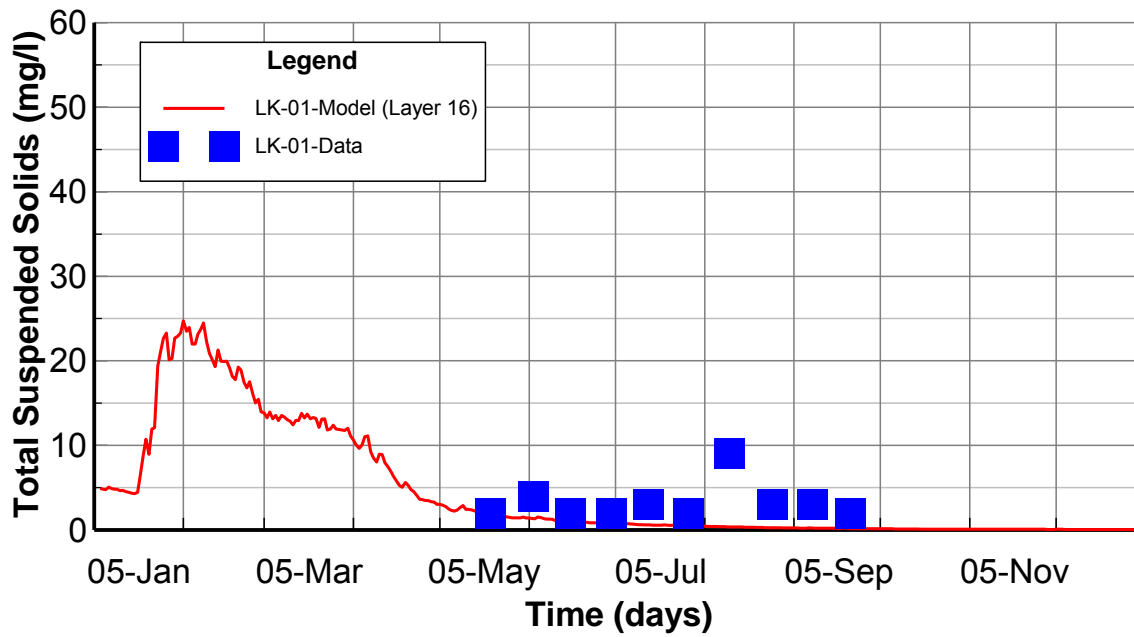


Figure 8-17. Surface Layer TSS Validation Plot at Station LK-01

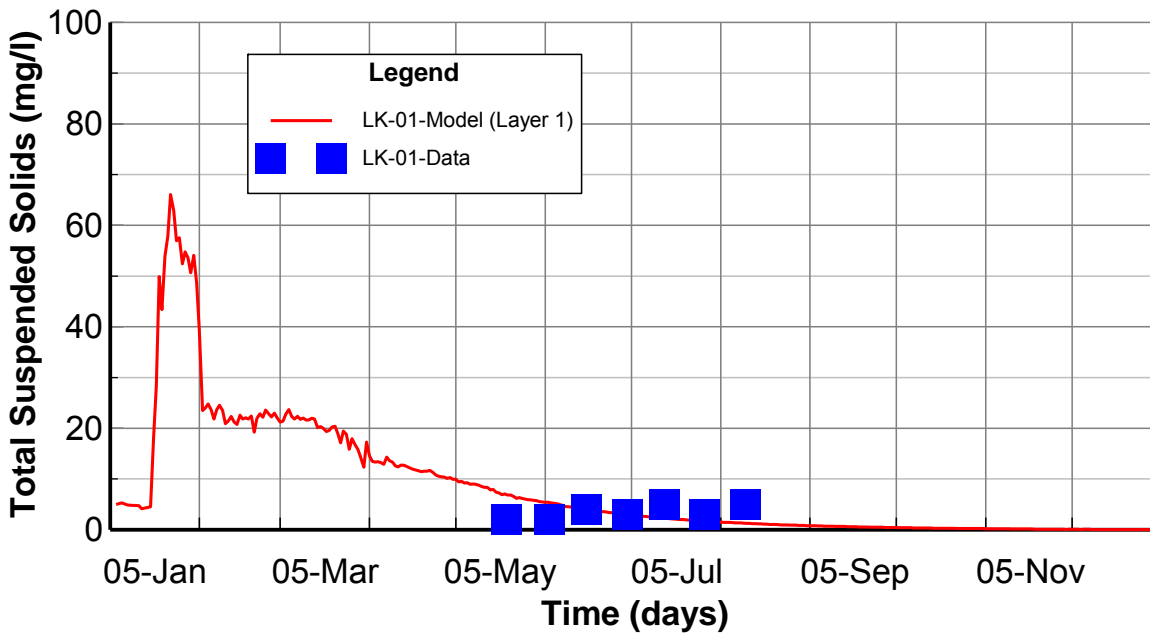


Figure 8-18. Bottom Layer TSS Validation Plot at Station LK-01

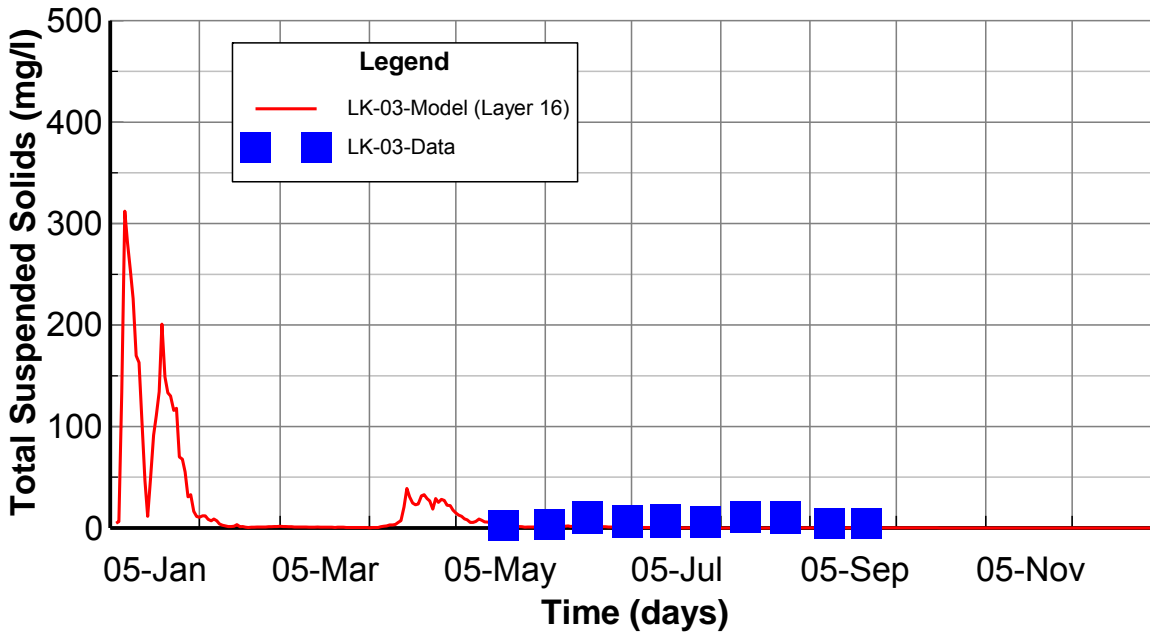


Figure 8-19. Surface Layer TSS Validation Plot at Station LK-03

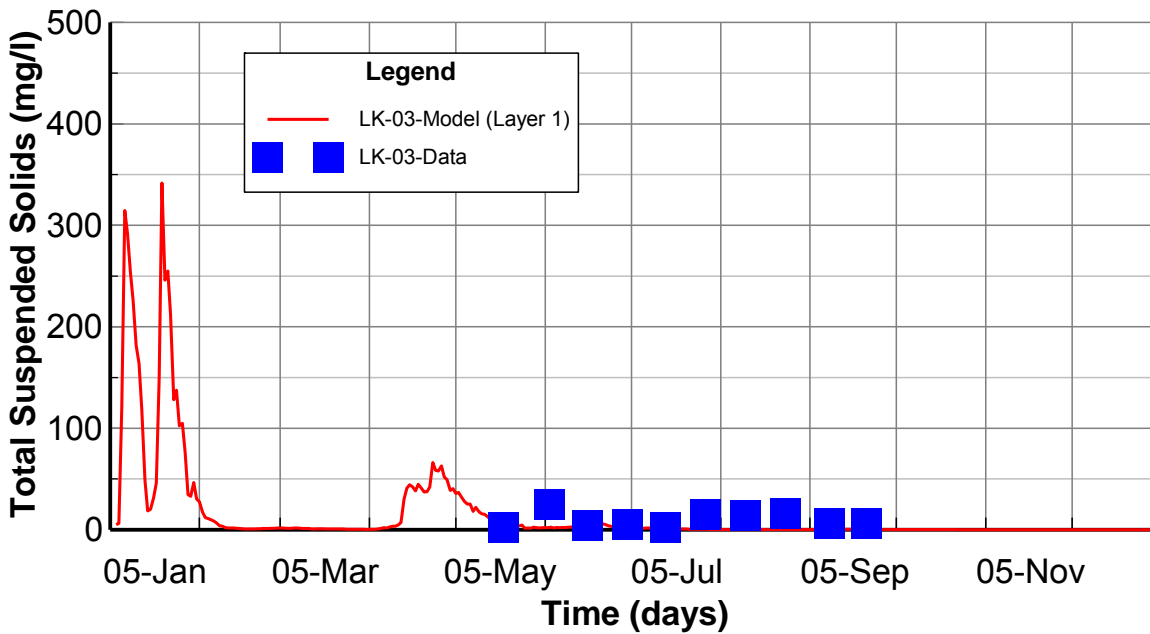


Figure 8-20. Bottom Layer TSS Validation Plot at Station LK-03

8.4 Dissolved Oxygen Calibration and Validation

Procedures used to calibrate dissolved oxygen included: 1) check the linkage between HSPF and EFDC to make sure that the setup of DO boundary conditions for the Lake EFDC model is correct; and 2) adjust the key parameters within reasonable ranges to obtain the best match with the observed data. Through the model calibration process, it was found that the most important parameters for the DO calibration were the SOD scaling factor for sediment diagenesis and the option used to represent reaeration. Lake DO is also strongly impacted in the lower layers by water temperature through stratification and in the surface layers by photosynthetic production of dissolved oxygen from algae growth.

Modeled oxygen results are presented for comparison to the observed data for the surface layer ($k=16$) and bottom layer ($k=1$). Dissolved oxygen calibration plots at LK-01 and LK-03 are given in Figures 8-21 through 8-24. Dissolved oxygen validation plots at LK-01 and LK-03 are given in Figures 8-25 through 8-28. The summary statistics of dissolved oxygen are given in Table 8-3.

The comparisons of dissolved oxygen vertical profiles at LK-01 and LK-03 are given in Figures 8-29 and 8-30. The complete calibration and validation time series plots and vertical profiles for all monitoring stations are given in APPENDIX J through APPENDIX M.

In general, the model results for both the surface and bottom layers followed with the seasonal trend of the measured oxygen, as can be seen in these model-data plots. However, during the validation period, the EFDC model generally underpredicted the surface layer dissolved oxygen (Figure 8-27) and underpredicted the bottom layer dissolved oxygen at Station LK-03 (Figure 8-28) after the end of July 2005. Observed DO at Station LK-03 ranges from ~8-14 mg/L during the months of May through July 2005. With water temperature ranging from ~25-30 °C, observed DO is characterized by supersaturated conditions of ~150% or more. Although model and observed surface chlorophyll are in reasonable agreement for this station (Figure 8-33), the photosynthetic contribution from algal growth to surface DO in the model does not match the consistently high levels of DO observed in the surface layer.

The calculated RMS errors ranged from 1.558 mg/L at the surface layer of station LK-01 to 3.334 mg/L at the bottom layer of station LK-03 shown in Table 8-3. The calculated relative RMS errors ranged from 15.3% at the bottom layer of station LK-04 to 30.3% at the surface layer of station LK-03. The model results are within or close to the defined model performance target of $\pm 20\%$ for dissolved oxygen.

For comparison at each station, model results are extracted as vertical “snapshots” at different times when the observed data are available. As can be seen in these model-data vertical profile plots shown in Figures 8-29 and 8-30, the model results are reasonably consistent with the observed dissolved oxygen for the well mixed winter conditions. For the summer stratified condition, the Tenkiller Ferry Lake EFDC model did not perform as well as the well mixed winter conditions.

There is significant correlation between DO, water temperature and water column stratification. Overall, the composite model performance for the relative RMS error for DO for the 4 stations is 24% ($n=203$ data pairs). Since the model results of DO are within, or close to, the defined model performance target of $\pm 20\%$, the model results for DO are deemed to be acceptable.

Table 8-3. Summary Statistics of DO (mg/l)

Station ID	Layer	Starting	Ending	# Pairs	RMS (mg/l)	Rel RMS (%)	Data Average (mg/l)	Model Average (mg/l)
LK-01	Layer 1	5/18/2005 12:25	9/26/2006 11:30	27	2.337	24.8	2.309	3.01
LK-01	Layer 16	5/18/2005 12:25	9/26/2006 11:30	27	1.558	26.9	9.198	8.27
LK-02	Layer 1	5/18/2005 9:33	9/26/2006 7:30	27	2.075	20.0	1.496	2.115
LK-02	Layer 16	5/18/2005 9:33	9/26/2006 7:30	27	2.243	24.2	9.243	8.205
LK-03	Layer 1	5/18/2005 14:34	9/26/2006 14:25	27	3.334	29.4	5.829	5.032
LK-03	Layer 16	5/18/2005 14:34	9/14/2006 14:10	26	2.271	30.3	10.289	8.617
LK-04	Layer 1	7/26/2005 16:40	9/26/2006 15:45	21	1.94	15.3	5.614	5.489
LK-04	Layer 16	7/26/2005 16:40	9/26/2006 15:45	21	2.212	20.5	9.915	9.362

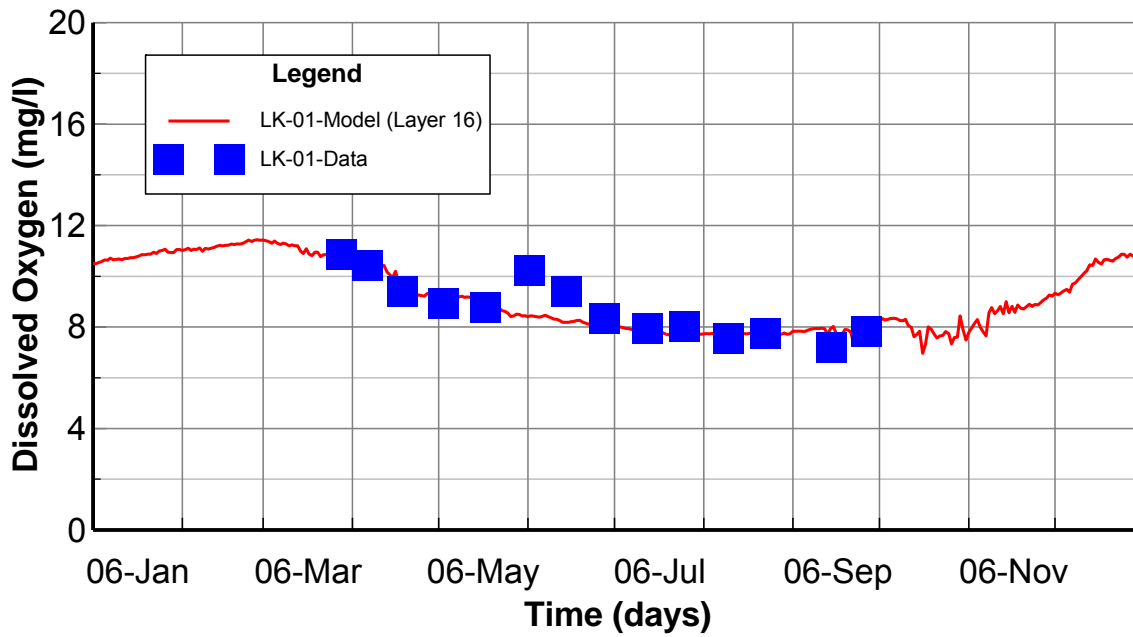


Figure 8-21. Surface Layer DO Calibration Plot at Station LK-01

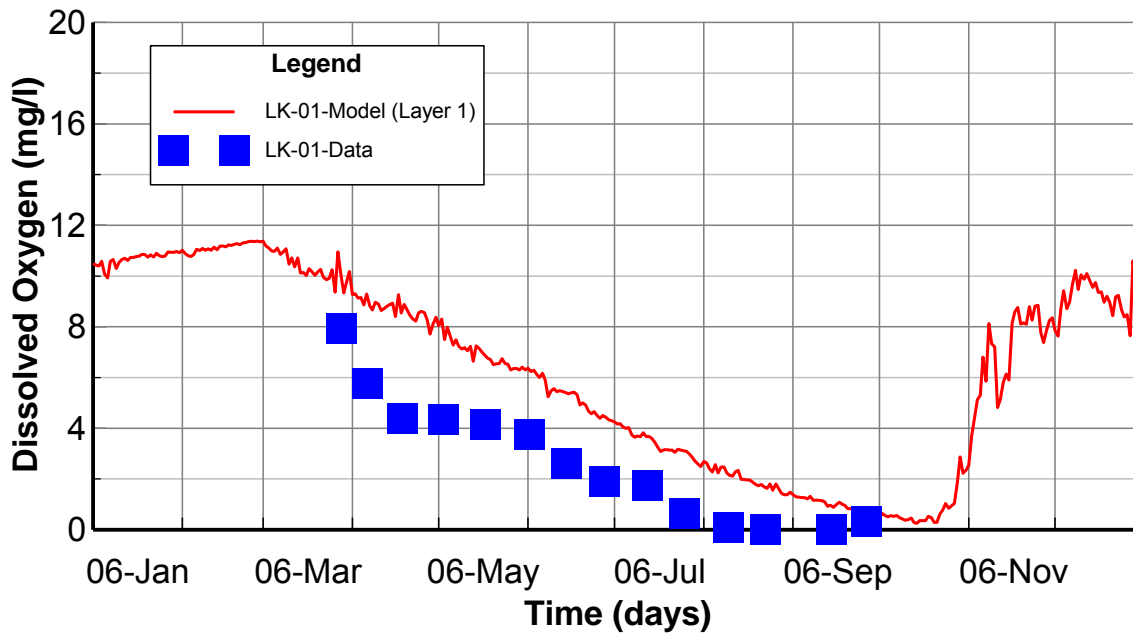


Figure 8-22. Bottom Layer DO Calibration Plot at Station LK-01

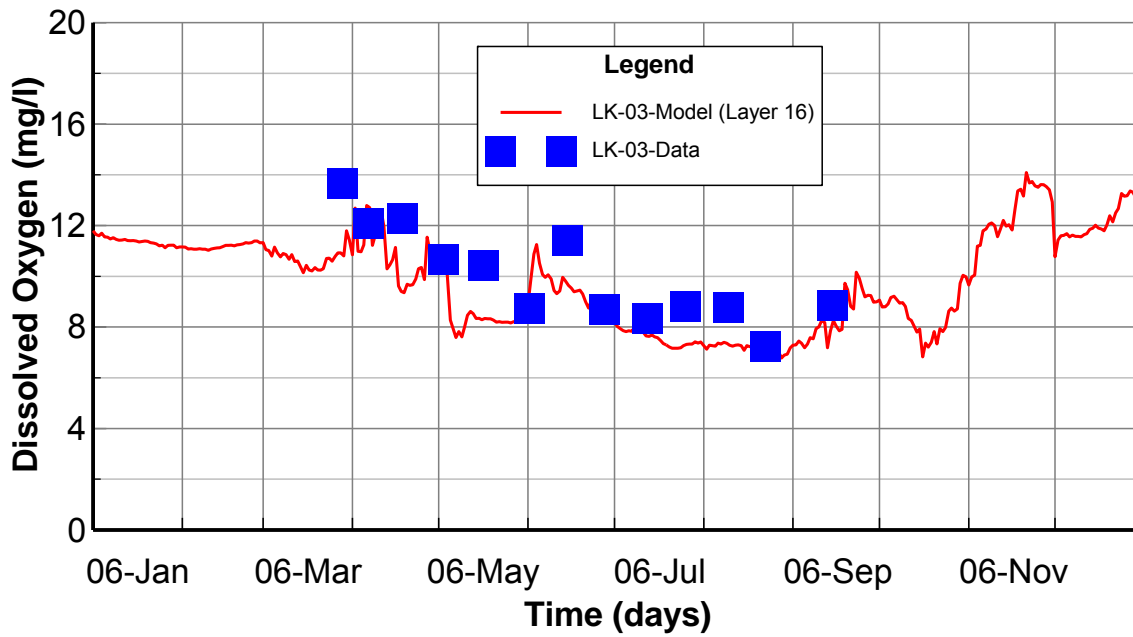


Figure 8-23. Surface Layer DO Calibration Plot at Station LK-03

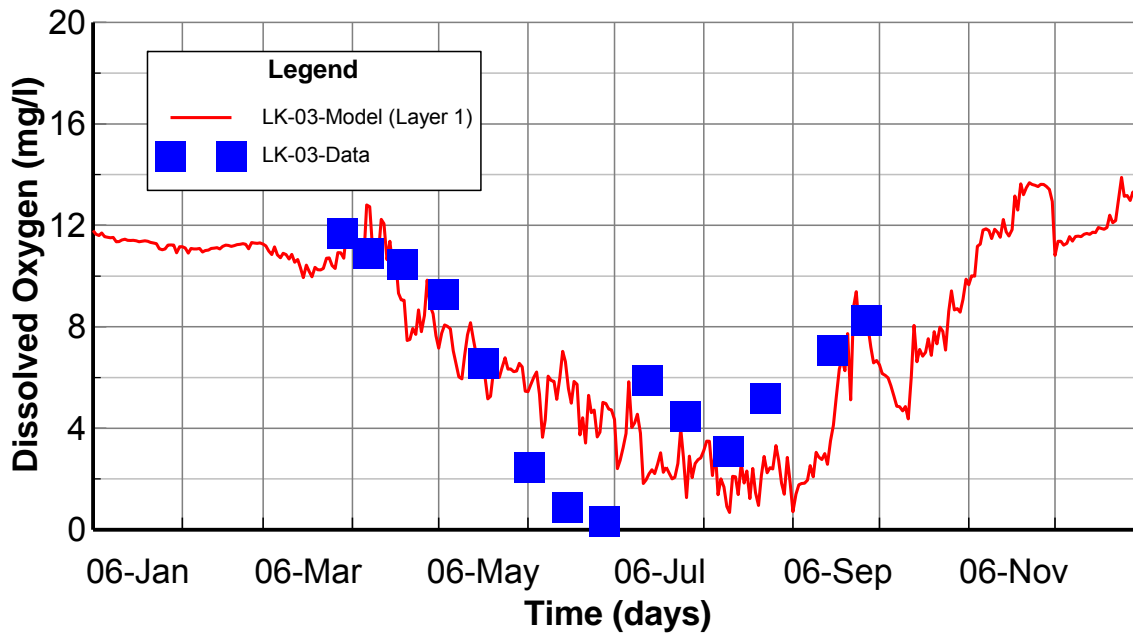


Figure 8-24. Bottom Layer DO Calibration Plot at Station LK-03

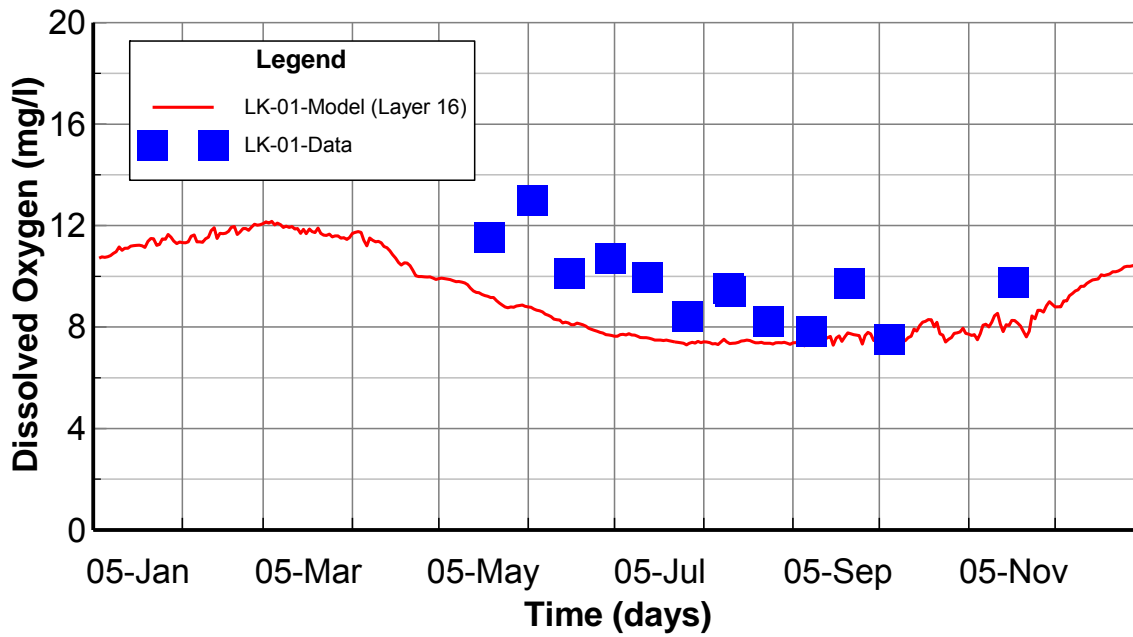


Figure 8-25. Surface Layer DO Validation Plot at Station LK-01

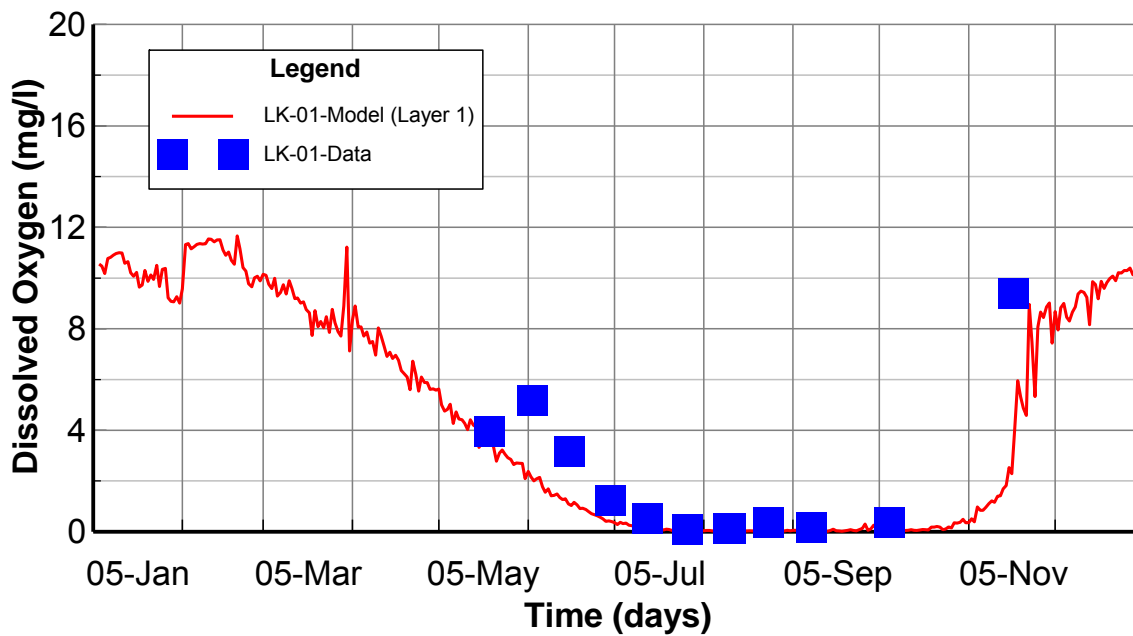


Figure 8-26. Bottom Layer DO Validation Plot at Station LK-01

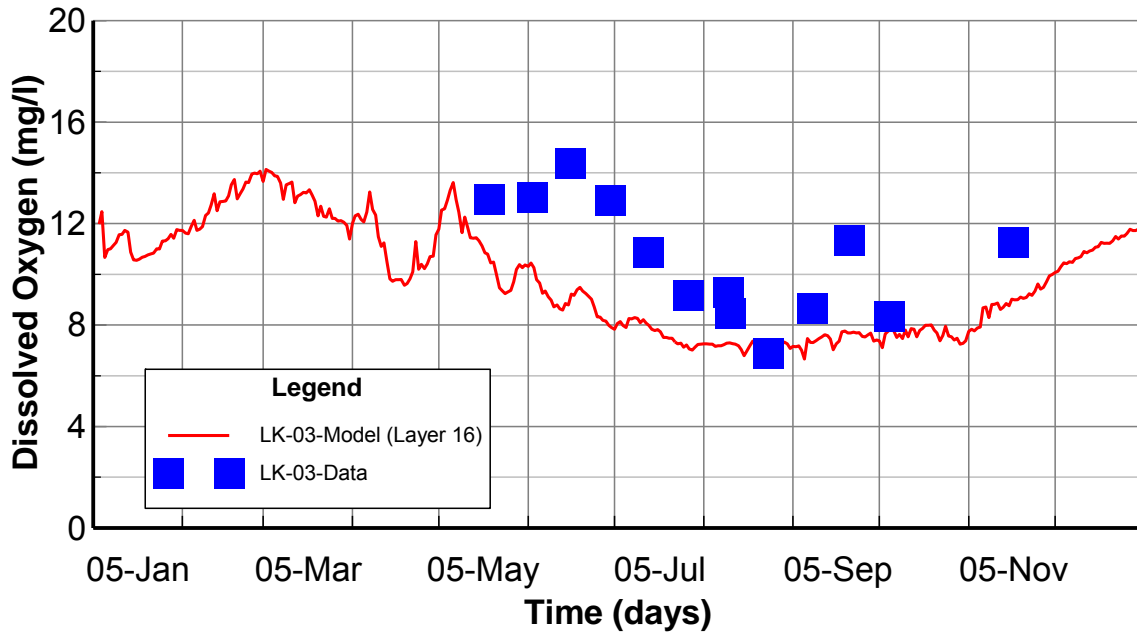


Figure 8-27. Surface Layer DO Validation Plot at Station LK-03

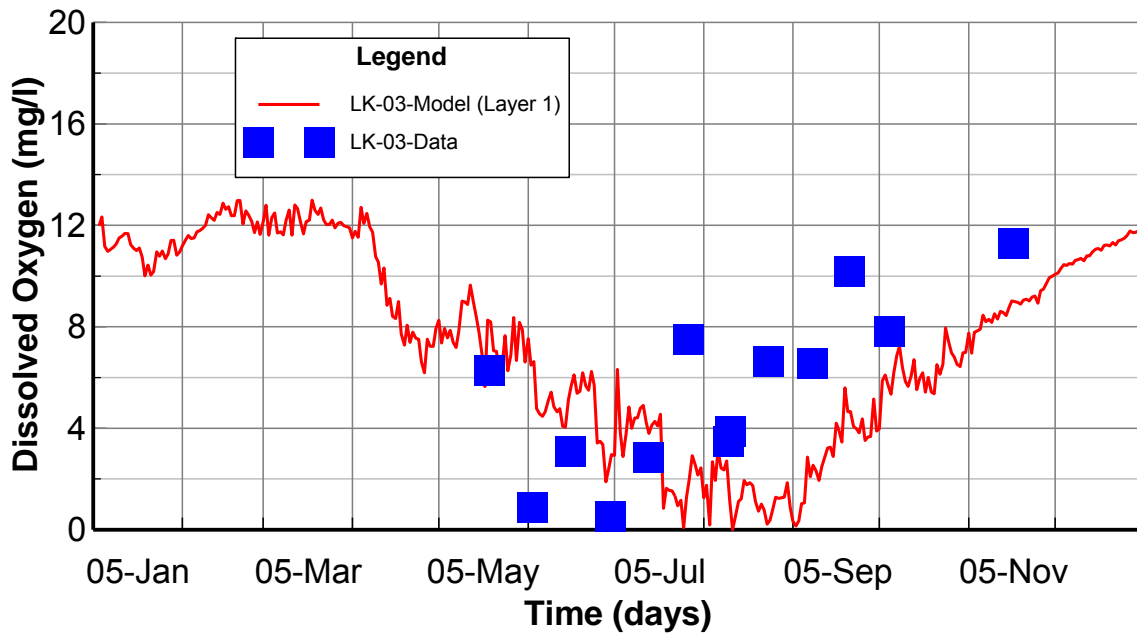


Figure 8-28. Bottom Layer DO Validation Plot at Station LK-03

TenKiller Hydrodynamic and Water Quality Model
Vertical Profiles: LK-01, Model Cell: 21, 12

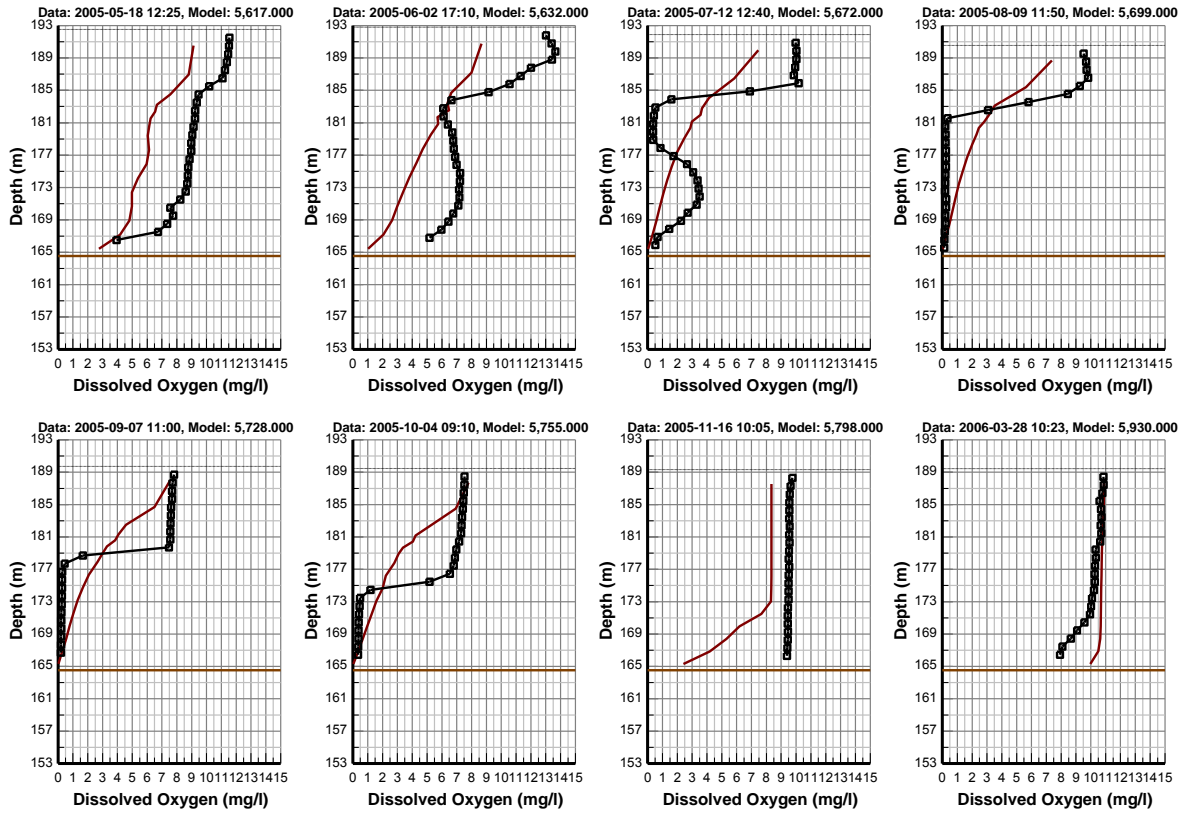


Figure 8-29. Dissolved Oxygen Vertical Profile Comparison Plot at Station LK-01 (18 May 2005 – 28 March 2006) (page 2-1)

TenKiller Hydrodynamic and Water Quality Model
Vertical Profiles: LK-01, Model Cell: 21, 12

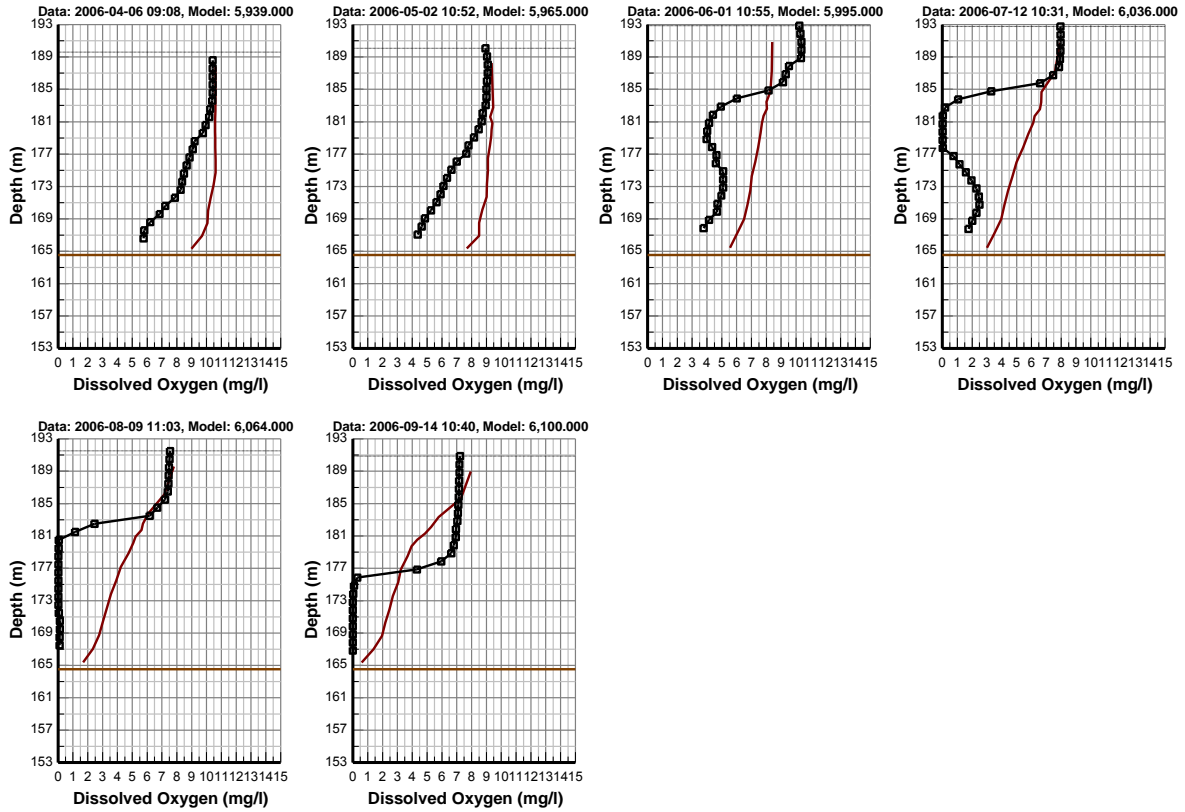


Figure 8-30. Dissolved Oxygen Vertical Profile Comparison Plot at Station LK-01 (6 April 2005 – 14 September 2006) (page 2-2)

TenKiller Hydrodynamic and Water Quality Model
 Vertical Profiles: LK-03, Model Cell: 21, 69

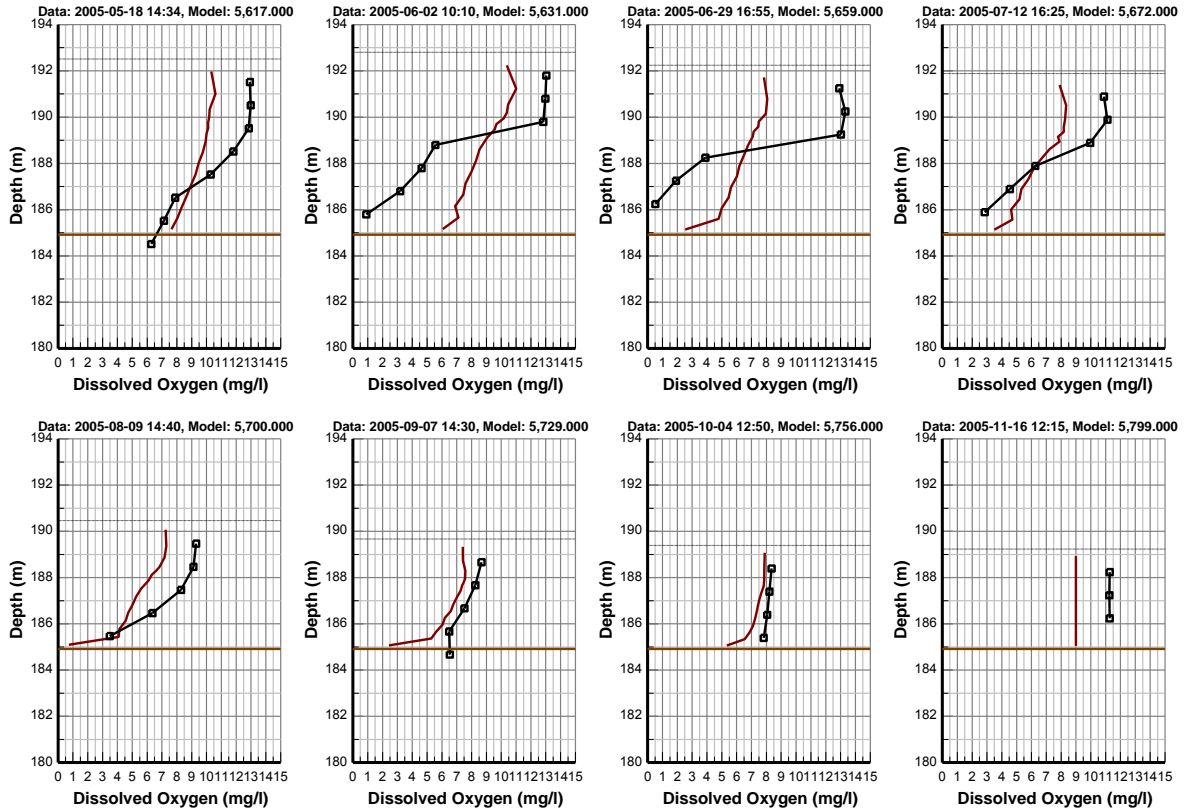


Figure 8-31. Dissolved Oxygen Vertical Profile Comparison Plot at Station LK-03 (18 May 2005 – 16 November 2005) (page 2-1)

TenKiller Hydrodynamic and Water Quality Model
 Vertical Profiles: LK-03, Model Cell: 21, 69

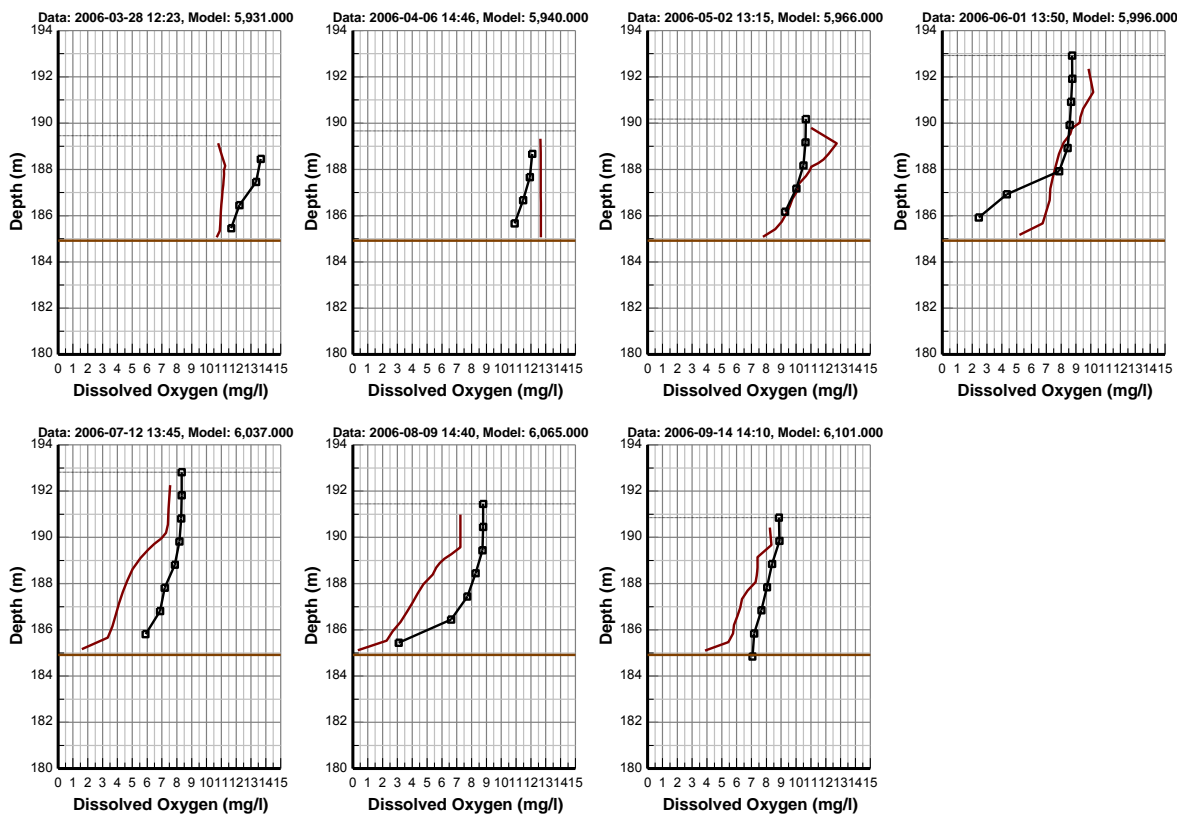


Figure 41. Dissolved Oxygen Vertical Profile Comparison Plot at Station LK-03 (28 March 2006 – 14 September 2006) (page 2-2)

8.5 Algae and Tropic State Index Calibration and Validation

Procedures used to calibrate algae (chlorophyll a) included: 1) check the linkage between HSPF and EFDC to make sure that the setup of algae boundary conditions for the Lake EFDC model is correct; and 2) adjust the key parameters within reasonable ranges to match the observed data. Through the model calibration process, it was found that the important parameters for algae included maximum algae growth rate, phosphorus half saturation for algae, basal metabolism rate, and predation rate of algae. The watershed loading of TPO4 also showed significant impact on the simulation of Algae.

Modeled algae biomass results (as Chlorophyll a) are presented for comparison to the observed data for the surface layer (k=16) and for the bottom layer (k=1). In the Tenkiller Ferry Lake model, cyanobacteria, diatom, and green algae were simulated to derive total algae biomass for comparison to chlorophyll a observations.

Chlorophyll a calibration and validation plots at LK-01 and LK-03 are given in Figures 8-32 through 8-39. The model performance statistics of chlorophyll a are given in Table 8-4. As can be seen in these model-data plots, the model results are in good agreement with measured biomass for the calibration period. In particular, The EFDC simulated chlorophyll a concentrations follow the seasonal trend of the observed chlorophyll a at Stations LK-03 and

LK-04. The complete calibration and validation time series plots for all monitoring stations are given in APPENDIX J and APPENDIX K.

The calculated RMS errors ranged from 4.24 µg/L at the surface layer of station LK-01 to 33.51 µg/L at the surface layer of station LK-04 as shown in Table 8-4. The calculated relative RMS errors ranged from 25.2% at the surface layer of station LK-04 to 67.0% at the bottom layer of station LK-04. Overall, the composite model performance for the relative RMS error for chlorophyll for the 4 stations is 28% (n=136 data pairs). Since the model results are well within the defined model performance target of ±100% for algae, the model results for algae are deemed to be acceptable.

Tenkiller Ferry Lake is classified as a Nutrient Limited Watershed (NLW) based on Carlson's (1977) Trophic State Index (TSI) because the chlorophyll-based TSI exceeds a numerical value of 62. Carlson's equation for the chlorophyll-based TSI is given below for Chlorophyll-a as µg/L. Using this equation a chlorophyll-based TSI value of 62 is seen to correspond to 24 µg/L chlorophyll-a.

$$TSI=9.81*\ln(Chl)+3.06$$

Model calibration results for chlorophyll are processed to compute Carlson's TSI based on chlorophyll (Figure 8-39). As can be seen in the model-data comparison for TSI at LK-03, the simulated TSI index is in good agreement with the observed TSI index as expected since the calculated TSI is based on the simulated chlorophyll using the above equation. It should be noted that the TSI target for chlorophyll is not used to assess the impact of watershed load reductions.

Table 8-4. Summary Statistics of Chlorophyll a (µg/l)

Station ID	Layer	Starting	Ending	# Pairs	RMS (ug/l)	Rel RMS (%)	Data Average (ug/l)	Model Average (ug/l)
LK-01	Layer 16	5/18/2005 12:05	9/26/2006 12:00	27	4.24	28.5	5.733	4.266
LK-02	Layer 16	5/18/2005 9:01	9/26/2006 8:00	26	9.267	56.9	7.881	11.728
LK-03	Layer 1	5/17/2005 15:22	9/14/2006 14:30	17	15.842	44.127	14.626	16.249
LK-03	Layer 16	5/17/2005 14:05	9/26/2006 14:40	25	15.212	37.194	14.593	20.749
LK-04	Layer 1	7/26/2005 16:40	9/26/2006 16:00	21	17.886	67.0	11.655	20.744
LK-04	Layer 16	7/26/2005 16:40	9/26/2006 16:00	22	33.51	25.2	25.418	15.463

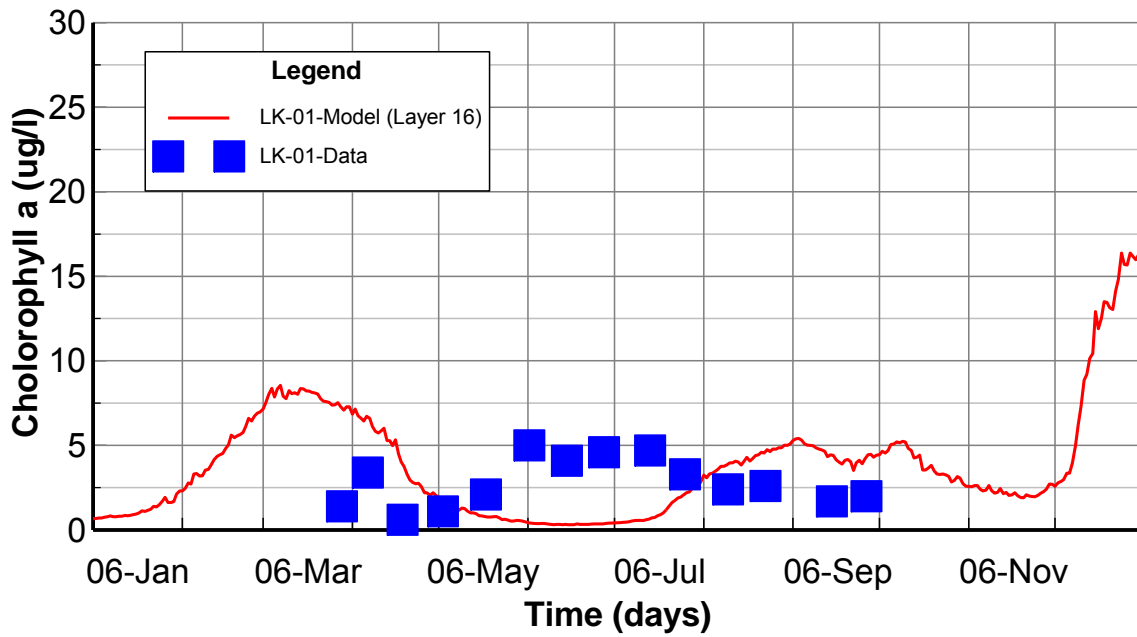


Figure 8-32. Surface Layer Chlorophyll a Calibration Plot at Station LK-01

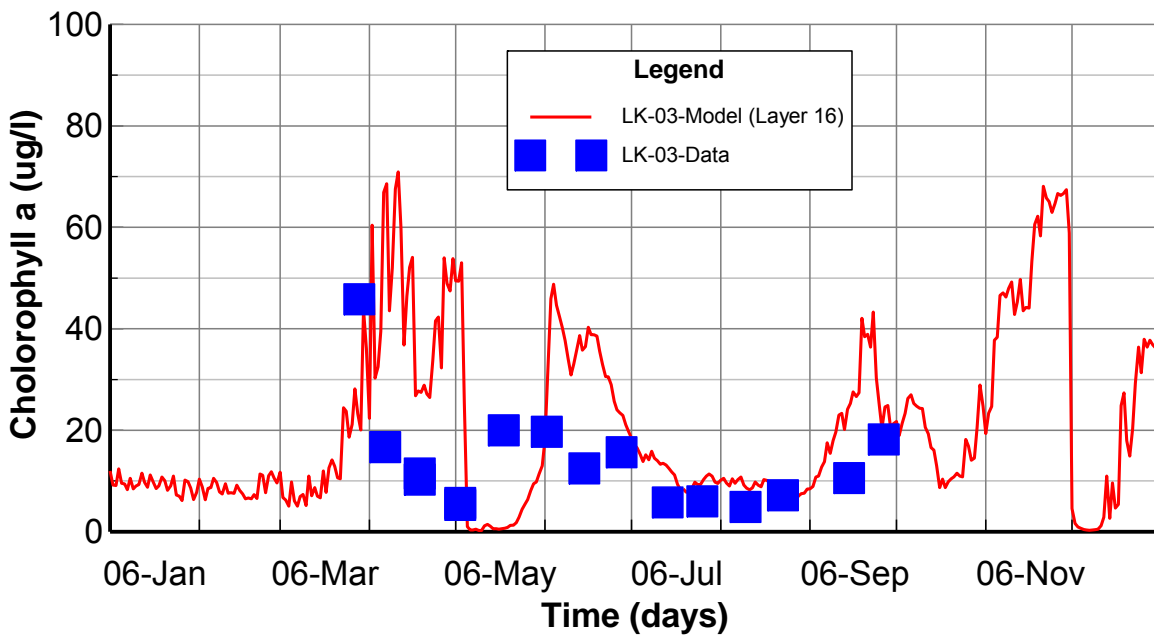


Figure 8-33. Surface Layer Chlorophyll a Calibration Plot at Station LK-03

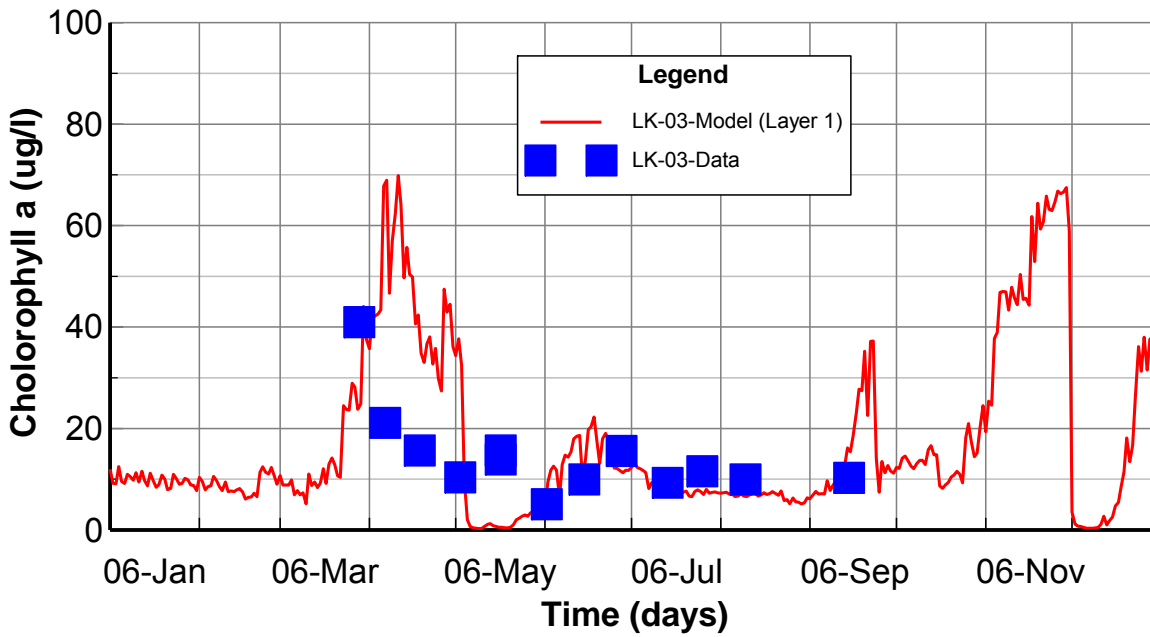


Figure 8-34. Bottom Layer Chlorophyll a Calibration Plot at Station LK-03

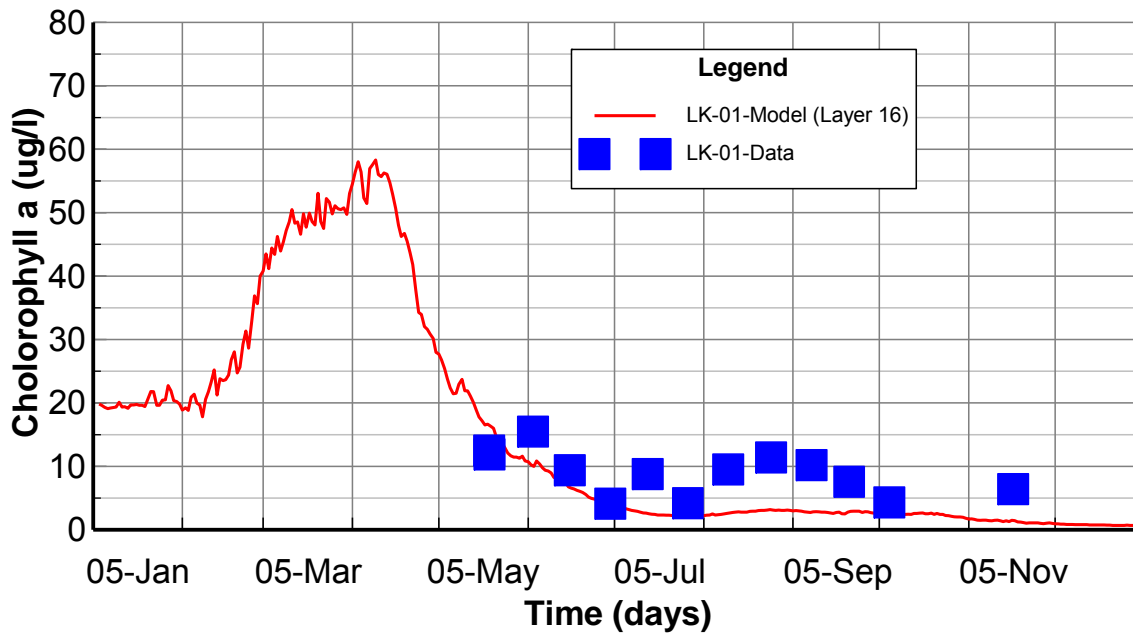


Figure 8-35. Surface Layer Chlorophyll a Validation Plot at Station LK-01

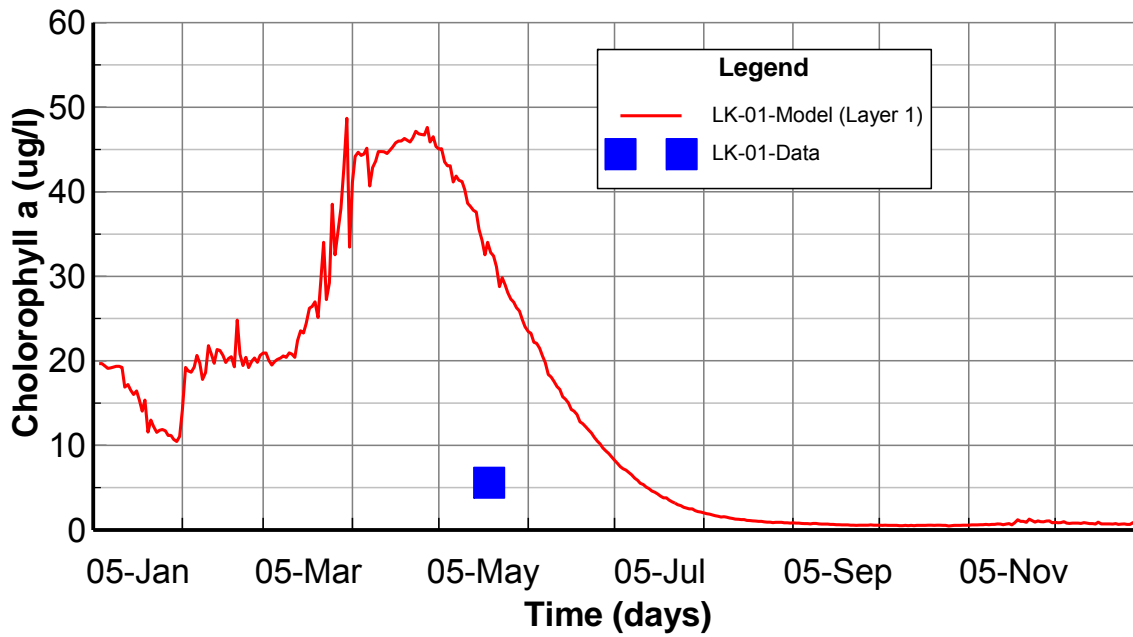


Figure 8-36. Bottom Layer Chlorophyll a Validation Plot at Station LK-01

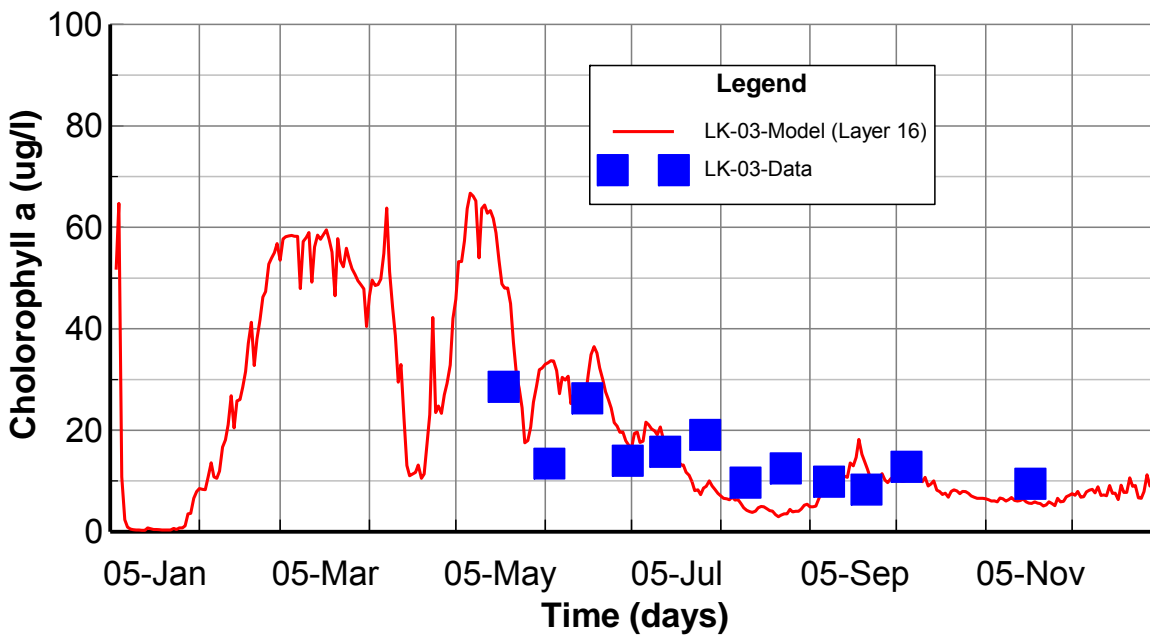


Figure 8-37. Surface Layer Chlorophyll a Validation Plot at Station LK-03

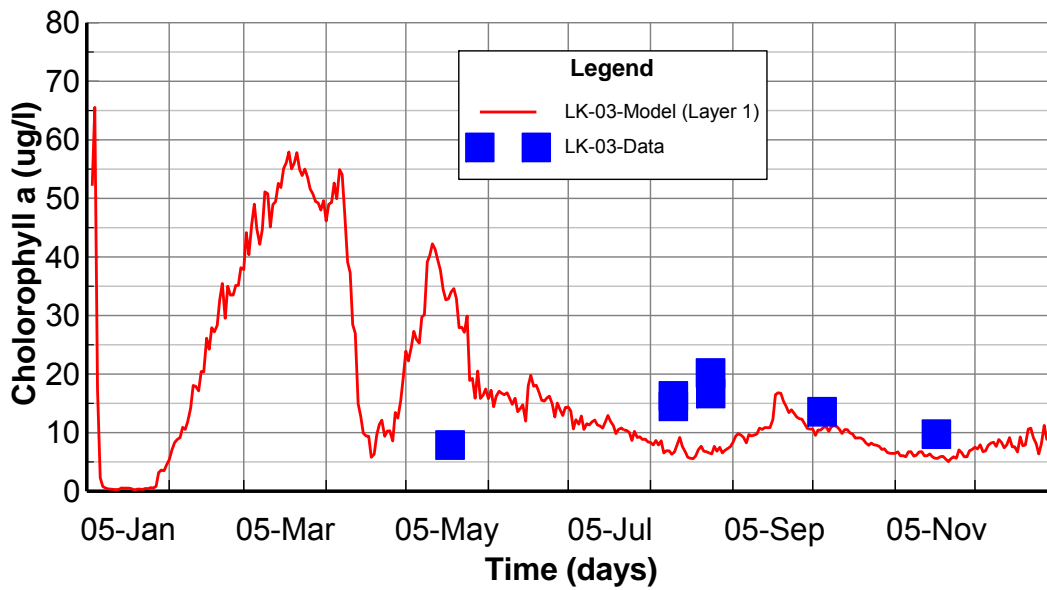


Figure 8-38. Bottom Layer Chlorophyll a Validation Plot at Station LK-03

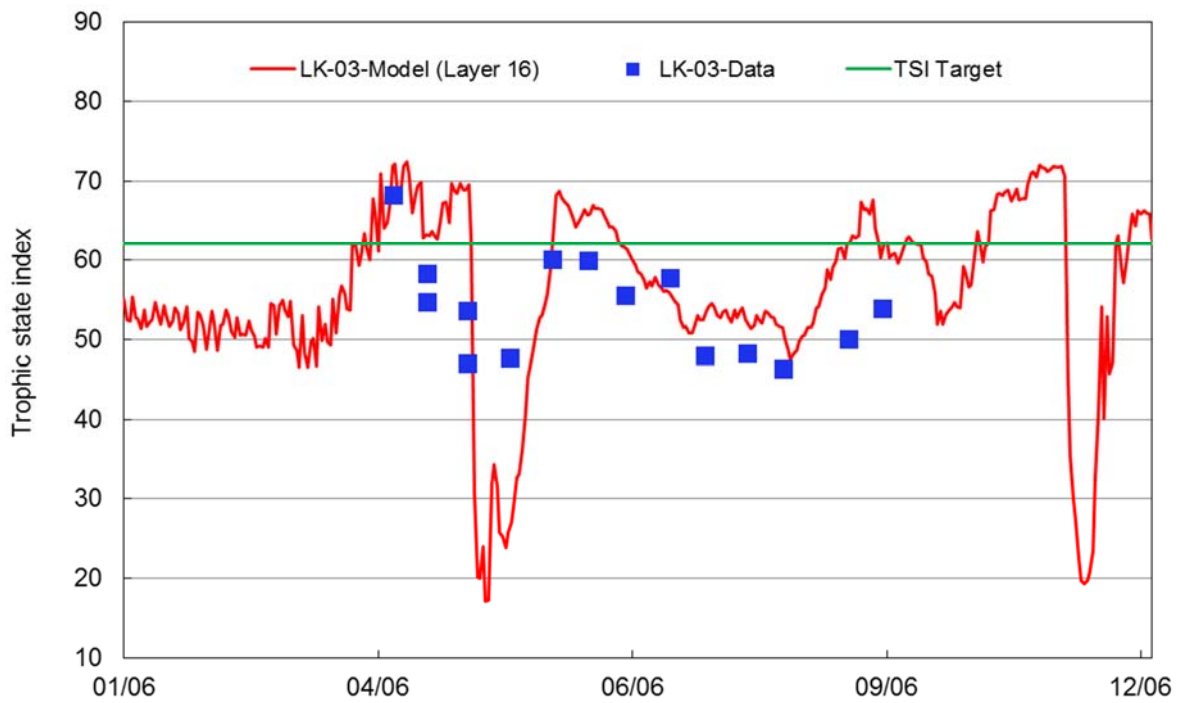


Figure 8-39. Comparison of Carlson's TSI for Chlorophyll-a and Oklahoma Water Quality Criteria at LK-03 for a Nutrient Limited Watershed

8.6 Organic Carbon Calibration and Validation

Procedures used to calibrate total organic carbon included: 1) check the linkage between HSPF and EFDC to make sure that the setup of TOC boundary conditions for the Lake EFDC model is correct; and 2) adjust the key parameters within reasonable ranges to match the observed data. Total organic carbon is strongly connected with the algae growth cycle; hence, algae-related parameters have a strong impact on the TOC model results. The settling velocity of refractory and labile organic matter also showed an impact on the distribution of TOC between the water column and the sediment bed.

Total organic carbon (TOC) model results are presented for comparison to the observed data for the surface layer (k=16) and bottom layer (k=1).

Total organic carbon calibration plots at LK-01 and LK-03 are given in Figures 8-40 through 8-43. Total organic carbon validation plots at LK-01 and LK-03 are given in Figures 8-44 through 8-47. The summary statistics of TOC are given in Table 8-5. As can be seen in these model-data plots, the model results are in fairly good agreement with the measured data for both calibration and validation periods.

The calculated RMS errors ranged from 0.742 mg/L at the bottom layer of station LK-03 to 1.154 mg/L at the bottom layer of station LK-04 as shown in Table 8-5. The calculated relative RMS errors ranged from 21.7% at the surface layer of station LK-02 to 100.0% at the bottom layer of station LK-01 (Table 8-5). The complete calibration and validation time series plots for all monitoring stations are given in APPENDIX J and APPENDIX K.

There is no defined model performance target for total organic carbon. Overall, the composite model performance for the relative RMS error for total organic carbon for the 4 stations is 51% (n=160 data pairs). Since the simulated total organic carbon followed the trend of the observed data reasonably well and the calculated relative RMS errors are within, or close, to $\pm 50\%$ in most of the cases, the model results of total organic carbon are deemed to be acceptable.

Table 8-5. Summary Statistics of TOC (mg/l)

Station ID	Layer	Starting	Ending	# Pairs	RMS (mg/l)	Rel RMS (%)	Data Average (mg/l)	Model Average (mg/l)
LK-01	Layer 1	5/18/2005 12:58	9/26/2006 12:00	15	1.04	100.0	1.813	0.978
LK-01	Layer 16	5/18/2005 12:05	9/26/2006 12:00	25	1.117	74.9	2.3	1.412
LK-02	Layer 1	5/18/2005 10:19	9/26/2006 8:00	15	0.848	68.4	1.92	1.185
LK-02	Layer 16	5/18/2005 9:01	9/26/2006 8:00	24	0.791	21.7	2.497	2.122
LK-03	Layer 1	5/17/2005 15:22	8/9/2006 14:50	13	0.742	63.4	2.182	2.423
LK-03	Layer 16	5/17/2005 14:05	9/26/2006 14:40	34	0.905	29.9	2.556	2.877
LK-04	Layer 1	3/28/2006 13:40	9/26/2006 16:00	14	1.154	40.4	1.969	2.815
LK-04	Layer 16	7/26/2005 16:40	9/26/2006 16:00	20	0.68	44.1	2.042	2.377

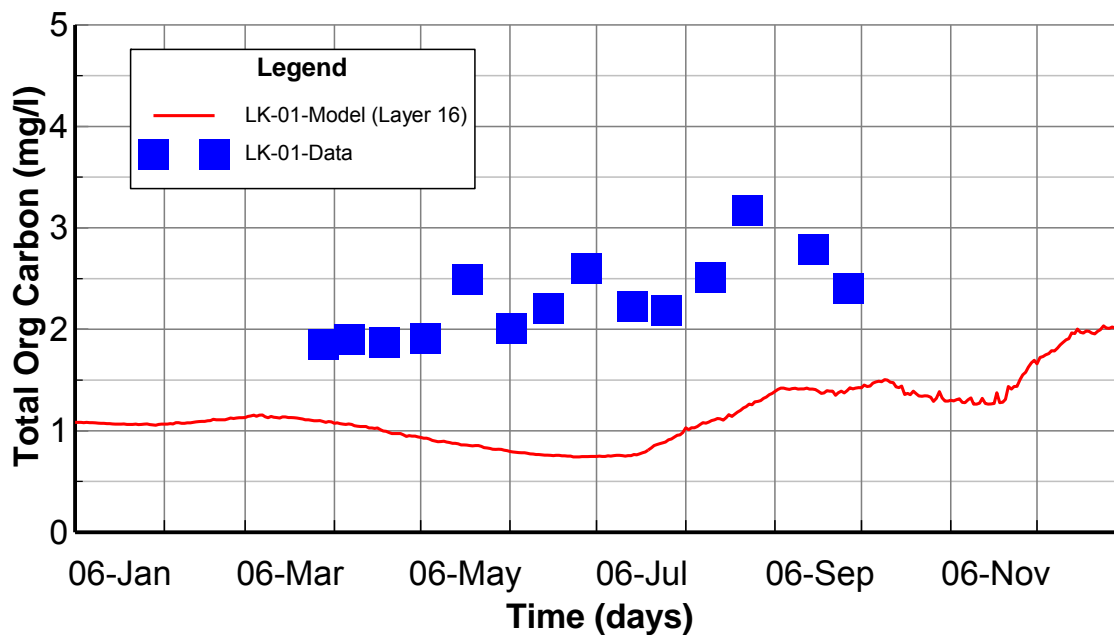


Figure 8-40. Surface Layer TOC Calibration Plots at Station LK-01

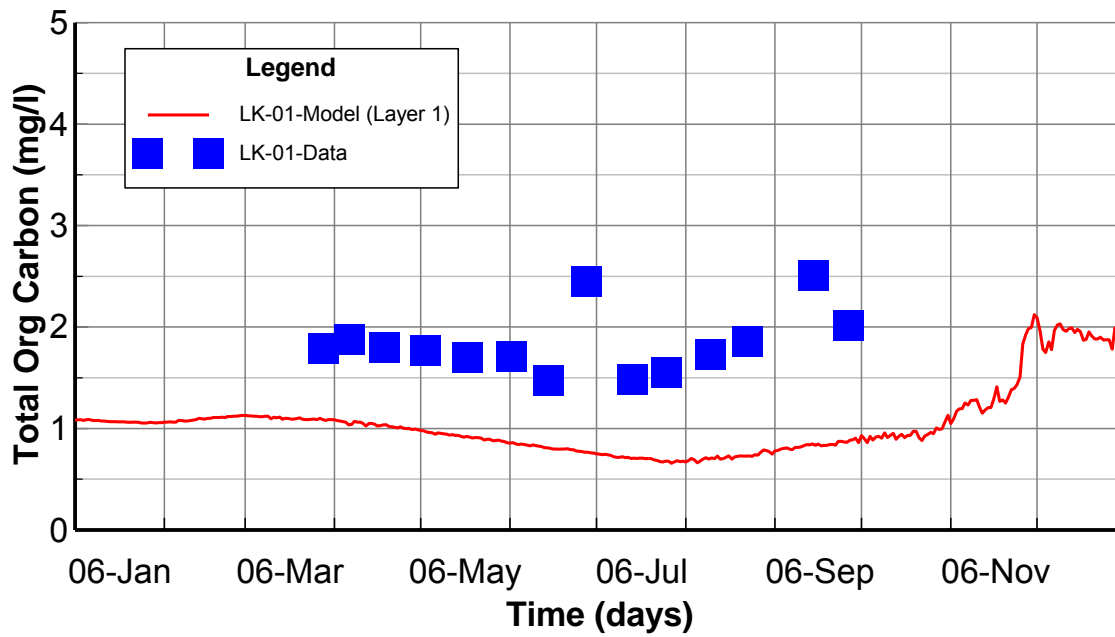


Figure 8-41. Bottom Layer TOC Calibration Plots at Station LK-01

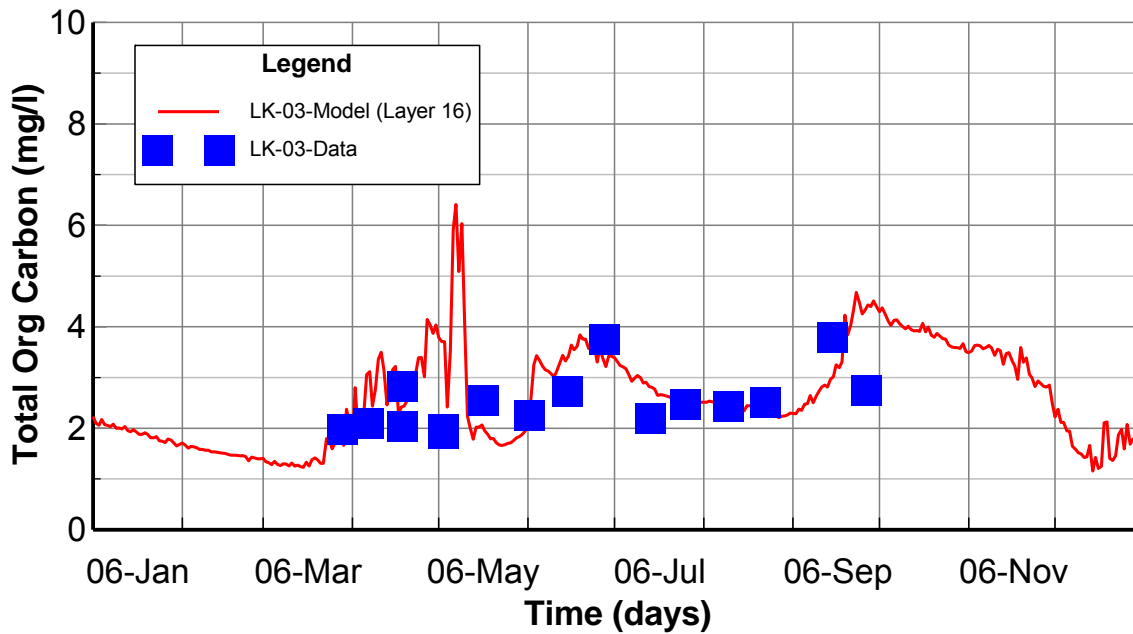


Figure 8-42. Surface Layer TOC Calibration Plots at Station LK-03

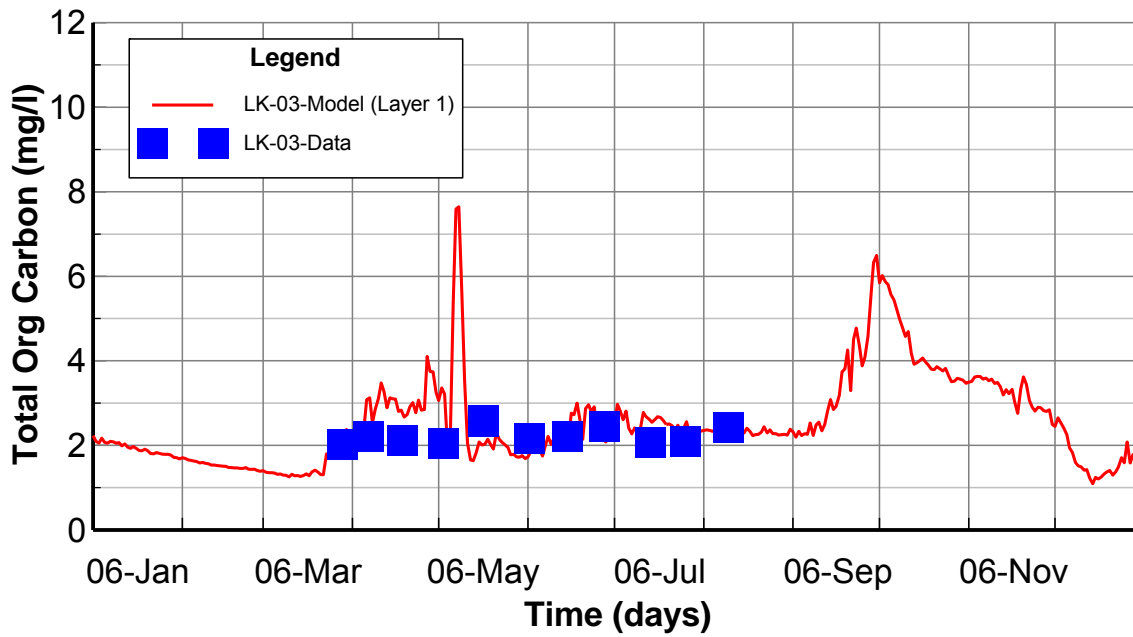


Figure 8-43. Bottom Layer TOC Calibration Plots at Station LK-03

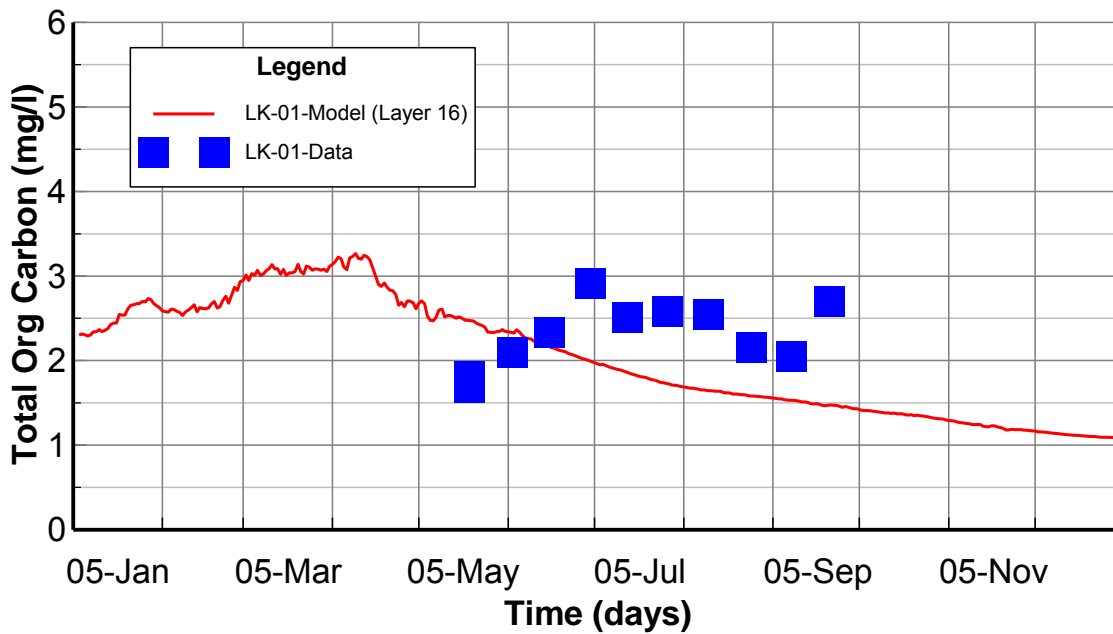


Figure 8-44. Surface Layer TOC Validation Plots at Station LK-01

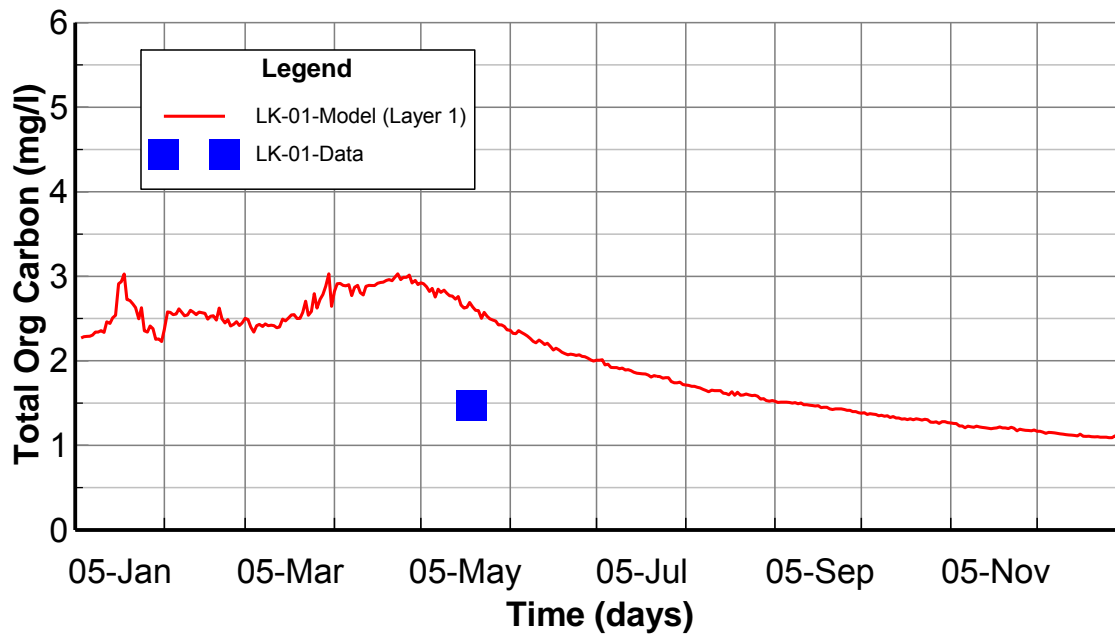


Figure 8-45. Bottom Layer TOC Validation Plots at Station LK-01

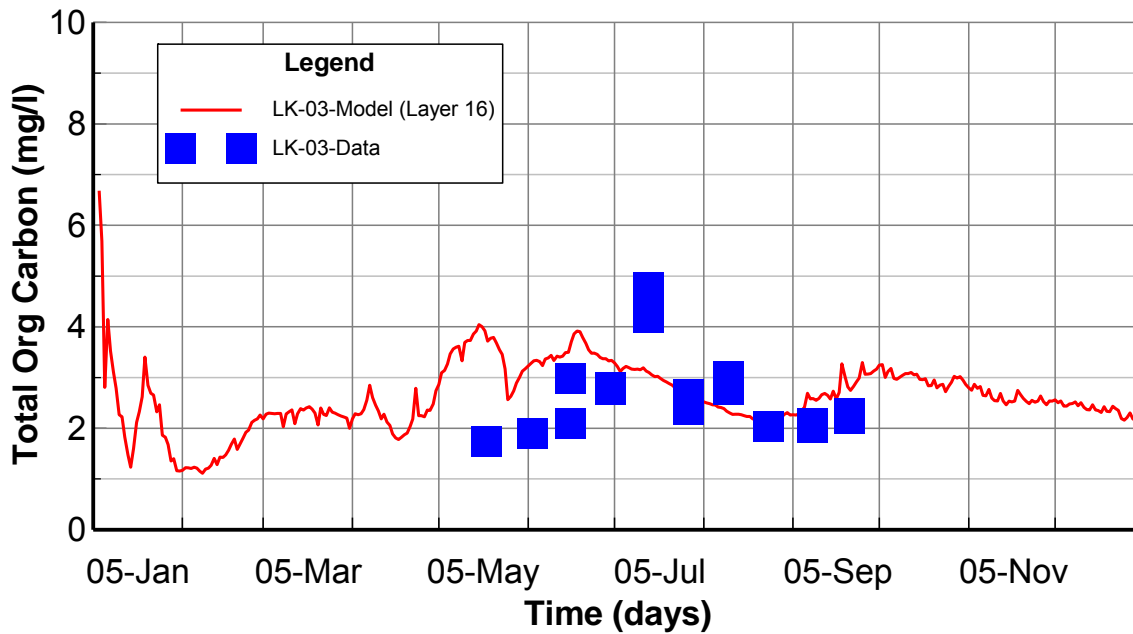


Figure 8-46. Surface Layer TOC Validation Plots at Station LK-03

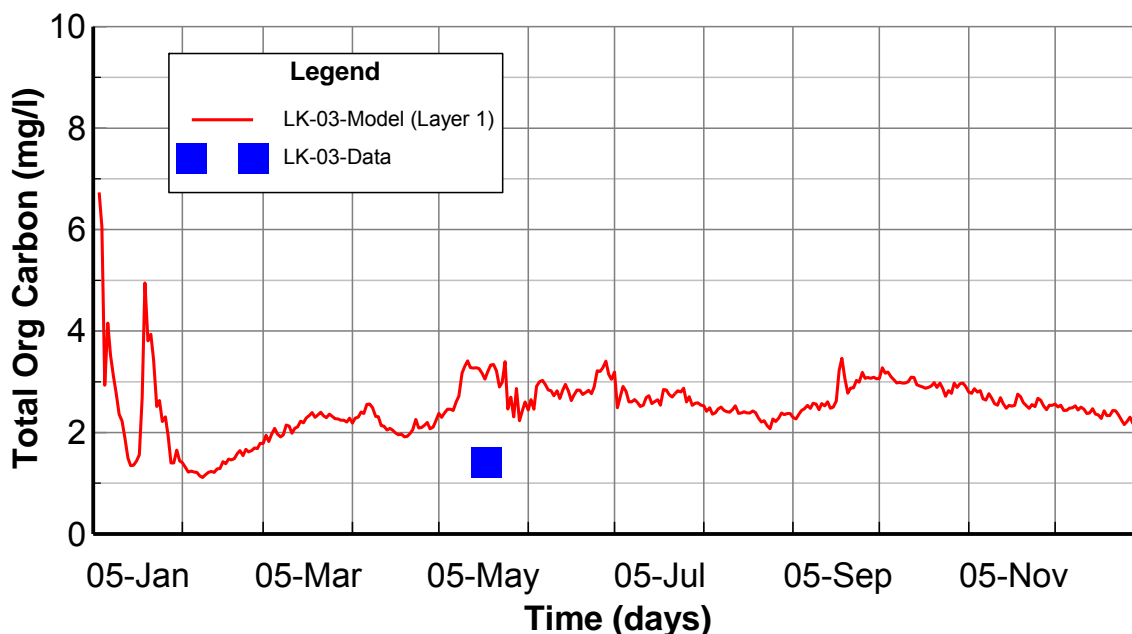


Figure 8-47. Bottom Layer TOC Validation Plots at Station LK-03

8.7 Nitrogen Calibration and Validation

Procedures used to calibrate nitrogen species included: 1) check the linkage between HSPF and EFDC to make sure that the setup of nitrogen boundary conditions for the Lake EFDC model is correct; and 2) adjust the key parameters within reasonable ranges to match the observed data.

Ammonia-N (NH_4), nitrite+nitrate-N (NO_3), and total Kjeldahl nitrogen (TKN) model results are presented for comparison to the observed data for the surface layer ($k=16$) and bottom layer ($k=1$). The ammonium calibration and validation plots at LK-01 and LK-03 are given in Figures 8-48 through 8-51. The TKN calibration and validation plots at Site 1 and Site 3 are given in Figures 8-52 through 8-55. The nitrate calibration and validation plots at LK-01 and LK-03 are given in Figures 8-56 through 8-63. The complete calibration and validation time series plots for all monitoring stations are given in APPENDIX J and APPENDIX K.

The majority of observed ammonia data were labeled as less than 0.1 mg/L, as shown in the calibration and validation plots. Considering the facts that the sample size of observed ammonia is too small ($N=3$ or 4 over 2005-2006) and the exact values of observed ammonia are below detection limit, the statistics for model performance are not provided. In most of the cases, the simulated ammonia data were less than or very close to the detection limit of 0.1 mg/L.

There are only two or three observed TKN data points from OWRB during 2005 to 2006; hence, the statistics are not provided. Generally, the EFDC simulated TKN values are seen to be close to the OWRB observed data.

Generally, the EFDC simulated NO₃ are consistently higher than the observed NO₃ data. Even though many calibration parameters have been tested, the NO₃ modeling performance was not improved. One likely reason for the model-data discrepancy might be the usually high NO₃ inputs from the HSPF-derived upstream boundaries for the Illinois River and Baron Fork Creek (Figures 8-64 and 8-65). In most of the cases, the NO₃ boundary inputs from the Illinois River are higher than 1.0 mg/L (Figures 8-64 and 8-65); however, the majority of the observed NO₃ data are lower than 1.0 mg/L. As shown in the plots for the Illinois River, the HSPF-derived upstream boundary data for NO₃ is greater than the observed NO₃ data for these rivers.

The calculated RMS errors of NO₃ ranged from 0.5 mg/L at the bottom layer of station LK-01 to 1.709 mg/L at the surface layer of station LK-04 in Table 8-6. The calculated relative RMS errors of NO₃ ranged from 38.1% at the bottom layer of station LK-01 to 121.7% at the surface layer of station LK-02 as shown in Table 8-6.

Due to observed data limitations, it is meaningless to calculate the model performance statistics for NH₄ and TKN. Hence, visual inspection is used as the major approach to evaluate the model performance for NH₄ and TKN. The majority of observed ammonia data were labeled as less than 0.1 mg/L. In most of the cases, the simulated ammonia data were less than or very close to 0.1 mg/L. Generally, the EFDC simulated TKN values are close to the OWRB observed data. Therefore, the model results of NH₄ and TKN are deemed to be acceptable.

In most of the cases, the calculated relative RMS statistics for NO₃ are less than 100%. All NO₃-related parameters were tested and calibrated, but significant improvement in model results was not obtained. The EFDC model results for NO₃ are significantly impacted by the watershed loadings simulated by HSPF. It was found that the HSPF simulated NO₃ results in the Illinois River, particularly in the calibration year of 2006, are higher than the observed NO₃ at the nearest USGS station at Tahlequah (less than 10 miles upstream) (Figure 8-64 and Figure 8-65). For the EFDC lake model, the elevated loading of HSPF-simulated NO₃ at the upstream boundary will simulate an accumulation of NO₃ over time. It is anticipated that the EFDC model performance for NO₃ would be improved if the watershed simulation of NO₃ was reduced to more closely reflect observed values. Considering the fact that Tenkiller Ferry Lake is a phosphorus-limited eutrophication lake and the calculated relative RMS for NO₃ are less than 100% in most of the cases, the model results of NO₃ are deemed to be acceptable.

Table 8-6. Summary Statistics of NO₃ (mg/l)

Station ID	Layer	Starting	Ending	# Pairs	RMS (mg/l)	Rel RMS (%)	Data Average (mg/l)	Model Average (mg/l)
LK-01	Layer 1	5/18/2005 12:58	9/26/2006 12:00	24	0.5	38.1	0.616	1.026
LK-01	Layer 16	5/18/2005 12:05	9/26/2006 12:00	25	1.071	88.8	0.286	1.314
LK-02	Layer 1	5/18/2005 10:19	9/26/2006 8:00	25	0.899	69.4	0.38	1.214
LK-02	Layer 16	5/18/2005 9:01	9/26/2006 8:00	24	1.24	121.7	0.203	1.414

Station ID	Layer	Starting	Ending	# Pairs	RMS (mg/l)	Rel RMS (%)	Data Average (mg/l)	Model Average (mg/l)
LK-03	Layer 1	5/17/2005 15:22	8/9/2006 14:50	22	1.084	52.5	0.362	1.221
LK-03	Layer 16	5/17/2005 14:05	9/14/2006 14:30	33	1.191	116.8	0.176	1.285
LK-04	Layer 1	7/26/2005 16:40	9/14/2006 15:40	18	1.037	78.5	0.347	1.153
LK-04	Layer 16	7/26/2005 16:40	9/14/2006 15:40	19	1.709	134.6	0.312	1.829

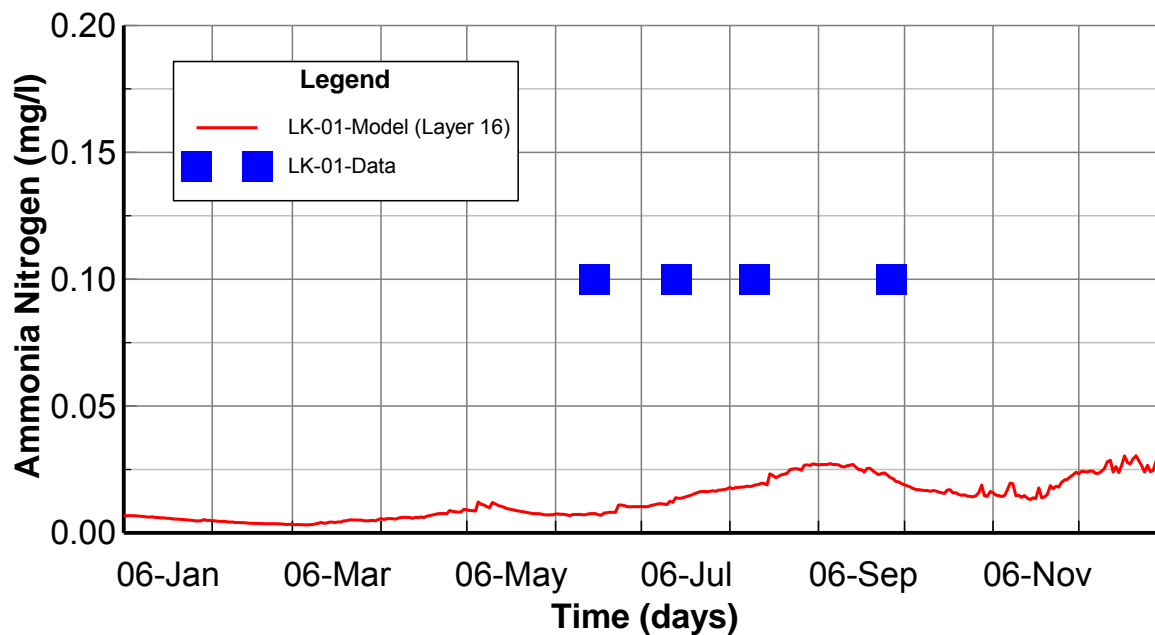


Figure 8-48. Surface Layer NH4 Calibration Plots at Station LK-01

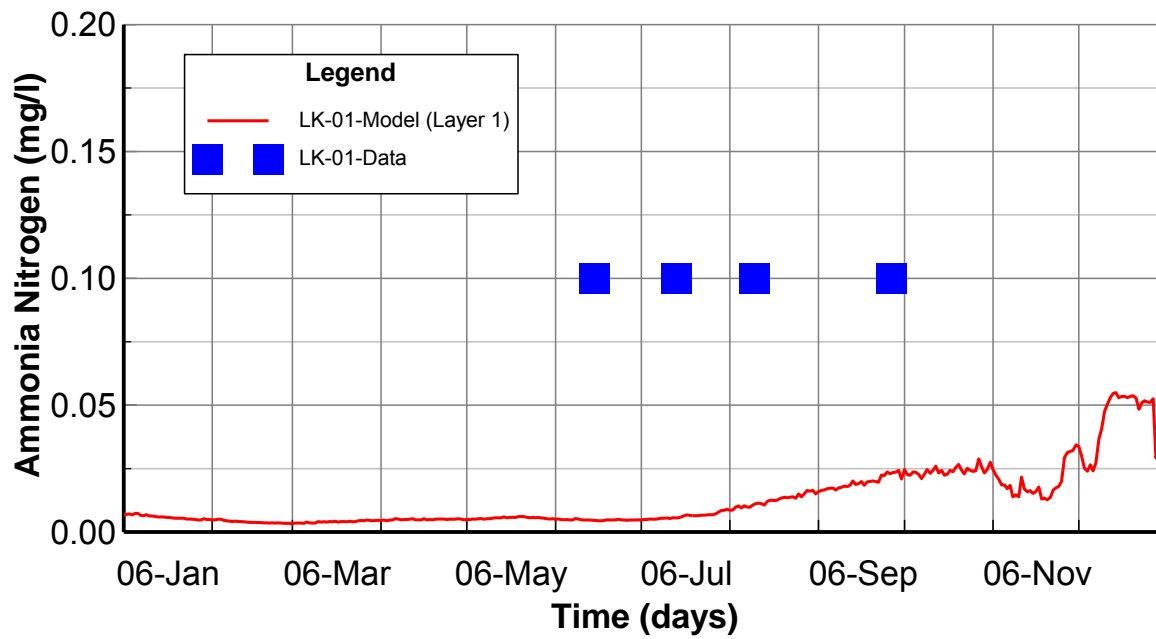


Figure 8-49. Bottom Layer NH4 Calibration Plots at Station LK-01

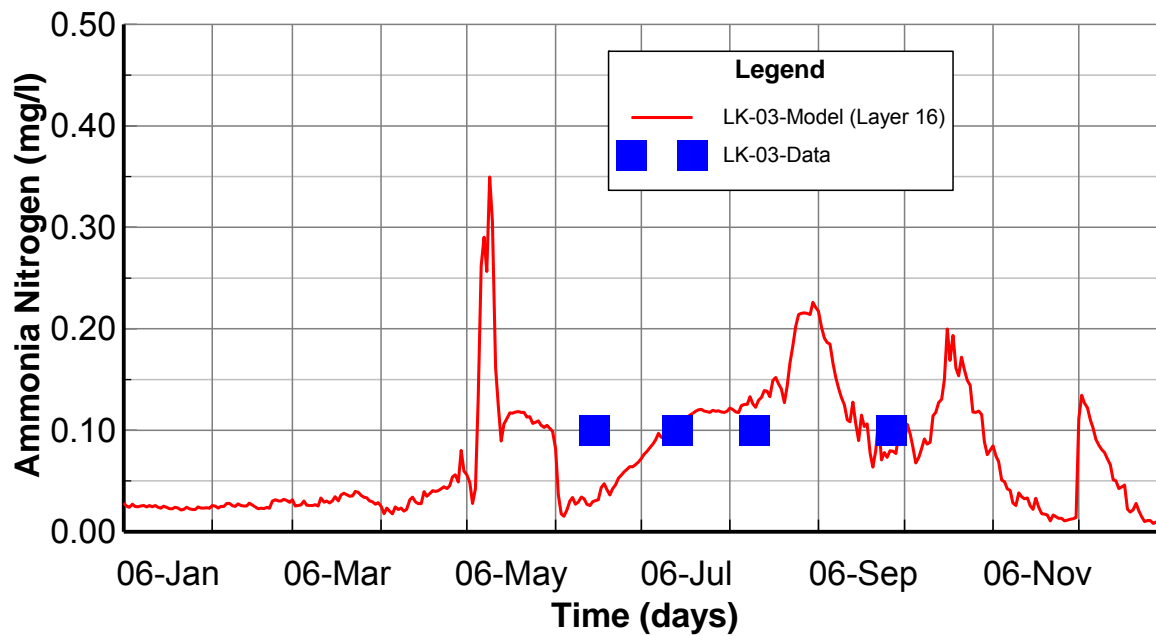


Figure 8-50. Surface Layer NH4 Calibration Plots at Station LK-03

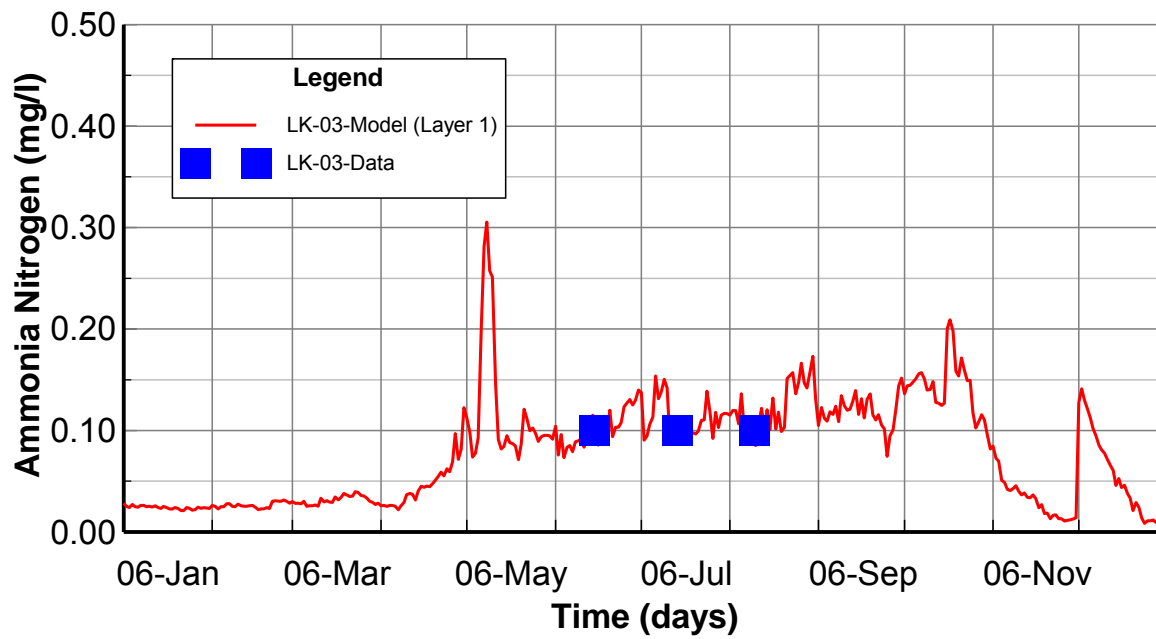


Figure 8-51. Bottom Layer NH4 Calibration Plots at Station LK-03

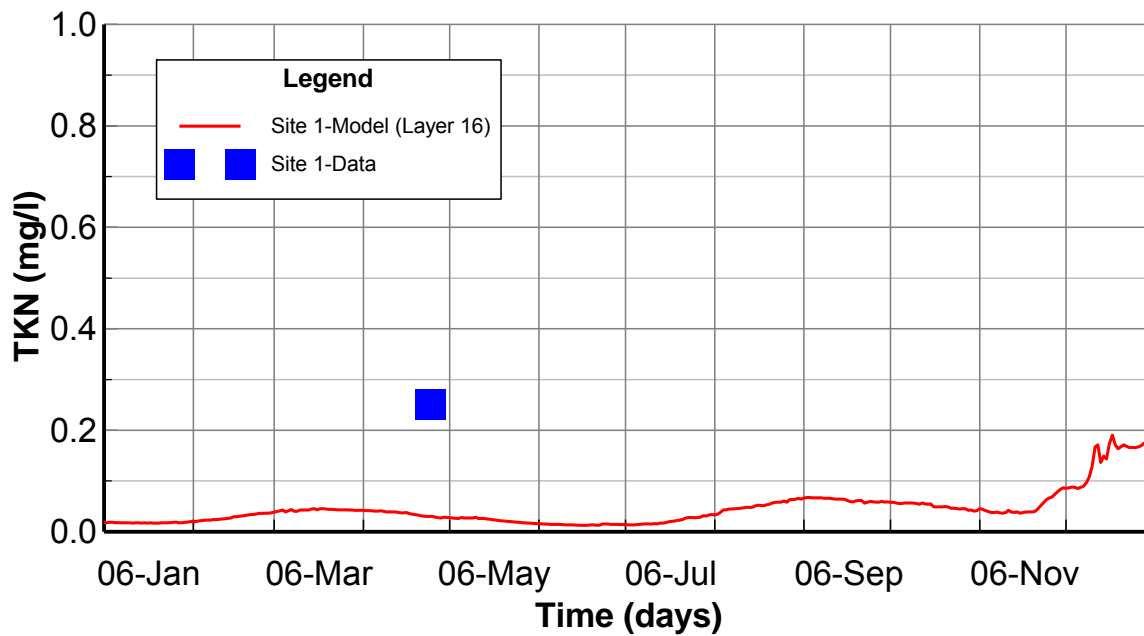


Figure 8-52. Surface Layer TKN Calibration Plots at Station Site1

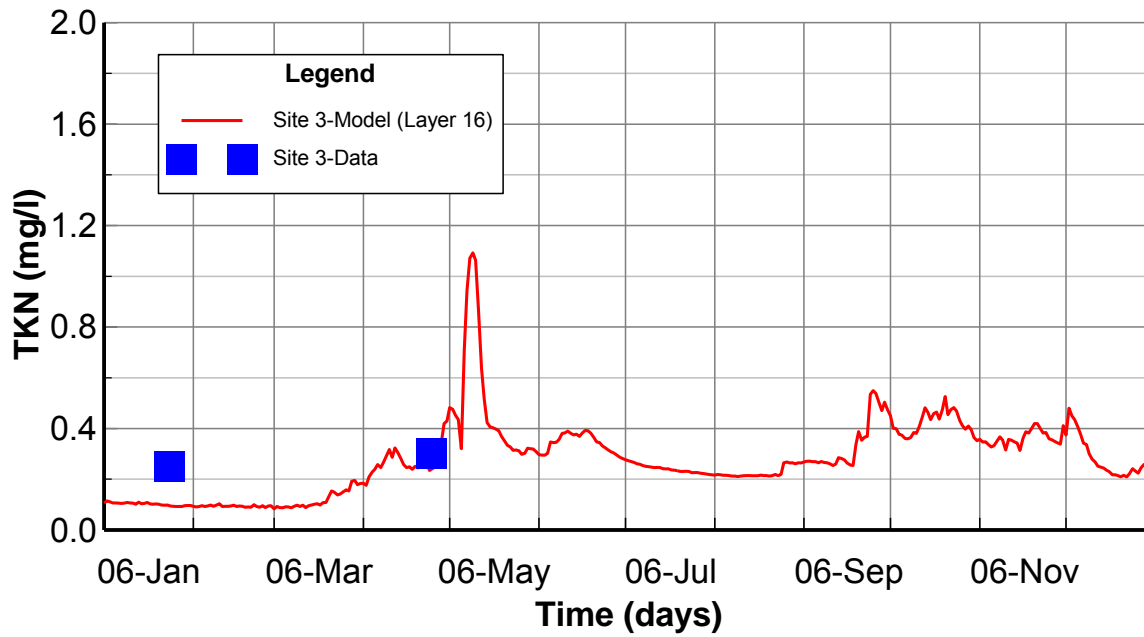


Figure 8-53. Surface Layer TKN Calibration Plots at Station Site3

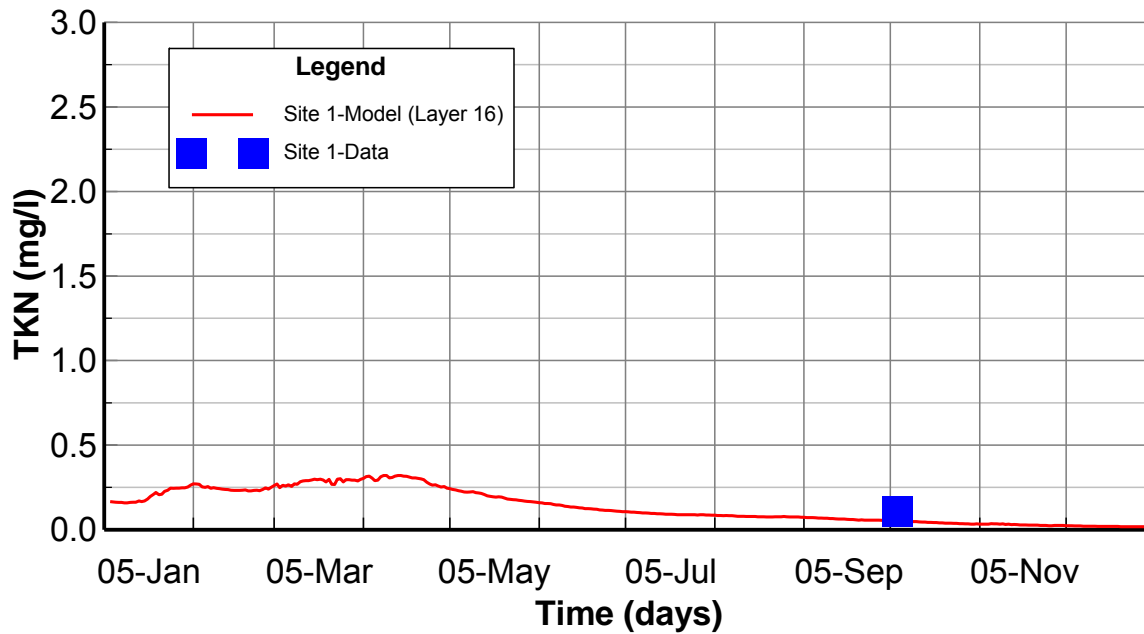


Figure 8-54. Surface Layer TKN Validation Plots at Station Site1

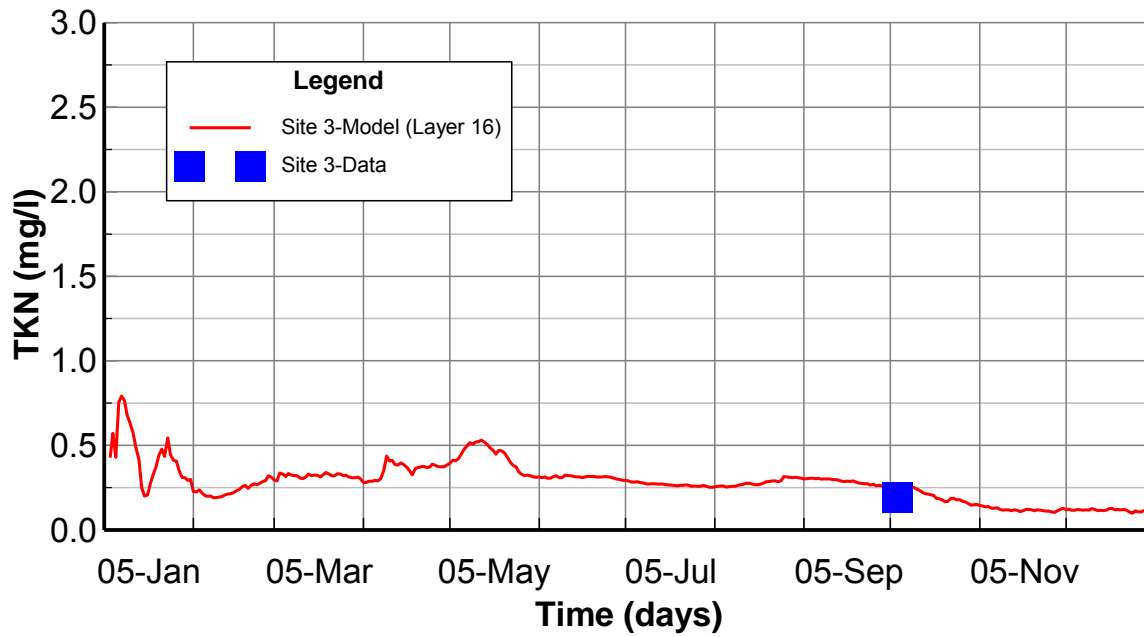


Figure 8-55. Surface Layer TKN Validation Plots at Station Site3

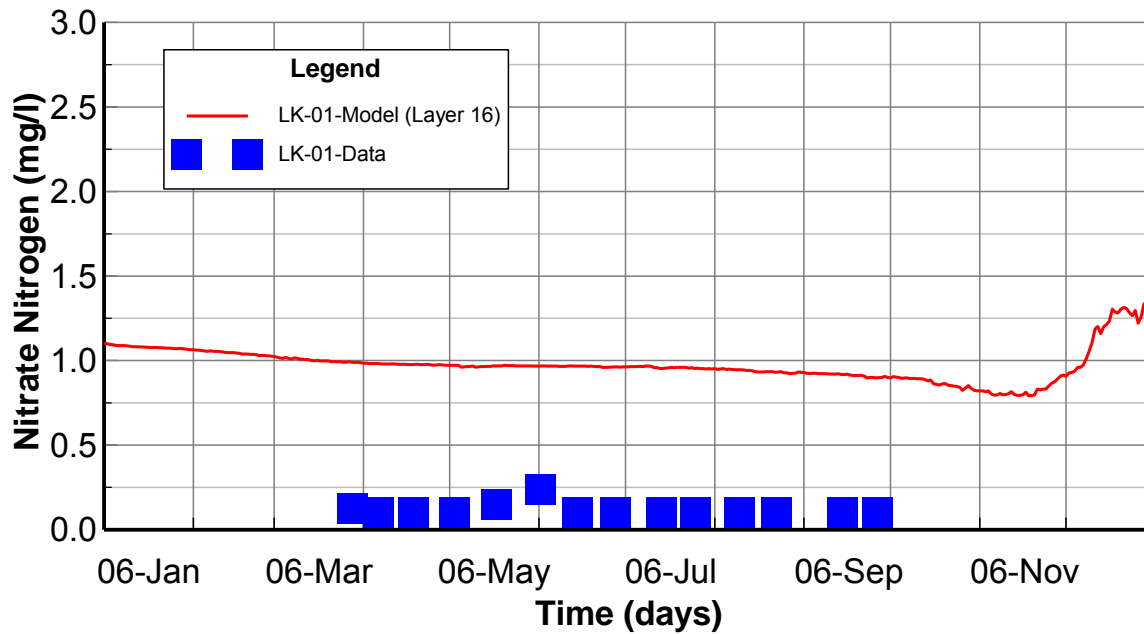


Figure 8-56. Surface Layer NO3 Calibration Plots at Station LK-01

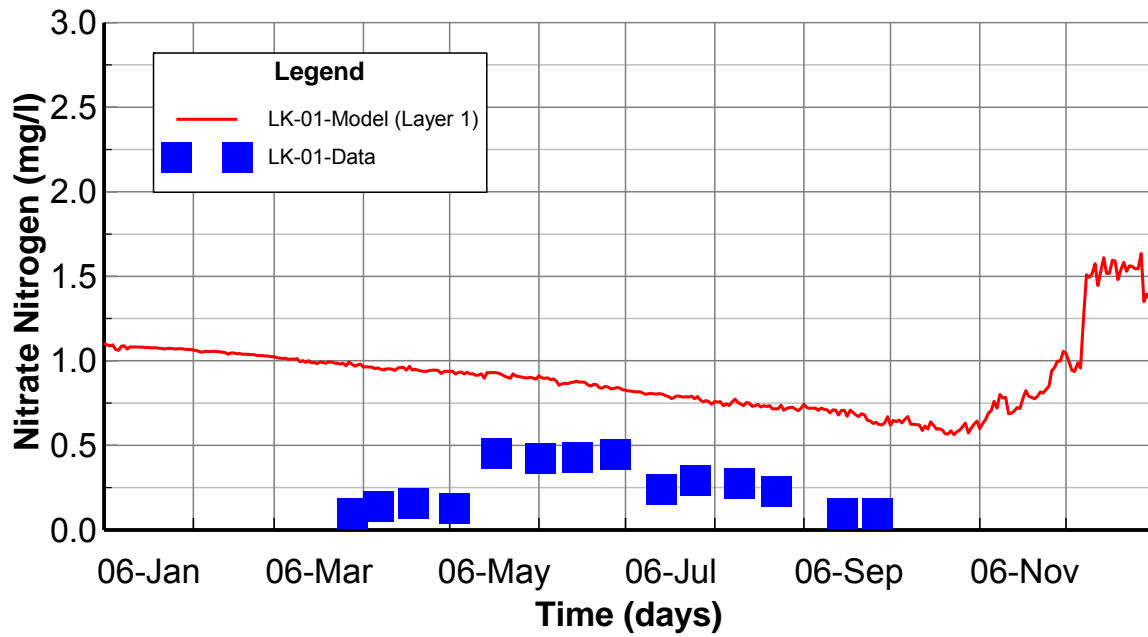


Figure 8-57. Bottom Layer NO3 Calibration Plots at Station LK-01

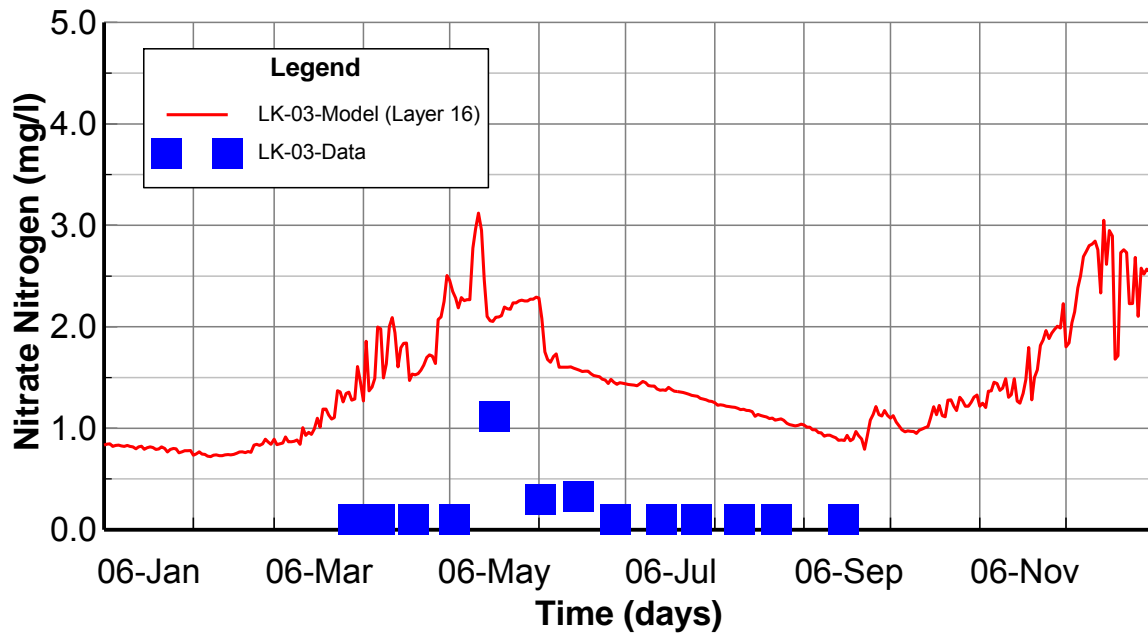


Figure 8-58. Surface Layer NO3 Calibration Plots at Station LK-03

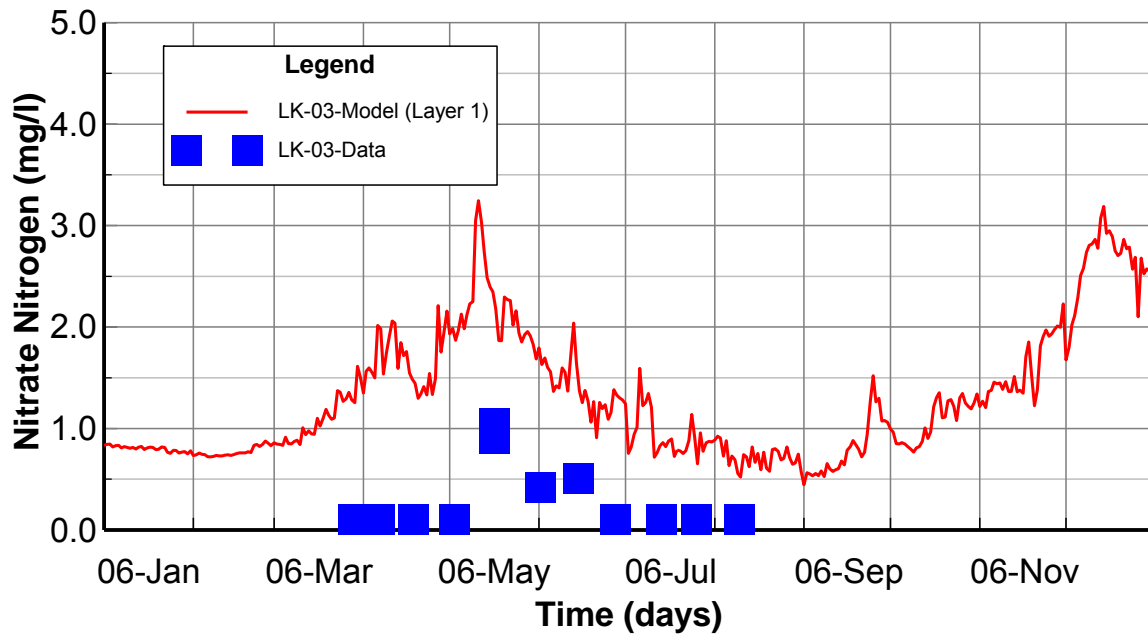


Figure 8-59. Bottom Layer NO3 Calibration Plots at Station LK-03

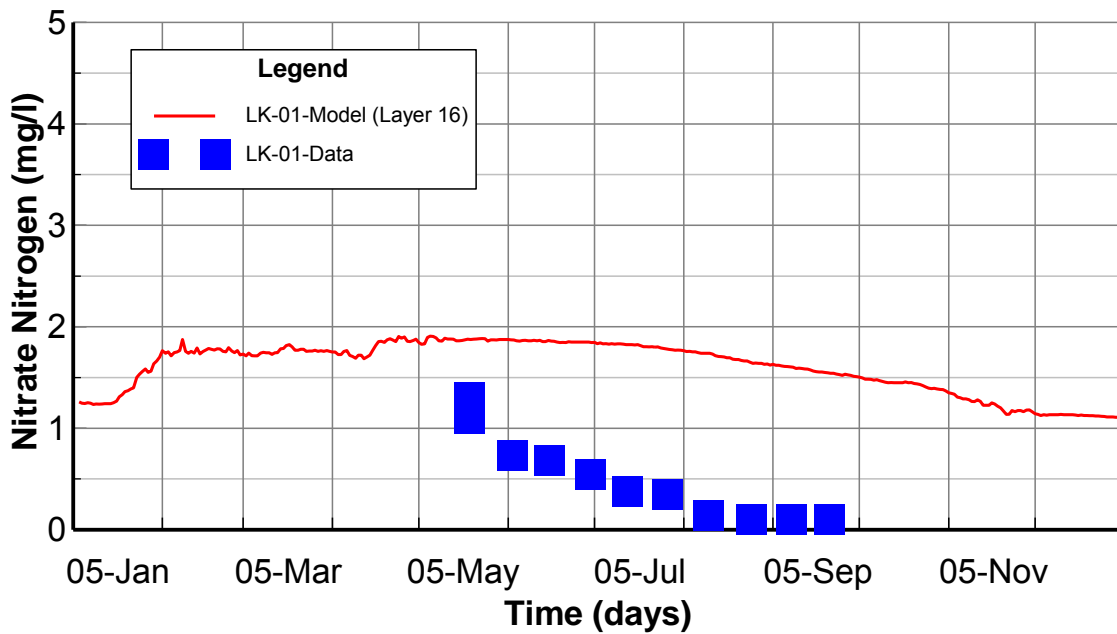


Figure 8-60. Surface Layer NO3 Validation Plots at Station LK-01

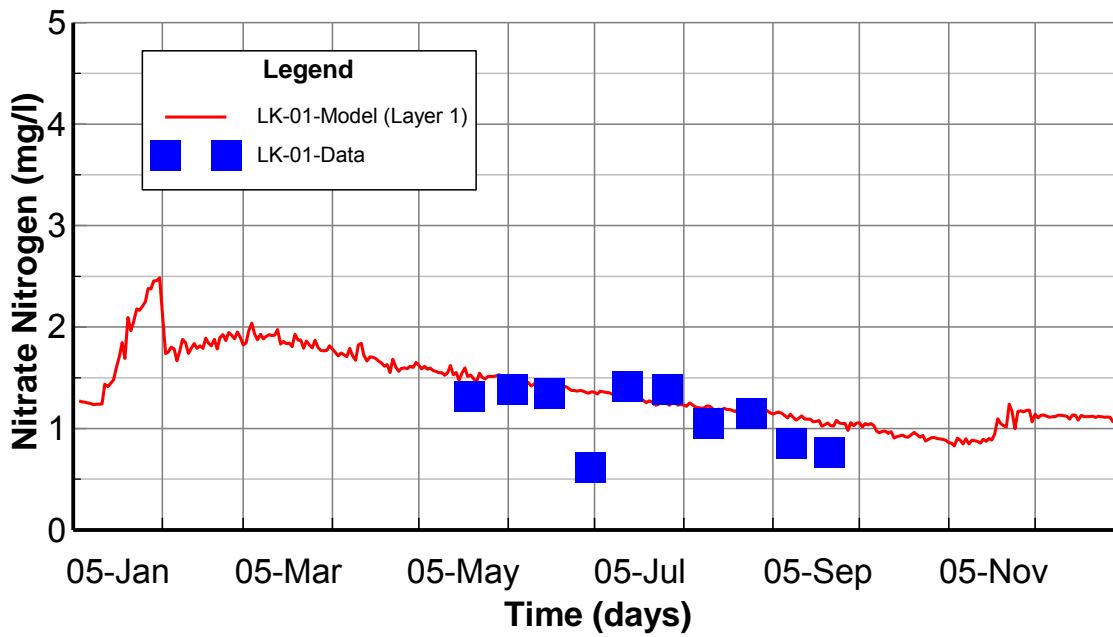


Figure 8-61. Bottom Layer NO₃ Validation Plots at Station LK-01

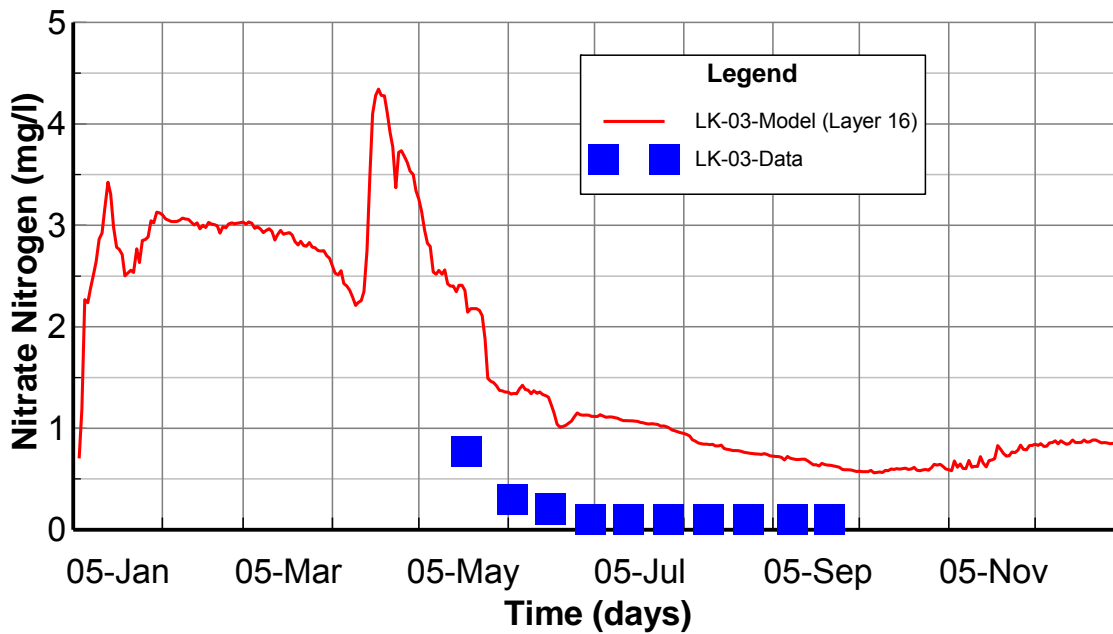


Figure 8-62. Surface Layer NO₃ Validation Plots at Station LK-03

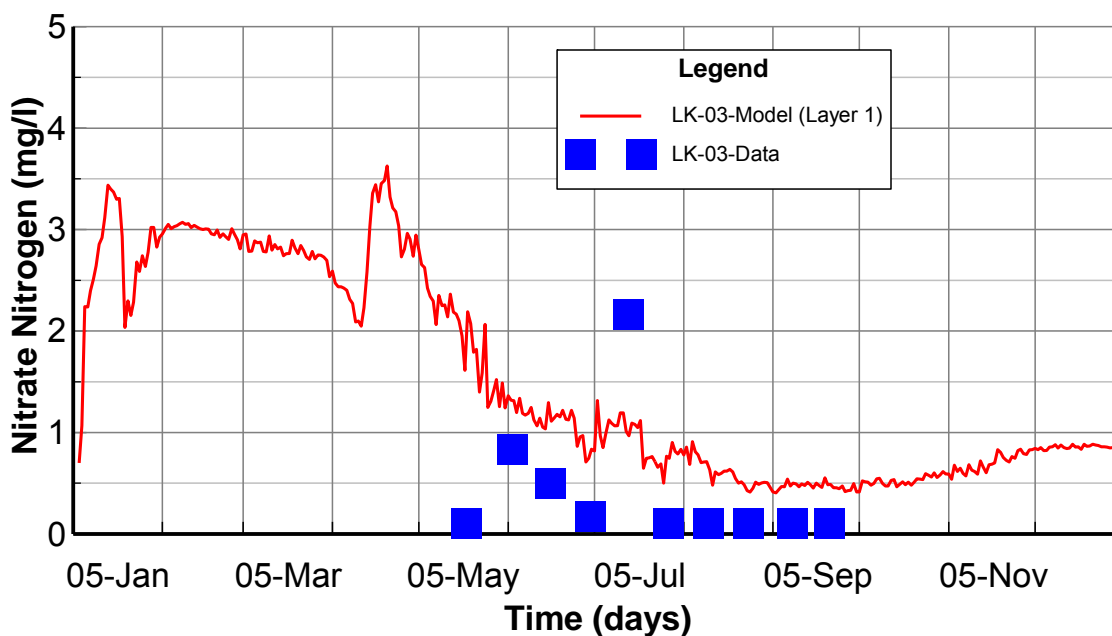


Figure 8-63. Bottom Layer NO₃ Validation Plots at Station LK-03

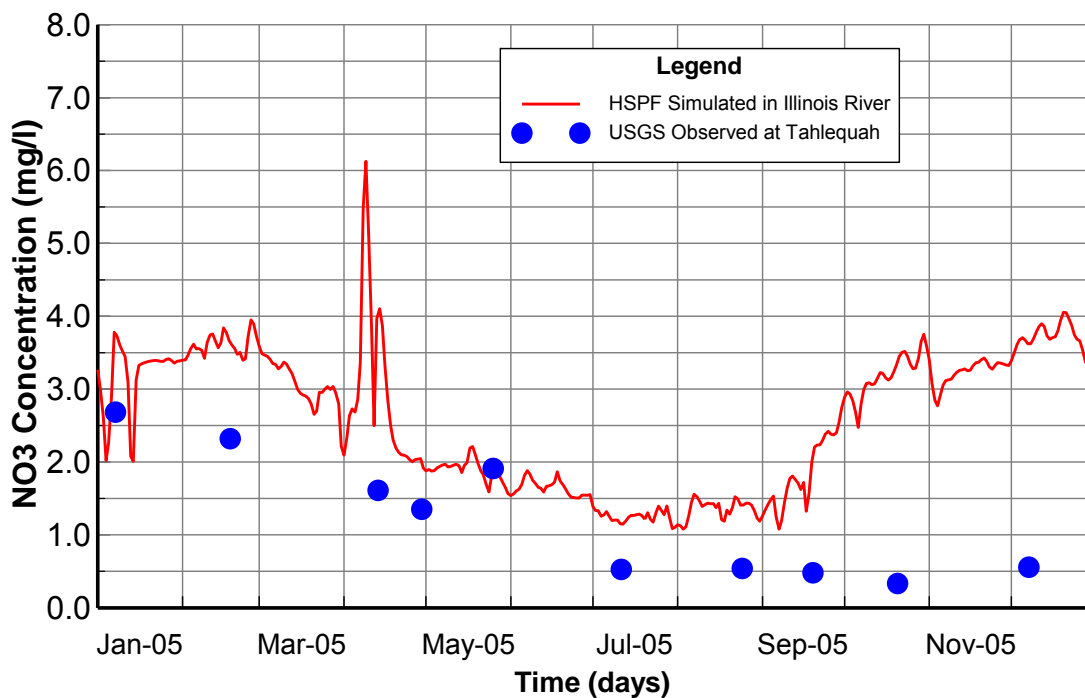


Figure 8-64. HSPF NO₃ Boundary at Illinois River in 2005. USGS Tahlequah station is approximately 9 miles upstream of the EFDC upstream boundary at Illinois River.

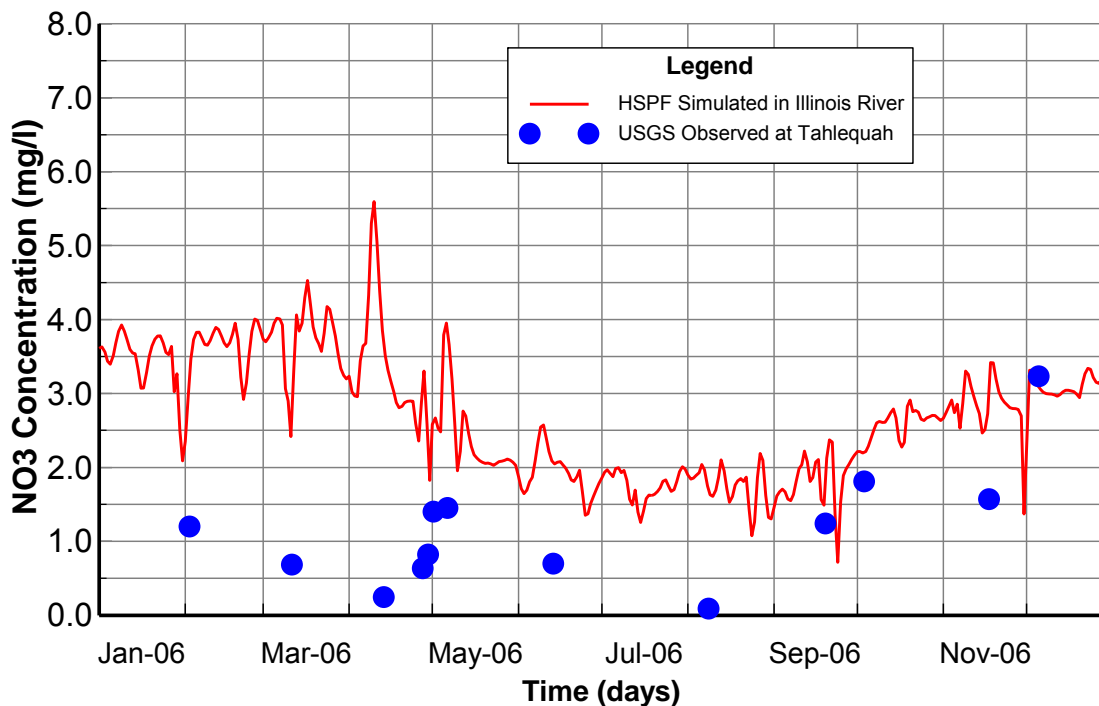


Figure 8-65. HSPF NO₃ Boundary at Illinois River in 2006. USGS Tahlequah station is approximately 9 miles upstream of the EFDC upstream boundary at Illinois River.

8.8 Phosphorus Calibration and Validation

Procedures used to calibrate phosphorus species include: 1) check the linkage between HSPF and EFDC to make sure that the setup of phosphorus boundary conditions for the Lake EFDC model is correct; and 2) adjust the key parameters within reasonable ranges to match the observed data.

Total phosphate (TPO₄) and total phosphorus (TP) model results are presented for comparison to the observed data for the surface layer (k=16) and bottom layer (k=1). The TPO₄ calibration plots at LK-01 and LK-03 are given in Figures 8-66 through 8-69. The TPO₄ validation plots at LK-01 and LK-03 are given in Figures 8-72 through 8-75. The TP calibration and validation plots at LK-01 and LK-03 are given in Figures 8-76 through 8-83. The calibration and validation time series plots for all monitoring stations are given in APPENDIX J and APPENDIX K.

As can be seen in the model-data plots, the model results are in reasonable agreement with measured TPO₄ and TP at station LK-01 and LK-02 for both calibration and validation periods. The EFDC simulated TPO₄ and TP at station LK-03 and LK-04 showed several spikes, particularly in May 2006, which are related to watershed model results provided by the HSPF upstream boundary inflows.

The HSPF-derived TPO₄ and flow boundaries for the Illinois River at Tahlequah are given in Figures 8-70 and 8-71. The figures show that the EFDC simulated TPO₄ spikes coincide with the peak flows and HSPF simulated TPO₄ loading in the Illinois River particularly during a storm event that occurred in late April and May 2006. Since the HSPF watershed model clearly overestimates phosphorus loading during the late April and May 2006 storm event, 3 sampling

dates in May 2006 were removed from the observed data set for TPO4 and TP for Station LK-03. The observed data sets were filtered to remove the impact of the significant overestimate of watershed loading in late April and May 2006 on the lake model response and the calculation of model performance statistics.

The calculated RMS errors of TPO4 ranged from 0.001 mg/L at the surface layer of station LK-01 to 0.104 mg/L at the surface layer of station LK-04 in Table 8-7. The calculated relative RMS errors of TPO4 ranged from 34.9% at the surface layer of station LK-01 to 420% at the surface layer of station LK-03 as in Table 8-7.

The calculated RMS errors of TP ranged from 0.008 mg/L at the bottom layer of station LK-01 to 0.141 mg/L at the bottom layer of station LK-04 (Table 8-8). The calculated relative RMS errors of TP ranged from 29.2% at the bottom layer of station LK-02 to 116.9% at the surface layer of station LK-04 (Table 8-8).

At station LK-01 and LK-02, the model results for TPO4 and TP are within or close to the defined model performance target of $\pm 50\%$ for nutrients with the highest relative RMS errors of 78 to 87% calculated for the surface layers of LK-02 and LK-01. However, at station LK-03 and LK-04, the model results for TPO4 and TP are higher than the defined model performance target of $\pm 50\%$ for nutrients.

In most of the cases, the calculated relative RMS errors of TPO4 are less than 100% with the exception of the surface layer for LK-04 (114%) and the surface and bottom layers for LK-03. The unusually large relative RMS errors for TPO4 at station LK-03 are 320% for the bottom layer and 421% for the surface layer. At the EFDC upstream boundary in the Illinois River, the HSPF-simulated TPO4 results showed higher peak values compared with the observed TPO4 concentrations at the nearest USGS station as shown in Figure 8-70. With the high peak flows simulated by HSPF shown in Figure 8-71, the TPO4 loads to the lake are even higher. The HSPF-simulated peak TPO4 concentrations move to the downstream end of the lake and cause the overestimation of TPO4 at station LK-03 during the late April-May storm event in 2006. Following the peak loading in April-May 2006, TPO4 observed in June through August 2006 is very low with many measured concentrations at the detection limit. This means that the actual concentration of TPO4 is either at the detection limit or is less than the detection limit. Model results for TPO4, also very low during the summer months of 2006, are consistent with the observed low values of TPO4 as a result of algal uptake of TPO4. The calibration and validation model results for chlorophyll for LK-03 (see Figure 8-33 and Figure 8-37) show good agreement with observed chlorophyll suggesting that the modeled uptake of TPO4 and the very low concentrations of simulated TPO4 are reasonable results for the model.

The very high relative RMS errors of 320% and 421% estimated for TPO4 at Station LK-03 result from two factors. The first factor is the overprediction of the TPO4 loading into the lake from the watershed model (see Figure 8-70) and the modeled in-lake response to the high loading during late April-May 2006. The second factor is the very low range of observed TPO4 (0.007 to 0.008 mg/L) that includes numerous measurements in both 2005 and 2006 that are at the detection limit for TPO4. The very low range of observed TPO4 skews the estimate of the relative RMS Error because the RMS Error is divided by the observed range. Overall, the composite model performance for the relative RMS error for the 4 stations for TPO4 is 142% and 65% for TP (n=171 data pairs). As shown by the composite relative RMS errors, model performance for TP of 65% is close to the target of $\pm 50\%$ and is also considerably better than the overall model performance for TPO4 (142%). Considering the fact that the calculated relative RMS errors of TPO4 and TP are within, or close to, the defined model performance

target of $\pm 50\%$ (with the exception of LK-03 for TPO4), the TPO4 and TP model results are deemed to be acceptable.

Table 8-7. Summary Statistics of TPO4 (mg/l)

Station ID	Layer	Starting	Ending	# Pairs	RMS (mg/l)	Rel RMS (%)	Data Average (mg/l)	Model Average (mg/l)
LK-01	Layer 1	6/29/2005 13:40	9/26/2006 12:00	22	0.003	34.9	0.003	0.005
LK-01	Layer 16	6/29/2005 13:40	9/26/2006 12:00	23	0.001	45.0	0.001	0.002
LK-02	Layer 1	6/29/2005 10:30	9/26/2006 8:00	23	0.02	57.6	0.013	0.019
LK-02	Layer 16	6/29/2005 10:30	9/26/2006 8:00	23	0.01	78.0	0.002	0.006
LK-03	Layer 1	6/29/2005 16:55	8/9/2006 14:50	19	0.026	320.131	0.002	0.018
LK-03	Layer 16	6/29/2005 16:55	9/26/2006 14:40	23	0.030	420.784	0.002	0.011
LK-04	Layer 1	7/26/2005 16:40	9/26/2006 0:00	21	0.079	73.2	0.051	0.066
LK-04	Layer 16	7/26/2005 16:40	9/26/2006 16:00	21	0.104	113.8	0.033	0.074

Table 8-8. Summary Statistics of TP (mg/l)

Station ID	Layer	Starting	Ending	# Pairs	RMS (mg/l)	Rel RMS (%)	Data Average (mg/l)	Model Average (mg/l)
LK-01	Layer 1	6/29/2005 13:40	9/26/2006 12:00	22	0.012	38.709	0.015	0.006
LK-01	Layer 16	6/29/2005 13:40	9/26/2006 12:00	23	0.008	87.118	0.011	0.003
LK-02	Layer 1	6/29/2005 10:30	9/26/2006 8:00	23	0.116	29.251	0.082	0.022
LK-02	Layer 16	6/29/2005 10:30	9/26/2006 8:00	23	0.012	60.329	0.015	0.013
LK-03	Layer 1	6/29/2005 16:55	8/9/2006 14:50	19	0.025	62.147	0.030	0.029

Station ID	Layer	Starting	Ending	# Pairs	RMS (mg/l)	Rel RMS (%)	Data Average (mg/l)	Model Average (mg/l)
LK-03	Layer 16	6/29/2005 16:55	9/26/2006 14:40	23	0.033	84.825	0.026	0.020
LK-04	Layer 1	7/26/2005 16:40	9/26/2006 0:00	21	0.141	37.225	0.158	0.126
LK-04	Layer 16	7/26/2005 16:40	9/26/2006 16:00	21	0.116	116.933	0.098	0.107

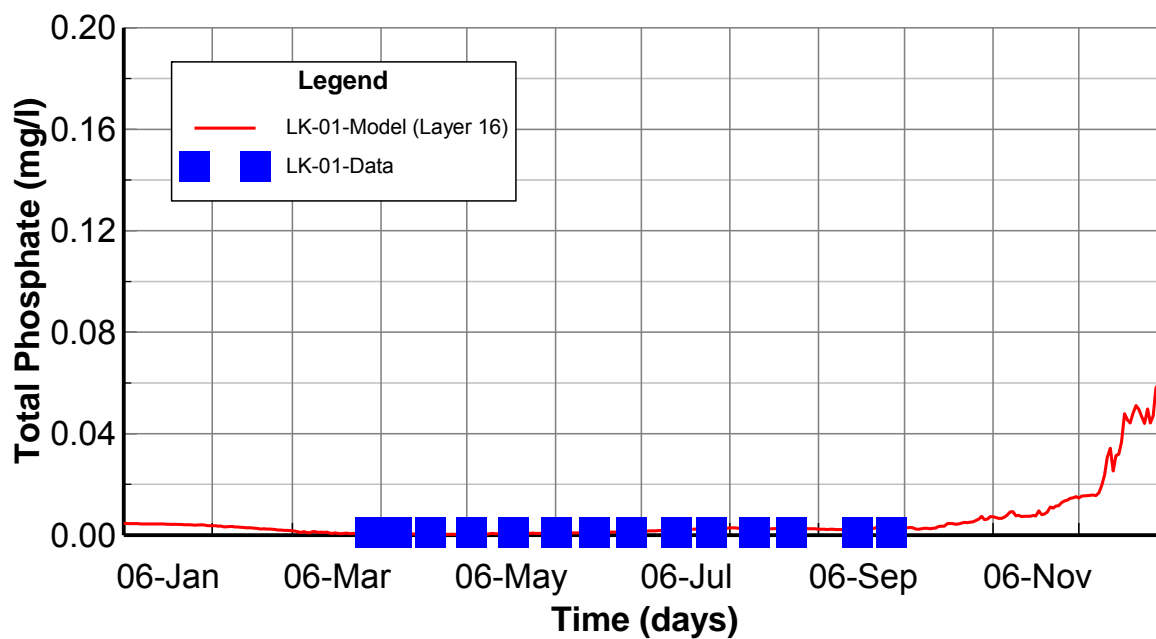


Figure 8-66. Surface Layer TPO4 Calibration Plots at Station LK-01

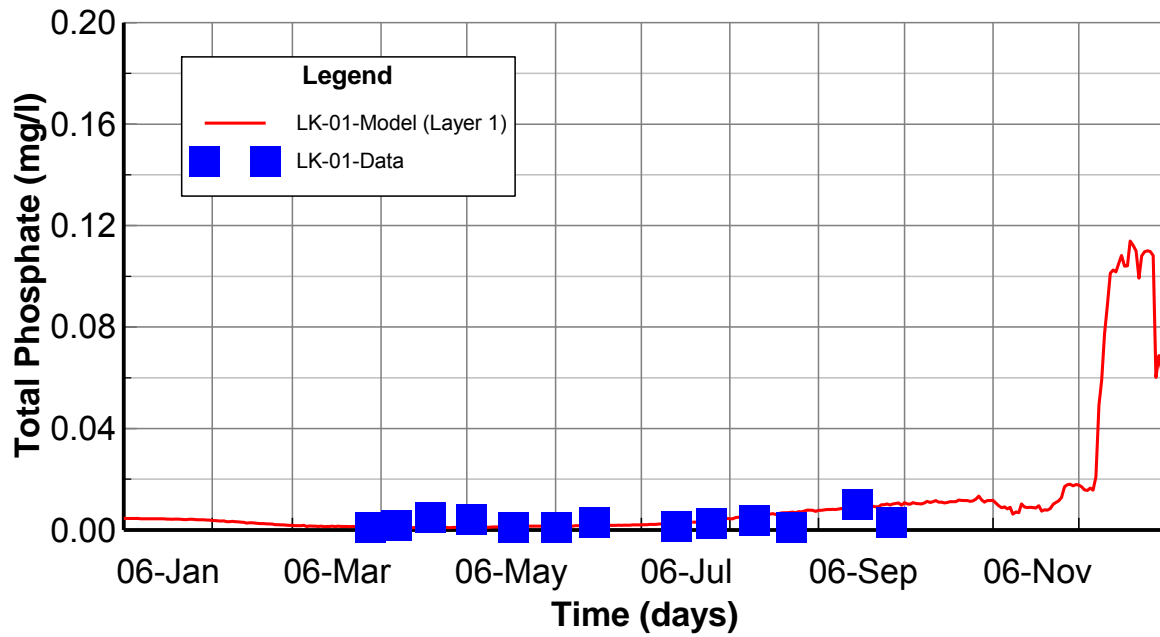


Figure 8-67. Bottom Layer TPO4 Calibration Plots at Station LK-01

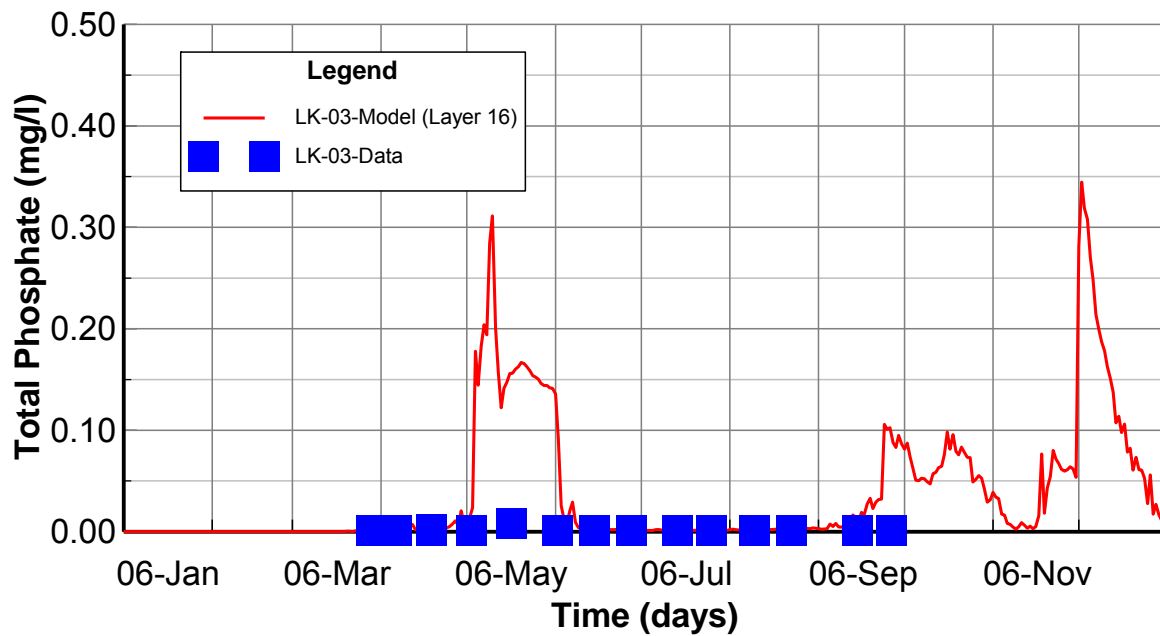


Figure 8-68. Surface Layer TPO4 Calibration Plots at Station LK-03

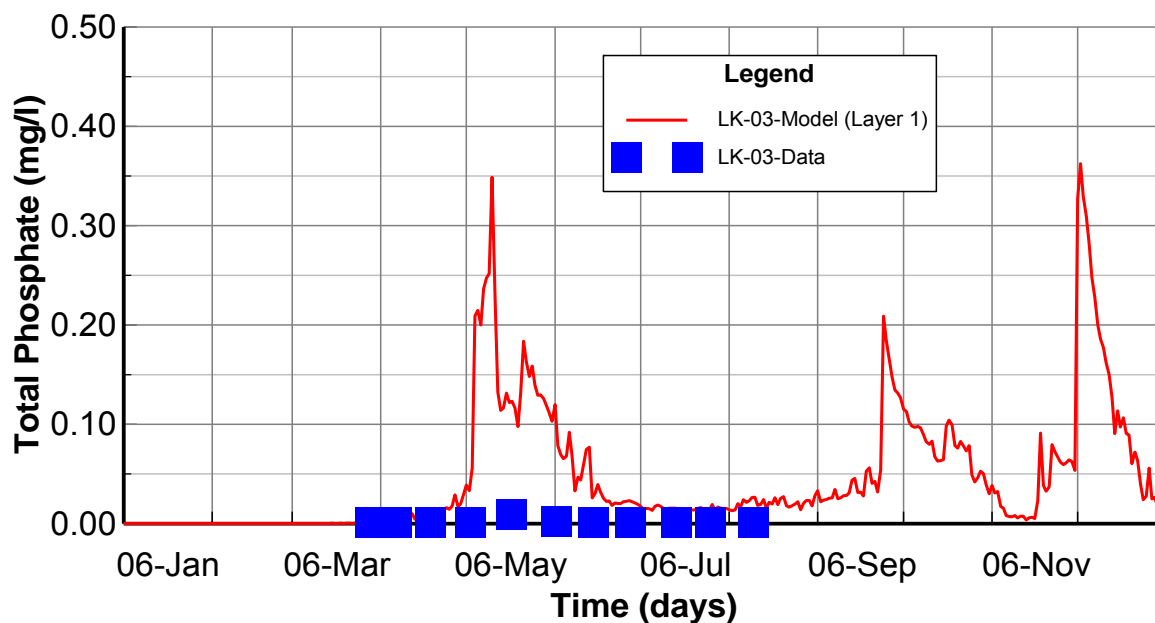


Figure 8-69. Bottom Layer TPO4 Calibration Plots at Station LK-03

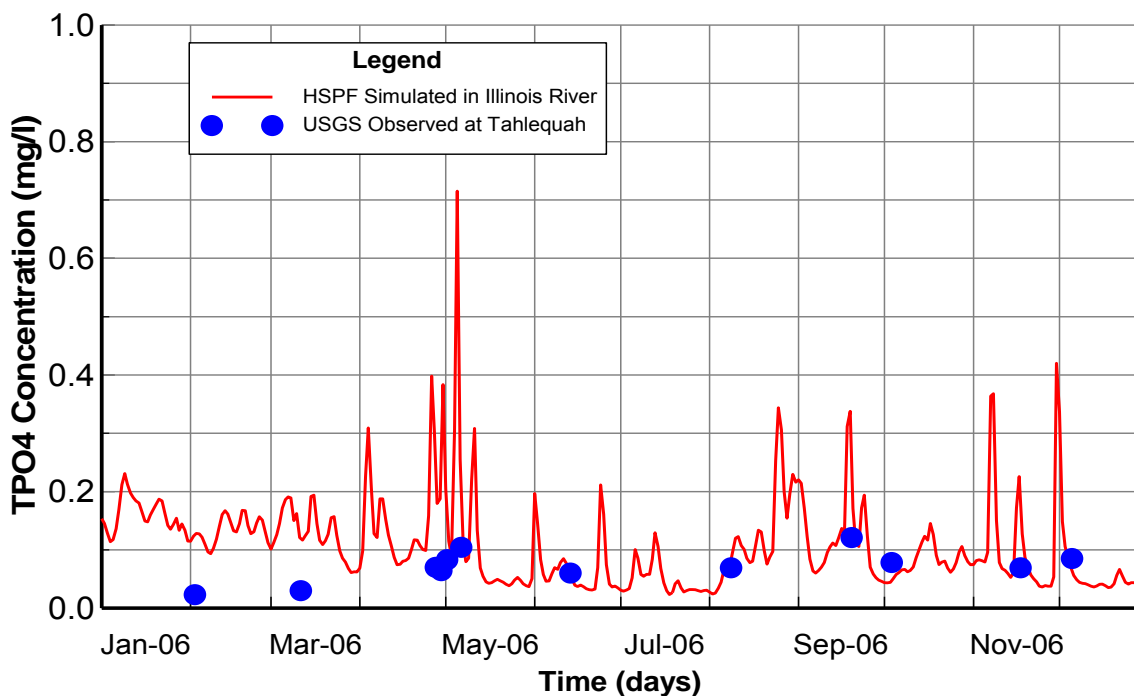


Figure 8-70. HSPF TPO4 Boundary in the Illinois River in 2006. USGS Tahlequah station is approximately 9 miles upstream of the EFDC upstream boundary at Illinois River.

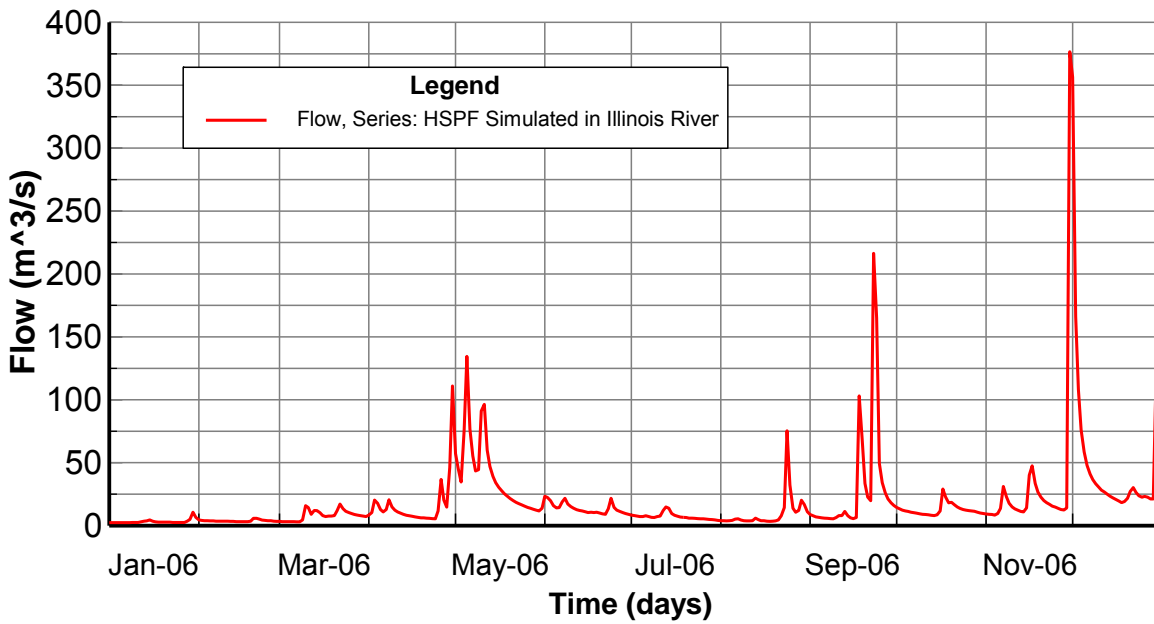


Figure 8-71. HSPF Flow Boundary in the Illinois River in 2006

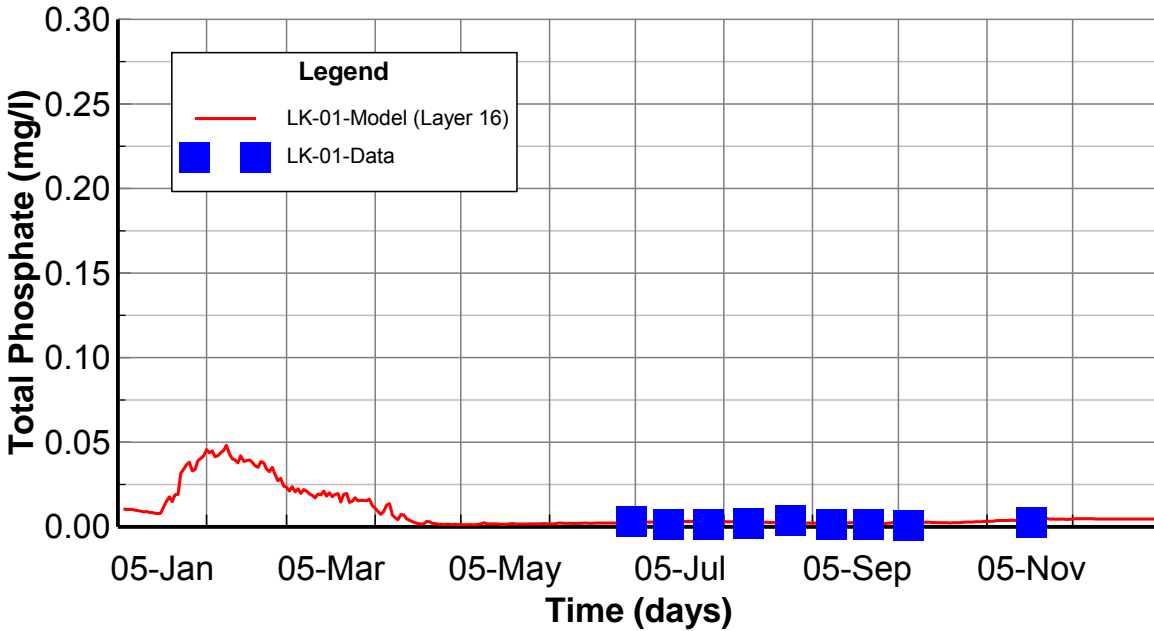


Figure 8-72. Surface Layer TPO4 Validation Plots at Station LK-01

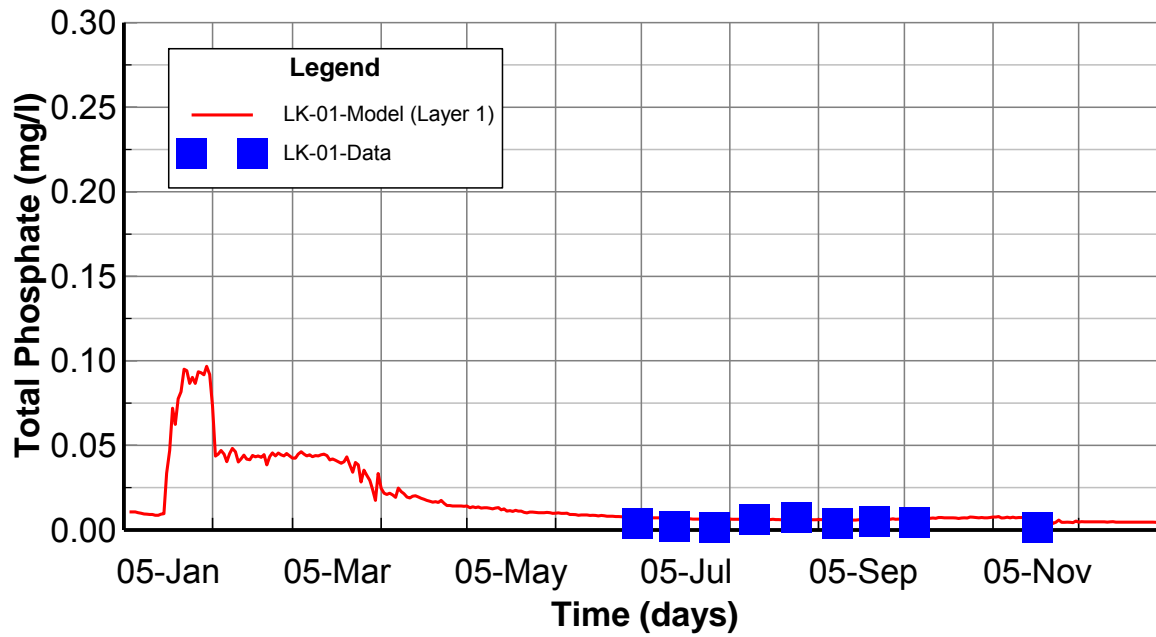


Figure 8-73. Bottom Layer TPO4 Validation Plots at Station LK-01

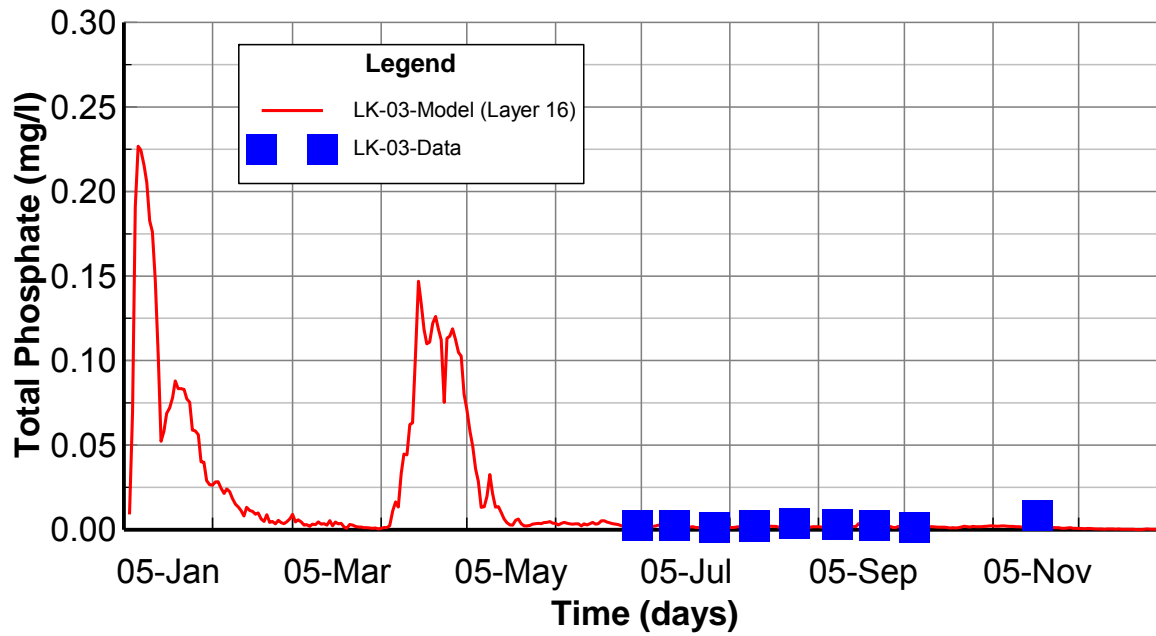


Figure 8-74. Surface Layer TPO4 Validation Plots at Station LK-03

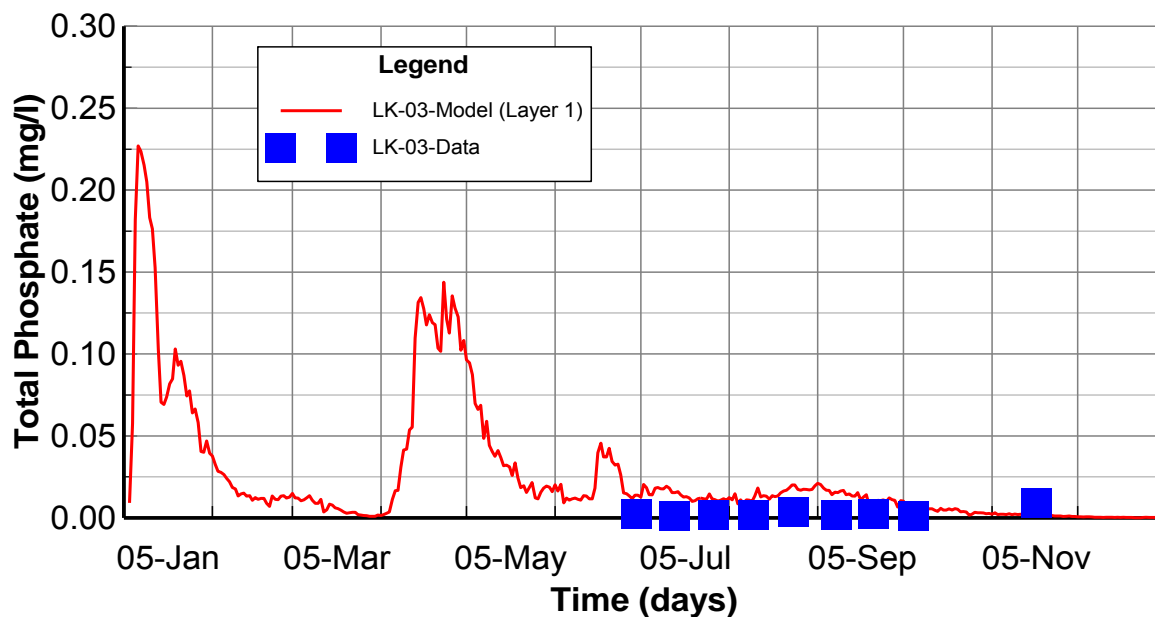


Figure 8-75. Bottom Layer TPO4 Validation Plots at Station LK-03

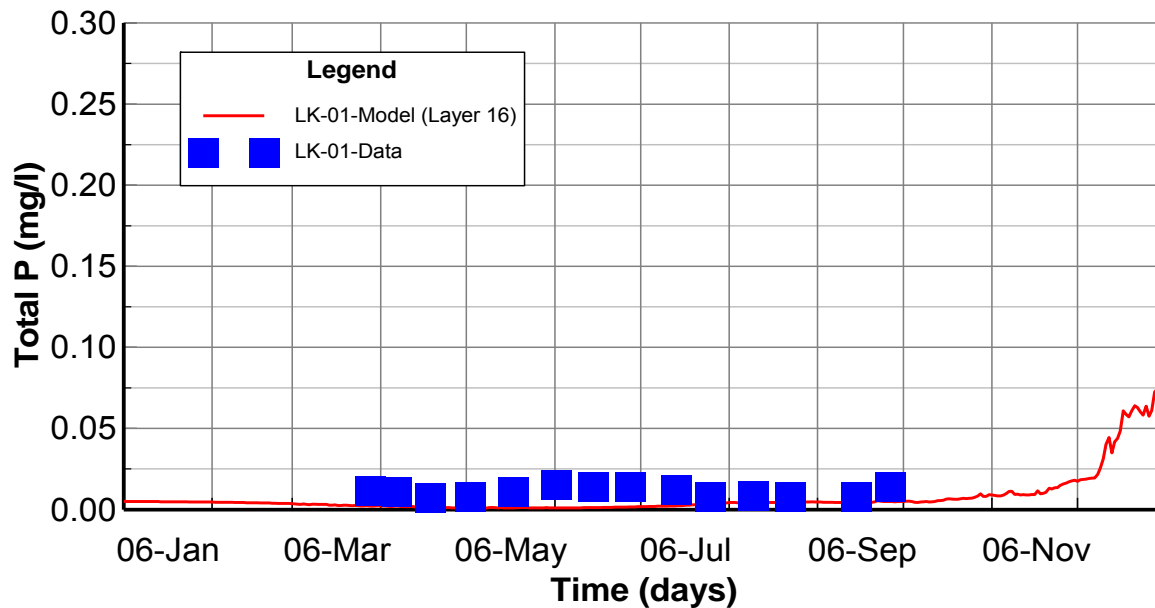


Figure 8-76. Surface Layer TP Calibration Plots at Station LK-01

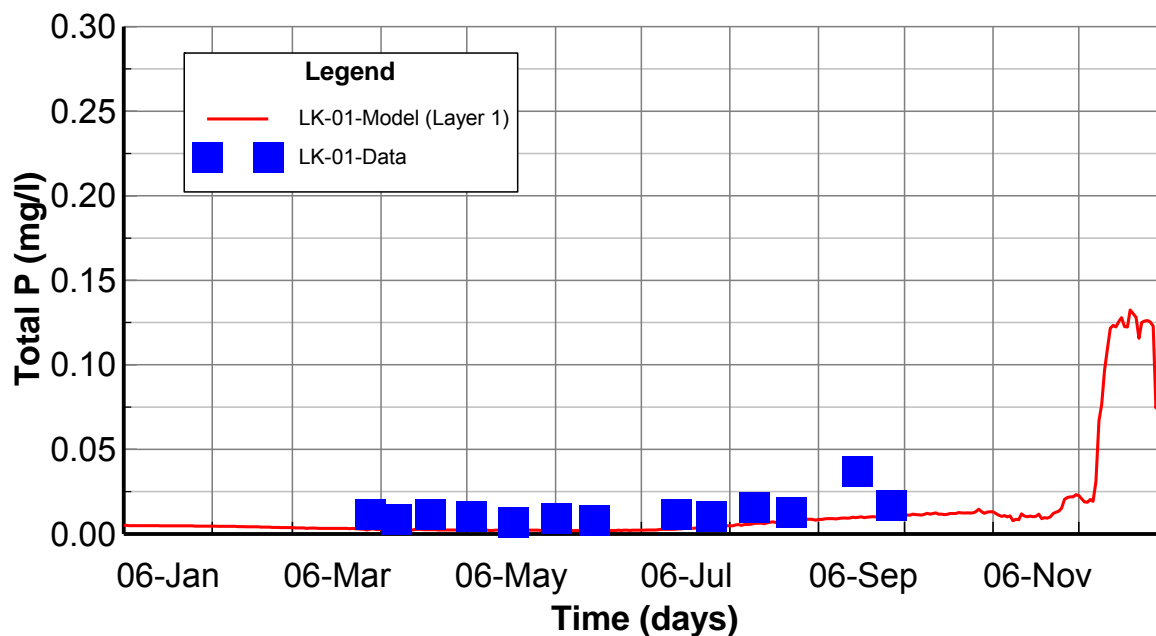


Figure 8-77. Bottom Layer TP Calibration Plots at Station LK-01

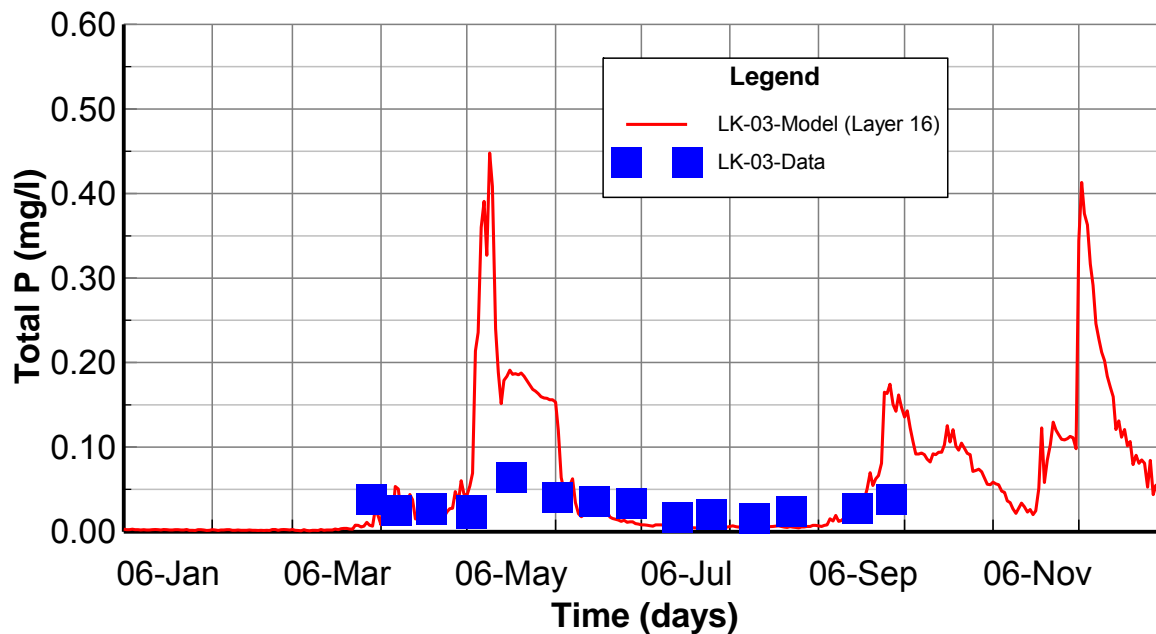


Figure 8-78. Surface Layer TP Calibration Plots at Station LK-03

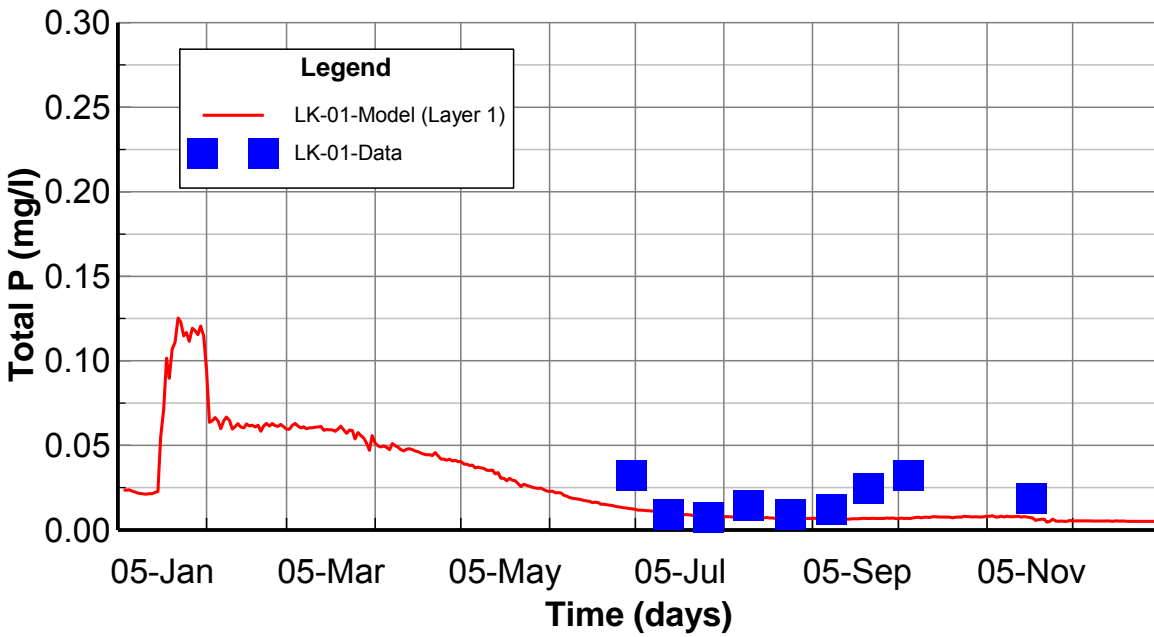


Figure 8-81. Bottom Layer TP Validation Plots at Station LK-01

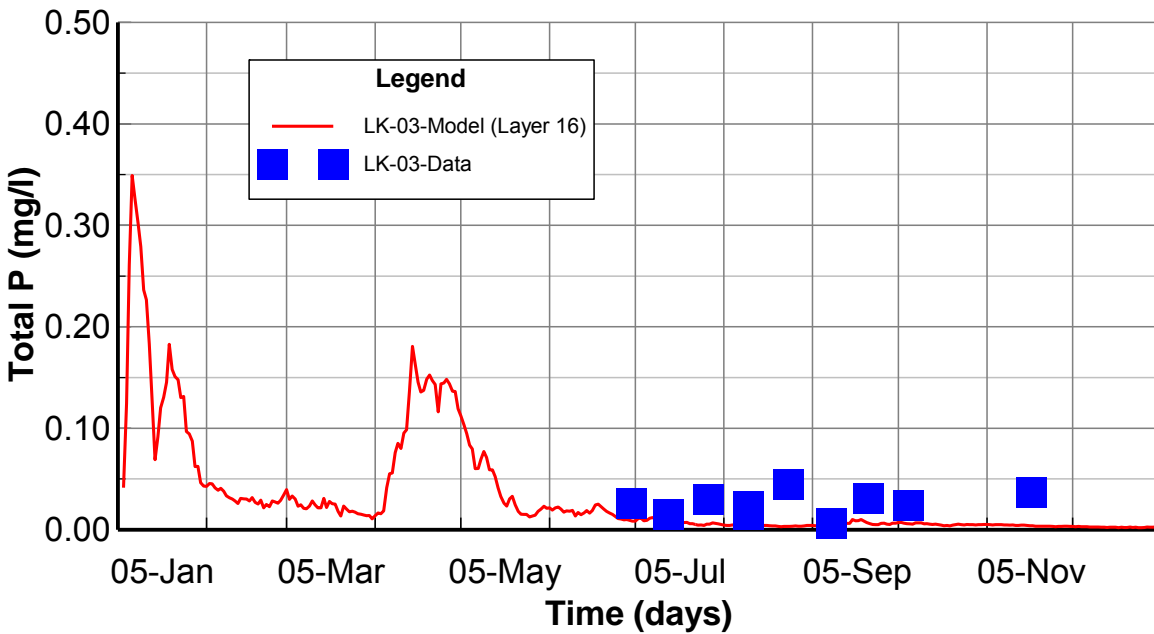


Figure 8-82. Surface Layer TP Validation Plots at Station LK-03

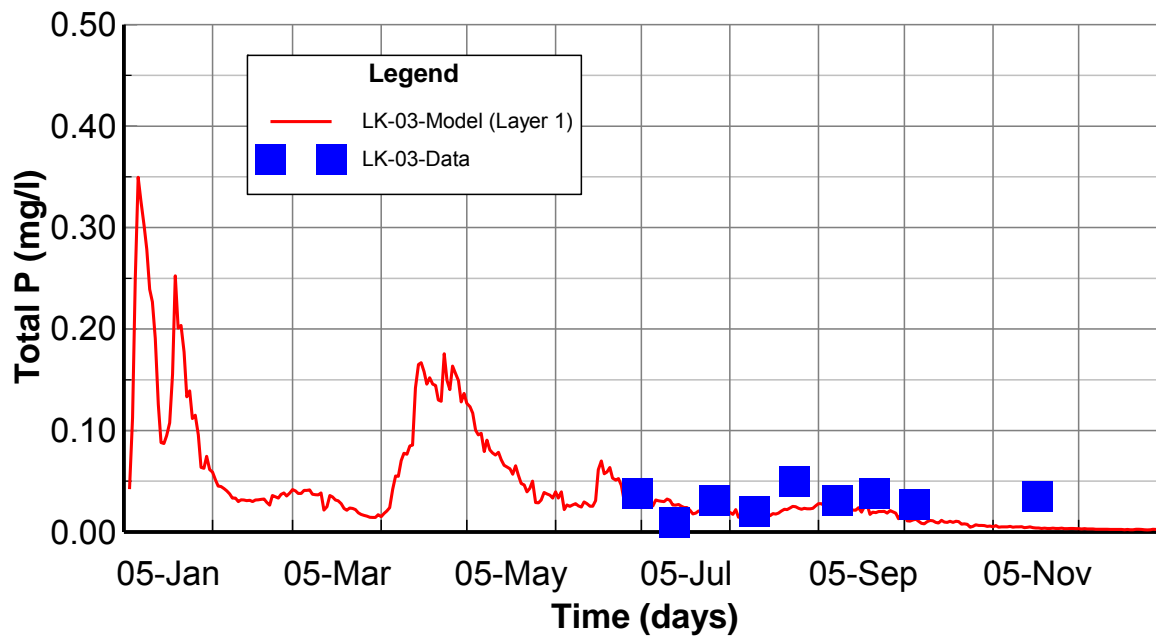


Figure 8-83. Bottom Layer TP Validation Plots at Station LK-03

Section 9 Summary and Conclusions

9.1 Summary

The Illinois River watershed (Hydrologic Unit Code 11110103) encompasses a drainage area of 1,052,032 acres in northwest Arkansas and northeast Oklahoma. The Illinois River, Baron Fork, Tahlequah Creek, Flint Creek and Caney Creek are the major streams in the watershed that drain into Tenkiller Ferry Lake, a 13,000 acre reservoir with 130 miles of shoreline. Downstream of the dam, the lower reach of the Illinois River flows 10 miles to the confluence with the Arkansas River. Nutrient loading from wastewater facilities, watershed runoff and large-scale agricultural poultry production are suspected of contributing to impairment of many segments of the Illinois River, other streams in the watershed and of Tenkiller Ferry Lake. The lake is on Oklahoma's 303 (d) list for impaired beneficial uses of Fish and Wildlife Propagation for warm water aquatic community life and Aesthetics. Tenkiller Ferry Lake was classified in 2006 as a Nutrient Limited Watershed (NLW) in Oklahoma Water Quality Standards based on Carlson's Trophic State Index (TSI). Causes of impairment have been identified as low dissolved oxygen in the hypolimnion and high algae biomass.

To provide a sound technical basis for TMDL determinations for the Illinois River watershed and Tenkiller Ferry Lake, EPA-supported public domain models have been selected to describe watershed hydrology and pollutant loading from the Illinois River watershed (HSPF); and hydrodynamics and water quality in Tenkiller Ferry Lake (EFDC). The linked watershed-lake model, calibrated and validated to data collected in the lake from 2005-2006, provides EPA and the States of Oklahoma and Arkansas with a mass balance-based model framework to simulate the water quality response within Tenkiller Ferry Lake to existing watershed loading. The watershed-lake model can be applied to model the potential response of in-lake water quality to alternative watershed load reduction scenarios; and to evaluate the effectiveness of load reduction scenarios on compliance with Oklahoma water quality standards and defined water quality targets for Trophic State Index (TSI) based on chlorophyll-a and dissolved oxygen for Tenkiller Ferry Lake. The watershed-lake model framework will be used to support development of TMDLs for Tenkiller Ferry Lake.

Using external flow and loading data provided by the HSPF watershed model and observed water quality data available from the OWRB and CDM/USGS surveys, the EFDC lake model was calibrated and validated for the 2-year period from January 2005 through December 2006. Model results were compared to observed data as (a) vertical profiles for water temperature and dissolved oxygen and (b) surface and bottom layer time series of water temperature, total suspended solids (TSS), dissolved oxygen, chlorophyll-a, nitrogen, phosphorus and total organic carbon.

The EFDC model incorporates internal coupling of organic matter production and deposition from the water column to the sediment bed with decomposition processes in the sediment bed that, in turn, produce benthic fluxes of nutrients and dissolved oxygen across the sediment-water interface. Tenkiller Ferry Lake, like many reservoirs, is characterized by seasonal thermal stratification and hypolimnetic anoxia. Summer anoxic conditions, in turn, are associated with internal nutrient loading from the benthic release of phosphate and ammonia into the water column that is triggered, in part, by low oxygen conditions. The water quality model, calibrated and validated to 2005-2006 data, accounts for the cause-effect interactions of water clarity, nutrient cycling, algal production, organic matter deposition, sediment decay, and sediment-water fluxes of nutrients and dissolved oxygen.

9.2 Conclusions

A previous EFDC model of Tenkiller Ferry Lake (DSSL, 2006), developed and calibrated to water quality data collected under the Clean Lakes Program in 1993-1994, was updated for calibration and validation using data collected by OWRB and CDM/USGS during 2005-2006. Based on recommendations provided in the previous modeling study, the horizontal and vertical resolution of the EFDC grid was increased significantly to better address seasonal water column stratification and new bathymetry data collected in 2005 was used to update the expanded resolution EFDC grid. While the 2005-2006 calibration and validation years provided the most robust data set, they were characterized by anomalous hydrologic conditions. Extreme drought conditions were observed throughout the Central Plains in 2005-2006 and lake levels in Tenkiller Ferry Lake, as well as many other reservoirs in Oklahoma, dropped to the lowest water levels recorded in decades.

The EFDC hydrodynamic and water quality model of Tenkiller Ferry Lake was calibrated to data available to describe lake water quality conditions from 2005-2006. Model results, in general, were in good agreement to observations and either met, or were close to, model performance targets for water temperature, dissolved oxygen, and chlorophyll-a. The performance targets were met at all stations for water temperature and chlorophyll-a. With the exception of Station LK-03 surface layer results, the performance target was met, or was close to the target for TSS at most stations. The performance target was met, or was only slightly higher than the target for surface and bottom layer dissolved oxygen at all stations.

Performance targets for nitrate, however, although close to the 50% target for bottom layer results (38-78%), were higher (89-135%) than the 50% target for surface layer nitrate. Evaluation of the watershed loading data simulated by the HSPF model for the Illinois River upstream boundary inputs to the lake model indicated that observed nitrate concentrations for 2005-2006 were lower than the nitrate loading provided by the watershed model.

Performance targets for surface and bottom layer orthophosphate (TPO₄) were either met, or were close to the performance target of 50% for the lacustrine stations LK-01 (35-45%) and LK-02 (57-78%) and the riverine station (LK-04) (73-113%). For the transition zone station (LK-03) (320-421%) between the river and the lake, however, the model results were much higher than the model performance target of 50% for phosphate. The high Relative RMS errors of 320% and 421% estimated for TPO₄ at LK-03 result from two factors. Evaluation of the watershed loading data provided by the HSPF model for the Illinois River upstream boundary inputs to the lake model, as with nitrate, showed that observed phosphate concentrations for 2005-2006 in the Illinois River at Tahlequah were much lower than the simulated phosphate loading provided by the watershed model. The second factor is the very low range of observed TPO₄ (0.007 to 0.008 mg/L) that included numerous measurements in both 2005 and 2006 that are at the detection limit for TPO₄. The very low range of observed TPO₄ thus skews the estimate of the Relative RMS Error because the RMS Error is divided by a very small value derived from the observed range.

Performance targets for surface and bottom layer total phosphorus (TP) were either met, or were very close to the performance target of 50% for the lacustrine stations LK-01 (39-87%) and LK-02 (29-60%). For the riverine station (LK-04) (37-117%) and the transition zone station (LK-03) (62-84%), however, the model results for TP were somewhat higher than the 50% target for TP.

The calibrated and validated HSPF watershed runoff model and the EFDC hydrodynamic and water quality model of Tenkiller Ferry Lake can provide EPA with a surface water model framework to support development of TMDLs and water quality management plans for Tenkiller Ferry Lake.

Section 10 References

- Anderson, K.A. and J.A. Downing. 2006. Dry and Wet Atmospheric Deposition of Nitrogen, Phosphorus and Silicon in an Agricultural Region. *Water, Air, and Soil Pollution*, 176:351-374.
- AQUA TERRA Consultants. 2010a. Quality Assurance Project Plan. Water Quality Modeling and TMDL Development for the Illinois River Watershed. Prepared for US EPA Office of Science and Technology, Washington DC, and US EPA, Region 6, Dallas TX. REVIEW DRAFT. April 23, 2010.
- AQUA TERRA Consultants. 2010b. Preliminary Data Review and Analysis for Water Quality Modeling and TMDL Development for the Illinois River Watershed. FINAL REPORT. Submitted to US EPA Region 6, and US EPA, Washington D.C. September 30, 2011. 98 p.
- AQUA TERRA Consultants. 2011. Data Review and Analysis for Water Quality Modeling and TMDL Development for the Illinois River Watershed. Submitted to US EPA Region 6, and US EPA, Washington D.C. REVIEW DRAFT. August 3, 2010. 98 p.
- AQUA TERRA Consultants. 2013. Simulation Plan for Water Quality Modeling and TMDL Development for the Illinois River Watershed. Prepared for US EPA Region 6, Dallas, TX. EPA PO # EP-11-6-000023. Submitted May 24, 2013.
- Arhonditsis, G.B. and M.T. Brett. 2005. Eutrophication model for Lake Washington (USA) Part I. Model description and sensitivity analysis. *Ecol. Model.* 187:140-178.
- Bicknell, B., J.C. Imhoff, J.L. Kittle, T.H. Jobes, A.S. Donigian. 2001. *Hydrological Simulation Program–Fortran. HSPF Version 12, User’s Manual*. Prepared by AQUA TERRA Consultants, Mountain View, CA in cooperation with Hydrologic Analysis Software Support Program, U.S. Geological Survey, Reston, VA. Prepared for National Exposure Research Laboratory, Office of Research and Development, U.S. Environmental Protection Agency, Athens, GA, EPA-March.
- Bicknell, B.R. and A.S. Donigian, Jr. 2012. Development of point source loads for Illinois River Watershed TMDL – Updated with additional data received from Springdale, Rogers, Fayetteville, and Lincoln. Memorandum to Quang Nguyen, EPA Region 6, Dallas TX. From AQUA TERRA Consultants. November 19, 2012.
- Blumberg, A.F., L.A. Khan and J. St. John .1999. Three-dimensional hydrodynamic model of New York Harbor Region. *Jour. Hydr. Engineering Div., Proc. ASCE*, 125(8):799-816, August.
- Cerco, C.F. and T.M. Cole. 1995. User’s Guide to the CE-QUAL-ICM Three-Dimensional Eutrophication Model: Release 1.0. Prepared for U.S. Army Waterways Experiment Station, Vicksburg, MS. Technical Report 95-15.
- Cerco, C.F., B.H. Johnson and H.V. Wang. 2002. Tributary refinements to the Chesapeake Bay Model. US Army Corps of Engineers, Engineer Research and Development Center, ERDC TR-02-4, Vicksburg, MS.

- Cole, T. and Wells, S.A. (2008) CE-QUAL-W2: A Two-Dimensional, Laterally Averaged, Hydrodynamic and Water Quality Model, Version 3.6, Department of Civil and Environmental Engineering, Portland State University, Portland, OR.
- Cooke, G.D., Welch, E.B., and Jones, J.R., 2011. Eutrophication of Tenkiller Reservoir, Oklahoma, from Nonpoint Agricultural Runoff. *Lake and Reservoir Management*. 27:256-270.
- Craig, P.M.. 2010. *User's Manual for EFDC_Explorer5: Pre/Post-Processor for the Environmental Fluid Dynamics Code*, Dynamic Solutions, LLC, Knoxville, TN.
- ODEQ 2008. *Water Quality in Oklahoma 2008 Integrated Report*. Appendix C: 303 (d) List of Impaired Waters. Oklahoma Department of Environmental Quality, Oklahoma City, OK, 376 pp.
- Daniel, T.C., J. Stead, P. DeLaune, A.N. Sharpley, T. Verkier, and D Fischel. 2009. Edge of Field Water Quality Monitoring from Various management Practices in the Ozark Highlands. Final Report 05-1300. Arkansas 319 Nonpoint Source Pollution Management Program. Arkansas Natural Resources Commission, Little Rock, AR. Available at <http://www.arkansaswater.org>.
- Dewald, T. 2006. NHDPlus User Guide. Prepared for the U.S. Environmental Protection Agency.
- Di Toro, D.M. 2001. *Sediment Flux Modeling*. Wiley Interscience, New York, NY.
- Donigian, Jr., A.S. 2000. *HSPF Training Workshop Handbook and CD*. Lecture #19. Calibration and Verification Issues, Slide #L19-22. EPA Headquarters, Washington Information Center, 10-14 January 2000. Presented and prepared for U.S. EPA Office of Water, Office of Science & Technology, Washington, DC.
- Donigian, A.S. Jr. 2002. Watershed Model Calibration and Validation: The HSPF Experience. WEF National TMDL Science and Policy 2002, November 13-16, 2002. Phoenix, AZ. WEF Specialty Conference Proceedings on CD-ROM.
- Donigian, A.S., and J.T. Love. 2003. Sediment Calibration Procedures and Guidelines for Watershed Modeling. WEF TMDL 2003, November 16-19, 2003. Chicago, Illinois. WEF Specialty Conference Proceedings on CD-ROM.
- Donigian, A.S. Jr., B.R. Bicknell, R.V. Chinnaswamy and P.N. Deliman. 1998a. Refinement of a Comprehensive Watershed Water Quality Model with Application to the Chesapeake Bay Watershed. Technical Report EL-98-6. U.S. Army Corps of Engineers, Waterways Experiment Station, Vicksburg, MS. 244p.
- Donigian, A.S. Jr., B.R. Bicknell, and J.C. Imhoff. 1995. Hydrological Simulation Program - FORTRAN (HSPF). Chapter 12. In: *Computer Models of Watershed Hydrology*. V.P. Singh (ed). Water Resources Publications. Littleton, CO. pp. 395-442.
- Donigian, A.S., Jr., B.R. Bicknell, and L.C. Linker. 1995b. Regional Assessment of Nutrient Loadings and Resulting Water Quality in the Chesapeake Bay Area. In: *Water Quality Modeling - Proceedings of the International Symposium*. April 2-5, 1995, Orlando, FL. C. Heatwole (ed.). American Society of Agricultural Engineers, St. Joseph, MO. pp. 294-302.

- Donigian, A.S. Jr., R.V. Chinnaswamy and P.N. Deliman. 1998b. Use of Nutrient Balances in Comprehensive Watershed Water Quality Modeling of Chesapeake Bay. Technical Report EL-98-5. U.S. Army Corps of Engineers, Waterways Experiment Station, Vicksburg, MS. 118p.
- Donigian, A.S., Jr., R.V. Chinnaswamy, and R.F. Carousel. 1995a. Watershed Modeling of Agrichemicals in Walnut Creek, IA: Preliminary Assessment of Contributions and Impacts. In: Water Quality Modeling - Proceedings of the International Symposium. April 2-5, 1995, Orlando, FL. American Society of Agricultural Engineers, St. Joseph, MI. pp. 192-201.
- Donigian, A. S., Jr., and N. H. Crawford. 1979. User's Manual for the Nonpoint Source (NPS) Model. Unpublished Report. Athens, Ga.: U.S. EPA Environmental Research Lab.
- Donigian, A. S., Jr., and H. H. Davis. 1978. User's Manual for Agricultural Runoff Management (ARM) Model. Report No. EPA-600/3-78-080. Athens, Ga.: U.S. EPA Environmental Research Lab.
- Donigian, A.S. Jr., J.C. Imhoff, B.R. Bicknell and J.L. Kittle. 1984. Application Guide for Hydrological Simulation Program - Fortran (HSPF), prepared for U.S. EPA, EPA-600/3-84-065, Environmental Research Laboratory, Athens, GA.
- Donigian, A.S. Jr and J.C. Imhoff. 2010. Model Selection for the Illinois River TMDL in AR/OK. Technical Memorandum prepared by AQUA TERRA Consultants for EPA Region 6. EPA Contract No. EP-C-06-29, Work Assignment No. 4-36. November 22, 2010. pp. 33.
- Donigian, A. S., Jr. and J. C. Imhoff. 2011. Model Selection for the Illinois River TMDL in AR/OK – FINAL. Technical Memorandum to Quang Nguyen and Claudia Hosch, US EPA Region 6., dated September 30, 2011. Prepared by AQUA TERRA Consultants, Mountain View, CA. 39 p.
- Donigian, A. S., J. T. Love, and R. A. Dusenbury. 2005. Tenkiller Re-Calibration and Extension. AQUA TERRA Consultants, Prepared for Dynamic Solutions, LLC and Oklahoma DEQ, Mountain View, California.
- Donigian, A.S. Jr., R. A. Park, and J. Clough. 2009. Tenkiller Ferry Lake Modeling Case Study - HSPF and AQUATOX. Submitted to Office of Water/Office of Science and Technology Standards and Health Protection Division U.S. Environmental Protection Agency, Washington, DC.
- Dynamic Solutions, LLC. 2006. 3-Dimensional Hydrodynamic EFDC Model of Lake Thunderbird, Oklahoma Model Setup and Calibration, Tasks 1A,1B(b) and 1B(c). Technical report prepared by Dynamic Solutions, Knoxville, TN for Oklahoma Dept. Environmental Quality, Water Quality Division, Oklahoma City, OK.
- Dynamic Solutions, LLC. 2012. 3-Dimensional Hydrodynamic EFDC Model of Lake Thunderbird, Oklahoma Model Setup and Calibration, Tasks 1A,1B(b) and 1B(c). Technical report prepared by Dynamic Solutions, Knoxville, TN for Oklahoma Dept. Environmental Quality, Water Quality Division, Oklahoma City, OK.
- Fisher, J.B. 2008. Expert Report. Prepared for State of Oklahoma in Case No. 05-CV-329-GKF-SAJ State of Oklahoma v. Tyson Foods, et al. (in the United States District Court for the Northern District of Oklahoma).

- Fisher, J.B., Olsen, R.L., Soster, F.M., Engle, B., and Smith, M. 2009. The History of Poultry Waste Contamination in the Illinois River Watershed as Determined from Sediment Cores Collected from Tenkiller Ferry Reservoir (Oklahoma, United States). Proc. 2009 International Symposium Environmental Science and Technology, Shanghai, China, June 2-5.
- FTN Associates, Ltd. 2012. Illinois River Watershed Partnership (IRWP). 2010. Watershed-Based Management Plan for the Upper Illinois River Watershed, Northwest Arkansas . Final Report, July 17, 2012.
- Green, W. R, (2013), Ambient conditions and fate and transport simulations of dissolved solids, chloride, and sulfate in Beaver Lake, Arkansas, 2006–10: U.S. Geological Survey Scientific Investigations Report 2013–5019, 50 p.
- Grip, W. M. 2008. Statement of Opinions, Wayne M. Grip, President, Aero-Data Corporation. Illinois River Watershed. Case No.: 4:05-cv-00329-GKF-SAJ United States District Court Northern District of Oklahoma. 29 pp.
- Grip, W. M. 2009. Statement of Opinions, Wayne M. Grip, President, Aero-Data Corporation. Illinois River Watershed. Case No.: 4:05-cv-00329-GKF-SAJ United States District Court Northern District of Oklahoma. 66 pp.
- Haggard, B.E. and T.S. Soerens. 2006. Sediment phosphorus release at a small impoundment on the Illinois River, Arkansas and Oklahoma, USA. *Ecol. Eng'r.* 28:280-287.
- Haggard, B.E., D.R. Smith and K.R. Brye. 2007. Variations in stream water and sediment phosphorus among select Ozark catchments. *J. Environ. Qual.* 36(6):1725-1734.
- Haggard, B.E. 2010. Phosphorus Concentrations, Loads, and Sources within the Illinois River Drainage Area, Northwest Arkansas, 1997-2008. *Journal of Environmental Quality* 39(6):2113-2120.
- Hamon, W.R. 1961, Estimating Potential Evapotranspiration. Hydraulics Division [Proceedings of the American Society of Civil Engineers](#). Vol. 87, pp. 107-120, 2817.
- Hamrick, J.M. 1992. *A Three-Dimensional Environmental Fluid Dynamics Computer Code: Theoretical and Computational Aspects*. Special Report No. 317 in Applied Marine Science and Ocean Engineering, Virginia Institute of Marine Science, Gloucester Point, VA. 64pp.
- Hamrick, J.M. 1996. *User's Manual for the Environmental Fluid Dynamics Computer Code*. Special Report No. 331 in Applied Marine Science and Ocean Engineering, Virginia Institute of Marine Science, Gloucester Point, VA.
- Hamrick, J.M. 2007. The Environmental Fluid Dynamics Code Theory and Computation Volume 3: Water Quality Module. Technical report prepared by Tetra Tech, Inc., Fairfax, VA.
- Harmel, R.D., C.T. Hann, and R. Dutnell. 1999. Bank Erosion and Riparian Vegetation Influences: Upper Illinois River, Oklahoma. *Trans. ASAE*, 42(5):1321-1329.
- Illinois River Watershed Partnership (IRWP). 2010. Watershed Management Plan for the Upper Illinois River Watershed, Northwest Arkansas . Amended Draft, May 28, 2010. 126 pp.
- Ji, Z-G. 2008. Hydrodynamics and Water Quality Modeling Rivers, Lakes and Estuaries. Wiley Interscience, John Wiley & Sons, Inc., Hoboken, NJ, 676 pp.

- Kaushai, S. and M. W. Binford. 1999. Relationship between C:N ratios of lake sediments, organic matter sources, and historical deforestation in Lake Pleasant, Massachusetts, US. *Jour. Paleolimnology*, 22:439-442.
- Massey, L.B. and B. Haggard. 2010. Water Quality Monitoring and Constituent Load Estimation in the Upper Illinois River Watershed, 2009. Prepared by Arkansas Water Resources Center, Fayetteville, AR. MSC Publication 363. Funded by Arkansas Natural Resources Commission Through Illinois River Watershed Partnership.
- Michael Baker, Jr., Inc. 2013. Quality Assurance Program Plan for Illinois River Watershed Nutrient Modeling Development. Prepared for US EPA Region 6, Dallas, TX. EPA Contract EP-C-12-052 Order No. 0002. Submitted September 30, 2013.
- Mishra, A., A.S. Donigian, Jr., and B.R. Bicknell. 2014. HSPF Watershed Modeling Phase 3 for the Crow wing, Redeye, and Long Prairie Watersheds: Calibration and Validation of Hydrology, Sediment, and Water Quality Constituents. Prepared for Minnesota Pollution Control Agency, St. Paul, MN. February 15, 2014.
- Nelson, et al. 2006. Illinois River 2005 Pollutant Loads at Arkansas Highway 59 Bridge. Publication No. MSC-332. Submitted to the Arkansas Soil and Water Conservation Commission. Arkansas Water Resources Center University of Arkansas Fayetteville, AK.
- Nolen, S., J. carroll, D. Combs, and J. Staves. 1989. Limnology of Tenkiller Ferry Lake, Oklahoma, 1986-1986. *Proc. Oklahoma Acad. Science*, Vol. 69: 45-55.
- OCC. 2010. Watershed Based Plan for the Illinois River Watershed. Prepared by Oklahoma Conservation Commission, Water Quality Division, Oklahoma City, OK. December 2010. 171 p.
- Oklahoma Conservation Commission (OCC). 2007. Illinois River Watershed Monitoring Program – National Monitoring Project. Prepared by Oklahoma Conservation Commission, Water Quality Division, Oklahoma City, OK. July 2007.
- Oklahoma Department of Environmental Quality (ODEQ). 2010 Oklahoma 303(d) List of Impaired Waters Appendix C. Online accessible at http://www.adeq.state.ar.us/ftproot/Pub/WebDatabases/PermitsOnline/NPDES/PermitInformation/AR0033910_Appendix%20C%202010%20List%20of%20Impaired%20Waters_20130528.pdf.
- Oklahoma State University. 1996. Diagnostic and Feasibility Study on Tenkiller Lake, Oklahoma. GP-016, Environmental Institute, Oklahoma State University.
- Olsen, R.B. 2008. Expert Report. Prepared for State of Oklahoma in Case No. 05-CV-329-GKF-SAJ State of Oklahoma v. Tyson Foods, et al. (in the United States District Court for the Northern District of Oklahoma).
- OWRB. 1996. Phase I, Diagnostic and Feasibility Study on Tenkiller Lake, Oklahoma, Final Report prepared by Oklahoma Ste University, Stillwater, OK for Cooperative “Clean Lakes” Project, US Environmental Protection Agency, Region VI, Dallas, Texas, 342 pp.
- OWRB. 2013. Lake Thunderbird Water Quality 2013. Oklahoma Water Resources Board, Oklahoma City, OK.
- Park, R, A.Y. Kuo, J. Shen and J. Hamrick.2000. *A Three-Dimensional Hydrodynamic-Eutrophication Model (HEM-3D): Description of Water Quality and Sediment Process*

- Submodels*. Special Report 327 in Applied Marine Science and Ocean Engineering, School of Marine Science, Virginia Institute of Marine Science, the College of William and Mary, Gloucester Point, Virginia.
- Romeis, J.J., C.R. Jackson, L.M. Risse, A.N. Sharpley, and D.E. Radcliffe. 2011. Hydrologic and Phosphorus Export Behavior of Small Streams in Commercial Poultry-Pasture Watersheds. *JAWRA*, 47(2):367-385.
- Runkel, R.L., C.G. Crawford, and T.A. Cohn. 2004. Load Estimator (LOADEST): A FORTRAN Program for Estimating Constituent Loads in Streams and Rivers. U.S. Geological Survey Techniques and Methods, Book 4, Chapter A5, 75 p.
- Saraswat, D., N. Pai, and M. Daniels. 2010. A Comprehensive Watershed Response Modeling for 12-Digit Hydrologic Unit Code "HUC" in Selected Priority Watersheds in Arkansas. Draft Report: Illinois River Watershed. Prepared for Arkansas Natural Resources Commission. Revised Report, May 2010. 118 p.
- Sharpley, A.N. 2009 (date approx.). Phosphorus-Based Nutrient Management in the Eucha-Spavinaw Watershed: Results, Accomplishments, and Opportunities. Executive Summary. University of Arkansas, Department of Crop, Soil, and Environmental Sciences, Division of Agriculture, Fayetteville, AR. 33p.
- Storm, D. E., and A.R. Mittelstee. 2014. Hydrologic Modeling of the Oklahoma/Arkansas Illinois River Basin Using SWAT 2012. Draft Report. Submitted to Oklahoma Conservation Commission. Personal communication from A. Mittelstee, February 6, 2014.
- Storm, D. E., P.R. Busteed, A.R. Mittelstee, and M.J. White. 2009. Hydrologic Modeling of the Oklahoma/Arkansas Illinois River Basin Using SWAT 2005. Draft Final Report. Submitted to Oklahoma Department of Environmental Quality. Biosystems and Agricultural Engineering Department, Division of Agricultural Sciences and Natural Resources, Oklahoma State University. October 8, 2009. 115 p. plus Appendices.
- Storm, D. E., M. J. White, and M. D. Smolen. 2006. Illinois River Upland and In-stream Phosphorus Modeling, Final Report. Pages 74 + Appendices. Department of Biosystems and Agricultural Engineering, Oklahoma State University, Stillwater OK.
- Tetra Tech, Inc. 2002. Minnesota River Basin Model: Model Calibration and Validation Report (Revised Draft). Prepared for the Minnesota Pollution Control Agency, St. Paul, MN.
- Tetra Tech, 2007. The Environmental Fluid Dynamics Code User Manual, US EPA Version 1.01, Tetra Tech, Inc., Fairfax, VA.
- Tortorelli, R.L., and B.E. Pickup. 2006. Phosphorus Concentrations, Loads, and Yields in the Illinois River Basin, Arkansas and Oklahoma, 2000-2004. U.S. Geological Survey Scientific Investigations Report 2006-5175. 38 p.
- US EPA Region 6 and OK DEQ. 2001. Water Quality Modeling Analysis in Support of TMDL Development for Tenkiller Ferry Lake and the Illinois River Watershed in Oklahoma (Draft). United States Environmental Protection Agency Region 6 and Department of Environmental Quality State of Oklahoma.
- Wells, S.A., V.I. Wells, and C.J. Berger. 2008. Water Quality and Hydrodynamic Modeling of Tenkiller Reservoir. Expert report prepared for State of Oklahoma in Case No. 05-CU329-GKF-SAJ State of Oklahoma v. Tyson Foods, et al. (in the United States District Court for the Northern District of Oklahoma)

White, M. 2009. Evaluation of Management Scenarios on Nutrient Loads in the Illinois River. Submitted to the Illinois River Watershed Partnership. Grassland Soil and Water Research Laboratory, Agricultural Research Service. US Department of Agriculture. March 9, 2009. 34 p.